The Role of DNA Damage and Extracellular Trap Formation in Atherosclerosis

Vickie Tang

A thesis submitted in fulfilment of the requirements for the award of the degree Doctor of Philosophy (Science)

October, 2020

School of Maths and Physical Sciences

Faculty of Science

University of Technology Sydney

Certificate of Original Authorship

I, Vickie Tang declare that this thesis, is submitted in fulfillment of the requirements for the award of PhD: Science, in the School of Maths and Physical Sciences at the University of Technology Sydney.

This thesis is wholly my own work unless otherwise referenced or acknowledged. In addition, I certify that all information sources and literature used are indicated in the thesis.

This thesis contains materials that have been published in [1] and is shown in Chapter 3. This publication includes the results shown in Figures 3.1, 3.2, 3.3, 3.4, 3.5, 3.6, 3.7, 3.8, 3.9, 3.10 and 3.11. I designed all the studies, analysed the data and wrote the drafts for the manuscript.

This document has not been submitted for qualifications at any other academic institutions.

This research is supported by the Australian Government Research Training Program.

Vickie Tang

Production Note:
Signature removed prior to publication.

31st October 2020

“Nothing in life is to be feared, it is only to be understood.
Now is the time to understand more, so that we may fear less.”

- **Marie Curie**

“Even miracles take a little time.”

- **Fairy Godmother**

“You have brains in your head. You have feet in your shoes.
You can steer yourself any direction you choose.
You're on your own. And you know what you know.
And you are the one who'll decide where to go...”

- **Dr Seuss**

Acknowledgements

Firstly, a huge thank you must go to my supervisors Prof Clare Hawkins, Prof Shanlin Fu and Dr Benjamin Rayner for providing constant support throughout my PhD. They have truly gone above and beyond to provide experience, guidance and a wealth of knowledge throughout this journey. Similarly, thanks must also go to the other members of the Inflammation Group at the Heart Research Institute and the Redox Biology Group at the University of Copenhagen. The members of both these groups provided insight, advice, personal experience and most importantly an empathetic shoulder to cry on when everything seemed to be going wrong.

Thanks must also go to people who were more than willing to share their experimental expertise with me. To Dr Allan Weimann and Prof Henrik Poulsen, thank you for sharing your knowledge in the detection of oxidized nucleosides with me. Also, thanks to Dr Dominic Love for teaching me how to perform the Seahorse experiments. A special thanks must also go to Pat Pisansarakit for all the tissue culture help over the years.

Throughout my PhD candidature, I was lucky enough to be surrounded by the most wonderful friends. Without their unwavering support, I would not have escaped with what's left of my sanity. To my friends I met in my time at the University of Copenhagen, thank you for making my move to a new country so seamless and memorable. My gratitude goes to the crew at the University of Technology Sydney, who have provided nothing but laughter and support. More specifically, my biggest thanks must go to Zohra,

who I was lucky enough to meet during our Honours year. Since then, she has been there for every lunch break and more importantly as emotional support. To my best friend, Shani, we have survived another massive milestone in our lives, and I couldn't be more thankful to have had you by my side as we've lived our best life together for the past 10 years. To my male twin and fellow gin lover, Ali, I will always be so grateful to have met you during the most stressful period of our lives. You have provided much needed encouragement and for that, I'll forever be indebted to you.

My most heartfelt thanks go to my family for whom I will be eternally grateful. To my parents, Selina and Thomas, thank you for providing nothing but love and support throughout the years. To Carrie and David, I will be ever so thankful for your company after a long day and for your constant push to finish this thesis (not to mention, thanks for also providing the best distractions, Joshua and Charlotte). Last but definitely not least, to my now husband, Justin, without whom this thesis truly would not exist. I am forever grateful for the company that you have provided, your poor attempts at distracting me from the mounting stress and for listening to me vent my frustrations even when you had no idea what I was talking about.

Table of Contents

Abstract

The primary cause of cardiovascular disease is atherosclerosis, which is an inflammatory disease resulting in plaque formation within blood vessels. Myeloperoxidase (MPO), an enzyme released by activated leukocytes in atherosclerosis catalyses the formation of hypochlorous acid (HOCl) which reacts readily with nucleic acids forming chlorinated nucleosides. There is increasing evidence that the formation of these chlorinated adducts has adverse effects, and elevated levels of these species are present in different inflammatory contexts, including atherosclerotic lesions.

The focus of Chapters 3 and 4 in this Thesis was to examine the effects of chlorinated nucleosides on endothelial cells (HCAEC) and smooth muscle cells (HCASMC) isolated from the human coronary artery. Studies in HCAEC and HCASMC showed that each of the chlorinated nucleosides studied incorporated into the RNA and DNA of these cells. However, only 8-chloroadenosine (8ClA) was shown to influence the metabolic activity and cell viability in HCAEC. 8ClA was converted to 8-ClATP, which was associated with alterations in the ability of HCAEC to perform glycolysis. Exposure of HCAEC to 8ClA also induced endoplasmic reticulum (ER) stress, resulting in apoptotic cell death and activation of the Nrf2 antioxidant stress response.

In Chapter 4, studies in HCASMC demonstrated that 8ClA and 5-chloro-2'-deoxycytidine (5CldC) decreased both the metabolic activity and proliferation of HCASMC. The effects of 8ClA on HCASMC were similar to those observed in HCAEC though less profound as the viability of HCASMC was unaffected, though some ER stress was apparent. In contrast, exposure of HCASMC to 5CldC resulted in alterations to pro-inflammatory

signalling, a large increase in the expression of MMP2 and MMP9 and phenotypic changes.

A potential source of chlorinated nucleosides under inflammatory conditions was explored in Chapter 5. The differentiation of PLB-985 cells into neutrophils was optimised, together with various treatment conditions to induce the productions neutrophil extracellular traps (NETs). The concentrations of modified nucleosides in both NET DNA and nuclear DNA of these cells was quantified using LC-MS/MS and it was shown that phorbol myristate acetate (PMA) and HOCl treatment gave 8-oxo-7,8-dihydro-deoxyguanosine (8oxodG) and 5CldC, respectively, in both NET and nuclear DNA.

Overall, the studies outlined in this Thesis provide insight into a potential new source of modified nucleosides in disease. These data show that chlorinated nucleosides are not only biomarkers of disease but can alter cellular function in both HCAEC and HCASMC. Therefore, these chlorinated adducts could play a role in the development and progression of atherosclerosis.

List of Figures

List of Tables

Abbreviations

Abbreviation	Definition
18S	18S ribosomal RNA
2-NBDG	2-(N-(7-nitrobenz-2-oxa-1,3-diazol-4-yl)amino)-2-deoxyglucose
3-ClTyr	3-chlorotyrosine
5ClC	5-chlorocytidine
5CldC	5-chloro-2'-deoxycytidine
5CldU	5-chloro-2'-deoxyuridine
5ClU	5-chlorouridine
5ClUra	5-chlorouracil
8ClA	8-chloroadenosine
8-ClATP	8-chloro-ATP
8Cl-cAMP	8-chloro-cyclic AMP
8CldA	8-chloro-2'-deoxyadenosine
8CldG	8-chloro-2'-deoxyguanosine
8ClG	8-chloroguanosine
8oxodG	8-oxo-7,8-dihydro-deoxyguanosine
8oxoG	8-oxo-7,8-dihydroguanosine
Ad	Adenosine
AMP	Adenosine monophosphate
ANOVA	Analysis of variance
ApoB-100	Apolipoprotein B-100

$ApoE^{-/-}$	Apolipoprotein E knockout mice
APS	Ammonium persulfate
ATF4	Activating transcription factor 4
ATF6	Activating transcription factor 6
ATP	Adenosine triphosphate
ATRA	All-trans retinoic acid
BCA	Bicinchoninic acid
BSA	Bovine serum albumin
CCCP	Carbonyl cyanide m-chlorophenyl hydrazone
cDNA	Complimentary DNA
CHOP	CCAAT-enhancer-binding protein homologous protein
CTP	Cytidine triphosphate
CVD	Cardiovascular disease
CX43	Connexin 43
Cyt	Cytidine
dC	2'-deoxycytidine
dG	2'-deoxyguanosine
DMEM	Dulbecco's Modified Eagle Medium
DMF	Dimethylformamide
DMSO	Dimethyl sulfoxide
DNA	Deoxyribonucleic acid
DNase	Deoxyribonuclease
ECAR	Extracellular acidification rate

ECD	Electrochemical detection
EDTA	Ethylenediaminetetraacetic acid
ELISA	Enzyme-linked immunosorbent assay
eNOS	Endothelial nitric oxide synthase
ER	Endoplasmic reticulum
ESI	Electrospray ionisation
ETC	Electron transport chain
FBS	Fetal bovine serum
FCCP	Carbonyl cyanide-4-(trifluoromethoxy)phenylhydrazone
FITC	Fluorescein isothiocyanate
FPG	Formamidopyrimidine DNA glycosylase
GADD34	Growth arrest and DNA damage-inducible protein 34
GAPDH	Glyceraldehyde 3-phosphate dehydrogenase
GCLC	Glutamate-cysteine ligase catalytic subunit
GC-MS	Gas chromatography mass spectrometry
GPx4	Glutathione peroxidase 4
GS	Glutathione synthetase
GTP	Guanosine triphosphate
HBSS	Hank's balanced salt solution
HCAEC	Human coronary artery endothelial cells
HCASMC	Human coronary artery smooth muscle cells
HDL	High-density lipoprotein
HEPES	4-(2-hydroxyethyl)-1-piperazineethanesulfonic acid

HO-1	Heme oxygenase 1
HPLC	High performance liquid chromatography
ICAM-1	Intercellular adhesion molecule-1
IFNγ	Interferon γ
IL-1	Interleukin-1
IL-10	Interleukin-10
IL-12	Interleukin-12
IL-13	Interleukin-13
IL-1β	Interleukin-1β
IL-4	Interleukin-4
IL-6	Interleukin-6
IL-8	Interleukin-8
IRE1	Inositol-requiring enzyme 1
Keap-1	Kelch-like ECH-associated protein 1
LC-MS	Liquid chromatography mass spectrometry
LC-MS/MS	Triple quadrupole liquid chromatography mass spectrometry
LDL	Low density lipoprotein
LOD	Limit of detection
LPS	Lipopolysaccharide
M1	Pro-inflammatory macrophage
M2	Anti-inflammatory macrophage
MMP2	Matrix metalloproteinase 2
MMP9	Matrix metalloproteinase 9

Mnase	Micrococcal nuclease
MPO	Myeloperoxidase
MRM	Multiple reaction monitoring
mRNA	Messenger RNA
NADH	Nicotinamide adenine dinucleotide
NADPH	Nicotinamide adenine dinucleotide phosphate
NETs	Neutrophil extracellular traps
NMR	Nuclear magnetic resonance
NQO1	NADPH quinone dehydrogenase 1
Nrf2	Nuclear factor erythroid-2-related factor 2
OCR	Oxygen consumption rate
Olfml3	Olfactomedin Like 3
OPN	Osteopontin
oxLDL	Oxidised low-density lipoprotein
PAD4	Peptidylarginine deiminase 4
PBS	Phosphate buffered saline
PERK	PKR-like endoplasmic reticulum kinase
PI	Propidium iodide
PMA	Phorbol 12-myristate 13-acetate
PVDF	Polyvinylidene fluoride
qPCR	Quantitative real time polymerase chain reaction
RIPA	Radioimmunoprecipitation assay
RNA	Ribonucleic acid

ROS	Reactive oxygen species
RPL13	Ribosomal protein L13
RPMI	Roswell Park Memorial Institute medium
S100A4	S100 calcium binding protein A4
SDS	Sodium dodecyl sulphate
SEM	Standard error of the mean
SOD1	Superoxide dismutase 1
SOD2	Superoxide dismutase 2
SR-AI	Scavenger receptor-AI
SR-AII	Scavenger receptor-AII
sXBP1	Spliced X-box binding protein 1
TBST	Tris-buffered saline with 0.1% Tween 20
TEMED	Tetramethylethylenediamine
TFA	Trifluoroacetic acid
TLR	Toll-like receptor
TNFα	Tumour necrosis factor α
TRAIL	Tumour necrosis factor related apoptosis inducing ligand
Trx	Thioredoxin
TXNIP	Thioredoxin interacting protein
UDG	Uracil DNA glycosylase
UPR	Unfolded protein response
UTP	Uridine triphosphate
VCAM-1	Vascular cell adhesion molecule-1

Publications and conference presentations arising from this thesis

Publications

Tang, V., Macer-Wright, J., Fu, S., Rayner, B., Hawkins, C., *Chlorinated Nucleosides - A Novel Inducer of Endothelial Dysfunction in Atherosclerosis?* Free Radical Biology and Medicine, 2016. **100**: p. S152.

Tang, V., Macer-Wright, J., Fu, S., Rayner, B., Hawkins, C., *A role for chlorinated nucleosides in the promotion of inflammation and endothelial dysfunction in atherosclerosis?* Free Radical Biology and Medicine, 2017. **108**: p. S30.

Tang, V., Macer-Wright, J., Rayner, B., Fu, S., Hawkins, C., *The effect of chlorinated nucleosides on vascular cell function.* Free Radical Biology and Medicine, 2018. **120**: p. S92-S93.

Tang, V., Rayner, B., Fu, S., Hawkins, C., *Role of chlorinated nucleosides in the promotion of vascular smooth muscle cell dysfunction.* Free Radical Biology and Medicine, 2018. **128**: p. S103-S104.

Tang, V., Fu, S., Rayner, B., Hawkins, C., *8-Chloroadenosine induces apoptosis in human coronary artery endothelial cells through the activation of the unfolded protein response.* Redox Biology, 2019. **26**: p. 101274.

Poster presentations

Tang, V., Macer-Wright, J., Fu, S., Rayner, B., Hawkins, C.

"Chlorinated Nucleosides - A Novel Inducer of Endothelial Dysfunction in Atherosclerosis?"

23rd Annual Meeting of Society for Redox Biology and Medicine, 16th – 19th November 2016, San Francisco, USA.

Tang, V., Macer-Wright, J., Fu, S., Rayner, B., Hawkins, C.

"A role for chlorinated nucleosides in the promotion of inflammation and endothelial dysfunction in atherosclerosis?"

OCC World Congress and Annual Society for Free Radical Research Europe, 21st – 23rd June 2017, Berlin, Germany.

Tang, V., Macer-Wright, J., Rayner, B., Fu, S., Hawkins, C.

"*The effect of chlorinated nucleosides on vascular cell function."*

19th Biennial Meeting of Society for Free Radical Research International, 4th – 7th June 2018, Lisbon, Portugal.

Tang, V., Rayner, B., Fu, S., Hawkins, C.

"*Role of chlorinated nucleosides in the promotion of vascular smooth muscle cell dysfunction."*

25th Annual Meeting of Society for Redox Biology and Medicine, 14th – 17th November 2018, Chicago, USA

Oral presentations

Tang, V., Macer-Wright, J., Fu, S., Rayner, B., Hawkins, C.

"The role of chlorinated nucleosides in endothelial dysfunction and atherosclerosis."

2017 Australian Society for Medical Research NSW Annual Scientific Meeting, 2nd June 2017, Sydney, Australia.

Tang, V., Macer-Wright, J., Fu, S., Rayner, B., Hawkins, C.

"*A role for chlorinated nucleosides in the development of endothelial dysfunction in atherosclerosis?"*

2017 Australian Atherosclerosis Society Annual Scientific Meeting, 25th – 27th October 2017, Sydney, Australia.

Tang, V., Rayner, B., Fu, S., Hawkins, C.

"Chlorinated nucleosides and their role in endothelial and smooth muscle cell dysfunction."

8th Joint Meeting of Society for Free Radical Research Australasia and Japan, 9th – 12th December 2017, Tokyo, Japan.

Awards received

Student Oral Finalist, Australian Atherosclerosis Society 2017, Sydney, Australia.

Young Investigator Finalist, Australian Society for Medical Research 2017, Sydney, Australia.

Young Investigator Travel Award, Society for Free Radical Research Australasia 2017, Tokyo, Japan.

Young Investigator Travel Award, Society for Free Radical Research Australasia 2018, Lisbon, Portugal.

July Paper of the Month, University of Technology Sydney 2019, Sydney, Australia.

Chapter 1 – Introduction

1.1. Overview

Atherosclerosis is the primary cause of cardiovascular disease (CVD) with CVD accounting for 30% of deaths in Australia [2]. Atherosclerosis is an inflammatory disease driven by the deposition of lipids within large blood vessels causing plaque formation [3]. This pathology involves many cell types throughout its development and progression. During the inflammatory process, cytokines and chemokines are released by endothelial cells causing the recruitment of cells to the site of inflammation [4].

During the inflammatory response, cells such as neutrophils and macrophages release myeloperoxidase (MPO), which has been demonstrated to have potent pro-inflammatory and pro-oxidative properties [5]. MPO catalyses the reaction between hydrogen peroxide and halides or pseudo halides causing the formation of multiple oxidants including hypochlorous acid (HOCl) [5]. HOCl readily reacts with most biomolecules causing the oxidation, modification and formation of chlorinated products such as chlorinated nucleosides [6]. There is evidence for HOCl-induced damage in multiple chronic inflammatory conditions including diabetes, cancer and CVD [7-10].

Chlorinated nucleosides are produced from the reaction between HOCl and DNA or RNA [6, 11-15]. These modified products are shown to be present in inflammatory fluids and diseased tissues [16-18], however whether chlorinated nucleosides are a marker of inflammation or have an ability to alter cellular metabolism and disease pathways is yet to be fully elucidated. Therefore, the influence of chlorinated nucleosides on the cellular

metabolism and survival of multiple vascular cell types was determined in this study. Whether these products were also produced from the process of neutrophil extracellular trap formation was also studied.

1.2. Cardiovascular disease and atherosclerosis

1.2.1. Significance of cardiovascular disease

CVD is a general term encompassing diseases relating to the heart and the blood vessels [19]. This includes conditions such as cardiomyopathy, stroke, heart failure, congenital heart disease and atherosclerosis, where many of these conditions can result in fatality. CVD remains one of the biggest killers in the world, despite advancements in therapeutic treatments. In Australia alone, CVD accounts for the death of one person every 12 minutes, affecting 1.2 million people in 2015 [2]. Overall, CVD is responsible for 30% of the deaths within Australia, and with an ageing population, these values are predicted to increase significantly [2].

Of these deaths and statistics recorded for Australians, atherosclerosis is the primary cause of CVD. Atherosclerosis is a chronic inflammatory disease characterised by the deposition of lipids within blood vessels causing plaque formation and consequential narrowing of the blood vessel [20]. In atherosclerosis, the fibrous cap is important in maintaining stability of the plaque. However, this can thin, leading to rupture of the atherosclerotic plaque, causing secondary cardiovascular events such as stroke and myocardial infarction [21]. There are multiple risk factors for the development of atherosclerosis including physical inactivity, smoking, obesity, diabetes, high blood

pressure, cholesterol and increasing age [2]. Atherosclerotic plaque development and progression are largely due to inflammation within the blood vessel and can be attributed to many biological pathways and their interaction with different vascular cell types [3].

1.2.2. Mechanisms responsible for the development and progression of atherosclerosis

Atherosclerosis is a progressive disease, which is driven by the inflammatory response within blood vessels [3]. Initially, the development and formation of an atherosclerotic plaque is in response to physical injury or chemical irritants causing the endothelial cells, lining the vessel wall, to dysfunction [4]. There are two responses that endothelial cells will exhibit due to physical stressors. When the endothelium is exposed to regular physical stress, for example, in laminar flow, endothelial cells will increase production of nitric oxide (NO) [22]. Under normal conditions, the production of NO causes vasodilation and decreases platelet aggregation within the vessel [23, 24]. Secondly, under physical stress, endothelial cells will increase expression of superoxide dismutase (SOD) to counteract increasing reactive oxygen species (ROS) [24]. However, these defence mechanisms can be impaired by physical factors such as bifurcations in blood vessels, increasing shear stress within the vessel [25, 26]. These mechanisms can also be influenced by chemical factors including high concentrations of circulating lipids, high blood glucose (for example, in Type 2 diabetes) and smoking [4]. In each of these cases, these factors influence homeostasis, causing increased permeability in the endothelium and the increased expression of pro-inflammatory cytokines and adhesion molecules [20, 27, 28].

The increase in permeability of the blood vessel allows for circulating lipoproteins such as low-density lipoprotein (LDL) into the tunica intima [29]. In the development of atherosclerosis, LDL can be oxidised to form oxidised LDL (oxLDL) by MPO in two instances. The first is via the direct oxidation of LDL in circulation by MPO at the surface of activated endothelial cells [30, 31]. However, due to the increased permeability of the blood vessel, LDL can migrate into the intima, where it binds to proteoglycans and begins to accumulate within the vessel wall. In this pro-inflammatory environment, there is an increase in oxidative stress, causing the formation of oxLDL [29]. This is significant as oxLDL can induce leukocyte recruitment in conjunction with adhesion molecules expressed by dysfunctional endothelial cells. Following this, resident macrophages uptake and retain oxLDL, causing the formation of foam cells [32]. Macrophages do not recognise oxLDL through their cell-surface LDL receptors, instead are recognised by scavenger receptors, which bind and internalise oxLDL in a non-regulated manner [33]. As these lipid-laden foam cells have impaired migration, this causes the formation of a fatty streak and an intermediate atherosclerotic lesion [33].

Smooth muscle cells also play a vital role in the formation of an atherosclerotic lesion from a fatty streak. During this process, smooth muscle cells migrate from the tunica media into the intima where there they become more proliferative and secrete cytokines reducing the production of extracellular matrix [34]. In addition, the smooth muscle cells play a vital role in the production and stabilisation of the fibrous cap [35]. The fibrous cap lies between the lumen and the core of the plaque, which contains macrophages, foam cells and extracellular matrix [34]. Smooth muscle cells provide structural integrity to the plaque and as they die within the fibrous cap, or through

alterations in the expression of extracellular matrix proteins, they can cause the thinning of the fibrous cap [34, 36].

Macrophages within the vessel wall undergo apoptosis and contribute to the formation of the necrotic core [37]. As macrophages undergo apoptosis, secondary necrosis occurs, as well as impaired clearance of dead cells [38]. Macrophages are the predominant phagocyte within an atherosclerotic lesion and as apoptosis occurs, there is a decrease in the population of functional macrophages [38]. The inability of these macrophages to clear the dead cells within the necrotic core causes an increase in the size of the necrotic core [37]. From this, complex atherosclerotic lesions form causing an occlusion within the artery, see Figure 1.1 [39]. As the fibrous cap thins and the necrotic core continues to grow, this makes the atherosclerotic plaque prone to rupture causing secondary pathologies such as stroke and myocardial infarction [21].

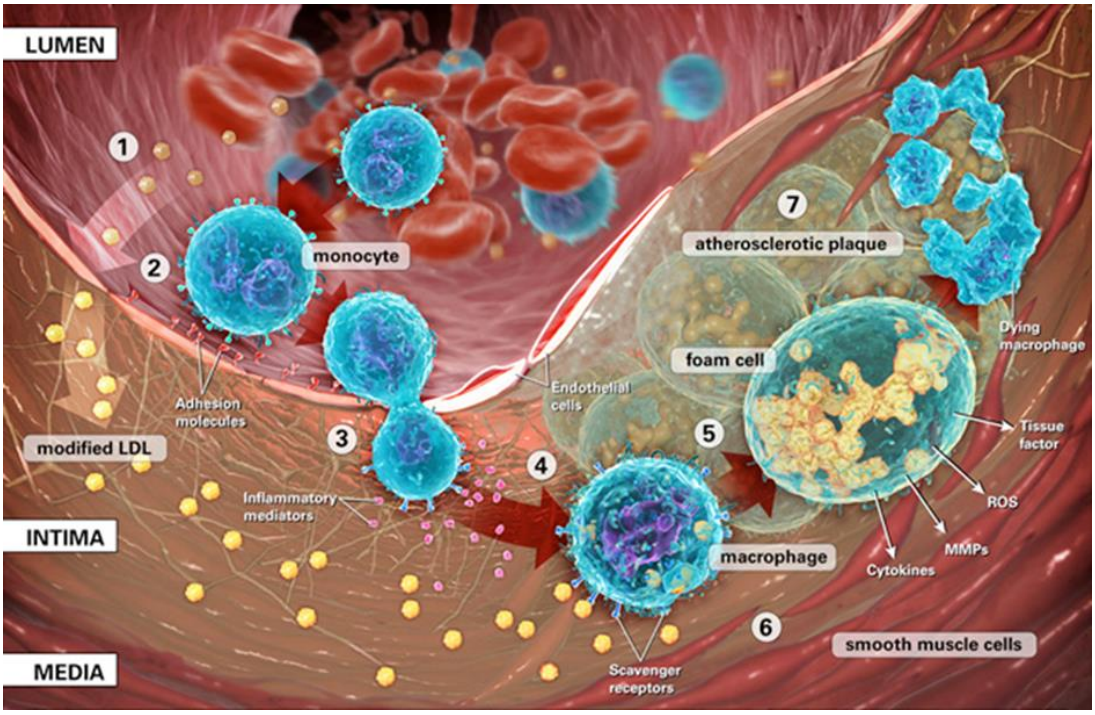

Figure 1.1: *Overview of the key steps involved in the development and progression of a plaque in atherosclerosis, reproduced from [39].*
1. Increased circulating LDL cause the endothelium to dysfunction, causing endothelial cells to release proinflammatory cytokines and adhesion molecules. 2. Monocytes are attracted to the endothelium and roll along the endothelium. 3. Monocytes then transmigrate into the tunica intima. 4. Monocytes mature into macrophages where they ingest modified low-density lipoprotein (LDL). 5. Lipid-laden macrophages form the foam cell. 6. Smooth muscle cells migrate to form the fibrous cap. 7. The atherosclerotic plaque is formed.

1.3. Cellular dysfunction involved in atherosclerosis

1.3.1. Endothelial dysfunction

Endothelial cells line blood vessels and are key in the regulation of homeostasis within the vasculature. The dysfunction of these cells lining the blood vessel is a driving force in the development and progression of atherosclerosis [4]. Endothelial cells regulate the transport and permeability of the blood vessel to plasma. The dysfunction of these cells causes the overexpression of adhesion molecules, such as intercellular adhesion molecule (ICAM) and vascular cell adhesion molecule (VCAM), causing the adhesion of

leukocytes and platelets to the vessel wall [40]. This results in the aggregation of these cells, resulting in the formation of a thrombus [4].

During the early stages of inflammation, the adhesion and aggregation of leukocytes to the vessel walls initiates the increased expression of various adhesion molecules, pro-inflammatory cytokines and chemokines [41]. During endothelial dysfunction in atherosclerosis, there is an overexpression of adhesion molecules such as ICAM and VCAM promoting the adhesion of monocytes to the endothelium [42]. The expression of adhesion molecules is promoted by the increased expression of pro-inflammatory cytokines including interleukin-1β (IL-1β) and tumour necrosis factor-α (TNFα) [42]. The overexpression of these factors plays a large role in the development and progression of atherosclerosis. At sites of inflammation, it has also been demonstrated that there is a significant increase in thrombotic factors and oxidative stress [40].

Previous studies have demonstrated that endothelial dysfunction is crucial in the early stages of atherogenesis [4]. These studies also suggest that those with risk factors for CVD, but without evidence of atherosclerosis still show signs of endothelial dysfunction evident through the inability of the endothelium to react to vasodilators including acetylcholine [4, 27, 43]. Endothelial nitric oxide synthase (eNOS) is a regulator of many functions in endothelial cells including vasodilation and the production of NO [22]. Endothelial dysfunction has been demonstrated to cause a significant impairment in the bioactivity of NO and an increase in the production of oxygen free radicals [44]. As NO is an inhibitor of the aggregation of platelets and adhesion to the endothelium, the decreased production of NO can cause detrimental outcomes [23, 24]. Other studies

show that endothelial dysfunction can be used as a predictor of CVD in patients with other risk factors for CVD [43].

1.3.2. Smooth muscle cell dysfunction

Though many studies implicate endothelial dysfunction in the development and progression of atherosclerotic disease, more recent studies suggest that smooth muscle cells also play a vital role in the initiation of disease development [35, 45]. In the wall of a blood vessel, smooth muscle cells are responsible for the formation of extracellular matrix [35]. When exposed to pro-atherogenic stimuli, smooth muscle cells can alter the type of extracellular matrix proteins that are expressed [46, 47]. These differences in the extracellular matrix produced, alter the lipid content within the vessel wall and increase the proliferation of cells that are adherent to the matrix [35].

In contrast to the role of smooth muscle cells in early atherogenesis, smooth muscle cells in advanced atherosclerosis play a vital role in stabilisation of the plaque and formation of the fibrous cap [21]. The stability of the atherosclerotic plaque is largely dependent on the thickness of the fibrous cap. As the fibrous cap thins, often due to the death of smooth muscle cells, the breakdown of collagen or disintegration of the extracellular matrix, causes the plaque to become prone to rupture [21]. Clinically, this can result in stroke or myocardial infarction. In most cases, this does not happen as the smooth muscle cells are able to repair the rupture in the lesion with advanced lesions often showing evidence of multiple sites of rupture and repair [21]. As this event can occur multiple times in an advanced lesion, this increases the size of the lesion and can cause occlusion of the blood vessel [48].

The repair of damaged blood vessels depends on a delicate balance of the proliferation, migration and the ability of the smooth muscle cells to synthesise extracellular matrix. Similarly, the stability of the plaque and plaque progression is dependent on the balance between proliferation / migration and cell senescence / death of the smooth muscle cells [34]. These properties are dependent on the smooth muscle phenotype and their ability to switch between contractile and synthetic phenotypes [49]. It has been demonstrated in rodent models that smooth muscle cells switch phenotypically in response to multiple stimuli including cytokines [50-52], extracellular matrix [53, 54], lipids [55] and ROS [56]. Smooth muscle cells in a synthetic phenotype have increased migratory and proliferative abilities and produce significantly larger amounts of collagen [57]. Synthetic smooth muscle cells can also uptake LDL more readily than contractile smooth muscle cells, forming foam cells, which implicates this phenotype with a higher prevalence in a diseased state [58].

1.3.3. Macrophages and foam cell formation

As an atherosclerotic lesion develops, circulating monocytes are recruited into the lesion site, where they differentiate into macrophages [33]. Within the lesion, macrophages ingest lipoproteins causing the formation of foam cells. The accumulation of these foam cells contributes to the increase of lipids within the lesion and increasing plaque growth [33]. Under these conditions, macrophages are unable to migrate leading to chronic inflammation and the progression of the plaque [59]. Macrophages are also responsible for increasing inflammation localised to this area by secreting ROS, pro-inflammatory cytokines and chemokines [60]. As these macrophages die within the lesion, they form the basis for the necrotic core in atherosclerosis [60].

Macrophages are highly plastic and exist broadly in two main phenotypes, pro-inflammatory (M1) and anti-inflammatory (M2) phenotypes [61]. Macrophages differentiate into the M1 phenotype from stimuli such as those regulated by toll-like receptors (TLR), interferon-γ (IFN-γ), lipopolysaccharide (LPS) and TNF-α [62]. M1 macrophages contribute to the inflammatory response by increasing production of ROS and NO as well as the increased expression of pro-inflammatory cytokines such as IL-1β, interleukin-6 (IL-6), interleukin-12 (IL-12) and TNF-α [62]. Due to the pro-inflammatory nature of the phenotype, macrophages in the M1 phenotype are found in larger populations within more progressive atherosclerotic lesions [62]. In contrast, M2 macrophages have anti-inflammatory properties and are differentiated into this phenotype following exposure to interleukin-4 (IL-4) or interleukin-13 (IL-13) [62]. These macrophages release interleukin-10 (IL-10) and the receptor agonist to interleukin-1 (IL-1), which are anti-inflammatory factors [62]. Due to their anti-inflammatory properties, M2 macrophages are found in higher populations in atherosclerotic lesions that are regressive [62].

The exposure of macrophages to both native and modified LDL is reported to result in the differentiation of macrophages into the M1 phenotype [63, 64] though this is controversial. Macrophage scavenger receptors have been shown to bind and internalised modified LDL through mechanisms that are not restricted by the content of cholesterol. It has been proposed that scavenger receptors are likely to play a vital role in the accumulation of cholesterol in macrophages causing the formation of foam cells [65]. Similarly, it has been demonstrated more recently that scavenger receptors activate signalling cascades responsible for the activation, inflammation and lipid

metabolism in macrophages [33]. In animal models of atherosclerosis including the apolipoprotein E knockout ($ApoE^{-/-}$) mice, it has been demonstrated that deletion of scavenger receptor-AI (SR-AI), scavenger receptor-AII (SR-AII) and CD-36 cause alterations in plaque progression [66].

SR-AI and SR-AII are expressed on the cell surface of macrophages and those that have formed foam cells [67]. Studies suggest that SR-AI and SR-AII are responsible for approximately 80% of the uptake of acetylated LDL [66, 68]. However, the affinity of these scavenger receptors to oxLDL is much lower, though SR-AI and SR-AII are able to recognise the apolipoprotein B moiety of oxLDL [69, 70]. In $ApoE^{-/-}$ murine models where SR-AI and SR-AII were deleted, it was demonstrated that there was a 58% decrease in the atherosclerotic lesion area when compared to $ApoE^{-/-}$ littermates [66], consistent with the presence of these scavenger receptors increasing the extent of plaque progression. CD36 is reported to bind to oxLDL rather than acetylated LDL. This scavenger receptor has been attributed to clearing approximately 60-70% of cholesteryl esters accumulated in macrophages that have been exposed to oxLDL modified by exposure to copper ions [68, 71, 72]. Studies with $ApoE^{-/-}$ mice that lack CD36 were shown to have significant decreases in the size of the atherosclerotic lesion [72]. This suggests that the uptake of oxLDL mediated by CD36 is a key driver of lesion formation in atherosclerosis [72].

1.3.4. Neutrophils and neutrophil extracellular trap formation

Neutrophils are the most abundant white blood cell accounting for 60 - 70% of leukocytes circulating in the human body [73]. They are the cell type most commonly

seen at sites of inflammation with their primary functions being phagocytic, engulfing invading pathogens such as bacteria and other microorganisms [19, 74]. However, neutrophils have also been shown to play vital roles in early and late stage atherosclerosis. In early stage lesions, neutrophils are localised to the subendothelial space and intima [75]. In contrast, studies in $ApoE^{-/-}$ mice show that in late stage plaques, neutrophils are found in the shoulder region and adventitia of the aorta [76]. Furthermore, there is evidence suggesting the correlation between lesion size and circulating neutrophil counts. It was determined that the depletion of neutrophils resulted in a marked reduction in atherosclerotic plaque size [75].

When protecting against invading pathogens and as a response to injury, neutrophils produce extracellular traps (NETs) forming a web-like structure of DNA that contains histones and antimicrobial proteins [77]. These structures are being increasingly implicated in lesion formation in atherosclerosis [74, 78-81]. There are two mechanisms by which NETosis occurs, suicidal and vital. Suicidal NETosis is the main mechanism by which NETs are released and occurs more slowly than in vital NETosis [74]. It is caused by the activation of nicotinamide adenine dinucleotide phosphate (NADPH) oxidase by invading pathogens, and pro-inflammatory molecules, such as interleukin-8 (IL-8) and phorbol myristate acetate (PMA) causing the release of the DNA structures through a ROS-dependent manner [82, 83]. The process begins with nuclear delobulation where the nuclear envelope becomes disassembled. Following this, the cell loses polarisation and the chromatin decondenses. Finally, the plasma membrane ruptures, allowing for the NET to be released [74]. In vital NETosis, neutrophils release nuclear DNA rapidly into the extracellular space without perforation of the cellular membrane in a ROS-

independent manner [84, 85]. This can occur independently of cell death and begins with the degranulation causing the release of granular proteins followed by the externalisation of nuclear chromatin. These processes are summarised in Figure 1.2.

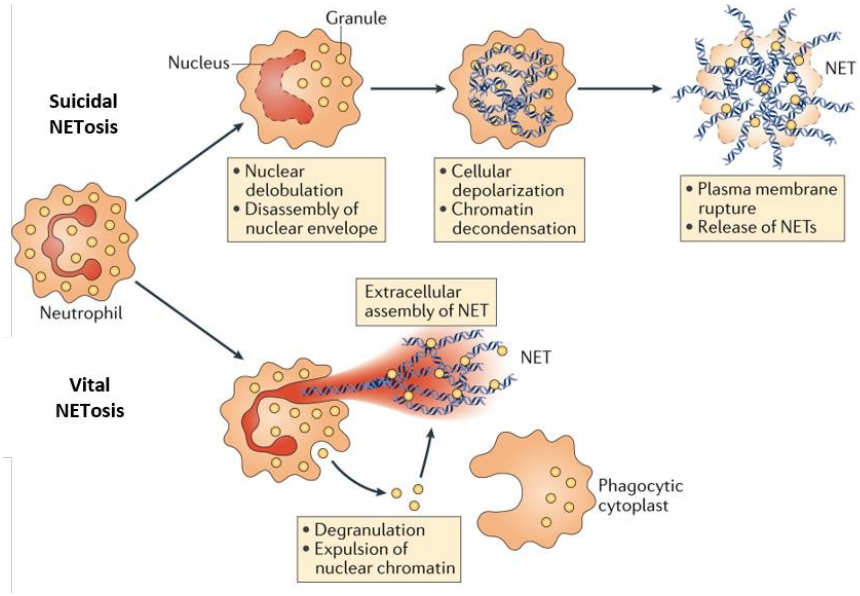

Figure 1.2: *Suicidal and vital neutrophil extracellular trap formation, reproduced from [74].*

NETs are present in both human and murine atherosclerotic lesions [81, 86-90]. In a murine model of atherosclerosis, it has been demonstrated that the formation of NETs may be due to cholesterol crystals [81]. The presence of NETs in the atherosclerotic lesion, is believed to drive the activation of macrophages causing an increase in the expression of pro-inflammatory cytokines [81]. Consequently, this recruits more leukocytes to the site of inflammation, thereby propagating the disease cycle.

Histone citrullination is a key process in NETosis, which results in chromatin decondensation owing to alterations in charge [91, 92]. Peptidylarginine deiminase 4 (PAD4) catalyses the citrullination of histones and is important in multiple processes including NETosis, haematopoiesis and apoptosis [93, 94]. PAD4-mediated citrullination

of histone causes the DNA-histone bond to be weakened, allowing for the release of DNA outside the nucleus [92, 95]. As such, studies have shown that chemical inhibition of PAD4 with Cl-amidine inhibits NET production in mouse and human neutrophils [90, 96, 97]. In a murine model of atherosclerosis, it was demonstrated that deletion of PAD4 prevented NET production and decreased lesion formation [90]. More recently, a study demonstrated that myeloid specific deletion of PAD4 significantly reduced NET production and decreased inflammatory response in the aorta showing a decrease in atherosclerotic burden [87]. This data supports a causal role of NETs in lesion formation.

It has also been well described that NETs have pro-thrombotic effects, with intact NETs shown to encapsulate platelets causing their activation and aggregation [98, 99]. NETs provide structure for the attachment of pro-coagulant molecules such as fibrinogen, fibronectin and von Willebrand factor [98], which provides stability to the fibrin network within a thrombus [100]. This is due to the increase in fibrin fibre size, providing more rigidity and stability, in turn, causing the thrombus dissolution time to be significantly longer [101].

In addition to the presence of citrullinated histones, NETs are characterised by the presence of key granule proteins, particularly neutrophil elastase and MPO, which is reported to retain its catalytic activity [102]. Although NETs contain MPO and are present in pro-inflammatory environments, what remains to be determined is whether damage occurs to these DNA and protein structures prior to or after the NETs have been released, and whether this has any biological role.

1.4. Myeloperoxidase and atherosclerosis

1.4.1. Chlorinated oxidant production

The infiltration of immune cells into the vessel wall and chronic inflammation results in the production of HOCl from the extracellular release of MPO [103, 104]. Activated leukocytes release MPO through a process of degranulation [5]. Membrane-bound NADPH oxidase on the neutrophil (or immune cell) converts oxygen to superoxide via a respiratory burst [105]. Superoxide in this environment dismutates to hydrogen peroxide (H_2O_2), which is converted to HOCl in the presence of chloride ions by MPO (summarised in Figure 1.3) [5]. HOCl is an extremely reactive oxidant, which reacts readily with almost all biomolecules including amines, with which it can form N-chloramines. This is significant as N-chloramines exhibit oxidising capacities similar to HOCl [106, 107].

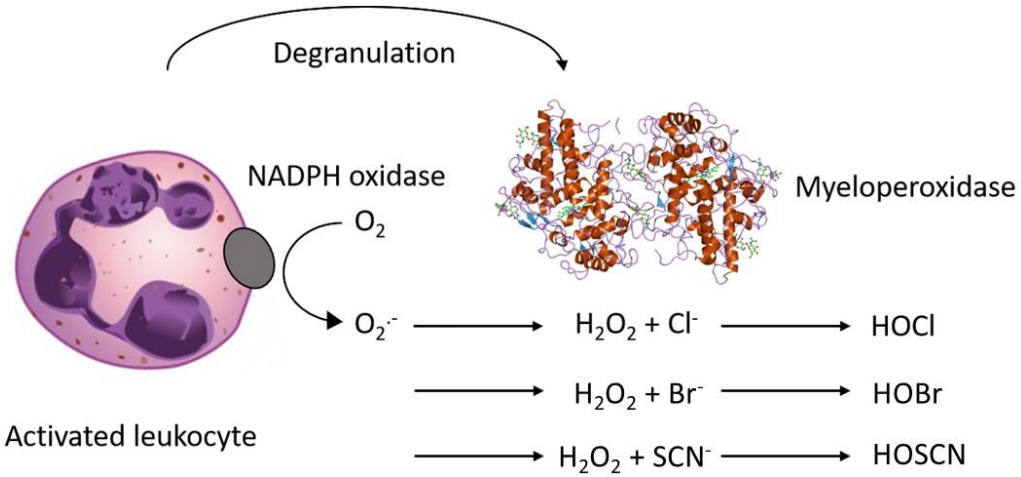

Figure 1.3: *Schematic of the formation of HOCl from myeloperoxidase.*

The formation of HOCl accounts for approximately 50% of hydrogen peroxide utilised by MPO under normal physiological concentrations of halide and pseudo halide ions [108, 109]. MPO also utilises bromide and thiocyanate ions to form hypobromous acid (HOBr) and hypothiocyanous acid (HOSCN), respectively [109]. However, the concentration of these hypohalous acids is dependent on the local halide and pseudo halide concentrations. Given significant evidence for the production of HOCl in chronic inflammatory pathologies [8, 9, 105], this oxidant is the focus of the current study.

1.4.2. MPO in atherosclerosis

Though the formation of HOCl through the actions of MPO and NADPH oxidase are part of a normal immune response, MPO has been shown within the literature to play a role in the development and progression of disease [110-115]. MPO has been implicated in not only atherosclerosis but also in other chronic inflammatory diseases including rheumatoid arthritis [114, 116], asthma [117], Alzheimer's disease [118, 119], cancer [120, 121], diabetes [122], multiple sclerosis [123] and kidney disease [124]. The detection of elevated biomarkers of HOCl-formation provides evidence or support for a role of this oxidant in disease progression.

MPO is widely recognised to be an independent risk factor for the development of coronary artery disease [125, 126]. Thus, in patients suffering from coronary artery disease, concentrations of MPO are significantly increased compared to those without disease [127]. MPO is elevated within the atherosclerotic lesion and is present in higher concentrations around the shoulder region of a plaque [113]. In addition, concentrations of macrophages expressing MPO are significantly increased in advanced plaques when

compared to early stage lesions [128]. In a more recent study, MPO has been shown to be relevant in plaque stability with increased MPO activity evident in unstable plaques [129]. In a murine model of atherosclerosis, where MPO was genetically deleted, it was found that the fibrous cap was thickened compared to those without gene deletion of MPO [129]. This suggests that MPO plays a role in the formation of an unstable atherosclerotic plaque. MPO has also been shown to be a good predictor of risk of myocardial infarction in patients suffering from unstable angina [130]. Similarly, studies have also shown that elevated levels of MPO are correlated to an increased risk in developing atherosclerosis [131-133].

In atherosclerosis, the accumulation of LDL within the vessel wall is a key driver of lesion formation [29]. Previous studies have shown that MPO plays a role in the oxidation of LDL via radical and non-radical pathways [134]. LDL is made up of a lipid core, which is encased in a phospholipid bilayer containing apolipoprotein B-100 (ApoB-100) [135]. HOCl has been demonstrated to oxidise both the protein and lipid components of LDL [136]. HOCl reacts with phospholipids, such as phosphatidyl serine, causing the formation of unstable chloramines [137]. The decomposition of these unstable chloramines results in the formation of radical intermediates, which cause lipid oxidation [137].

Thus, the protein moiety of LDL is believed to be the primary target of HOCl. In addition, to the phospholipid head groups, protein chloramines can also be formed on the lysine side chains, which have also been proposed to promote the secondary oxidation of the LDL lipids [138]. Another prominent target on ApoB-100 are the methionine residues

[139]. The exposure of ApoB-100 to HOCl induces the oxidation of methionine residues to form methionine sulfoxide [139]. Furthermore, tyrosine residues on ApoB-100 are a major target for lipid peroxidation by HOCl, which forms the HOCl-specific damage biomarker, 3-chlorotyrosine (3-ClTyr) [7, 113, 140]. This implicates MPO in atherogenesis as there are increased concentrations of 3-ClTyr in the circulating LDL of CVD patients as well as within an atherosclerotic plaque [141].

In addition to the formation of modified LDL, MPO has also been reported to decrease the atheroprotective effect of high-density lipoprotein (HDL). Studies have demonstrated that low concentrations of HDL within the plasma have been strongly correlated to a higher risk of CVD [142]. The major mechanism by which HDL is thought to exhibit atheroprotective effects is through reverse cholesterol transport, which removes cholesterol from the arterial wall [143]. MPO impairs the ability of HDL to support cholesterol efflux from lipid-laden macrophages [144, 145]. Furthermore, oxidised HDL competes with native HDL as a ligand for scavenger receptors, impairing the transport of cholesterol from tissues to the liver for removal [146]. In addition to these findings, *in vitro* studies with reconstituted HDL showed that exposure to MPO caused the protective effects of HDL to be diminished and the increased expression of the pro-inflammatory cytokine, VCAM, in endothelial cells [147]. Overall, given that HDL has been demonstrated to have anti-inflammatory, anti-thrombotic and anti-oxidative effects, these effects exhibited on HDL by MPO may promote atherogenesis.

1.4.3. HOCl-induced modifications of proteins

MPO-derived oxidants are potent and have the ability to modify most biomolecules including DNA, RNA, lipids and protein [106, 148-151]. *In vivo,* proteins are thought to be the main target for HOCl owing to the abundance of proteins within a biological system. When isolated proteins are exposed to HOCl, it has been demonstrated that damage occurs mostly to the amino acid side chains [152]. The most readily oxidised amino acids by HOCl are cysteine and methionine residues, followed by histidine, cystine, tryptophan, lysine and tyrosine in terms of the second order rate constants [153]. In general, HOCl-induced protein oxidation is irreversible, leading to the inhibition of enzymes, crosslinking, protein unfolding and can make the protein more or also less vulnerable to protein degradation [154].

HOCl reacts more readily with amino acid side chains than with the protein amide backbone [155]. HOCl has been shown to react with sulfur-containing amino acid side chains. Sulfenyl chlorides are formed upon the reaction of HOCl with cysteine and can further react to produce multiple products [156, 157]. Sulfenyl chloride intermediates are highly reactive with thiols, causing the formation of disulfides. The hydrolysis of sulfenyl chloride intermediates forms sulfenic acid and other oxy acids [156]. Furthermore, sulfenyl chlorides are also reported to decompose to form a thiyl radical [154]. It has also been postulated that the reaction of cystine with HOCl forms sulfenyl chlorides. In contrast, sulfenyl chlorides derived from cystine are hydrolysed to form thiosulfinates as well as sulfinic and sulfonic acids [158]. When methionine is present on the N-terminal residue, HOCl reacts to form dehydromethionine, which has been suggested as a biomarker for MPO-induced damage [159, 160]. A study on children with

cystic fibrosis showed elevated levels of dehydromethionine and methionine sulfoxide in samples taken from the bronchoalveolar fluid [161].

N-chloramines form from the reaction of HOCl with histidine and lysine residues. This is significant as the oxidising capacity of HOCl is retained when N-chloramines are formed [162]. Furthermore, when N-chloramines are formed on protein lysine residues, the chlorine can be transferred within the protein or to other substrates, which results in the regeneration of the parent amine [163]. Similarly, N-chloramines formed on histidine residues can transfer the chlorine to other residues within the protein to increase stability [164]. N-chloramines have also been shown to transfer chlorine to the exocyclic amines of nucleic acid bases to form chlorinated nucleosides [6].

HOCl has also been described to react with aromatic tyrosine residues. HOCl or reactive chloramines react with tyrosine to form 3-ClTyr and 3,5-dichlorotyrosine [165, 166]. 3-ClTyr is produced by HOCl-specific damage to protein and has therefore been used as a biomarker in inflammatory fluids and diseases tissue [167-171]. HOCl-induced modifications on protein have been shown to alter immunity, as well cause the activation of neutrophils [172], implicating HOCl-induced damage in disease. Overall, the reaction of HOCl with proteins, specifically amino acid residues alters the function of proteins and can cause tissue damage during chronic inflammation.

1.4.4. Reactions of hypochlorous acid with lipids

In general, when HOCl reacts with lipids, HOCl reacts with the double bonds present in unsaturated fatty acids, phospholipids and cholesterol [173]. This leads to the formation of chlorohydrins, oxysterols or peroxides [173]. Studies have indicated that HOCl can

cause lipid peroxidation in lipoproteins and in liposomes [173]. Chlorohydrins have been shown *in vitro* to alter cell permeability and viability by disruption of the lipid bilayer [174, 175]. Oxysterols have been shown to be present in disease with elevated levels present in patients with atherosclerosis [176]. Furthermore, the incubation of macrophages with oxysterols has been shown to increase the expression of pro-inflammatory cytokines suggesting that oxysterols can alter cell signalling [177].

Another target of HOCl is phospholipids, which exist in high concentrations in biological membranes [178]. Phospholipids are important targets for oxidation and chlorinated by HOCl, in particular those with polar head groups (for example, amino acid residues in phosphatidylserine) or unsaturated fatty alcyl residues [179]. In the cardiovascular system, the most abundant phospholipids present in plasma membranes are plasmalogens and are prevalent in neutrophils, smooth muscle cells and cardiomyocytes [180-184]. Plasmalogens result from the reaction between a fatty aldehyde and glycerol and are characterised by an ethanolamine or choline headgroup [185]. In the presence of HOCl, the primary amine headgroups of ethanolamine are oxidised to form chloramines, dichloramines, chlorimines and nitriles. Though these products were demonstrated to be produced *in vitro*, only the lysophosphatidylcholine chlorohydrin has been identified in human atherosclerotic plaques [186].

Plasmalogens contain a vinyl-ether bond, which makes these phospholipids more susceptible to oxidative damage by HOCl compared to those with an alcyl residue [187]. The cleavage of the vinyl ether bond results in the formation of α-chloro fatty aldehydes [180]. In human neutrophils activated with phorbol ester, the α-chloro fatty aldehyde,

2-chlorohexadecanal was shown to accumulate [188]. Furthermore, it was shown in this study that HOCl targets plasmalogens present in endothelial cells, thereby impacting neighbouring cells [189]. Similarly, HOCl also targets LDL-associated plasmalogens, which leads to the production of 2-chlorohexadecanal. This is supported by the 1400-fold increase in 2-chlorohexadecanal present in human atherosclerotic lesions when compared to healthy human aortic tissue [190]. Therefore, these HOCl-modified products have been shown to accumulate in human atherosclerotic tissue and the vessel wall.

1.4.5. HOCl-induced modifications of nucleic acids

The modification of DNA and RNA is prevalent at sites of inflammation and also in diseased states such as cancer [191, 192]. Mutations in DNA occur following reaction with HOCl and N-chloramines through crosslinking, DNA strand breaks and also through the disruption of hydrogen bonding [192, 193]. Also, the decomposition of N-chlorinated nucleobases has been demonstrated to result in formation of radicals causing cleavage of DNA strands [194, 195].

The reaction of HOCl with nucleotides, nucleosides and nucleobases yields both unstable and stable chlorinated products: N-chloramines and carbon-chlorine products, respectively [194-198]. In the formation of N-chloramines, a hydrogen attached to the endo- or exocyclic nitrogen is replaced by a chlorine atom. The stability of N-chloramines is dependent on the position of the nitrogen on the compound. N-chloramines formed on an exocyclic amine such as those formed on cytidine are more stable than those formed on endocyclic amines such as uridine [199]. These products are unstable due to

the nature of the nitrogen-chlorine bond and are often reaction intermediates which ultimately react to form compounds such as 5-hydroxycytosine, 5-hydroxyuracil, thymine glycol or hypoxanthine [200, 201]. Given that these products can also be produced via the reaction of nucleosides with other oxidants [197], they are unsuitable as a biomarker of HOCl-induced damage.

N-chloramines also react with the aromatic rings of nucleosides giving rise to a more stable carbon-chlorine bond. These reactions with nucleosides forms chlorinated nucleosides such as 8-chloro-(2'-deoxy)adenosine (8-Cl(d)A), 8-chloro-(2'-deoxy)guanosine (8-Cl(d)G), 5-chloro-(2'-deoxy)cytosine (5-Cl(d)C) and 5-chlorouridine (5-ClU) [13, 196, 197, 200-203], see Figure 1.4. When parent ribose nucleosides were exposed to HOCl or N-chloramines, 5ClC was formed to the greatest extent when compared to 8ClG and 8ClA, with only low levels of 8ClA being produced [6]. Similarly, the reaction of HOCl or N-chloramines with parent deoxyribose nucleosides formed 5CldC to the greatest extent, followed by 8CldG, with small concentrations of 8CldA formed [6]. In addition, reactions of HOCl with cells also forms these chlorinated nucleoside products [6, 13].

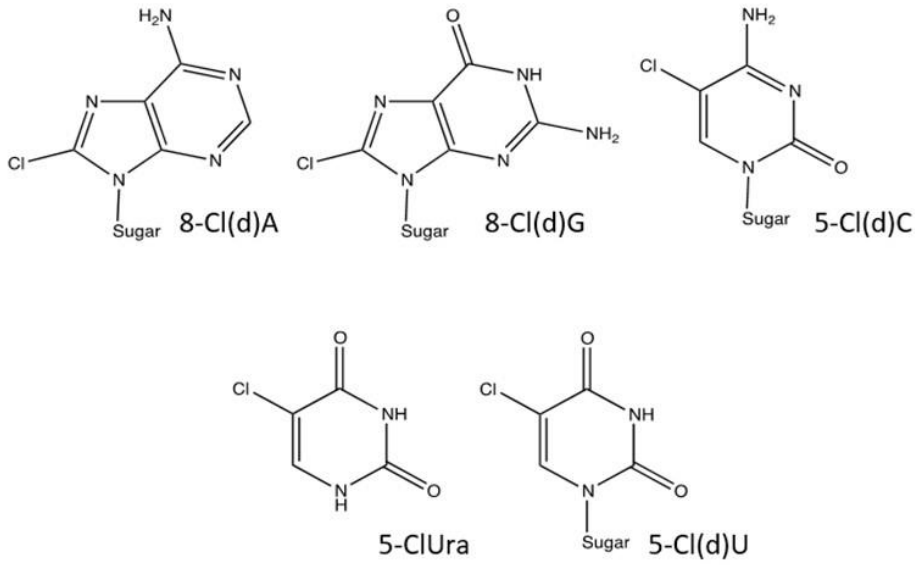

Figure 1.4: *Structures of chlorinated nucleosides.*

1.5. Biomarkers of inflammation in disease

1.5.1. DNA damage products as biomarkers

Biomarkers are products that can be quantified in a disease state and provide an indication as to health, severity of disease or response to treatment. As such, their discovery is important in the identification of disease mechanisms and targets, as well as in the development or studies of therapeutic intervention [204]. DNA damage products are being explored as biomarkers within the literature as there has been evidence of their presence in inflammation and pathologies such as cancer and atherosclerosis [205-210]. There are a variety of DNA damage products that are formed *in vivo* with some providing insight into the origin and oxidant causing their formation [204].

The most well studied nucleic acid damage products are 8-oxo-7,8-dihydroguanosine (8oxoG) and 8-oxo-7,8-dihydro-deoxyguanosine (8oxodG) [211-216]. 8oxoG and 8oxodG levels have been shown to be elevated in inflammatory diseases such as cancer [215], CVD [217, 218] and diabetes [211, 212]. Previous studies in the urine of diabetic patients have shown the presence of 8oxoG, which may provide a non-invasive biomarker [219]. Furthermore, in patients newly diagnosed with diabetes, 8oxoG has been demonstrated to be excreted in the urine with higher levels predicting long term mortality [220]. Similarly, elevated levels of the DNA oxidation marker, 8oxodG, has been correlated to diabetes [211]. However, in contrast to 8oxoG, 8oxodG levels have not been shown to correlate with mortality in diabetic patients [221]. Though 8oxoG and 8oxodG have been shown to be a potential non-invasive biomarker in diabetes, a limitation to the use of these products is that they can be artefactually formed by conditions such as heat [222, 223].

Chlorinated DNA damage products have been demonstrated to be elevated in animal models of oxidative stress. In particular, chlorinated nucleosides have been shown to be a viable candidates as biomarkers in diseased states. In rodents exposed to LPS, elevated levels of 8CldG were detected in the liver, 2 to 12 h after exposure [18]. In these animals, it was also demonstrated that there were elevated levels of 8CldG excreted in the urine 24 h after exposure to LPS [18]. Another chlorinated nucleoside, 5ClUra has been shown to be detected in inflammatory tissue after bacterial infection [17]. In addition, studies on human atherosclerotic lesions were conducted and it was shown that concentrations of 5ClUra were 10 times those found in healthy aortic tissue [16]. Given these findings, this implicates HOCl induced damage on DNA in inflammation and atherosclerosis.

Though there is evidence for DNA damage in these diseased states, there are limitations to the use of these products as biomarkers for disease. The main limitation is the abundance of DNA damage products compared to those of lipids, proteins or other metabolites [204]. This requires more sensitive methods of detection for modified nucleic acids when compared to other modified biomolecules. Another limitation with the use of modified nucleic acids as biomarkers is the invasive nature of the procedures required to sample the DNA [204]. Similarly, the tests and multitude of pathologies that could be analysed using samples isolated by invasive methods would be limited due to the amount of sample that could be taken from the site. The exception to this would be a biomarker detectable within venous blood.

1.5.2. Detection of DNA damage products

Over time, the methods of detecting modified nucleic acids *in vivo* have evolved. Initial studies in the separation of chlorinated nucleosides (in particular 5ClC, 5ClU and 5ClUra) formed from the reaction of DNA with HOCl, utilised paper chromatography [196]. Other studies have been conducted using thin layer chromatography and ultraviolet-visible spectrometry to identify 5ClC and 5ClUra after exposing the respective parent nucleoside to HOCl [197, 203].

More recently, studies in this area have used more definitive methods of detection and quantification of DNA damage products. These include the use of gas chromatography – mass spectrometry (GC-MS), liquid chromatography – mass spectrometry (LC-MS) and nuclear magnetic resonance (NMR) spectroscopy. A study of chlorinated nucleosides performed using LC-MS determined the limit of detection (LOD) to be 0.1 pmol for each

chlorinated nucleoside (8ClA, 8ClG, 5ClC, 8CldA, 8CldG and 5CldC) by monitoring m/z of the molecular ion and the fragment ion formed from cleavage of the nucleoside at the sugar moiety (*m/z* summarised in Table 1.1) [14].

Table 1.1: *Mass fragmentation of chlorinated nucleosides detected using LC-MS.*

Compound	**Molecular ion (*m/z*)**	**Fragment ion (*m/z*)**
8ClA	302	107
8ClG	318	186
5ClC	278	146
8CldA	286	170
8CldG	302	186
5CldC	262	146

Furthermore, Noyon et al. validated an LC-MS/MS method in the detection of chlorinated nucleosides in biological matrices [224]. In this study, it was determined that the limit of quantification (LOQ) of 5CldC, 5ClC, 8oxoG and 8oxodG was 5 fmol. Experiments also showed that the LOQ of 8ClG was 0.2 fmol [224]. The results from this study showed evidence for the detection of 8ClG being 75-fold more sensitive than a previously published method [13]. Furthermore, the detection of 8oxodG was found to be 4-fold more sensitive than methods published by Henriksen et al [225]. However, a limitation of this study was that other chlorinated nucleosides such as 8ClA and 8ClA were not detected by this method [224].

For many studies, LC-MS is the preferred method of analysis due to the ease of sample preparation compared to GC-MS where a derivatisation step is required in order to increase sample volatility. Another limitation in the use of GC-MS is the artefactual formation of DNA damage during sample preparation for example the oxidation of 2'-deoxyguanosine to form 8oxodG. Multiple studies have used HPLC as a method of separating chlorinated nucleosides followed by analysis and quantification using LC-MS [17, 226].

Other studies have published methods of GC-MS sample preparation where derivatisation temperatures have been lowered to reduce formation of artefactually produced modified nucleosides. Previous studies have used thermal or acid hydrolysis techniques in order to form the nucleosides from DNA, where more recently, studies have turned to using enzymatic methods such as the use of DNA glycosylase repair enzymes [227-229]. On the other hand, a study was published comparing the use of GC-MS and LC-MS in detecting chlorinated nucleosides, which found that using either method, there were negligible amounts of chlorinated DNA artefacts formed from sample preparation. However, it was determined that GC-MS had a faster sample turn around and was twice as sensitive as the LC-MS method tested [230].

Though the artefactual formation of chlorinated DNA artefacts may not be a huge concern when studying DNA damage products, the artefactual oxidation of samples during preparation for analysis needs to be explored. The product of oxidative DNA damage, 8oxodG is often used as a measure of oxidative stress within a system. The formation of oxidised DNA damage products including 8oxodG can be induced by heat

through increasing ROS, therefore incorrect sample storage or preparation can result in an overestimation of their true concentrations in samples [222].

Another method used in the study of DNA damage is the use of the Comet assay, which is a single cell gel electrophoresis assay [231]. This technique is dependent on the unwinding of the chromatin in the DNA of cells that have been embedded into agarose. During electrophoresis, the DNA is drawn towards the anode resulting in comet-like images when the DNA is stained by a fluorescent DNA probe such as Sytox Green [231]. The size of the comet-tail is proportional to the amount of strand breaks and the frequency of strand breaks is taken from the intensity of DNA fluorescence in the comet tail [231]. This method has been utilised with various repair enzymes in order to study specific DNA damage products. For example, the use of formamidopyrimidine DNA glycosylase (FPG) allows for the detection of the oxidised purines, 8oxoG and 8oxodG, as well as ring-opened purines [232]. The misincorporation of uracil into DNA can also be determined by the Comet assay using uracil DNA glycosylase (UDG), which is the repair enzyme responsible for removal of uracil from DNA [233]. Furthermore, Comet assay can detect crosslinks between DNA as the formation of the comet-tail is inhibited in this case. DNA crosslinks can therefore be determined by the inhibition of normal DNA comet-tail formation after treatment with H_2O_2 [231].

A different approach used by several studies includes the use of antibodies in order to detect these DNA damage products. A study conducted by Asahi et al. used a primary monoclonal antibody against 8ClG in order to determine the presence of 8ClG after rodents were exposed to LPS [18]. It was demonstrated that this method had limitations

owing to the inability of the concentrations of 8ClG to be quantified due to a lack of specificity as the antibody was 10 times more reactive to 8-bromoguanosine [18]. Similarly, antibodies against 8oxodG are often used in order to detect 8oxodG within tissue samples.

More recently, enzyme linked immunosorbent assays (ELISA) have been developed in order to quantify 8oxodG in saliva, urine, serum, plasma, tissue, cell lysates and supernatants. Though ELISA is a quantitative method of determining 8oxodG, the results of this method are not comparable to those obtained by LC-MS methods [234]. This is due to the ELISA antibody recognising both free 8oxodG and 8oxodG incorporated into the DNA where LC-MS methods often only measure the free nucleoside.

1.6. DNA damage in disease

1.6.1. Cancer

It has been well studied within the literature that damage to DNA during inflammation can be detrimental, leading to the development of cancer [191, 206]. Cancer is not only a disease caused by increased proliferative activity, but in many cases can be due to agents that promote damage to DNA [191]. Cells that continue to proliferate despite having become mutagenic or having sustained DNA damage continue to thrive in the inflammatory environment of cancer [191]. These environments contain an abundance of growth factors and inflammatory cells, which lead to tumour metastasis [191].

In a cancerous environment, there is a significant increase in ROS, which can cause modifications to DNA [235]. These DNA damage products, for example 8oxodG are formed due to ROS-mediated inflammation during tumorigenesis [236]. 8oxodG is mutagenic due to its tendency to pair with adenine during DNA replication [237]. The primary enzyme which removes 8oxodG from DNA is OGG1, which cleaves the glycosylic bond [238]. Though the damage in cancer produced by oxidative DNA damage was believed to be due to the mispair of 8oxodG with adenine, recent studies have demonstrated that free 8oxodG also has mutagenic properties [239]. Although there is evidence linking DNA damage to cancer, the evidence for the link to diabetes and CVD is also becoming clearer within the literature.

1.6.2. Diabetes

DNA damage has been linked to diabetes with studies showing that some DNA damage products may correlate with clinical markers [10]. It has been well described in the literature that there is an increased incidence of DNA damage in the blood cells of those with Type 2 diabetes when compared to those without [201, 240-243]. More recently, it has been shown that patients suffering from Type 2 diabetes are more susceptible to mutagens and have impaired DNA repair mechanisms [244]. The sustained increase in glucose levels alter the ability of cells to express insulin-dependent mRNA required to activate DNA repair pathways, which may explain the observations described [244].

The most well studied DNA damage product in diabetes is 8oxodG [240]. 8oxodG has been demonstrated to be relevant in this context due to an increase in ROS in a diabetic environment. ROS such as the hydroxyl radical, superoxide anion, peroxynitrite and

peroxyl radicals can produce not only oxidative DNA damage but other modifications including DNA strand breaks [201]. Many studies have shown that there is a significant increase in the excretion of 8oxodG in diabetic urine compared to age matched controls [245-247]. In addition to this, it has been demonstrated that diabetic patients with complications have significantly increased levels of 8oxodG excreted in their urine when compared to diabetic patients without complications [248]. Though these observations have been made, there has been no link described between 8oxodG levels and mortality rates in diabetic patients [221, 249].

Studies have also been able to provide a link between the urinary excretion of the RNA oxidation product, 8oxoG and diabetes [212, 214, 221, 249, 250]. These studies suggest that 8oxoG is a viable biomarker for diabetes. The urinary excretion of 8oxoG is a good predictor of mortality in patients with newly diagnosed diabetes independent of other risk factors such as sex, age, smoking, blood pressure and pre-existing CVD [249]. Moreover, in urine collected 6 years after diagnosis with diabetes, it was determined that increased levels of 8oxoG at this follow up corresponded to an increase risk in mortality [221]. Similarly, a decreased urinary excretion of 8oxoG in diabetic patients had a decreased risk in mortality showing that 8oxoG was not only a predictor of mortality but also a risk factor [221]. These data provide evidence for the efficacy of the use of modified nucleosides as a biomarker in disease.

1.6.3. CVD and atherosclerosis

In CVD, it has been proposed that an increase in oxidative stress, increased DNA damage and limited DNA repair contributes to atherogenesis [251]. The oxidative damage

observed in atherosclerosis is largely due to the production of ROS (such as the production of the superoxide and hydroxyl radical) in the inflammatory environment leading to the progression of disease [252]. In atherosclerosis, it has been demonstrated that there is a significant increase in DNA single and double strand breaks and elevated concentrations of 8oxodG due to increased ROS in this disease state [208, 253]. Some studies have shown a correlation between the concentrations of 8oxodG detected with the severity of disease [208, 253]. It has also been shown within the literature that in atherosclerotic lesions, there is an increase in staining for 8oxodG when using immunohistochemistry methods and a significant increase in DNA repair pathways, for both base excision repair and other non-specific pathways [207].

Not only is there evidence for the presence of oxidative DNA damage in the context of atherosclerosis, studies have also demonstrated that there is also chlorination of DNA within a lesion [16]. As previously mentioned in this chapter, a study performed by Takeshita et al., showed that concentrations of 5ClUra were found to be 10-fold higher within an atherosclerotic lesion when compared to healthy aortic tissue [16]. Whether this chlorinated nucleoside is a by-product of the disease process or whether it propagates disease progression remains to be determined.

1.7. Biological reactivity of chlorinated nucleosides

1.7.1. Cellular consequences

The biological reactivity or cellular consequences of chlorinated nucleosides are yet to be fully elucidated, however there are some studies demonstrating their incorporation

into nucleotides, DNA and RNA [1, 6]. The incorporation of these modified nucleosides has been demonstrated to cause mutagenesis, which has been implicated in diseased states such as atherosclerosis and cancer [16, 254]. In these pathologies, inflammation is an important component causing the development and progression of disease.

A study published in 2015 showed that 5ClC showed mutagenic properties *in vitro* and *in vivo* [255]. This chlorinated nucleoside is mutagenic as it remains unidentified by DNA polymerases, which only recognise this modification 25% of the time. There were two mechanisms proposed by which this process occurs, that 5ClC was converted to a more toxic product or 5ClC was intrinsically mutagenic [255, 256]. Studies on the mutagenesis of 5ClC demonstrated that 5ClC base-paired with guanine 95% of the time and adenine for the other 5%. These findings are significant as 5ClC is the most readily formed chlorinated nucleoside [256]. Another study showed that only 5ClC incorporated into the RNA of epithelial prostatic cells and EA.hy926 endothelial cells causing alterations in RNA synthesis and translation [256].

5ClUra incorporates into the DNA of a human leukemia cell line [257]. In these cells, 5ClUra could not be distinguished from thymine during DNA replication when the template strand contained 5ClUra or thymine [257]. Similarly, when 5ClUra and adenosine formed based pairs in DNA, the base pair was not targeted for removal by glycosylases due to their thermodynamic stability and hydrogen bonding similarities to a base pair of thymine and adenine [258].

In a murine macrophage cell line, J774.A1, ribose chlorinated nucleosides, 8ClA, 8ClG and 5ClC were shown to incorporate into RNA [259]. In contrast, only 5CldC incorporated

into the DNA of J774.A1 cells but not 8CldA and 8CldG [259]. These cells were shown to be able to clear levels of 5ClC from cellular RNA as well as 8ClA and 8ClG to a lesser extent. However, when J774.A1 cells were exposed to 8ClG and 5ClC, there was a significant increase in the expression and secretion of pro-inflammatory cytokines and chemokines, including IL-1β [259]. However, though there were alterations to the expression of pro-inflammatory genes, there were no observed differences to proliferation or viability of the cells under the conditions used.

In contrast to this, the prolonged exposure of J774.A1 cells to 8ClA caused alterations in metabolism and induced apoptotic cell death [260]. When these cells were exposed to 8ClA, there was a significant increase in the incorporation into the nucleotide pool to form 8-ClATP. The formation of this product did not alter basal mitochondrial respiration or glycolysis, however, it was demonstrated to significantly increase maximal respiration and spare respiratory capacity [260]. In addition, these cells were shown to have altered antioxidant responses and DNA damage repair.

These data demonstrate that chlorinated nucleosides can have mutagenic effects as well as incorporate into RNA and DNA of cells causing other effects influencing homeostasis. With this knowledge, chlorinated nucleosides have been used therapeutically particularly in the context of cancer [261, 262].

1.7.2. Chlorinated nucleosides as therapeutic agents

Though some chlorinated nucleosides have been shown to cause mutagenic effects, there is also evidence demonstrating the therapeutic benefits of these compounds. *In vitro* studies with 5CldC have shown that this chlorinated nucleoside works as a

radiosensitiser [263]. In HEp-2, RIF-1 and S-180 mammalian cell lines, co-treatment with 5CldC and tetrahydrouridine, caused the cells to be more sensitive to X-ray [263]. In addition, when these cells were pre-incubated with inhibitors of pyrimidine synthesis, this sensitivity was increased [263].

Studies performed with human cancers in nude mice have demonstrated similar effects to those in cell lines [264]. It was shown that *in vivo,* deoxycytidine kinase converts 5CldC to 5-CldCMP, which is further converted to 5-CldUMP by dCMP deaminase [265]. Following this, 5-CldUMP has been shown to be anabolised and selectively incorporated into DNA of cancerous tumours as 5CldU [265]. This works as a radiosensitiser as X-rays directed to tumour DNA with incorporated 5CldU, causing the Cl atom to be released. From this, a uracyl radical is formed causing strand breaks to occur within the tumour DNA [264]. The cell is then no longer able to adequately replicate, causing death of the cancerous cells [264].

Another chlorinated nucleoside that has been demonstrated to have therapeutic benefits is 8ClA. *In vitro* studies using leukemic cell lines have shown that exposure to 8ClA causes the formation of 8-Cl-cAMP resulting in apoptotic cell death [266]. The cell death observed was proposed to occur through two major mechanisms, either through the depletion of ATP or by inhibiting anti-apoptotic proteins [266]. Following these mechanisms, 8ClA is phosphorylated by multiple enzymes, for example, adenosine kinase to form the chlorinated analogue of ATP, 8-ClATP [266]. Similarly, the formation of 8-ClADP has been demonstrated to compete with ADP, also causing the depletion of intracellular ATP [267].

In addition to these effects observed in chronic lymphocytic leukemia cells, 8ClA has been demonstrated to induce apoptosis in myeloma [266, 268, 269], breast cancer [270, 271] and mantle cell lymphoma [272] cell lines. The ability of 8ClA to induce these outcomes on cancerous cell types has resulted in a Phase I clinical trial of intravenous infusions of 8ClA in the treatment of chronic lymphocytic leukemia [261]. More recently, Phase I/II clinical trials of intravenous infusions of 8ClA in the treatment of refractory and relapsed acute myeloid leukemia are also in completion [262]. Though these chlorinated nucleosides have been and continue to be studied in the treatment of disease, whether 8ClA, 5CldC and other chlorinated nucleosides are involved in the progression of other pathologies, remains to be defined.

1.8. Summary

Although MPO has been shown to play a vital role in the immune response, the generation of MPO-derived oxidants such as HOCl has been strongly linked to the development and progression of atherosclerosis [110, 113, 115]. Studies show that HOCl is a strong oxidant, capable of reacting with DNA and RNA to form chlorinated nucleosides [13, 196]. Though chlorinated nucleosides have been implicated in diseases such as atherosclerosis and diabetes, whether these compounds are biomarkers or whether they propagate disease progression remains to be fully elucidated. Studies have shown the toxicity of 8ClA and mutagenic properties of 5ClC, however, the implications of exposure many of the other chlorinated nucleosides in the context of atherosclerosis remains unknown.

Another well known contributor to the progression of atherosclerosis is the production of NETs. The structures of NETs have been well defined to be strands of DNA as well as histones and antimicrobial factors, which are expelled in response to injury or other stressors. One of the antimicrobial factors present on NET DNA include MPO. However, whether MPO attached to these NETs produce HOCl, which could react to NET DNA to form chlorinated nucleosides remains unknown.

1.9. Hypotheses and aims

Therefore, the objective of this project was to determine the effect of exposure to chlorinated nucleosides in human coronary artery endothelial cells (HCAEC) and human coronary artery smooth muscle cells (HCASMC). Also, this study aimed to examine whether any chlorinated nucleosides were formed on the DNA of NETs in a human neutrophil cell line (PLB-985).

1.9.1. Hypotheses

This project explored two specific hypotheses, which were that: the formation of chlorinated nucleosides under chronic inflammatory conditions will influence the function of vascular cells, promoting the development and progression of atherosclerosis. The second hypothesis was that neutrophil extracellular traps may be a source of chlorinated nucleosides in inflammatory environments.

1.9.2. Project aims

1. To determine the extent of uptake and turnover of chlorinated nucleosides with different vascular cell models (HCAEC and HCASMC).
2. To assess whether chlorinated nucleosides influence cellular function and pro-inflammatory signalling pathways in vascular cells.
3. To establish whether neutrophil extracellular traps are a potential physiological source of chlorinated nucleic acids.

Chapter 2 – Materials and Methods

2.1. Materials

Solutions and chlorinated nucleoside stocks were prepared using nanopure water, which was filtered through a Milli-Q system unless otherwise stated (Millipore Waters, Australia). Materials and chemicals were sourced from various companies that are stated in Appendix 1.

2.2. Chlorinated nucleosides and all-trans retinoic acid (ATRA)

Stock solutions of chlorinated nucleosides, 8ClA, 8ClG, 5ClC and their deoxyribose forms, 8CldA, 8CldG and 5CldC were made to a concentration of 500 µM in Milli-Q water. Parent nucleosides adenosine (Ad), cytidine (Cyt), 2'-deoxyguanosine (dG) and 2'-deoxycytidine (dC) were made to a concentration of 5 mM in Milli-Q water. A stock solution of all-trans retinoic acid (ATRA) was made to 10 mM in dimethyl sulfoxide (DMSO). Chlorinated nucleosides and ATRA stock solutions were stored in aliquots at –80˚C prior to dilutions in appropriate cell culture media for cell treatments.

2.3. Cell culture

2.3.1. Human coronary artery endothelial cell culture

Human coronary artery endothelial cells (HCAEC) (Cell Applications) were cultured in MesoEndo cell culture medium (Cell Applications) under sterile conditions at 37˚C with 5% CO_2. For each experiment, a minimum of 3 separate donors (details outlined in Table

2.1) were cultured and passaged for experiments by enzymatic digestion using trypsin-EDTA (0.025% trypsin and 0.01% EDTA in PBS) to form a cell suspension. Cell density was normalised to 5 × 10^4 cells/mL (unless otherwise specified) and cells at or between passages 3 – 6 were plated in MesoEndo cell culture medium and were allowed to adhere to the plate overnight prior to treatment. 8ClA, 8ClG, 5ClC, 8CldA, 8CldG and 5CldC (4, 8 and 16 µM) were prepared in MesoEndo cell culture medium sterile filtered, and incubated with the cells for 2, 6, 24, 48 and 72 h.

Table 2.1: *Human coronary artery endothelial cell donor information.*

Donor Number	Gender	Age	Ethnicity
2366	Male	60	Caucasian
2315	Male	19	Hispanic
2863	Male	16	Caucasian

2.3.2. Human coronary artery smooth muscle cell culture

Human coronary artery smooth muscle cells (HCASMC) (Cell Applications) were cultured in smooth muscle cell growth medium (Lonza) under sterile conditions at 37˚C with 5% CO_2. For each experiment, a minimum of 3 separate donors (details outlined in Table 2.2) were cultured and passaged for experiments by enzymatic digestion using trypsin-EDTA (0.025% trypsin and 0.01% EDTA in PBS) to form a cell suspension. Cell density was normalised to 1 × 10^5 cells/mL (unless otherwise specified) and passages 3 – 6 were plated in smooth muscle cell growth medium and allowed to adhere to the plate overnight prior to treatment. 8ClA, 8ClG, 5ClC, 8CldA, 8CldG and 5CldC (4, 8 and 16 µM)

were prepared in smooth muscle cell growth medium sterile filtered and incubated with the cells for 2, 6, 24, 48 and 72 h.

Table 2.2: *Human coronary artery smooth muscle cell donor information.*

Donor Number	Gender	Age	Ethnicity
1522	Male	54	Black
1559	Male	22	Black
2989	Male	27	Caucasian

2.3.3. PLB-985 cell culture and differentiation

PLB-985 cells were cultured in RPMI-1640 supplemented with 10% fetal bovine serum (FBS), 100 U/mL penicillin and 0.1 mg/mL streptomycin under sterile conditions in T175 cm^2 tissue culture flasks. Cells were cultured in a humidified environment with 5% CO_2 at 37˚C. PLB-985 were allowed to proliferate in suspension culture with passaging every second day by removing 20 mL of cell suspension and replacing the volume removed with 20 mL of RPMI-1640 supplemented with 10% FBS, 100 U/mL penicillin and 0.1 mg/mL streptomycin. Cells between passages 3 and 20 were normalised to a density of 3×10^3 cells/mL and were differentiated into a neutrophil-like state by incubation in T175 cm^2 flasks in RPMI-1640 with 1% FBS, 1.3% DMSO and 2 µM ATRA for 72 h prior to each experiment.

2.3.3.1. Determination of PLB-985 morphology with May-Grünwald-Giemsa staining

The successful differentiation of PLB-985 (myelomonoblasts) into a neutrophil-like granulocyte was determined using morphological analysis with May-Grünwald-Giemsa

staining. Non-differentiated PLB-985 cells and PLB-985 cells differentiated in 1 µM and 2 µM ATRA were normalised to a density of 2×10^5 cells/sample in 200 µL 50% RPMI-1640 (with 10% FBS, 100 U/mL penicillin and 0.1 mg/mL streptomycin) and 50% PBS. Cells were cytocentrifuged using a Cytospin 3 (Thermo Fisher Scientific) at 20 *× g* for 10 min onto microscope slides. Slides were then allowed to dry in a fume cabinet for 1 h, before fixing in methanol for 5 min, and staining with 55% May-Grünwald in 45% Phosphate buffer (pH 6.5) for 10 min. A second stain, 10% Giemsa in 90% Phosphate buffer was then applied for 15 min prior to submersion of the slides in Phosphate buffer for 5 min. Slides were then briefly washed in Milli-Q H_2O for 1 min to remove residual stain prior to allowing it to dry. Once slides had been allowed to dry for at least 1 h, coverslips were mounted onto each slide using PERTEX. The slides were then allowed to dry in the fume cabinet overnight prior to imaging using an Olympus Bx43 microscope.

2.4. Neutrophil extracellular trap release

2.4.1. Qualitative detection of NETs by microscopy with Sytox Green staining

In order to determine the production of NETs, extracellular release of DNA was determined by using the DNA specific stain, Sytox Green, with microscopic imaging. PLB-985 cells differentiated in 2 µM ATRA for 72 h were counted and normalised to a density of 5×10^5 cells/mL, then plated into 4-well chamber slides (4×10^5 cells/well), which were pre-coated with poly-*l*-lysine. Cells were allowed to adhere to the slides for 1 h in a humidified environment with 5% CO_2 at 37˚C. In experiments with PMA, each well was gently washed with HBSS supplemented with 0.5% FBS to remove residual RPMI-1640.

Each well was then treated with 25, 50 and 100 nM PMA in HBSS supplemented with 0.5% FBS and incubated at 37˚C for 4 h. in experiments with HOCl, each well was washed gently with RPMI-1640 supplemented with 0.5% FBS. Wells were then treated with 0.5, 0.75 and 1 mM HOCl diluted in RPMI-640 with 0.5% FBS and incubated at 37˚C for 4 h. After incubation, an equal volume of 8% (v/v) formaldehyde in PBS was added to each well to fix the cells with incubation for 15 min. After removal of media and formaldehyde, a second fixative of 4% (v/v) formaldehyde in PBS was added and the slides were further incubated for 15 min. Slides were then gently washed twice with HBSS prior to the addition of 2 µM Sytox Green for 10 min to stain extracellular DNA. The stain was aspirated from each well and the chambers were removed. Slides were left to dry for 10 min before adding a coverslip with ProLong Gold antifade mountant. After allowing the slides to dry overnight in the dark, each chamber was imaged using the FITC filter on an Olympus Bx43 fluorescence microscope.

2.4.2. Quantification of NETs by fluorescence

2.4.2.1. Quantification of NETs by Sytox Green staining

The quantification of NET production was performed by staining extracellular DNA with Sytox Green, followed by measurement of fluorescence using a plate reader. PLB-985 were differentiated as above and plated into a 24-well plate (5×10^5 cells/well) or black 96-well plate (2×10^5 cells/well) prior to treatment with PMA (10, 20, 25, 50 and 100 nM). In the black 96-well plates, 2 µM Sytox Green was added and the plate was analysed at excitation and emission wavelengths of 504 and 523 nm, respectively, using a plate reader, every hour for 4 h. Cells plated in the 24-well plates were treated with

PMA (10, 20, 25, 50 or 100 nM) for 4 h. Following treatment, 40 U/mL of deoxyribonuclease (DNase) was added to each well and incubated for 15 min before inactivation with 5 mM EDTA. The supernatant was then centrifuged (200 × *g* for 5 min) to remove cells, followed by staining of remaining NETs with 2 µM Sytox Green. The stained supernatant (200 µL) was then transferred into a black walled 96-well plate and analysed using a SpectraMax M3 plate reader at excitation and emission wavelengths of 504 and 523 nm, respectively.

2.4.2.2. Quantification of NETs by PicoGreen staining

The quantification of NET production was also performed by staining extracellular DNA with PicoGreen, followed by measurement of fluorescence using a plate reader. After differentiation and stimulation of PLB-985 (5×10^5 cells/well) with HOCl (0.25, 0.5, 0.75 or 1 mM) or PMA (10, 25, 50 or 100 nM) for 4 h, 0.5 mU/mL of micrococcal nuclease (MNase) was added and samples were incubated at 37 ˚C with 5% CO_2 for 15 min. MNase was then inactivated by addition of 5 mM EDTA prior to centrifugation to remove the cell pellet. An equal volume of 1:200 dilution of PicoGreen reagent in 10 mM Tris base buffered with 1 mM EDTA was then added to the supernatant. This was then transferred into a black 96-well plate and incubated for a further 10 min. Following incubation, fluorescence was recorded at excitation and emission at 488 and 520 nm, respectively using a SpectraMax M3 plate reader.

2.5. Quantification of unmodified and modified nucleosides using liquid chromatography triple quadrupole mass spectrometry (LC-MS/MS)

2.5.1. Nucleic acid isolation

2.5.1.1. Isolation of DNA, RNA and protein from HCAEC and HCASMC

The incorporation of chlorinated nucleosides into the DNA or RNA of HCAEC or HCASMC was determined by LC-MS/MS. HCAEC or HCASMC (1×10^6 cells) were plated in a T175 cm^2 flask with chlorinated nucleosides (8 µM) and incubated for 2, 6, 24, 48 and 72 h at 37˚C. Following treatment, DNA and RNA was isolated from the cells using the Isolate II RNA/DNA/Protein Extraction Kit (Bioline) following the manufacturer's protocol. Cells in each sample were lifted into suspension using 5 mL of trypsin-EDTA (0.025% trypsin and 0.01% EDTA in PBS) and centrifuged at 220 × *g* for 5 min to pellet the cells. PBS (5 mL) was then added into each sample to resuspend and wash the cells. Samples were then centrifuged at 220 × *g* for 5 min and the supernatant was removed prior to the addition of 300 µL of Lysis Buffer TX. Samples were then stored at – 20˚C until separation or immediately transferred to a DNA isolation column.

Once lysed samples were transferred to the DNA column, the columns were centrifuged at 14 000 × *g* for 1 min and the flow through (A) was transferred to a microcentrifuge tube for isolation of RNA. Wash buffer W1 (500 µL) was then added to the column and centrifuged at 14 000 × *g* for 1 min. This was then repeated with wash buffer W2 with the flow through discarded. The column was centrifuged for 2 min at 14 000 × *g* in order to dry the column. DNA elution buffer (100 µL) was then added to each sample and centrifuged for 2 min at 200 × *g*, followed by 14 000 × *g* for 1 min to elute DNA.

In order to isolate RNA, 100% ethanol was added (200 µL) to the flow through sample (A) and vortexed to mix. The resulting solution was transferred to the RNA and protein isolation column and centrifuged at 3500 × *g* for 1 min. The flow through from this solution (B) was then transferred into a microcentrifuge tube for isolation of protein. To the column, 400 µL of wash buffer W1 was added, followed by centrifugation at 14 000 × *g* for 1 min with the flow through discarded. The wash step was then repeated twice more prior to drying the column by centrifugation at 14 000 × *g* for 2 min. RNA was eluted by addition of RNA elution buffer (50 µL) followed by centrifugation at 200 × *g* for 2 min then 14 000 × *g* for 1 min.

To isolate protein from each sample, 500 µL of nuclease-free water and 40 µL of protein binding buffer was added to the flow through from the RNA column (B). Samples were then transferred into the RNA and protein column and centrifuged at 5 200 × *g* for 2 min with flow through discarded. Wash buffer 3 (500 µL) was added to each sample and centrifuged at 5 200 × *g* for 2 min. To elute the protein, 100 µL of protein elution buffer was added to each sample and centrifuged at 5 200 × *g* for 2 min. Protein neutralisation buffer (9.3 µL) was then added to each sample. DNA, RNA and protein samples were all stored at -80˚C until further analysis.

2.5.1.2. Isolation of DNA from extracellular traps released by PLB-985

The presence of chlorinated nucleosides on NETs released by PLB-985 was determined by LC-MS/MS. Differentiated PLB-985 cells were normalised to a density of 1×10^7 cells/sample before treatment to induce NETs in T75 cm^2 cell culture flasks. After incubation with PMA (50 nM) or HOCl (0.75 mM) for 4 h, traps were digested with DNase

(40 U/mL) for 10 min. 5 mM EDTA was then added in order to inactivate the DNase. Samples were centrifuged for 5 min at 200 × g in order to pellet the cells. The supernatants were then transferred into 50 mL centrifuge tubes where DNA was precipitated by adding a one tenth volume of 3 M sodium acetate (pH 5.2) followed by 2 volumes of absolute ethanol, and incubation at – 20 ˚C overnight. The samples were then centrifuged at 4 ˚C for 30 min at 14 000 × g to pellet DNA. The supernatant was removed, and the DNA pellet was lysed using the lysate buffer in the DNA isolation kit (QIAGEN). The initial cell pellet was washed once with PBS and centrifuged at 200 × g for 5 min. The pelleted cells were then lysed using the lysis buffer from the DNA extraction kit. Once the lysis buffer had been added to precipitated DNA and cell pellet, the extraction kit was used to isolate DNA.

2.5.2. Hydrolysis and dephosphorylation of DNA and RNA

DNA or RNA concentration was measured using a Nanodrop spectrophotometer and each sample was adjusted to 500 ng of DNA or RNA. Samples were hydrolysed using 2 U Nuclease P_1 with addition of an equal volume of 300 mM sodium acetate and zinc sulfate solution, pH 5.3 and incubated for 2 h at 37˚C. Samples were then dephosphorylated using 10 U alkaline phosphatase with the addition of an equal volume of a 500 mM Tris-HCl and 1 mM EDTA solution at pH 8.0 for 1 h at 37˚C. A liquid-liquid extraction was performed using 5 volumes of chloroform. After addition of chloroform, the sample was vortexed and centrifuged to separate into two layers. The top aqueous layer was collected, transferred to a new tube and centrifuged at 16 000 *× g* for 10 min through a 10 kDa centrifugal filter followed by then centrifuged at 16 000 *× g* for 10 min through a 0.22 µm filter. The filtrate was subjected to solid phase extraction using a C18 vacuum

cartridge. Solid phase extraction was performed by conditioning the cartridge with 80% methanol, equilibration with 0.1% TFA in H_2O, addition of sample, followed by washing with 0.1% TFA in H_2O and elution using 80% methanol. Samples were then evaporated for 4 h (to dryness) using a Speedivac at 40 ˚C prior to resuspension in 50 µL of H_2O.

2.5.3. Detection of chlorinated and parent nucleosides by LC-MS/MS

A Discovery C18 column (5 µm pore size, 25 cm × 2.1 mm) (Sigma Aldrich) was used to achieve chromatographic separation of chlorinated and parent nucleosides (Appendix 2). 20 µL of each sample was injected and eluted according to the mobile phase composition in Table 2.3 using 5 mM ammonium formate in H_2O (Buffer A) and 5 mM ammonium formate in 50% (v/v) acetonitrile (Buffer B) adapted from [6]. Detection of each compound was completed by UV absorbance at 260 nm using an Agilent Technologies 1290 detector. Confirmation was achieved by ESI-positive triple-quadrupole mass spectrometry using selected reaction monitoring (SRM) with mass fragmentation summarised in Table 2.4 as previously described [6, 13]. Mass fragmentation was achieved with nitrogen as the collision gas, held at a temperature of 290˚C, with a flow rate of 11 L/min. The capillary voltage applied was 4000 V in order to ionise each sample with a sheath gas flow of 12 L/min at a temperature of 400 ˚C. Collision energies for both the qualifier and quantifier ions were determined by direct injection into the MS with monitoring using Mass Hunter Optimizer Software (Agilent).

Table 2.3: *Mobile phase composition to separate chlorinated and parent compounds.*

Time	Buffer B (%)
0 – 10	0
10 – 50	0 – 20
50 – 60	20 – 50
60 – 65	50 – 100
65 – 70	100
70 – 75	100 – 0

Table 2.4: *Mass fragmentation of unmodified and chlorinated nucleosides.*

Compound	Parent ion (m/z)	Qualifier ion (m/z)	Qualifier Collision Energy	Quantifier ion (m/z)	Quantifier Collision Energy
8ClA	302.2	153.0	53	169.9	17
8ClG	318.1	169.0	45	186.0	13
5ClC	278.1	128.9	41	145.9	17
Adenosine	268.1	118.9	49	136.1	17
Guanosine	284.1	135.0	33	151.9	17
Cytidine	244.1	95.0	47	112.0	17
8CldA	286.1	116.9	13	169.9	9
8CldG	302.1	132.9	35	186.0	13
5CldC	262.1	93.0	35	145.9	9
2’-deoxyadenosine	252.2	119.0	41	135.9	9
2’-deoxyguanosine	268.1	110.1	45	151.9	37
2’-deoxycytidine	228.1	58.8	37	111.9	9

2.5.4. Detection of 8CldG in NETs

Detection of 8CldG was performed using an Acquity C18 UPLC column (1.8 µm pore size, 10 cm × 2.1 mm) (Waters) maintained at a temperature of 11˚C. A 25 µL injection of each sample was eluted under the gradient outlined in Table 2.5, where mobile phase A is 0.5% (v/v) of acetic acid in H_2O and mobile phase B is 100% acetonitrile. 8CldG was measured using negative ESI triple-quadrupole mass spectrometry by monitoring mass fragmentation of 300.1 → 184.00 and of the heavy isotope 302.1 → 186.00. In order to determine the presence of 8CldG, confirmation was determined by a ratio of peak area of the light isotope : heavy isotope of approximately 3 : 1.

Table 2.5: *Gradient elution of 8CldG.*

Time (min)	Flow (µL/min)	Mobile phase B (%)
0 - 1.5	200	0
1.5 – 2.0	200	0 – 6.0
2.0 – 9.0	200	15.8
9.0 – 9.1	200	15.8 – 100
9.1 – 11.0	200	100
11.0 – 11.1	250	100 – 0
11.1 – 18.9	300	0
18.9 – 19.0	200	0

2.6. Quantification of unmodified and chlorinated nucleotides using high performance liquid chromatography (HPLC)

2.6.1. Lysis of HCAEC and HCASMC

The incorporation of 8ClA into the nucleotide pool of HCAEC or HCASMC to form 8-ClATP was determined by HPLC. HCASMC or HCAEC (2×10^5 cells) were plated into 6-well cell culture plates overnight to allow attachment, after which, the cells were treated with 8ClA and Ad (16 µM) for 24 and 48 h. Treatment media was then removed and cells were washed twice with PBS prior to enzyme dissociation using trypsin-EDTA (0.025% trypsin and 0.01% EDTA in PBS) to lift cells into suspension. Cells from triplicate wells were then pooled and washed with PBS twice with centrifugation prior to removal of PBS and cell lysis using 500 µL of H_2O.

2.6.2. Extraction of the nucleotide pool

A 10 µL aliquot of each sample was removed for protein quantification by a BCA assay to normalise each sample to protein concentration. 500 µL of 0.8 M perchloric acid was added to the remaining sample followed by centrifugation at 400 × *g* for 5 min. The supernatant was kept and transferred to a separate tube. This process was then repeated with 500 µL of 0.4 M perchloric acid added to the pellet. Supernatants were then combined and neutralised to pH 7 using 10 M potassium hydroxide. Samples were centrifuged at 400 × *g* for 5 min in order to remove any precipitate. The supernatant was then transferred into 0.22 µm spin filter columns and centrifuged at 16 000 × *g* for 10 min prior to storage at – 20 ˚C until analysis using HPLC.

2.6.3. Detection of chlorinated nucleotides

Nucleotides were detected using a Shimadzu HPLC system coupled with a Shimadzu SPD-M20A PDA detector set at a wavelength 254 nm. Separation was achieved using a ZORBAX SAX HPLC column (5 µm pore size, 4.6 x 250 mm) column maintained at 30 ˚C. A 50 µL injection of each sample was made and eluted at a flow rate of 1.5 mL/min. A gradient elution was performed using an exponential curve with an initial mobile phase composition of 60% 0.005 M $NH_4H_2PO_4$ (pH 2.8) and 40% 0.75 M $NH_4H_2PO_4$ (pH 3.6) to a final mobile phase composition of 100% 0.75 M $NH_4H_2PO_4$ (pH 3.6) over 50 min. The final mobile phase composition was then maintained for 5 min prior to the composition being returned to initial mobile phase composition with a 5 min hold at 60% 0.005 M $NH_4H_2PO_4$ (pH 2.8) and 40% 0.75 M $NH_4H_2PO_4$ (pH 3.6) before injection of the next sample.

2.6.4. Standard curves and quantification of parent and chlorinated nucleotides

Standard curves were prepared for each nucleotide, ATP, CTP, GTP, UTP and 8-ClATP, ranging from 0 – 20 µM with each compound diluted in H_2O. Each standard solution was filtered through a 0.22 µm centrifugal filter as per the cell sample procedure described above, followed by analysis by HPLC. A mixed standard was made by combining equal volumes of each nucleotide and injections of 10, 20, 30, 40 and 50 µL were separated by HPLC. Concentrations of each nucleotide in the cell samples was determined by extrapolating from the standard curve followed by normalisation to protein concentration, with values reported in nmol/mg protein.

2.7. Cellular assays

2.7.1. Metabolic activity by PrestoBlue Cell Viability Reagent

The metabolic activity of treated HCAEC and HCASMC was assessed using the PrestoBlue Cell Viability Reagent (ThermoFisher Scientific) which measures metabolic activity, following the manufacturer's protocol. HCASMC or HCAEC (1×10^4 cells) were plated into a 96-well plate and allowed to adhere overnight in a humidified environment maintained at 37 ˚C with 5% CO_2. Cells were then treated with chlorinated nucleosides, 8ClA, 8ClG, 5ClC, 8CldA, 8CldG and 5CldC (4, 8 and 16 μM) diluted in MesoEndo cell culture media (HCAEC) or smooth muscle cell growth media (HCASMC) for 24, 48 and 72 h. 2 h prior to the end of the incubation period, 22 μL of PrestoBlue reagent was added to each well and reincubated at 37˚C. Fluorescence was then determined by plate reader with excitation and emission at wavelengths 560 and 590 nm, respectively. The results were normalised to the non-treated control in each case.

2.7.2. Proliferation assay

The proliferation of HCASMC was determined after treatment by staining with trypan blue to exclude dead cells and cell counting using a haemocytometer. HCASMC (10^5 cells) were plated into 12-well plates and allowed to incubate overnight at 37˚C with 5 % CO_2. Cells were then treated with 8ClA, 5ClC, 8CldG and 5CldC (16 μM) for 24, 48, 72 and 96 h. After each incubation time, cells were de-adhered from the plate using trypsin-EDTA (0.025% trypsin and 0.01% EDTA in PBS) prior to cell counting using a haemocytometer with trypan blue staining to exclude non-viable cells. Total cell number was then calculated for each sample in triplicate.

2.7.3. ATP assay

The ATP concentration in cells was determined in experiments with 8ClA and Ad with the ATPlite Luminescence assay system (Perkin Elmer). HCAEC or HCASMC (10^4 cells) were seeded into black 96-well plates overnight before treatment with 8ClA or Ad (8 µM) for 24 and 48 h. Concentrations were then determined as outlined in the manufacturer's manual. Briefly, a standard curve was made ranging from 0 – 20 µM ATP in cell culture medium. Mammalian cell lysis solution (50 µL) was then added into each well including standard curve samples. The plate was placed onto an orbital shaker for 5 min, after which, 50 µL of substrate (Luciferase/Luciferin) was added to each well. The plate was placed on an orbital shaker for a further 5 min, followed by dark adaption for 10 min. A measure of luminescence at 570 nm was then taken using the SpectraMax L microplate luminometer.

2.7.4. BCA assay

Protein concentration was determined in cell lysates using the BCA assay. A standard curve was made using bovine serum albumin (BSA) at concentrations from 0 – 2 mg/mL diluted in H_2O. Standards and samples (10 µL) were pipetted into a 96-well plate in triplicate prior to the addition of 190 µL of BCA reagent (1 : 50 dilution of 5% $CuSO_4$ (w/v) in BCA Reagent A (2.5 mM sodium bicinchoninate, 189 mM sodium carbonate, 8.25 mM sodium tartrate, 100 mM sodium hydroxide and 113 mM sodium bicarbonate, pH 11.25)). The plate was then incubated at 60˚C for 30 min followed by measurement of absorbance at 562 nm using a SpectraMax M2e plate reader.

2.7.5. GAPDH activity assay

The activity of GAPDH was determined by monitoring the formation of NADH measured by the increase in absorbance at 340 nm. After treatment with 8ClA and Ad (8 µM), HCAEC (10^5 cells) were washed twice with PBS prior to lysis using Milli-Q H_2O. Lysates were then added to 20 mM NAD^+ dissolved in a buffer of 45 mM sodium pyrophosphate / 60 mM sodium phosphate (pH 7.4). Glyceraldehyde 3-phosphate (180 µM) was then added to each sample immediately prior to analysis. The formation of NADH was monitored using SpectraMax M2e Microplate Reader (Molecular Devices) at an absorbance of 340 nm, over time at 37˚C. The activity of GAPDH was normalised to protein as determined using the BCA assay.

2.7.6. Glucose uptake assay

Glucose uptake was assessed using the Glucose Uptake Cell-Based Assay Kit (Cayman Chemical). HCAEC (1×10^4 cells) were treated with 8ClA (8 µM) and Ad (8 µM) for 48 h, after which the treatment media was aspirated and replaced with glucose-free HBSS, with or without apigenin (50 µM) for 1 h. 2- 2-deoxy-2-[(7-nitro-2,1,3-benzoxadiazol-4-yl)-amino]-D-glucose (2-NBDG; 250 µM), a fluorescent analogue of glucose, was then incubated with each sample before the supernatant was replaced with the Cell-based assay buffer. The fluorescence present within the cells was imaged using a FITC filter on an Olympus Bx43 microscope. The change in fluorescence was then detected at an excitation and emission of 485 and 535 nm, respectively, using a SpectraMax M2e plate Reader.

2.7.7. Seahorse assay

The Seahorse XF Analyser was used in order to determine any alterations to ATP production by oxidative phosphorylation or glycolysis. Mitochondrial respiration was assessed in HCAEC that were exposed to 8ClA or Ad by determining the oxygen consumption rate (OCR). OCR was measured using a Seahorse XF24 Extracellular flux analyser and the Cell Mito Stress Test Kit (Agilent). HCAEC were plated in a Seahorse XF24 cell culture microplate (3.2×10^4 cells) and allowed to adhere to the plate for 1 h. After 1 h, the supernatant was gently aspirated before the addition of 8ClA or Ad (8 µM) for 48 h. HCAEC were then washed with Seahorse XF DMEM supplemented with 20 mM glucose, 40 µM L-glutamine and 80 µM sodium pyruvate. The plate was incubated at 37˚C while OCR was measured before and after injection of multiple inhibitors; oligomycin (1.7 µM), carbonyl cyanide-p-trifluoromethoxyphenylhydrazone (FCCP, 0.7 µM) and rotenone / antimycin A (0.5 µM). The plate was allowed to equilibrate in the XF analyser for 12 min. After equilibration, the plate was mixed for 3 min and OCR rate was measured. This was repeated before and after each injection of each inhibitor. Once completed, each sample was washed twice with PBS, then lysed using 25 µL of RIPA buffer (20 mM Tris-HCl (pH 7.5), 150 mM NaCl, 1 mM Na_2EDTA, 1 mM EGTA, 1% NP-40, 1% sodium deoxycholate, 2.5 mM sodium pyrophosphate, 1 mM b-glycerophosphate, 1 mM Na_3VO_4, 1 µg/ml leupeptin) in order to perform the DC protein assay (Section 2.7.8) for protein normalisation. From the OCR obtained, multiple measures of mitochondrial respiration were calculated (see Figure 2.1).

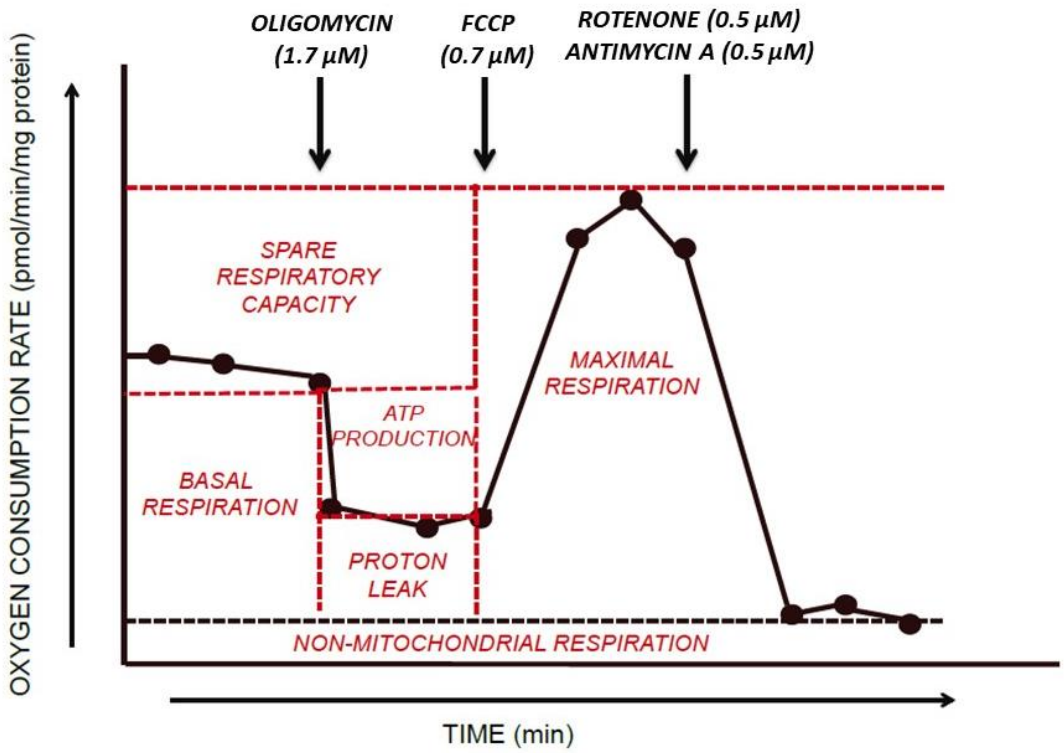

Figure 2.1: *Measures of mitochondrial respiration using a Seahorse Analyser (modified from [273]).*

The Mito-stress test uses the Seahorse XF24 Analyser in order to determine measurements of mitochondrial respiration. Initially, the basal respiration was determined by measuring oxygen consumption rate (OCR). Oligomycin (1.7 µM) was then added into each sample and the OCR was recorded in order to determine the proton leak. From this, ATP production was calculated as the difference in OCR between basal respiration and proton leak. An injection of FCCP (0. 7 µM) was then made and the recorded OCR was representative of maximal respiration. The spare respiratory capacity was then determined from the difference in OCR between maximal and basal respiration. Both rotenone (0.5 µM) and antimycin A (0.5 µM) was injected in order to stop mitochondrial respiration, where the corresponding OCR showed non-mitochondrial respiration.

The glycolytic ability of HCAEC (3.2×10^4 cells) that were exposed to 8ClA or Ad (8 µM) for 48 h was determined by measuring extracellular acidification rate (ECAR). Following treatment, HCAEC were washed using Seahorse XF DMEM supplemented with 40 µM L-glutamine and incubated at 37˚C. ECAR was then measured prior and following an injection of 10 mM glucose. Results were normalised to protein concentration using the DC protein assay (Section 2.7.8).

2.7.8. DC protein assay

The concentration of protein in samples from the Seahorse assay was determined using the DC protein assay kit (Bio-Rad). After analysis of OCR and ECAR using the Seahorse XF24 Extracellular flux analyser, the supernatant was removed, and each sample was gently washed twice with HBSS. To each sample, 25 µL of RIPA buffer was added to each well and the cells were gently scraped into solution. The resulting solutions were stored at – 20˚C until analysis. Standards were prepared using BSA to concentrations of 0 µg to 50 µg diluted in RIPA buffer to a total volume of 25 µL. Solution S (100 µL) was added to Solution A (5 mL) and 125 µL of the mixture was added to each standard or sample. Solution B (1 mL) was then added to each standard or sample and pipetted to mix prior to incubation at room temperature for 15 min. Samples and standard were then transferred to a 96-well plate and absorbance was read at 750 nm on a SpectraMax M2e plate reader.

2.7.9. Lactate assay

The extent of glycolysis was confirmed using the glycolysis cell-based assay kit (Cayman Chemical) to determine the concentrations of lactate released into the extracellular environment, following the manufacturer's protocol. HCAEC (10^4 cells) were plated into 96-well culture plates, followed by treatment with 8ClA or Ad (8 µM) for 48 h. After treatment, the plate was then centrifuged at 220 × *g* for 5 min. 10 µL of supernatant was then transferred into a new 96-well plate containing 90 µL of assay buffer. Reaction solution (100 µL) was then added into each well in order to start the reaction. This process was repeated with standard solutions of L-lactate ranging from 0 - 10 mM with 10 µL added to standard wells instead of supernatant in order to produce a standard

curve. Following addition of reaction solution to each well, the plate was incubated at room temperature for 30 min on an orbital shaker. The absorbance was then determined at 490 nm using a SpectraMax M2e plate reader. Concentrations of each sample was then determined by extrapolation from the standard curve.

2.7.10. MMP activity assay

The activity of MMP2 and MMP9 was determined by gelatin zymography, modified from a method published by Frankowski, et al. [274]. Gels for zymography were prepared by casting 8% separating gels (0.08% acrylamide, 0.1% SDS, 0.1% APS and 0.01% TEMED in 0.375 M Tris, pH 8.8) containing 0.15% gelatin with a 6% stacking gel (0.06% acrylamide, 0.1% sodium dodecyl sulfate (SDS), 0.1% ammonium persulfate (APS) and 0.01% tetramethylethylenediamine (TEMED) in 0.125 M Tris, pH 6.8). Cell media (25 µL) was added to each well with 5 µL of loading buffer (0.313 M Tris-HCl, pH 6.8, 10% SDS, 50% glycerol and 0.05% bromophenol blue) and the chamber was filled with SDS-PAGE running buffer (3% Tris-base, 1.4% glycine and 1% SDS (w/v) in H_2O). The gels were then run at 110 V for 60 min or until the dye front reached the base of the gel.

After gel electrophoresis, the gels were activated and stained using Coomassie brilliant blue. The gel was removed from the gel plates and washed with gel washing buffer (2.5% Triton X-100 in water) for 15 min on an orbital shaker. The gel was then washed twice more with gel washing buffer for 15 min each time. The gel was then incubated in development buffer (50 mM Tris, pH 7.4, 10 mM $CaCl_2$, 0.02% NaN_3 in water) for 42 h at 37˚C.

Once the gel had been developed, it was then stained using Coomassie blue solution (12.5% (w/v) Coomassie brilliant blue R-250 solution in 1% acetic acid and 45% ethanol) for 1 h at room temperature on an orbital shaker. The staining solution was removed and replaced with a solution of 25% ethanol and 10% acetic acid in water for 15 to 30 min, until there were visible white bands on the gel. After this, the solution was discarded and replaced with a solution of 5% ethanol and 7.5% acetic acid in H_2O to further destain for 3 h or until clear white bands were observed against the blue gel background. After destaining, the gels were placed in deionised water and washed on an orbital shaker for 30 min. The gels were then imaged on a document scanner and density of the white band was determined using ImageJ software.

2.8. Flow cytometry

2.8.1. Fluo-4AM – Calcium accumulation in the cytosol

Fluo-4AM is a fluorescent stain that binds to cytosolic calcium causing an increase in fluorescence at 488 nm. The accumulation of calcium within the cytosol was measured using Fluo-4AM (Invitrogen) and flow cytometry. Cultured HCAEC or HCASMC (2×10^5 cells) were treated with 8ClA, Ad, 5CldC or dC (8 µM) in 6-well plates for 24 h and washed twice with calcium free HBSS. Cells were then stained with 5 µM Fluo-4AM in calcium-free HBSS for 45 min in the dark at 37˚C prior to gentle scraping to lift the cells into suspension. Samples were then stored on ice until analysis using a FACSverse flow cytometer (BD Biosciences). Samples were gated side scatter versus forward scatter where cell debris and doublet cells were excluded to give Population 1. A histogram of

Population 1 was plotted as Count versus FITC-fluorescence where a right shift in the histogram corresponds to increased calcium accumulation. Percentage Fluo-4AM binding for each treatment was compared to the control using the geometric mean of the FITC fluorescence area.

2.8.2. Annexin V/propidium iodide – Cell death by apoptosis and necrosis

Annexin V and propidium iodide are used in conjunction with flow cytometry in order to determine the extent of cell death by apoptosis and necrosis, respectively. Following apoptosis, phosphatidylserine is externalised on the cell membrane, which binds to Annexin V, whereas propidium iodide chelates DNA and is taken up by necrotic cells. HCAEC or HCASMC (2×10^5 cells) were treated with 8ClA, Ad, 5CldC or dC (8 µM) prior to washing twice with PBS. Cells were then lifted into suspension using trypsin-EDTA (0.025% trypsin and 0.01% EDTA in PBS) before washing twice with PBS. Samples were then resuspended in Annexin V binding buffer (10 mM HEPES, 140 mM NaCl, 2.5 mM $CaCl_2$, pH 7.4) with 5 µL of Annexin V and propidium iodide stains. Each sample was then vortexed and incubated in the dark at 37˚C for 15 min before being placed on ice until analysis using a FACSverse flow cytometer (BD Biosciences). Samples were gated as side scatter versus forward scatter where Population 1 was drawn to exclude dead cells and doublet cells (Figure 2.2A). A plot of propidium iodide versus Annexin V was quadrant gated to show live population (black), propidium iodide positive cells (red) and Annexin V positive cells (green) (Figure 2.2B).

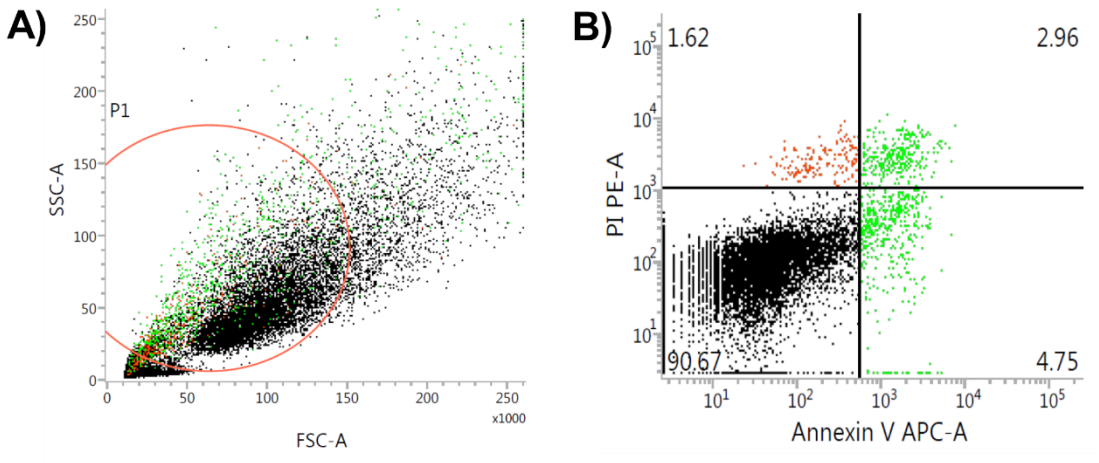

Figure 2.2: *Representative population and quadrant gating for necrosis and apoptosis. A) Gating of the population of cells for Annexin V and propidium iodide staining with flow cytometry to give Population 1, excluding doublet and dead cells. B) Representative quadrant gating of propidium iodide versus Annexin V fluorescence of control cells in Population 1 to show live (black), necrotic (red) and apoptotic (green) cells. The percentage of cell population in each quadrant was determined using BD FACSVerse Software.*

2.8.3. KI-67 – Cell proliferation

2.8.3.1. Cell treatment and ethanol fixation

The population of proliferating cells was determined by analysing the expression of KI-67, a protein expressed in all active phases of the cell cycle but absent in resting cells [275]. HCASMC (2×10^5 cells) were treated with 8ClA, 5CldC, Ad and dC prior to washing twice with PBS. Cells were then lifted into suspension using trypsin-EDTA (0.025% trypsin and 0.01% EDTA in PBS) and washed twice with PBS. Ice-cold ethanol (70 %) was added dropwise into the cell pellet whilst vortexing, to give a total volume of 5 mL. Each sample was then incubated at – 20˚C overnight prior to staining with KI-67.

2.8.3.2. Sample staining with KI-67

After incubation at – 20˚C overnight, each sample was centrifuged in order to form a cell pellet. The ethanol fixative was then aspirated, and cells were washed with 10 mL of PBS

supplemented with 1% FBS. Cells were again pelleted by centrifugation prior to a second wash, aspirating the supernatant and addition 500 µL of PBS with 1% FBS. KI-67 stain (5 µL; 0.06 µg) was then added to each sample and incubated at room temperature for 30 min in the dark prior to analysis using a FACSverse flow cytometer (BD Biosciences). Samples were gated side scatter versus forward scatter where cell debris and doublet cells were excluded to give Population 1. A histogram of Population 1 was plotted as Count versus APC-fluorescence where a right shift in the histogram corresponds to increased KI-67 binding. Percentage KI-67 binding for each treatment was compared to the control using the geometric mean of the APC fluorescence area.

2.8.4. JC-1 – Mitochondrial membrane depolarisation

The JC-1 stain is taken up into the mitochondria of cells where it forms aggregates, producing red fluorescence. Alterations to the mitochondrial membrane potential reflecting increased mitochondrial membrane permeability result in leakage of JC-1 into the cytosol where green fluorescence is exhibited [276]. Therefore, the extent of mitochondrial dysfunction can be determined by calculating the red : green fluorescence ratio. HCASMC (2×10^5 cells) were treated with 8ClA, 5CldC, Ad or dC (8 µM) prior to washing twice with PBS. Cells were lifted into suspension using trypsin (0.025% trypsin and 0.01% EDTA in PBS) followed by centrifugation at 220 × *g* for 5 min. The cell pellet was washed with PBS followed by centrifugation at 220 × *g* for 5 min. The supernatant was removed and PBS (500 µL) was then added into each well with 5 µL of JC-1 stain followed by incubation in the dark for 30 min. In the positive control samples, 1 µL of 50 mM CCCP was added to decouple the mitochondria in addition to the stain. Samples were then analysed using a FACSverse flow cytometer with cells plotted on a side scatter

vs forward scatter plot. Population 1 was then drawn to exclude dead and doublet cells (Figure 2.3A). Results were reported as a ratio of red : green fluorescence in population 1 (Figure 2.3B) for triplicate samples.

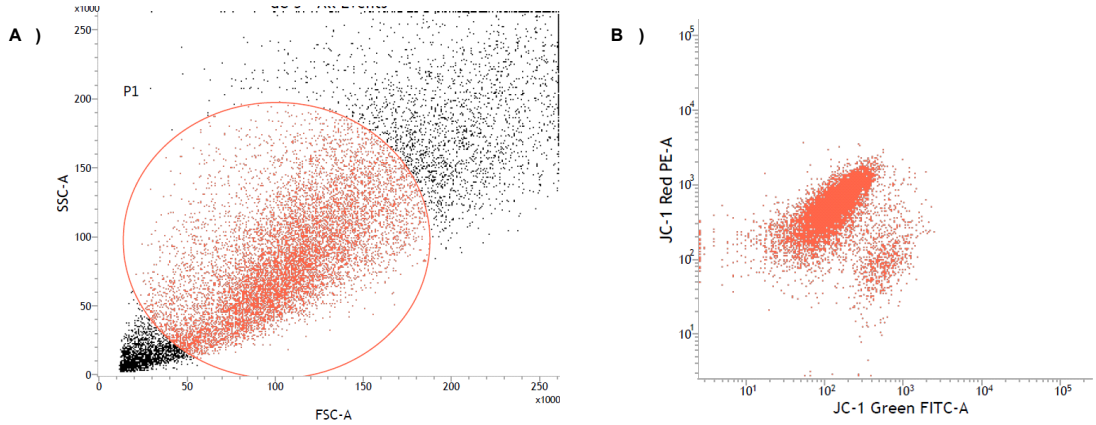

Figure 2.3: *Representative population gating for JC-1 staining to determine mitochondrial membrane depolarisation.*
A) Gating of the population of cells for JC-1 staining with flow cytometry to give Population 1. B) Representative plot of JC-1 red fluorescence vs JC-1 green fluorescence of population 1. The ratio of red : green fluorescence was determined using FACSVerse software.

2.9. Gene expression by quantitative real time polymerase chain reaction

2.9.1. Cell lysis and extraction of RNA

Cellular RNA was extracted using the ReliaPrep RNA Cell Miniprep System (Promega) as stated in the manufacturer's manual. Cells were washed twice with PBS prior to cell lysis using the BL + TG buffer supplied and vortexed for 30 s. An aliquot of isopropanol was added and again, the plate was vortexed. These samples were then subjected to RNA extraction or stored at – 80˚C to be extracted later.

For RNA extraction, the cell lysates were transferred to the extraction columns and centrifuged at 14 000 × *g* for 30 s. Samples were washed using the RNA wash solution

with centrifugation at 14 000 × *g* for 30 s. The DNase I incubation mix was then added to each column and allowed to incubate at room temperature for 1 h. After incubation with DNase I, column wash solution was added to each sample and the columns were centrifuged at 14 000 × *g* for 30 s. Columns were then washed a further two times using the RNA wash solution, where the first wash was centrifuged at 14 000 × *g* for 30 s, and the second wash centrifuged at 16 000 × *g* for 2 min. RNase-free water was added to each sample and left at room temperature for 5 min prior to centrifugation to elute RNA at 14 000 × *g* for 1 min.

2.9.2. RNA quantification

RNA concentration was then quantified using a Nanodrop Spectrophotometer (Thermo Scientific). A blank measurement was determined using the spectrophotometer by determining the absorbance of nuclease-free H_2O. Following this, 2 µL of each RNA sample was loaded onto the lower pedestal, with measurement of absorbance made at wavelengths ranging from 220 to 350 nm. This was repeated for each RNA sample with the lower pedestal cleaned with a lint-free tissue in between each use. RNA concentration was then determined using the Beer-Lambert equation based on the absorbance of the sample at 260 nm. The purity of the RNA sample was determined by using the ratio of absorbances measured at 260 and 280 nm (260/280 ratio). RNA samples were taken as pure with a 260/280 ratio between 1.8 and 2.0. Samples with ratios outside of these values were not used to synthesise cDNA.

2.9.3. cDNA synthesis

After RNA concentration was determined, concentrations were normalised to 500 ng per reaction. Reverse transcription to produce cDNA was performed using the iScript cDNA synthesis kit. To each sample, 2.5 µL of iScript reverse transcriptase and 10 µL of 5 × iScript reaction mix was added. The total volume of each reaction was then corrected to 50 µL using nuclease-free H_2O. Samples were thermocycled at 25°C for 5 min, held at 42°C for 30 min, 85°C for 5 min, finishing with an infinite hold at 4°C.

2.9.4. Quantitative real time polymerase chain reaction (qPCR)

After thermocycling, cDNA was diluted by a factor of 3 and qPCR was performed using iQ SYBR Green Supermix (BioRad) with primer sequences outlined in (Table 2.6). Samples were plated into a 384-well plate with each well containing 5 µL of iQ SYBR Green Supermix, 0.4 µL of forward primer (20 µM), 0.4 µL of reverse primer (20 µM), 1.2 µL of nuclease-free water and 3 µL of diluted cDNA sample. The PCR plate was heated to 95°C for 3 min, annealed at 60°C for 30 s, extended at 72°C for a further 30 s, over 40 cycles prior to denaturation for 2 min at 95°C. A dissociation curve was plotted every 0.5°C between 65 and 95°C at the end of each cycle. Samples were then compared to a standard curve from 1 : 10 dilutions of cDNA for each primer pair before normalisation to two housekeeping genes, RPL13 and 18S ribosomal RNA.

Table 2.6: *qPCR forward and reverse primer sequences.*

Gene	Forward sequence	Reverse sequence
18S	GAGGATGAGGTGGAACGTGT	TCTTCAGTCGCTCCAGGTCT
ATF4	TGGTCAGTCCCTCCAACAAC	TCCATTTTCTCCAACATCCAA
Calponin	CTGACTCCCGAGTACCCAGA	TGCCATGCAGGGAGAGGG
CHOP	GGAGCTGGAAGCCTGGTATG	GCAGGGTCAAGAGTGGTGAAG
CX43	TCTTCATGCTGGTGGTGTCC	ACCACTGGTCGCATGGTAAG
Decorin	TGCTTTCTGTTGCAGGTTGG	GTGGGGGTCTTGCTTTTTGG
Desmin	CAACAGCGACATAGCCCATC	AAAGCGTAGGCCTCAGGTCA
GADD34	TCCTCTGGCAATCCCCCATA	TGGTTTTCAGCCCCAGTGTT
GCLC	TCCAGGTGACATTCCAAGCC	GAAATCACTCCCCAGCGACA
GPx4	AGACCCGAAAATCCAGCGTG	CAAGCCCCTACGCAGAAAGA
GS	CCCTAGCCGGTTTGTGCTAA	CCAAAGATGCCCAGCTCTGA
HO-1	TTCAAGCAGCTCTACCGCTC	GGGGCAGAATCTTGCACTTT
ICAM	GGCTGGAGCTGTTTGAGAAC	ACTGTGGGGTTCAACCTCTG
MMP2	GCTACGATGGAGGCGCTAAT	TCAGGTATTGCACTGCCAACT
MMP9	TTCAGGGAGACGCCCATTTC	TGGGTGTAGAGTCTCTCGCT
NQO1	TCCACAATAGCTGACGGCTG	TGTCAAGCCAGTCACCAAGG
Olfml3	GGACACACCATGTCCCAGAG	GTTATAGCGGAGGCTGGCAT
OPN	AGGCATCACCTGTGCCATAC	GGCCACAGCATCTGGGTATT
RPL13	AGATGGCGGAGGTGCAG	GTTGATGCCTTCACAGCGTA
S100A4	TCTTGGTTTGATCCTGACTGCT	ACTTGTCACCCTCTTTGCCC
SOD1	AAAGATGGTGTGGCCGATGT	CAAGCCAAACGACTTCCAGC

SOD2	TCTGTTGGTGTCCAAGGCTC	ACAGTAGAGCATCTCTCCCAA
sXBP1	GCTGAGTCCGCAGCAGGT	GTCCAGAATGCCCAACAGG
Trx	GTGAAGTCAAATGCACGCCA	GCAGATGGCAACTGGTTATGT
TXNIP	TCGGCTTTGAGCTTCCTCAG	AGCAGACACAGGTGCCATTA
VCAM	CAGACAGGAAGTCCCTGGAA	TTCTTGCAGCTTTGTGGATG

2.10. Protein expression

2.10.1. Lysis of whole cell samples

Protein expression was determined by Western blot in HCAEC (2×10^5 cells) after treatment in 6-well plates with 8ClA or Ad (16 µM). For whole cell experiments, treated cells were lysed using 100 µL of cell lytic reagent (Sigma Aldrich) with 1% (v/v) protease inhibitor cocktail (Sigma Aldrich). The concentration of protein was determined in each sample by performing a BCA assay, and samples were normalised to contain 5 µg protein.

2.10.2. Nuclear and cytoplasmic extraction

For nuclear translocation studies, cytoplasmic and nuclear fractions were isolated using the NE-PER Nuclear and Cytoplasmic extraction kit (ThermoFisher Scientific) as per manufacturer's instructions. HCAEC (5×10^5 cells) were treated with 8ClA or Ad (8 µM) in T25 cm^2 cell culture flasks. Cells were washed twice with PBS then lifted into suspension using trypsin-EDTA (0.025% trypsin and 0.01% EDTA in PBS). Each sample was centrifuged at 220 × *g* to pellet cells prior to lysis with 200 µL of ice-cold cytoplasmic

extraction reagent (CER) I reagent. Each sample was then vortexed for 15 s to resuspend the pellet and incubated on ice for 10 min. 11 µL of ice-cold CER II reagent was added to each sample before vortexing for 5 s and placing on ice for 1 min. The sample was vortexed again for 5 s, then centrifuged at 16 000 × *g* for 5 min at 4˚C. The supernatant (cytoplasmic fraction) was transferred into a clean microcentrifuge tube and placed on ice while the pellet was resuspended in 100 µL of nuclear extraction reagent (NER) reagent. The tube containing NER reagent was then vortexed for 15 s and placed on ice for 10 min with this process repeated for a total of 40 min. Following this, each tube was centrifuged at 16 000 × *g* for 10 min at 4˚C and the supernatant (nuclear fraction) was transferred to a clean microcentrifuge tube, and placed on ice. The concentration of protein was determined using a BCA assay and normalised to contain 10 µg protein for the cytosolic fraction and 5 µg for nuclear fractions.

2.10.3. Reducing protein samples and gel electrophoresis

Protein samples were reduced using the Nu-PAGE system. Each sample was normalised to the appropriate concentration of protein (as stated Sections 2.10.1 and 2.10.2) in a total volume of 16.25 µL in H_2O. NuPAGE LDS sample buffer (6.25 µL) and NuPAGE reducing agent (2.5 µL) was then added into each sample and mixed by pipetting. Samples were heated at 70˚C for 10 min for the reducing reaction to occur and centrifuged at 10 000 × *g* for 5 min.

The supernatant of reduced samples was loaded onto 10-well 4-12% Bis-tris gels (Life Technologies) with one well containing Precision Plus Protein Kaleidoscope molecular mass marker (Bio-Rad) followed by electrophoresis at 200 V for 35 min. Gels were then

transferred onto polyvinylidene fluoride (PVDF) membranes using the iBlot 2 transfer machine (ThermoFisher Scientific) with cycling at 20 V for 7 min. The PVDF membrane was blocked in 5% (w/v) BSA in Tris-buffered saline (20 mM Tris-HCl, pH 7.4, 153 mM NaCl) with 0.1% (v/v) Tween-20 (TBST) overnight.

2.10.4. Protein probing, imaging and quantification

The blocking buffer was removed and replaced with a solution containing the primary antibody. For the determination of the protein expression of TXNIP, a 1 : 1000 dilution of rabbit anti-TXNIP primary antibody in 5% (w/v) BSA in TBST was added to the PVDF membrane containing whole cell lysates. The Western blot was then incubated overnight at 4˚C on a plate rocker. Following incubation with the primary antibody, the membrane was washed 3 times for 5 min each time with TBST. A 1 : 2000 dilution of anti-rabbit IgG in 5% (w/v) BSA in TBST was added to the membrane and incubated at room temperature on a plate rocker for 2 h. The membrane was washed 3 times for 5 min with TBST prior to imaging and quantification. The membrane was then incubated with Western lighting – plus ECL (Perkin Elmer), followed by imaging using the ChemiDoc imaging system (Bio-Rad).

When determining the nuclear translocation of ATF4, the blocking buffer was removed after overnight incubation. A 1 : 1000 dilution of rabbit anti-ATF4 primary antibody in 5% (w/v) BSA in TBST was added to the PVDF membrane for 2 h at room temperature on a plate rocker. The membrane was washed 3 times for 5 min with TBST. A 1 : 2000 dilution of anti-rabbit IgG in 5% (w/v) BSA in TBST was added to the membrane and incubated at room temperature on a plate rocker for 1 h. The membrane was washed

for 5 min with TBST prior to the addition of Western lighting – plus ECL (Perkin Elmer) to achieve chemiluminescence. Imaging of the membrane was performed using a ChemiDoc imaging system (Bio-Rad).

After imaging, each membrane was stripped of the antibodies by incubation with Restore Western blot stripping buffer (Thermo Scientific) for 15 min on a plate rocker. The membranes were then washed with TBST for 5 min on a plate rocker prior to blocking the membrane overnight at 4˚C on a plate rocker with 5% (w/v) BSA in TBST. The protein loading was determined by addition of a 1 : 1000 dilution of mouse anti-β-actin primary antibody in 5% (w/v) BSA in TBST to the PVDF membrane and incubated at room temperature on a plate rocker for 1 h. The membrane was washed 3 times for 5 min with TBST, then a 1 : 2000 dilution of anti-mouse IgG in 5% (w/v) BSA in TBST (20 mM Tris-HCl, pH 7.4, 153 mM NaCl) with 0.1% (v/v) Tween-20) was added to the membrane and incubated at room temperature on a plate rocker for 1 h. After incubation, the blot was washed for 5 min with TBST and imaged with Western lighting – plus ECL (Perkin Elmer) and the ChemiDoc imaging system (Bio-Rad).

For studies determining the nuclear translocation studies, staining with Ponceau S was used as the loading control. Ponceau S staining solution (0.1% (w/v) in 5% acetic acid) was added to the membrane and incubated at room temperature on a plate rocker for 10 min. The membrane was then washed with H_2O on a plate rocker until red bands were visible against a white membrane prior to imaging using the ChemiDoc imaging system. The densitometry of protein bands was determined for each protein using ImageJ software and normalised to the β-actin or ponceau S loading control.

2.11. Statistical analysis

GraphPad Prism 7.0 (GraphPad Software) was used in order to plot all graphs in this thesis. Statistical analysis was also performed using this software to determine significance to $p < 0.05$ using one-way or two-way analysis of variance (ANOVA) with Dunnett's post-hoc multiple comparisons test between treated and non-treated control samples. Experimental results were plotted at mean ± standard error of the mean (SEM) of at least 3 biological replicates.

Chapter 3 – Effect of chlorinated nucleosides on endothelial cell function

3.1. Introduction

As described in Chapter 1, during chronic inflammation, activated leukocytes infiltrate the wall of a blood vessel propagating the development of atherosclerotic lesions and further disease progression [3]. At sites of inflammation, MPO is released, causing the formation of multiple oxidants including HOCl, which reacts readily with many biomolecules including DNA, RNA and protein, causing their oxidation and modification [104]. This oxidant causes damage to surrounding cells and tissue and is linked to the development of many disease states including atherosclerosis [126, 277]. MPO has also been shown as a risk factor for cardiovascular disease and a prognostic marker for the outcome of patients after myocardial infarction [127, 278].

The reaction of HOCl with DNA and RNA results in the formation of stable chlorinated products, including chlorinated nucleosides such as 8ClA, 8ClG, 5ClC, 8CldA, 8CldG and 5CldC [6, 18, 224, 279]. Chlorinated nucleosides have been shown to be present as biomarkers of chronic inflammation in multiple pathologies, with elevated levels seen in plasma, inflammatory fluids and urine [17, 18, 256]. Their presence has also been demonstrated in diseased tissues from multiple pathologies including atherosclerosis [16]. Though these modified nucleosides have been shown to be present in multiple pathologies, whether their presence can further propagate disease remains to be elucidated.

It has been previously established within the literature that the incorporation of chlorinated nucleosides into the DNA has mutagenic effects, implicating these compounds in the disease progression of cancer [9]. However, these properties have been used to a therapeutic advantage, as chlorinated nucleosides have also been used to kill cancer cell lines. 5CldC has previously been used in studies as a sensitising agent prior to radiotherapy, while 8ClA has been shown to be toxic to many cancer cell lines including breast cancer [270, 271], mantle cell lymphoma [272], myeloma [266, 268, 269] and chronic lymphocytic leukemia [280].

Furthermore, 8ClA has been used in clinical trials as a chemotherapeutic agent in the treatment of chronic lymphocytic leukemia and acute myeloid leukemia [261, 262]. In each of these instances, the mechanism by which 8ClA causes the death of these malignant cells is either through the depletion of ATP stores within the cell or through the inhibition anti-apoptotic proteins [269, 270, 280]. In these studies, it was demonstrated that 8ClA was phosphorylated by enzymes including adenosine kinase to the chlorinated analogue of adenosine triphosphate, 8-ClATP. Previous studies utilising 8ClA and 8Cl-cAMP, used concentrations of 10 µM [266, 271, 272, 281], which has been previously shown to be achievable levels within plasma in animal studies and clinical trials, respectively [282, 283].

More recently, a study has demonstrated that 8ClA has effects on non-malignant J774.A1 macrophage-like cells [259, 260]. Exposure of J774.A1 cells to 8ClA resulted in the incorporation of this chlorinated nucleoside into the cellular RNA [259] and into the nucleotide pool to form 8-ClATP [260]. Interestingly, although ATP synthase has been

shown to be inhibited in malignant cells, it was demonstrated that there was no significant difference in the ability to synthesise ATP in the mitochondria [260]. In J774.A1 cells, it was determined that there was activation of Nuclear factor erythroid-2-related factor 2 (Nrf2) and the increased mRNA expression of thioredoxin interacting protein (TXNIP), showing an increase in antioxidant responses. Though the depletion of ATP is not observed in J774.A1 cells exposed to 8ClA, an apoptotic mechanism of cell death was demonstrated as in malignant cell types [260].

The endoplasmic reticulum (ER) of cells plays a vital role in the synthesis, modification and folding for various proteins. There are many alterations within homeostasis, which can induce a state of ER stress including significant alterations in Ca^{2+} stores, oxidative stress, hypoxia and the activation of inflammatory pathways [284]. When ER stress is sustained, the unfolded protein response (UPR) becomes activated. The UPR is a major pathway deciding cell fate within these conditions, signalling for either cell survival or cell death by apoptosis [284]. This pathway has been shown to be activated under the inflammatory environment within an atherosclerotic lesion, with previous studies demonstrating that UPR pathway activation can cause endothelial damage and plaque instability in the progression of atherosclerotic disease [285, 286]. Previous studies have also shown that activation of the UPR, causes alterations within cellular homeostasis through alterations in antioxidant responses and other signalling pathways relating to stress within cells [287].

This current Chapter examined the incorporation of chlorinated nucleosides, 8Cl(d)A, 8Cl(d)G and 5Cl(d)C into the DNA and RNA of HCAEC and their effect on the metabolic

activity and cell survival. Previous studies have demonstrated that 8ClA caused significant decreases in the metabolic activity of HCAEC following exposure for 24 h and 48 h. 8ClA was also shown to incorporate into the nucleotide pool of HCAEC to form 8-ClATP [288]. Thus, further experiments were performed in this Chapter under comparable conditions to examine whether as a consequence, any stress related pathways are activated, which could be relevant in the context of atherosclerotic disease.

3.2. Hypothesis and aims

Previous studies demonstrated that 8ClA induced metabolic changes in HCAEC as well as incorporated into the nucleotide pool [288]. It was hypothesised that chlorinated nucleosides would incorporate into the DNA or RNA of HCAEC, promoting the development or progression of atherosclerosis. Therefore, the experiments in this chapter aimed to determine the extent of incorporation and clearance of chlorinated nucleosides from the DNA and RNA. Studies also aimed to determine the consequence of the exposure of HCAEC to chlorinated nucleosides in terms of cell function and viability.

3.3. Methods

HCAEC (Cell Applications) were cultured in MesoEndo cell culture medium (Cell Applications) under sterile conditions at 37˚C with 5% CO_2 and were obtained from a minimum of 3 separate donors. Treatments of 8ClA, 8ClG, 5ClC, 8CldA, 8CldG and 5CldC

(4, 8 and 16 µM) were made in MesoEndo cell culture medium and incubated with the cells for 2, 6, 24, 48 and 72 h, as described in Section 2.3.1.

The incorporation and clearance of chlorinated nucleosides from cellular DNA and RNA was quantified by LC-MS/MS. Firstly, DNA and RNA were isolated from chlorinated nucleoside treated HCAEC using the Bioline Isolate II DNA/RNA/Protein extraction kit (Section 2.5.1). Samples were then prepared for analysis as described in Section 2.5.2 and quantified by LC-MS/MS, as described in Section 2.5.3. The metabolic activity of HCAEC after treatment with chlorinated nucleosides was determined using PrestoBlue Cell Viability reagent, explained in Section 2.7.1.

The concentration of ATP in HCAEC treated with 8ClA was determined using the ATPlite luminescence assay system, shown in Section 2.7.3. Samples for the determination of the incorporation of 8ClA into the nucleotide pool to form 8-ClATP were prepared as outlined in Sections 2.6.1. and 2.6.2. Concentrations of nucleotides were quantified by chromatographic separation using HPLC (Section 2.6.3) and extrapolation from standard curves (Section 2.6.4). Final nucleotide concentrations were then normalised to protein concentration determined by BCA assay (Section 2.7.4).

Mitochondrial respiration in HCAEC exposed to 8ClA was determined by measuring OCR using the MitoStress Test Kit and Seahorse XF Analyser, as described in detail in Section 2.7.7. OCR was measured during sequential injections of oligomycin (1.7 µM), FCCP (0.7 µM) and rotenone / antimycin A (0.5 µM). Similarly, the effects of 8ClA on glycolysis was determined by Seahorse XF analyser by measuring ECAR before and after injection of 10 mM glucose (Section 2.7.7). The differences in OCR and ECAR were normalised to

protein concentration determined by performing the DC Protein Assay, shown in Section 2.7.8.

GAPDH activity in HCAEC treated with 8ClA was measured by monitoring the formation of NADH at an absorbance of 340 nm, as described in Section 2.7.5. GAPDH activity was normalised to the concentration of protein in each sample determined by BCA assay (Section 2.7.4) The uptake of glucose in HCAEC exposed to 8ClA was analysed using the Glucose Uptake Cell-Based Assay Kit (Section 2.7.6). After treatment, cells were exposed to 2-NBDG, with or without the positive control, apigenin. Fluorescence was then imaged using an Olympus Bx43 microscope at excitation and emission of 485 and 535 nm, respectively. The change in fluorescence was detected using a SpectraMax M2e Microplate Reader at an excitation and emission of 485 and 535 nm.

The expression of mRNA was determined for multiple genes by qPCR as described in Section 2.9. After treatment, cells were lysed and RNA was extracted using the ReliaPrep RNA Cell Miniprep System (Section 2.9.1). For each sample, the concentration of RNA was quantified (Section 2.9.2) and normalised to 500 ng sample for cDNA synthesis using the iScript cDNA synthesis kit. qPCR was then performed using iQ SYBR Green Supermix (Section 2.9.3) using forward and reverse primer sequences outlined in Table 2.6. The mRNA expression of each gene of interest was then normalised to 2 housekeeping genes, 18S ribosomal RNA and RPL13.

The protein expression of TXNIP and nuclear translocation of ATF4 in HCAEC that were exposed to 8ClA was determined using Western blot (Section 2.10). Cell samples were lysed as described in Sections 2.10.1 and 2.10.2. A BCA assay (Section 2.7.4) was

performed to normalise protein concentration prior to reducing samples using the Nu-PAGE system. Samples were then loaded onto 4-12% Bis Tris gels and separated by mass using gel electrophoresis (Section 2.10.3). Protein expression was then determined by protein probing with primary and secondary antibodies, followed by quantification using ImageJ software (Section 2.10.4).

Flow cytometry was used in order to examine calcium accumulation within the cytosol and the mechanism of cell death. After treatment with 8ClA, cell samples were prepared for calcium accumulation studies by staining with Fluo-4AM (Section 2.8.1) followed by analysis using a FACSverse flow cytometer. Cell death by apoptosis or necrosis was also determined using flow cytometry in HCAEC that were exposed to 8ClA by staining with Annexin V and propidium iodide, respectively (Section 2.8.2).

3.4. Results

3.4.1. Chlorinated nucleosides incorporate into the cellular DNA and RNA

The effects of chlorinated nucleosides on the metabolic activity and ATP stores of HCAEC have previously been determined [288]. It was shown that exposure to 8ClA caused a significant decrease in metabolic activity in HCAEC after a 24 and 48 h exposure period. 8ClA was also demonstrated to incorporate into the nucleotide pool of HCAEC to form 8-ClATP. Therefore, the current study examined whether chlorinated nucleosides incorporated into the DNA or RNA of HCAEC over a 72 h period. When HCAEC were exposed to 8ClA, 8ClG and 5ClC (16 µM), each chlorinated nucleoside was incorporated into the RNA (Figure 3.1A-C). The extent of incorporation was time and nucleoside

dependent with incorporation of 8ClA increasing over 24 h. The incorporation of 8ClA into the RNA was greater than that of both 8ClG and 5ClC (16 µM), where maximal levels were reached after 6 h of treatment (Figure 3.1A-C). Evidence for incorporation into DNA was also obtained in HCAEC exposed to the deoxyribose chlorinated nucleosides, 8CldA, 8CldG and 5CldC (16 µM) (Figure 3.1D-F). The maximal incorporation of chlorinated deoxyribose nucleosides was reached at 48 h, with the highest extent of incorporation of 8CldG compared to 8CldA and 5CldC. In each of these experiments, there were no chlorinated nucleosides detected in controls, which had no treatment, nor were there alterations in parent nucleosides with treatment. There was also no evidence for the incorporation of chlorinated deoxyribose nucleosides into RNA or ribose nucleosides into DNA.

Further experiments were performed to examine the stability of chlorinated nucleosides within the RNA and DNA and the ability of the HCAEC to clear chlorinated nucleosides from the DNA or RNA once the exogenous source had been removed. HCAEC were incubated in the presence of each chlorinated nucleoside for 24 h, after which, the cells were washed and re-incubated in complete media in the absence of chlorinated nucleoside for a further 48 h. In most cases, there was no significant change in the concentrations of chlorinated nucleoside incorporated in the DNA or RNA after washing and re-incubation for 48 h when compared to incubation with treatment for 24 – 72 h. The exception to this was evident when cells were treated with 8ClA, where a decrease in 8ClA within the RNA was observed after re-incubation when compared to 24 h treatment. When HCAEC are exposed to 8CldG, a decrease was shown when compared

to 48 and 72 h treatment. A non-significant decrease in incorporation was also observed when cells were exposed to 5ClC and 5CldC.

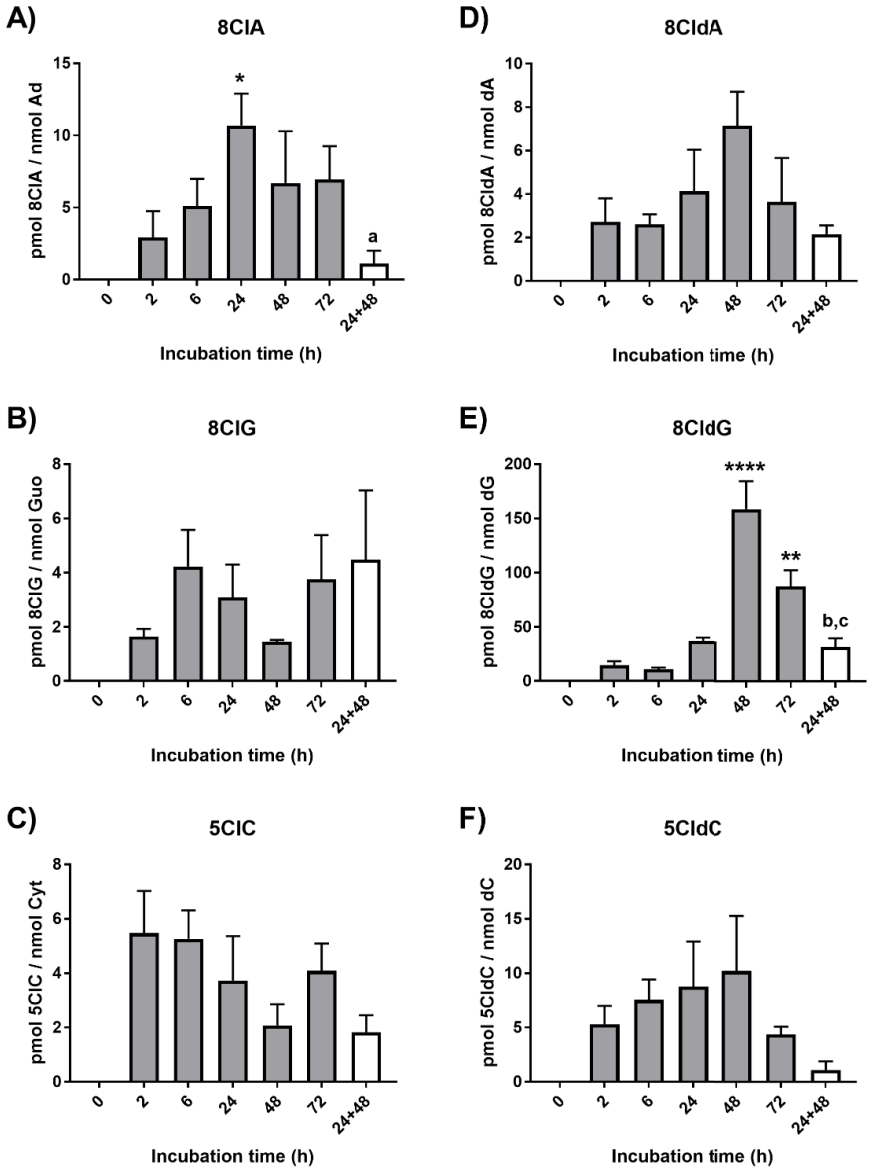

Figure 3.1: *Chlorinated nucleosides incorporate into the DNA and RNA of HCAEC.*
*HCAEC (1 × 10^6 cells) were treated with 16 µM 8ClA (A), 8ClG (B), 5ClC (C), 8CldA (D), 8CldG (E) or 5CldC (F) for a period of 2 – 72 h (grey) or incubated with the chlorinated nucleoside for 24 h prior to washing and re-incubation without treatment in complete media for 48 h (white). After treatment, DNA and RNA was extracted, then hydrolysed and dephosphorylated prior to analysis by LC/MS. The concentration of chlorinated nucleoside is shown as a 1:1000 ratio with parent nucleoside where results show the mean ± SEM of experiments performed with at least 3 separate donors. *, ** and **** show a significant difference (p < 0.05, 0.01 and 0.0001, respectively) in incorporation of chlorinated nucleoside when compared to non-treated control. a, b and c show a significant decrease (p < 0.05) in chlorinated nucleoside compared to 24, 48 and 72 h, respectively. Statistics were calculated using a one-way ANOVA with Sidak's multiple comparison test.*

3.4.2. 8ClA does not alter ATP production by oxidative phosphorylation in HCAEC

Given that treatment with 8ClA caused a decrease in metabolic activity and alterations to ATP stores after 48 h as shown in previous studies, alterations in mitochondrial respiration were assessed. The Mito Stress test was used with the Seahorse analyser in order to measure the oxygen consumption rate (OCR). By measuring the OCR, prior, during and after a series of injections of inhibitors of the electron transport chain, any alterations in the cells ability to undergo mitochondrial respiration would become apparent. A series of injections were made of oligomycin, FCCP and rotenone/antimycin A which inhibit ATP production, uncouple the mitochondria and inhibit Complexes I/III, respectively were added and parameters of mitochondrial function were calculated (outlined in Figure 2.1).

Studies assessed HCAEC after treatment with 8ClA at varying concentrations (4, 8 and 16 μM) and Ad (16 μM) for 48 h as significant decreases in metabolic activity were observed at this time point, together with a decrease in ATP. The OCR of HCAEC exposed to 8ClA (4, 8 and 16 μM) and Ad (16 μM) for 48 h was determined prior to and after injections of oligomycin, FCCP and a mixture of rotenone/antimycin A. The changes in OCR were plotted as a graph of OCR vs Time to a show a real-time respiratory profile of 8ClA and Ad treated HCAEC (Figure 3.2).

Baseline respiration was determined prior to injection of oligomycin (1.7 μM) and the OCR was recorded in order to determine the proton leak. From this, ATP production was calculated as the difference in OCR between basal respiration and proton leak. An injection of FCCP (0. 7 μM) was then made and the recorded OCR was representative of

maximal respiration. The spare respiratory capacity was then determined from the difference in OCR between maximal and basal respiration. Both rotenone (0.5 μM) and antimycin A (0.5 μM) was injected in order to stop mitochondrial respiration, where the corresponding OCR showed non-mitochondrial respiration (Figure 3.2).

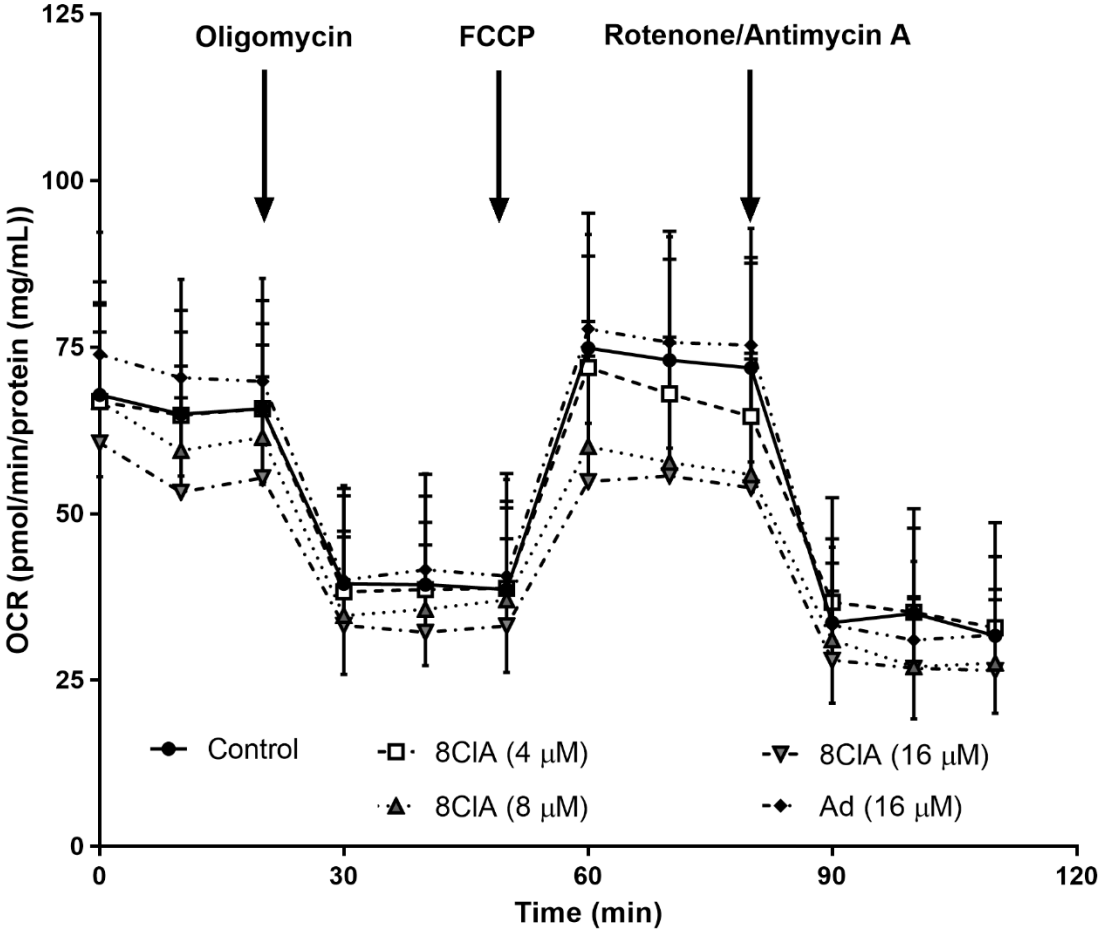

Figure 3.2: *The effect of 8ClA on the mitochondrial respiration of HCAEC.*
HCAEC (3.2 × 10^4 cells) were treated with varying concentrations of 8ClA (4, 8 and 16 μM) and Ad *(16 μM) for 48 h prior to assessing mitochondrial respiration by measuring oxygen consumption rate (OCR). OCR was measured prior and during injections of oligomycin (1.7 μM), FCCP (0.7 μM) and rotenone/antimycin A (0.5 μM). These data show the mean ± SEM of 3 experiments using different cell donors with 4 biological replicates.*

As described above, measurements of mitochondrial function were calculated from the OCR of HCAEC treated with 8ClA and Ad for 48 h. It was demonstrated that there were no alterations in basal respiration (prior to injections) in these cells between each treatment and when compared to non-treated control cells (Figure 3.3A). After addition of oligomycin, it was demonstrated that there were no significant changes to the ATP coupler response in 8ClA-treated HCAEC when compared to non-treated control cells (Figure 3.3D). Similarly, the addition of FCCP to each sample showed no significant changes to the electron transport chain accelerator response (Figure 3.3C). When the final injection of rotenone/antimycin was added to shut down the mitochondria, it was demonstrated that there were no significant differences in the non-mitochondrial respiration of HCAEC exposed to 8ClA when compared to non-treated control (Figure 3.3B). Furthermore, when ATP production, coupling efficiency and spare respiratory capacity were calculated from the OCR reported after injections of ETC inhibitors, there were no significant differences observed between 8ClA treated cells and non-treated control cells (Figure 3.3D-F). However, the variation between cell donors in each of the experiments is large and therefore may contribute to the lack of significant changes in measures of mitochondrial respiration (see Figure 3.2 and Figure 3.3).

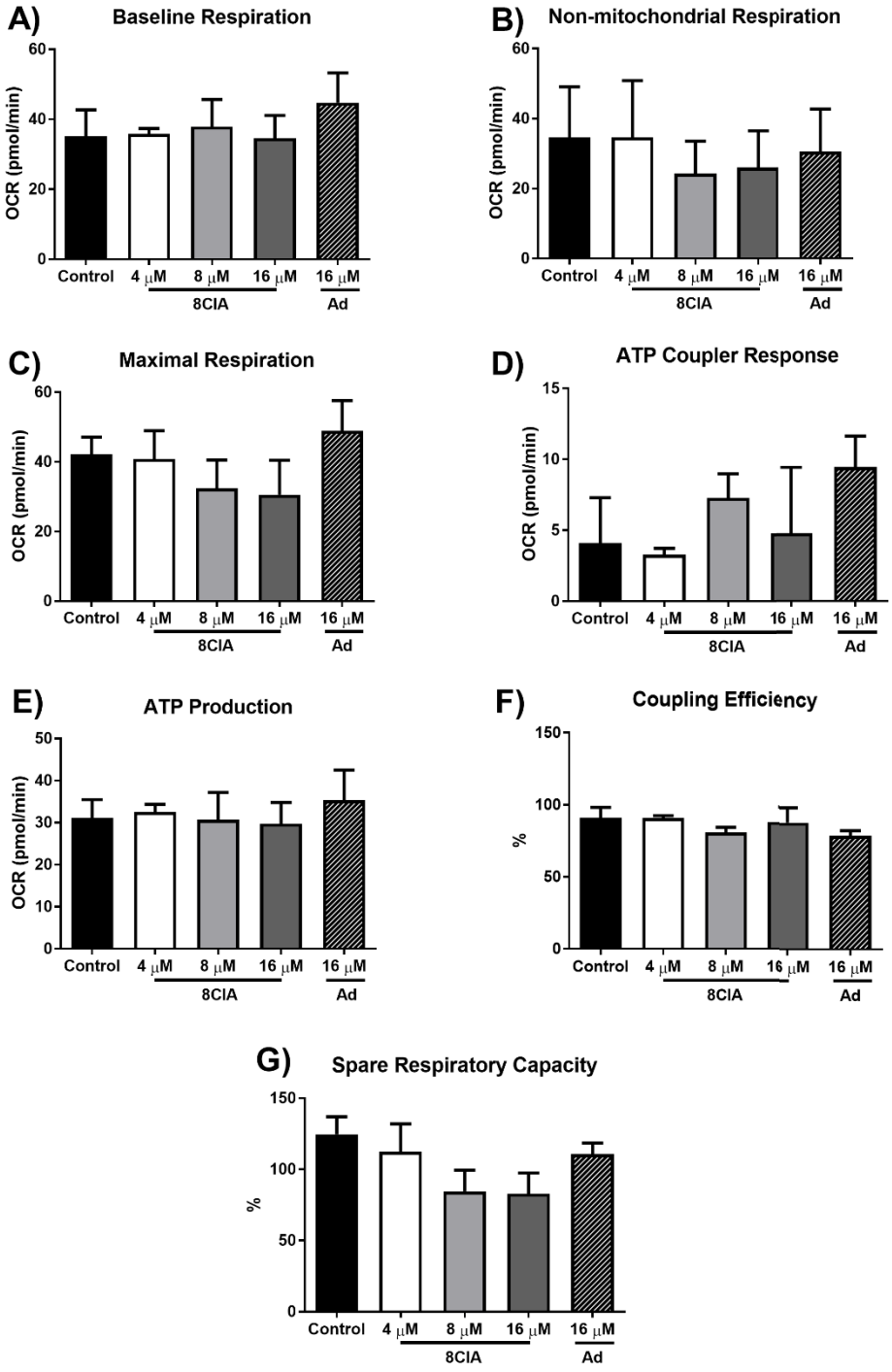

Figure 3.3: *Mitochondrial respiration remains unaltered after treatment with 8ClA.*
The mitochondrial respiration of HCAEC (3.2 × 10^4 cells) were treated with varying concentrations of 8ClA (4, 8 and 16 µM) and Ad *(16 µM) for 48 h followed by measurement with a Seahorse XF Analyser and the Mitostress Test. From measuring the OCR, the basal respiration (A), non-mitochondrial respiration (B), maximal respiration (C), ATP coupler response (D), ATP production (E), coupling efficiency (F) and spare respiratory capacity (G) were calculated. The graphs represent mean ± SEM of at least 3 biological replicates using 3 individual cell donors. No significant differences were observed between treatment and control when analysed using a one-way ANOVA with Dunnett's multiple comparison post-hoc test.*

3.4.3. Exposure to 8ClA causes decreases ATP synthesis by glycolysis

In cells, glycolysis is the other key cellular pathway responsible for the production of ATP. Therefore, the effect of 8ClA on glycolysis in HCAEC treated was assessed using Seahorse analyser. Alterations in extracellular acidification rate (ECAR) was determined with and without injection of glucose (10 mM). Basal glycolysis (ECAR in the absence of glucose) in 8ClA treated HCAEC remained unchanged compared to control (Figure 3.4A). However, once an injection of glucose was made, there was a significant decrease in the ECAR of cells that had been exposed to 8ClA when compared to non-treated and Ad controls (Figure 3.4A, B). This suggests that with 8ClA treatment, HCAEC have a decreased ability to undergo glycolysis.

Following this, the release of L-lactate into the extracellular environment of HCAEC was determined after exposure to 8ClA and Ad using the glycolysis cell-based assay kit. L-lactate is an end product of glycolysis and therefore a decrease of L-lactate release into the cell media would further support a decrease in glycolysis. Results show that the concentration of L-lactate excreted into the extracellular environment was markedly decreased when HCAEC were exposed to 8ClA when compared to non-treated control and Ad treated cells, which supports the data showing a blunted ability to perform glycolysis (Figure 3.4C). There were no significant changes in glycolysis as reflected by L-lactate concentrations in the media in Ad treated cells, supporting a causal role for the chlorination of the nucleoside in the effects observed.

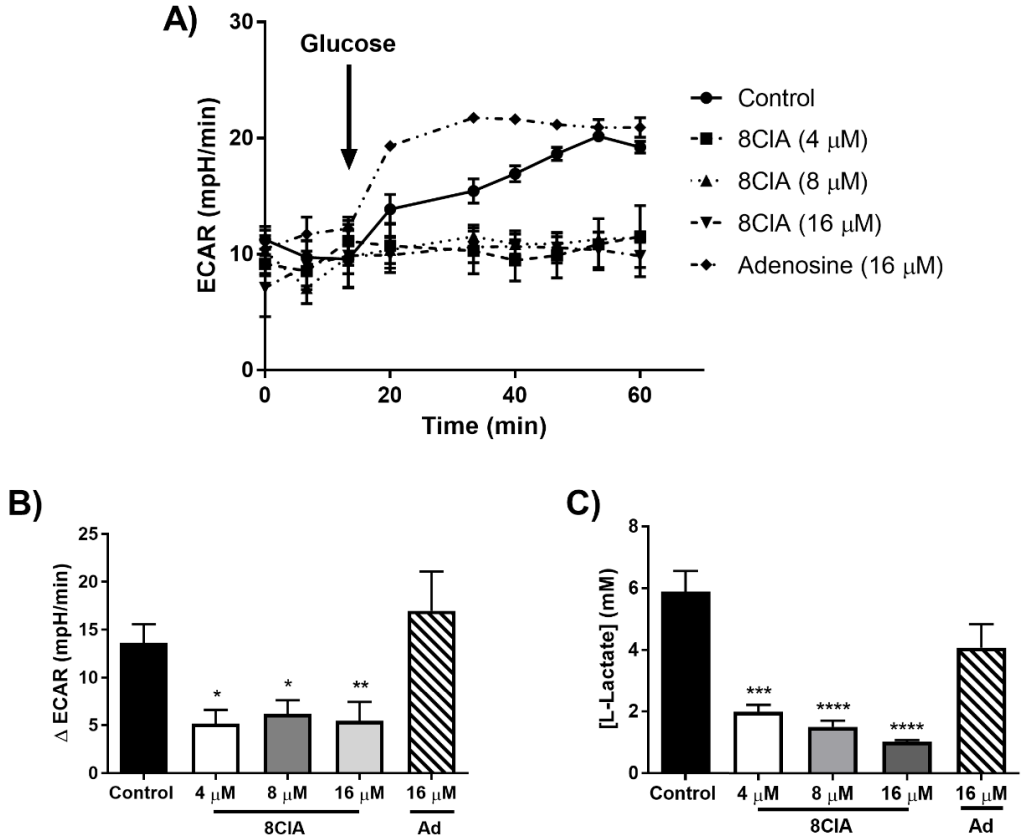

Figure 3.4: *Treatment of HCAEC with 8ClA induces changes in glycolysis and GAPDH activity.*

The glycolytic rate of HCAEC (3.2 × 10^4 cells) treated with 8ClA (4, 8 and 16 μM) and Ad *(16 μM) was measured using a Seahorse XF Analyser before and after addition of glucose (10 nM)(A and B). The excretion of L-Lactate into the extracellular environment (C) was determined using the glycolysis cell-based assay kit. Results represent mean ± SEM of 3 biological replicates performed with 3 independent cell donors. *, **, *** and **** represent a statistically significant decrease ($p < 0.05$, 0.01, 0.001 and 0.0001, respectively) compared to control experiments using a one-way ANOVA with Dunnett's multiple comparisons test.*

3.4.4. 8ClA treatment does not alter glucose uptake in HCAEC but decreases GAPDH activity

Glycolysis is the process by which glucose is broken down into pyruvate and lactate following the uptake of glucose into cells [289]. Therefore, given the effect on the glycolytic ability demonstrated on HCAEC after exposure to 8ClA, whether this was due to alterations in glucose uptake was examined. The uptake of glucose with and without

treatment of 8ClA in HCAEC was determined using the fluorescent analogue of glucose, 2-NBDG.

When 2-NBDG is taken up into cells, it exhibits fluorescence at an excitation and emission of 475 and 550 nm, respectively. HCAEC that were non-treated, exposed to 8ClA (8 µM), Ad (8 µM) or apigenin were stained with 2-NBDG prior to imaging by microscopy with a FITC filter in order to confirm uptake of 2-NBDG into the cells (Figure 3.5A-D). Further experiments quantified the fluorescence of 2-NBDG in HCAEC exposed to 8ClA, Ad and apigenin using a plate reader. Results showed that when HCAEC were treated with 8ClA for 24 or 48 h, there was no alteration in the uptake of glucose when compared to non-treated and Ad control (Figure 3.5E, F). However, when cells were incubated in the presence of the positive control, apigenin (an inhibitor of Glut-1), it was demonstrated that there was a significant decrease in uptake for 2-NBDG (Figure 3.5E, F).

As it was found that alterations in glycolytic activity were not due to alterations in the ability of HCAEC to uptake glucose, the activity of GAPDH, a glycolytic enzyme, was assessed. After HCAEC were exposed to 8ClA (8 µM) or Ad (8 µM), samples were lysed in H_2O followed by addition of NAD^+ and glyceraldehyde 3-phosphate after which the formation of NADH was monitored over time at an absorbance of 340 nm. When HCAEC were exposed to 8ClA, it was found that there was a marked decrease in GAPDH activity when compared to non-treated control (Figure 3.6). However, when the cells were treated with non-chlorinated Ad, there was also a decrease in GAPDH activity, though smaller than treatment than 8ClA (Figure 3.6).

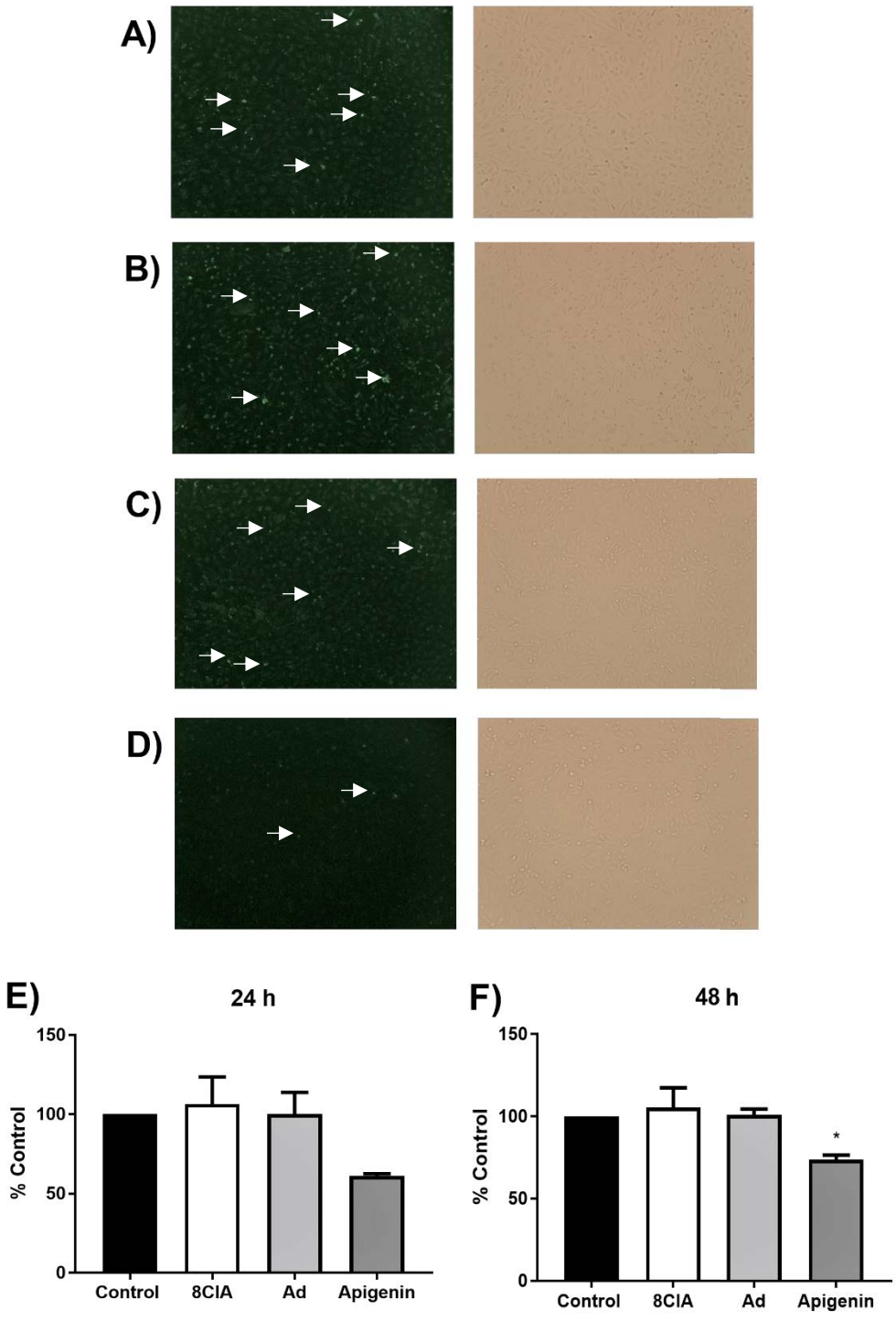

Figure 3.5: *The effect on glucose uptake when HCAEC are exposed to 8ClA.*
*The glucose uptake of HCAEC (5 × 10^4 cells) that were untreated (A), treated with 8ClA (8 µM) (B), Ad (8 µM) (C) and apigenin (50 µM) (D) was imaged by FITC and brightfield microscopy after staining with 2-NBDG (250 µM). The fluorescence of 2-NBDG was also measured using a plate reader at an excitation and emission of 485 and 535 nm, respectively, after 24 (E) and 48 h (F) of treatment. White arrows on A-D show positive staining with 2-NBDG * demonstrated a significant decrease ($p < 0.05$) in fluorescence when compared to control determined by one-way ANOVA with Dunnett's posthoc multiple comparison test.*

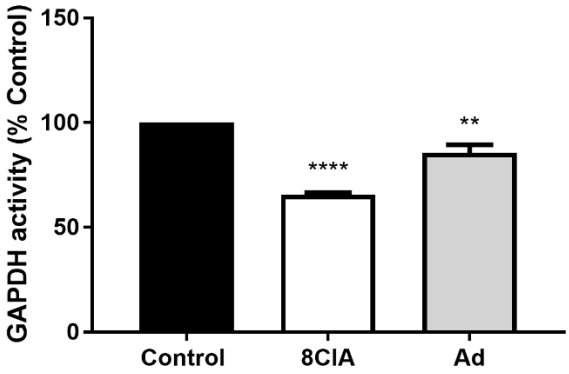

Figure 3.6: *The effect 8ClA on GADPH activity in HCAEC.*
*The activity of GAPDH in HCAEC (10^5 cells) exposed to 8ClA or Ad (8 µM) was determined by monitoring the formation of NADH at an absorbance of 340 nm over time at 37 ˚C using a plate reader. Results represent mean ± SEM for 3 experiments performed with 3 independent cell donors in triplicate. ** and **** represent a statistically significant decrease ($p < 0.01$ and 0.0001, respectively) compared to control experiments using a one-way ANOVA with Dunnett's multiple comparisons test.*

3.4.5. Treatment with 8ClA causes ER stress

Due to the effects of 8ClA on the cellular metabolism of HCAEC, further studies were performed to examine changes in the expression of genes related to stress signalling pathways. The mitochondria and ER communicate closely during homeostasis through the mitochondrial-associated ER membrane, which helps to regulate ATP production, calcium regulation and apoptosis [290]. As 8ClA caused alterations to ATP production by glycolysis, the effect of 8ClA on ER stress in HCAEC was studied.

HCAEC were exposed to 8ClA or Ad (8 µM) for 6 h prior to the extraction of nuclear and cytoplasmic protein fractions. It was demonstrated by Western blot that treatment with 8ClA induced an increase in the nuclear translocation of ATF4 from the cytosol into the nucleus (Figure 3.7A, B). This is consistent with activation of the UPR via the PERK signalling pathway, supported by experiments performed using tunicamycin, a known

activator of the UPR, which also increased nuclear translocation of ATF4 (Figure 3.7A). Similarly, there were also significant increases in other genes downstream of ATF4 associated with the UPR, including CCAAT-enhancer-binding protein homologous protein (CHOP) and growth arrest DNA damage inducible 34 (GADD34) (Figure 3.7D, E). HCAEC that were exposed to 8ClA also had increased mRNA expression of spliced x-box binding protein 1 (sXBP1) (Figure 3.7F), which is a marker of ER stress related to the ATF6 and IRE1 signalling pathways of the UPR. These increases in mRNA expression were not observed when HCAEC were treated with Ad, consistent with a role for the chlorination of Ad in these data.

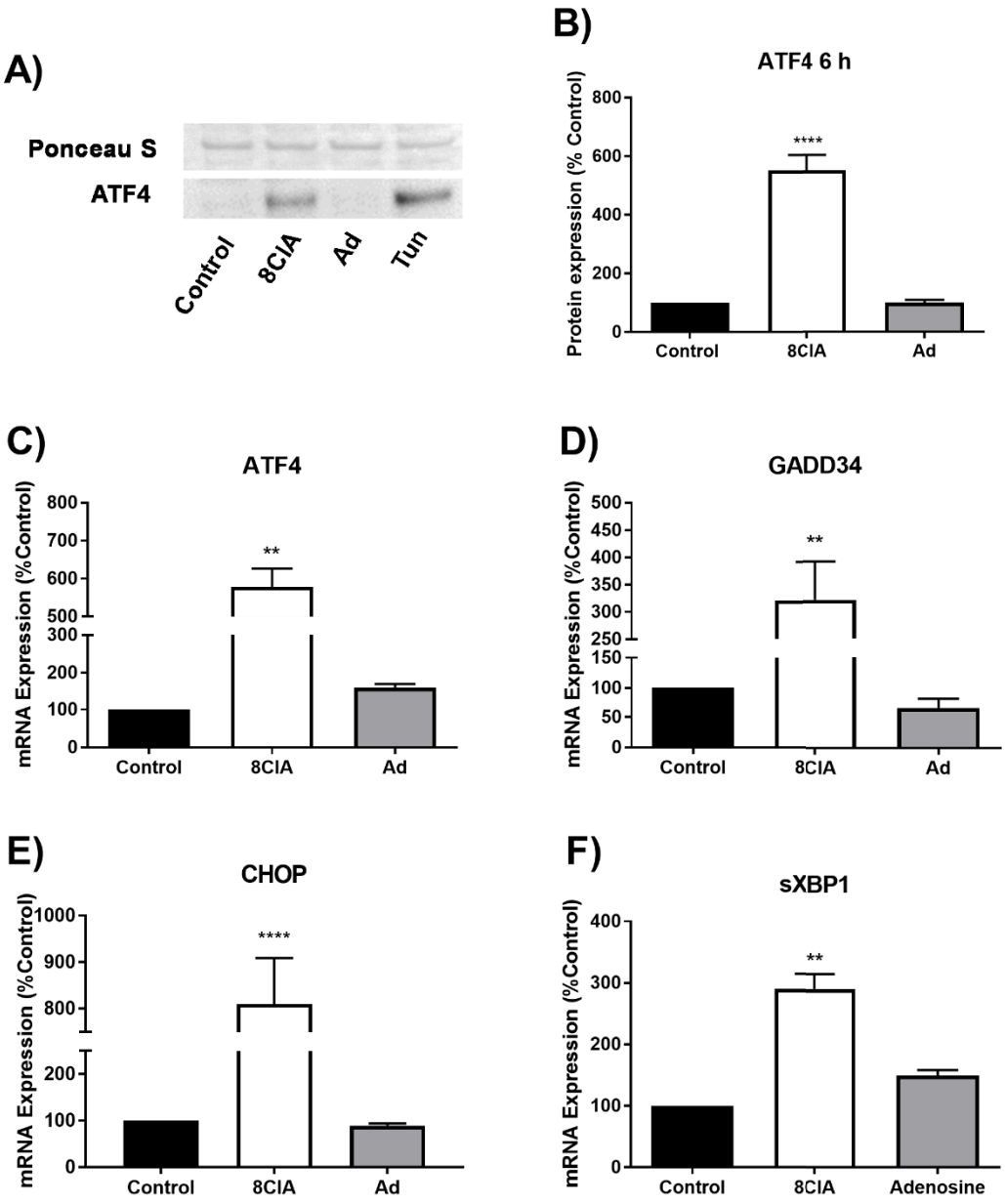

Figure 3.7: *Treatment with 8ClA causes ER stress and activates the unfolded protein response.*

Activation of the UPR was assessed in HCAEC (10^5 cells) treated with 8ClA or Ad *(Ad, 8 µM) for 6 h prior to analysis of ATF4 translocation from the cytosol into the nucleus as determined by Western blot (A and B). Other markers of ER stress were examined using qPCR after 24 h exposure to determine the mRNA expression of ATF4 (C), GADD34 (D), CHOP (E) and sXBP1 (F) when compared to two housekeeping genes, 18S and RPL13. Results show the mean ± SEM of 3 independent cell donors, completed in triplicate. ** and **** show a significant increase ($p < 0.01$ and 0.0001, respectively) in mRNA expression when compared to control using a one-way ANOVA with Dunnett's multiple comparison test.*

3.4.6. Exposure to 8ClA alters antioxidant responses in HCAEC

ER stress has been associated with the activation of cellular antioxidant responses including the Nrf2-Keap1 pathway [291]. Studies then focussed on the mRNA expression of antioxidant genes associated with Nrf2 after HCAEC were exposed to 8ClA. It was found that when HCAEC were treated with 8ClA (8 µM) for 24 h, that there was a significant increase in mRNA expression compared to control and Ad of NADPH dehydrogenase quinone 1 (NQO1), glutamate-cysteine ligase catalytic subunit (GCLC) and heme-oxygenase 1 (HO-1) (Figure 3.8A-C), which is consistent with the activation of Nrf2. Another major protein associated with the regulation of oxidative stress and inflammation is thioredoxin-interacting protein (TXNIP) [292, 293]. Exposure of HCAEC to 8ClA, but not Ad only resulted in a significant increase in mRNA and protein expression of TXNIP (Figure 3.8D-F).

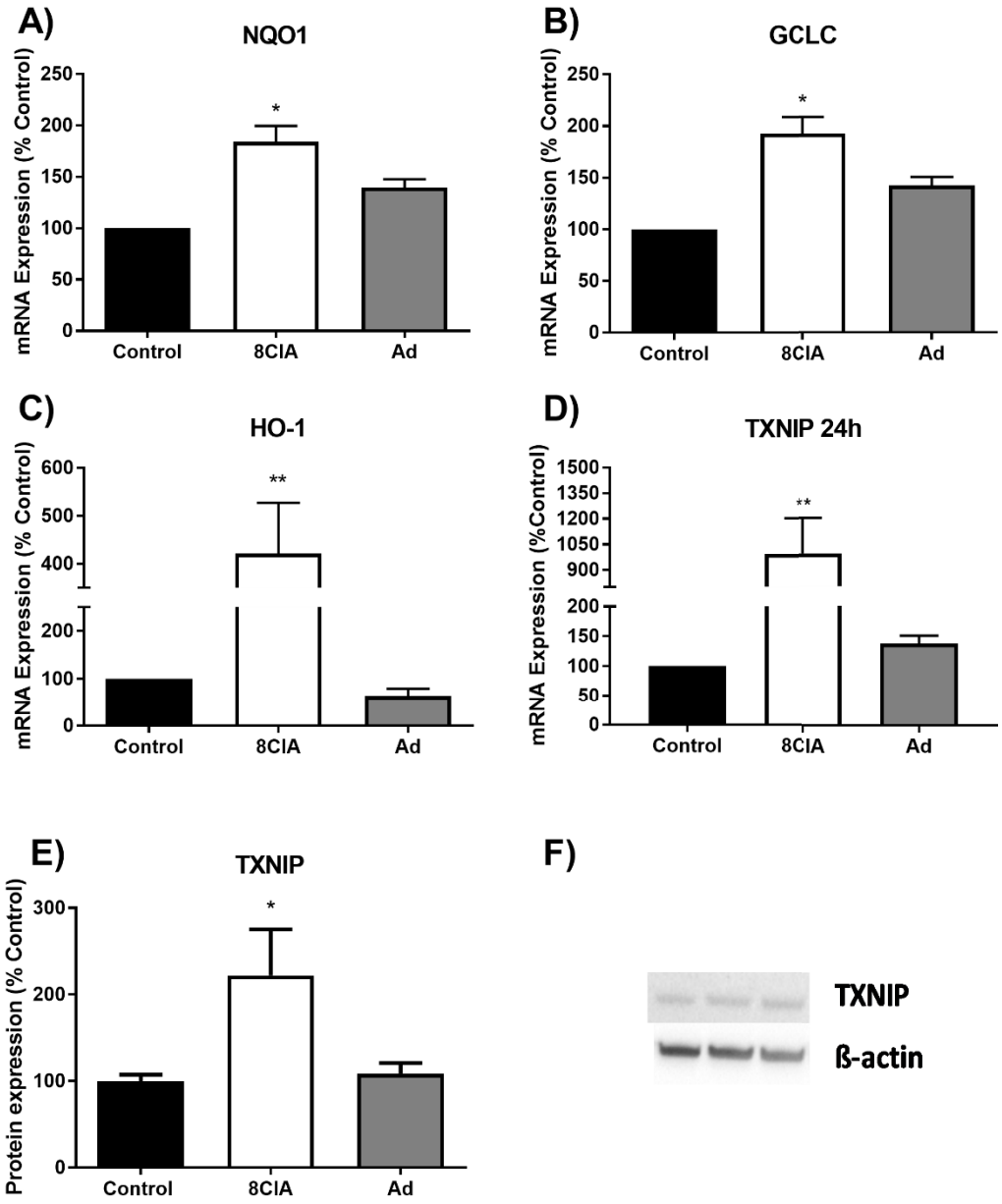

Figure 3.8: *HCAEC exposed to 8ClA have altered expression of Nrf2-related and other antioxidant responses.*

*The mRNA expression in HCAEC (10^5cells) treated with 8ClA or Ad (8 µM) for 24 h was analysed to determine alterations in antioxidant responses, NQO1 (A), GCLC (B), HO-1 (C) and TXNIP (D) when compared to 2 housekeeping genes, 18S and RPL13. The protein expression of TXNIP after 24 h treatment was determined by Western blot and normalised to the protein expression of ß-actin (E and F). * and ** ($p < 0.05$ and 0.01, respectively) show a significant increase in mRNA or protein expression when compared to control using a one-way ANOVA with Dunnett's multiple comparison test.*

Given the marked increase in TXNIP, the mRNA expression of other antioxidant response genes was also determined by qPCR. Superoxide dismutases (SOD) are the main antioxidant defence mechanism against superoxide, and therefore the mRNA expression of SOD1 and SOD2 was determined after HCAEC were exposed to 8ClA (8 µM) for 24 h. SOD1, the isoform found in the cytoplasm, was found to be significantly decreased when compared to control cells (Figure 3.9A). However, these differences were similar to those observed with Ad-treated control cells. When HCAEC were exposed to 8ClA (8 µM), the mRNA expression of SOD2 (the isoform present in the mitochondria) remained unchanged compared to non-treated control cells. Interestingly, the incubation of HCAEC with Ad (8 µM) caused a significant decrease in SOD2 gene expression when compared to non-treated control (Figure 3.9B).

Studies were then performed in order to determine the mRNA expression of glutathione-dependent antioxidant responses. The genes related to the glutathione antioxidant response, glutathione peroxidase 4 (GPx4) and glutathione synthetase (GS) remained unchanged in HCAEC exposed to 8ClA (8 µM) for 24 h (Figure 3.9C, D). However, in contrast, mRNA expression of GS was shown to be significantly decreased in Ad-treated HCAEC when compared to non-treated control (Figure 3.9D). Furthermore, the mRNA expression of thioredoxin (Trx), which plays a key role in the antioxidant response and redox signalling was determined in HCAEC exposed to 8ClA (8 µM). It was found that there were no significant changes in the expression of Trx between 8ClA-treated or Ad-treated cells with non-treated control (Figure 3.9E).

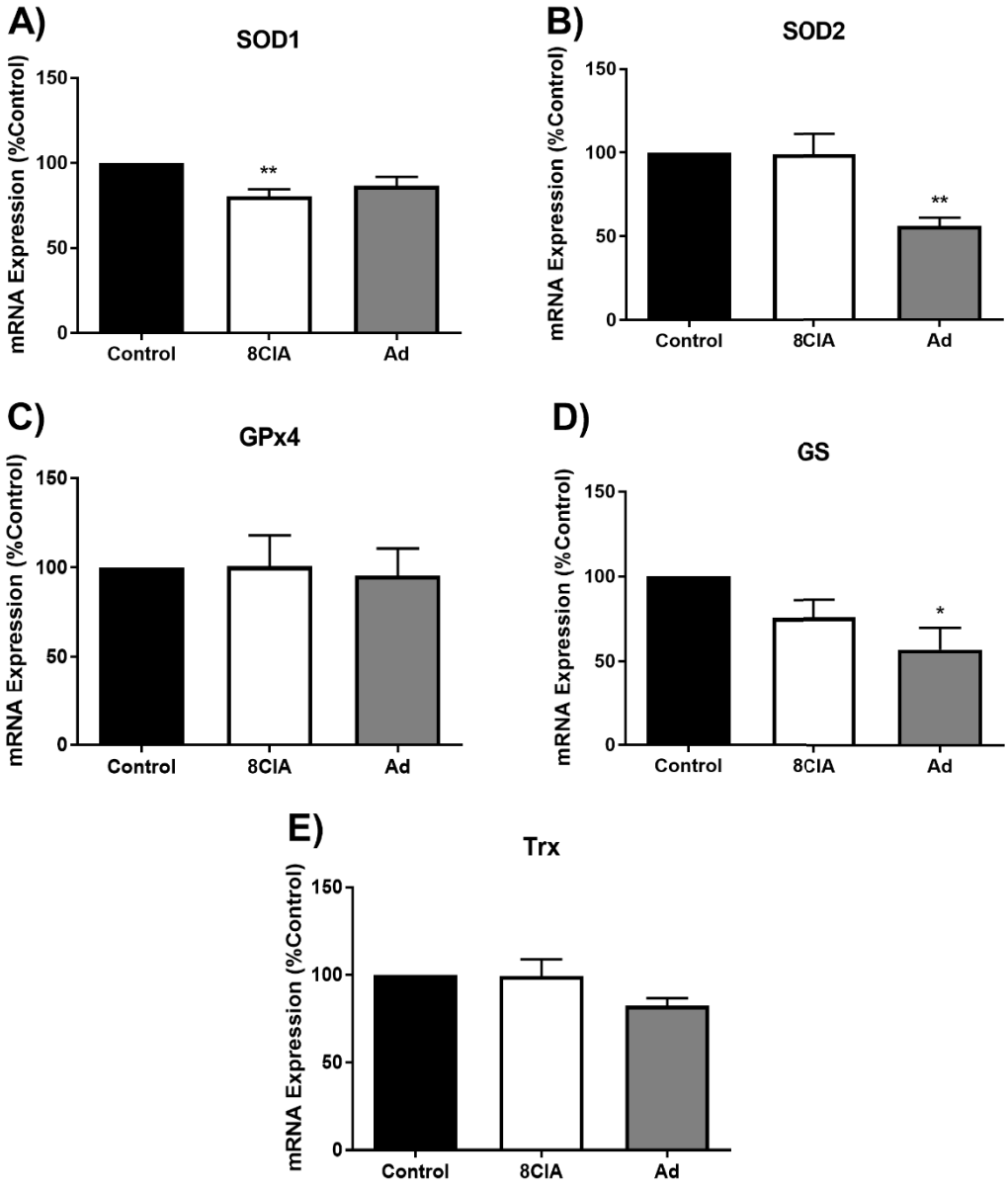

Figure 3.9: *Treatment with 8ClA does not alter some antioxidant responses in HCAEC.*
*The mRNA expression of other antioxidant responses, SOD1 (A), SOD2 (B), GPx4 (C), GS (D) and Trx (E) was determined by qPCR after HCAEC were treated with 8ClA or Ad (8 µM) for 24 h. Expression was compared to 2 housekeeping genes 18S and RPL13 with experiments performed in triplicate with 3 cell donors. The data represents mean ± SEM, where * and ** show a significant difference ($p < 0.05$ and 0.01, respectively) in mRNA expression compared to control using a one-way ANOVA with Dunnett's multiple comparison test.*

3.4.7. 8ClA causes increased calcium accumulation and induces apoptotic cell death

Sustained ER stress can induce changes to the storage of calcium intracellularly and promote apoptotic cell death [294, 295]. The accumulation of calcium in the cytosol, which could result from release from the ER during increased oxidative stress, was measured using Fluo-4AM staining with flow cytometry. HCAEC treated with 8ClA (8 µM) for 24 h had significantly increased accumulation of calcium within the cytosol when compared to control and Ad treated cells (Figure 3.10A). To assess whether the changes in calcium accumulation were associated with ER stress and UPR activation, experiments were performed with an inhibitor of the PERK pathway, as PERK is upstream of ATF4, which was shown to be upregulated in HCAEC exposed to 8ClA. In HCAEC pre-treated with an inhibitor of PERK (GSK2606414) prior to exposure to 8ClA (8 µM), the increase in calcium accumulation within the cytosol is not observed (Figure 3.10B). This suggests that the accumulation of calcium in the cytosol was due to activation of the PERK pathway of the UPR.

Further studies were performed in order to determine whether the accumulation of calcium in the cytosol was related to PERK activation and the marked increase in gene expression of CHOP, a molecule responsible for apoptotic cell death signalling, which could be responsible for the observed decrease in cell viability. Staining with Annexin V and propidium iodide with flow cytometry was then performed in order to determine the mechanism of cell death by apoptosis or necrosis, respectively, when HCAEC were treated with 8ClA (8 µM). After treatment with 8ClA (8 µM) for 48 and 72 h, HCAEC had a significantly increased population of Annexin V positive cells showing a larger apoptotic population (Figure 3.11). Data also showed that there was a slight increase in

propidium iodide positive cells (though not significant) showing a minor increase in the population of necrotic cells (Figure 3.11C, D). These data suggest that when HCAEC are exposed to 8ClA, the main mechanism by which cell death occurs is through apoptosis.

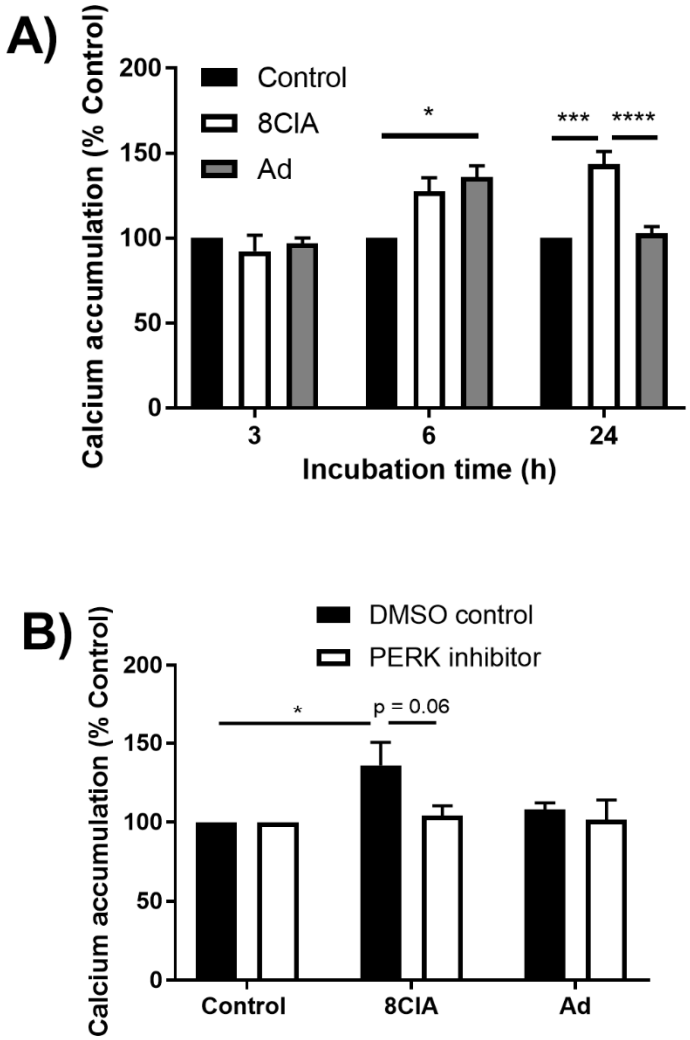

Figure 3.10: *Exposure of HCAEC to 8ClA causes calcium to accumulate in the cytosol.*
*The changes in the cytosolic calcium in HCAEC (A) was determined in HCAEC after 3, 6 and 24 h incubation with 8ClA and Ad (8 μM) using Fluo-4AM staining. Calcium accumulation was also assessed with pre-treatment using an inhibitor of PERK (GSK2606414) followed by treatment with 8ClA for 24 h (B). Experiments were completed with 3 biological replicates of 3 independent cell donors where results are mean ± SEM. *, *** and **** show a significant difference (p < 0.05, 0.001 and 0.0001) in viability when compared to control using a two-way ANOVA with Dunnett's multiple comparison test.*

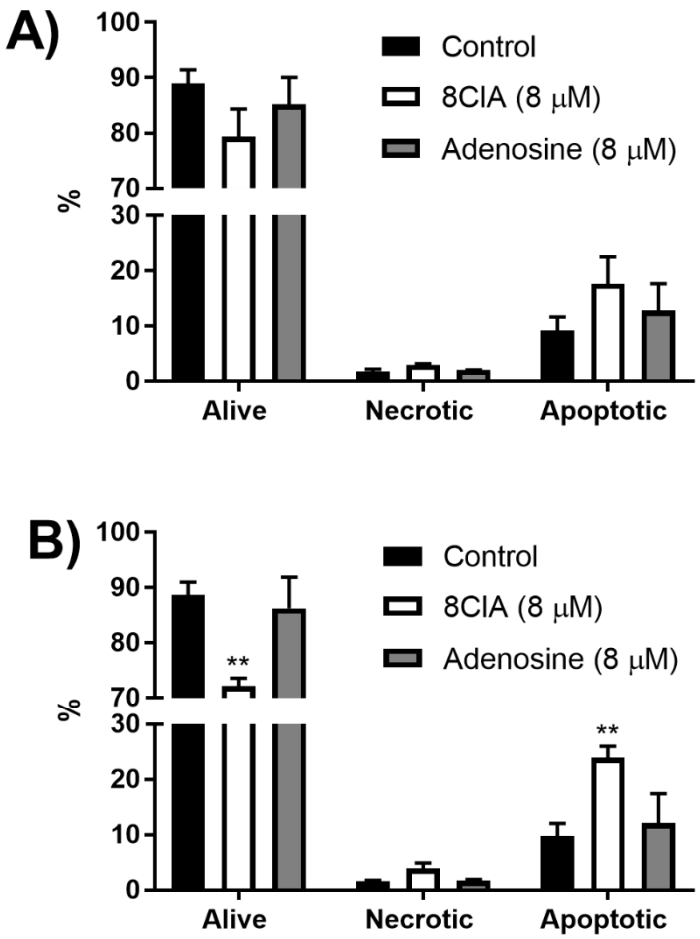

Figure 3.11: *8ClA exposure induces apoptotic cell death in HCAEC.*
*The viability of HCAEC (1 × 10^5 cells) after treatment with 8ClA or Ad (8 μM) for 48 (C) or 72 h (D) was determined using Annexin V and propidium iodide staining. Experiments were completed with 3 biological replicates of 3 independent cell donors where results are mean ± SEM. ** shows a significant difference (p <0.01) in viability when compared to control using a two-way ANOVA with Dunnett's multiple comparison test.*

3.5. Discussion

There are many studies within the literature identifying the presence of chlorinated nucleosides in multiple inflammatory pathologies [16-18, 256]. During inflammation, there is an increase in the generation of the MPO-derived oxidant, HOCl. HOCl reacts with most biomolecules, such as DNA and RNA, forming stable chlorinated compounds [104]. What remains to be elucidated is the role of chlorinated nucleosides in disease progression. Previously, it has been shown that chlorinated nucleosides incorporated into DNA have mutagenic consequences and their presence can initiate the growth of tumour cells in inflammatory cancers [9]. The experiments performed in this Chapter determined the effect of chlorinated nucleosides on the cellular function of HCAEC, given the role that MPO plays in endothelial cell damage and the presence of chlorinated products in atherosclerotic lesions [16, 126].

This study demonstrated that ribose chlorinated nucleosides, 8ClA, 8ClG and 5ClC incorporated into the RNA of HCAEC. It was found that there was no incorporation of deoxyribose nucleosides incorporating into RNA and ribose nucleosides into DNA, which correlates to previous studies that showed that ribonucleotide reductase lacks affinity towards chlorinated nucleosides [256, 269]. This was supported by studies performed in J774.A1 macrophages, where 8ClA, 8ClG and 5ClC were shown to incorporate into cellular RNA and not into DNA [259]. In contrast, it has previously been shown that 8ClA can incorporate into the DNA of human gliomal cells, however it is postulated that this is specific to cell type [296]. Deoxyribose chlorinated nucleosides 8CldA, 8CldG and 5CldC were shown to incorporate into the cellular DNA of HCAEC. However, in studies with J774.A1 cell lines, it was demonstrated that only 5CldC incorporated into the

cellular DNA but there was no evidence for the incorporation of 8CldA or 8CldG in these cells [259].

The incorporation of each chlorinated nucleoside increased over time, reaching maximal levels within 24 – 48 h of exposure. Previous studies demonstrated that treatment of EA.hy926 cells, which are an endothelial cell line, with the chlorinated nucleosides 8Cl(d)G and 5Cl(d)C, resulted in the accumulation of these modified nucleosides into the nucleotide pool, with only 5ClC incorporating into the RNA [256]. This could be due to the difference in cell types and of reactivities between cell lines and the primary cells utilised in this study. Studies using primary epithelial prostate cells for example, found the incorporation of chlorinated nucleosides to be 40 – 227 times greater than in the EA.hy926 cell line, supporting the increased accumulation in primary cell types [256]. Therefore, the levels of incorporation of 8ClA shown in this study are supported by studies performed in other cell types.

The ability of HCAEC to clear or repair chlorinated nucleosides from their DNA and RNA was determined by 48 h re-incubation without chlorinated nucleoside in the cell culture media after an initial 24 h exposure period. In this study it was shown that there was a significant decrease of 8ClA evident in the RNA of HCAEC exposed to 8ClA under these conditions. This decrease was not observed when HCAEC were treated with 8ClG or 5ClC under these conditions. Previous studies showed that 8ClA destabilises the RNA as the nucleoside takes a *syn*-conformation as opposed to the favoured *anti*-conformation [269]. Similarly, previous studies demonstrated that the incorporation of 5ClC into the RNA of EA.hy926 cells also cause destabilisation of the RNA [256]. However, in the

current study, it was found that after 48 h re-incubation following 24 h exposure that there was a non-significant decrease in the presence of 5ClC within the RNA. This could be due to the inconsistencies found between each individual HCAEC donor used in this study. In contrast, clearance studies in J774.A1 cells showed evidence for the significant removal of 5ClC from the RNA but not 8ClA or 8ClG [259]. This could be due to the difference in cell types or also due to the increased re-incubation time (72 h) used in that study allowing for the chlorinated nucleoside to be excised or converted to another compound by deamination [259].

Similarly, decreases in accumulation of deoxyribose chlorinated nucleosides were also observed after re-incubation, especially when exposed to 8CldG and 5CldC. This could be due to the larger amounts of these modified nucleosides that incorporated over the 24 h exposure period when compared to 8CldA. Moreover, this may be due to differences in the ability of the chlorinated nucleosides to penetrate into the cell and subsequently the ability of RNA reductase/DNA polymerases to incorporate them into the DNA. Previous studies have demonstrated that 8CldG incorporates to a greater extent compared to other chlorinated nucleosides in endothelial and prostate cells [256], which supports the trends demonstrated in this current study. Another study showed that in J774.A1, that 5CldC incorporates more readily into DNA than 8CldG [259], however these differences could again be attributed to the use of primary endothelial cells. In the literature, whether cells are able to clear and/or repair chlorinated nucleosides from the DNA is unclear. In this study, the decrease of 5CldC from the HCAEC after re-incubation in absence of 5CldC could be due to the deamination of 5CldC to 5ClU rather than clearance of the chlorinated nucleoside [200]. Whether

5CldC is deaminated to form 5ClU, rather than cleared from the DNA could be determined in a future study using GC-MS, as previously described by Jiang et al.[15].

Though each of the chlorinated nucleosides examined in this study were able to incorporate into the DNA or RNA of HCAEC, only 8ClA caused alterations in the metabolic activity of these cells. The decrease in metabolic activity observed in HCAEC occurred over similar timepoints to those seen with the incorporation of 8ClA into the RNA and also the incorporation into the nucleotide pool to form 8-ClATP. These incorporations occurred together with a significant decrease in glycolysis but not mitochondrial respiration, with HCAEC ultimately undergoing apoptosis. Previous studies have demonstrated the toxicity of 8ClA and its potency in inducing apoptotic cell death in multiple cancer cell lines, leading to its use as an agent in the treatment of chronic lymphocytic leukemia [261, 262, 280]. In the case of cancer cell lines, the mechanism causing apoptosis when treated with 8ClA has been attributed to the formation of 8-ClATP and subsequent depletion of ATP stores [267, 271, 280]. In contrast, a study using murine macrophages demonstrated that 8ClA did not cause depletion of ATP stores unlike in malignant cells [260]. Other studies have shown cell death to be a result of cellular signalling, causing autophagy or anti-apoptotic protein transcription [271, 280].

In cancer cell lines, the autophagy reported was due to the activation of AMPK which was induced through the depletion of ATP when cells were exposed to 8ClA [271]. In this previous study, activation of AMPK caused the signalling of mTOR to be reduced, resulting in the phosphorylation of Unc5-like kinase 1 [271]. When 8Cl-cAMP was used, experiments demonstrated a marked increase in AMPK activity with a significant

decrease in ATP. Whether these similarities exist with the experimental conditions used in this study with HCAEC, remains to be determined. However, in the current study, it seems that the decrease in ATP concentration is evident after longer exposure (48 h) when compared to those observed in cancer cell lines. In the present study with HCAEC, the depletion of ATP is not observed at earlier time points and this may be due to the cells abilities to use glycolysis to compensate, which was shown by decrease in ECAR, extracellular lactate and activity of GAPDH. This may be why there are no alterations observed in HCAECs ability to perform mitochondrial respiration. A previous study has shown that exposure of cells to 8ClA, causes decreased glycolytic ability [271]. However, it was shown that the alterations in glycolysis were due to changes in glucose uptake in this case, and were accompanied by a decrease in mitochondrial respiration, which were not observed in this study.

Treatment of HCAEC with 8ClA caused significant alterations to antioxidant cellular signalling responses, increased ER stress and activation of the UPR. In some cases, (such as SOD2 and GS), a decrease in gene expression is also seen on exposure of the cells to Ad. The reason for this is not certain, but likely reflects the known biological reactivity of Ad [297]. The mechanism by which ER stress is activated is unclear, however it may be due to the alterations in bioenergetics that were observed given the role of the ER in cell metabolism. In general, the activation of the UPR works to restore homeostasis to promote cell survival. However, in cases where homeostasis cannot be restored and ER stress is sustained, cellular signalling within UPR induces apoptosis by a CHOP-dependent pathway [287]. This study demonstrated activation of both the PERK and IRE1 parts of the UPR, causing the translocation of ATF4 into the nucleus, increased

mRNA expression of GADD34 and CHOP, ultimately inducing apoptosis in these cells. As 8ClA induces activation of the UPR, this may have significance in lesion development as activation of UPR has previously been shown to cause damage to the endothelium and instability of an atherosclerotic plaque [285, 286].

In HCAEC treated with 8ClA, the data also supports activation of the transcription factor, Nrf2, with a significant increase in the mRNA expression of many associated antioxidant response genes including HO-1, GCLC and NQO1. As Nrf2 has been demonstrated to exhibit pro-atherogenic effects such as inflammation, redox regulation, foam cell formation and macrophage polarisation [298], the ability of 8ClA to activate this pathway in HCAEC could be significant in the progression of atherosclerosis. In the current study, the activation of Nrf2 may be related to the induction of ER stress, as PERK can phosphorylate Nrf2, promoting Nrf2 to dissociate from Keap1 [287]. In this study, it was also demonstrated that treatment of HCAEC with 8ClA induced increased expression of TXNIP, which is important in maintaining glucose metabolism. TXNIP has previously been shown to increase ER resident protein disulphide isomerase activity, promoting protein folding, with studies showing an increase in TXNIP expression when ER stress was induced [299-301]. The overexpression of TXNIP has also been shown to induce redox stress and promote apoptotic cell death [300], which may contribute to the apoptosis evident in the current study.

The results from this study show that HCAEC, when exposed to 8ClA have altered cellular metabolism resulting in ER stress, increased expression of antioxidant responses and apoptotic cell death. In both early and late stage atherosclerosis, ER stress has been

shown to play an integral role, leading to endothelial dysfunction [285, 286]. The concentrations that chlorinated nucleosides are present within inflammatory tissues and whether they are sufficient to induce these outcomes in a diseased state remains unknown. Though, previous studies have demonstrated that the levels of chlorinated nucleosides used within this study are similar to concentrations obtained when cells are exposed to physiologically relevant concentrations of HOCl [6, 13].

The concentrations of 8ClA used in the current study are comparable to those found in plasma levels from previous studies and in clinical trials using 8Cl-cAMP, which has been demonstrated to work via the same mechanism [266, 282, 283]. This may have significance in patients receiving chemotherapeutic doses of 8ClA intravenously, where the concentrations used in this study are relevant as it may cause collateral damage to the endothelium. Overall, these data suggest that 8ClA could contribute to disease progression during chronic inflammation and potentially provide a biomarker for the diagnosis of disease.

3.6. Summary

In this chapter, HCAEC were treated with various chlorinated nucleosides likely to be produced during inflammation *in vivo.* It was demonstrated that ribose chlorinated nucleosides incorporated into RNA and deoxyribose chlorinated nucleosides incorporated into DNA. Though each nucleoside was demonstrated to incorporate into the cellular RNA or DNA, only exposure to 8ClA caused a significant decrease in metabolic activity in HCAEC. The extent of incorporation of other chlorinated

nucleosides may induce alterations to cell function, which might not have adverse effects to metabolic activity. These effects may still promote inflammation as seen in other cells types, however these effects still need to be elucidated in HCAEC.

In this study, 8ClA was demonstrated to activate the UPR via PERK in addition to activation of Nrf2. Ultimately, the sustained ER stress and alterations in antioxidant responses resulted in a significant increase in calcium accumulation, which could be inhibited by inhibition of PERK and HCAEC were shown to die by apoptosis. These findings may have implications in the development and progression of atherosclerosis. This is indicated by the endothelial dysfunction when HCAEC were exposed to 8ClA, which is a hallmark in atherosclerosis. This data shows that the presence of chlorinated nucleosides in inflammatory conditions can further exacerbate cellular dysfunction which may contribute to pathogenesis. Moreover, these findings may highlight pathways by which chlorinated nucleosides could contribute to disease progression.

The next Chapter extends these studies to examine the effects of chlorinated nucleosides on vascular smooth muscle cell function, using human coronary artery smooth muscle cells (HCASMC) as a model.

Chapter 4 – Effect of chlorinated nucleosides on human coronary artery smooth muscle cells

4.1. Introduction

In the previous chapter, it was determined that chlorinated nucleosides, in particular 8ClA have detrimental effects in relation to the survival of HCAEC. It raised the question as to whether similar effects would be observed when other cells vital to the formation of atherosclerotic lesions, such as vascular smooth muscle cells, are exposed to 8ClA and other chlorinated nucleosides.

Many studies show the clear role of endothelial cell dysfunction in atherosclerosis [4, 302, 303]. However, more recently, there have been studies emerging to show the role of smooth muscle cells in the initiation and progression of atherosclerosis [34]. Smooth muscle cells have both damaging and protective effects in atherosclerosis. The cross talk between immune cells and vascular smooth muscle cells can promote plaque growth, size, composition and stability [304]. Within the vessel wall, smooth muscle cells are responsible for the production of extracellular matrix [47]. When these cells are exposed to pro-atherogenic stimuli, the expression of extracellular matrix proteins changes, altering the lipid content with the vessel wall and the proliferation of vascular smooth muscle cells [35]. Furthermore, smooth muscle cells can also release cytokines, which effect endothelial function, causing endothelial cells to overexpress adhesion molecules and pro-inflammatory cytokines [34, 305, 306]. This causes downstream effects by increasing chemotaxis of monocytes into the developing plaque [306].

Smooth muscle cells play a vital role in atherogenesis, causing plaque stabilisation in the later stages of plaque formation. Plaque stability is often correlated to the thickness of the fibrous cap, so as the fibrous cap thins, the plaque becomes more prone to rupture. This occurs due to the death of the smooth muscle cells, breakdown of collagen or the disintegration of the matrix by proteases such as matrix metalloproteinases (MMPs) [21]. This is clinically relevant as the rupture of an atherosclerotic plaque can result in myocardial infarction or stroke. However, in many cases, the smooth muscle cells repair the rupture in the plaque causing the lesion to increase in size. As the lesion increases in size, this can cause an occlusion within the blood vessel [34].

Plaque stability, progression and the repair of damaged blood vessels is dependent on the balance between the migration, proliferation and extracellular matrix synthesis [34]. The ability of vascular smooth muscle cells to migrate and proliferate is due to their phenotype. Smooth muscle cells can switch between two phenotypes: contractile and synthetic [307]. Synthetic smooth muscle cells are more migratory and proliferative, producing larger amounts of collagen [307] and have increased mRNA expression of markers such as desmin and calponin [308]. Cells in this phenotype are also able to take up more LDL than contractile smooth muscle cells, which can contribute to the formation of foam cells, which are prevalent in atherosclerotic lesions [57]. In contrast, smooth muscle cells exhibiting a contractile phenotype are significantly decreased after vascular injury, where smooth muscle cells are shown to switch to a synthetic phenotype to help with repair [309]. Smooth muscle cells in the contractile phenotype express different markers to synthetic smooth muscle cells including osteopontin (OPN),

connexin-43 (CX43), Olfactomedin Like 3 (Olfml3), S100 Calcium Binding Protein A4 (S100A4) and decorin [307].

In the literature, it has been shown using rodent models of atherosclerosis that smooth muscle cells can switch phenotypes in response to different stimuli. These include cytokines [50-52], extracellular matrix [53, 54], lipids [55] and ROS [56]. In normal arterial tissue, smooth muscle cells exhibit a range of markers including smooth muscle cell α-actin, smooth muscle cell myosin heavy chain and smoothelin [310]. However, both smooth muscle cells *in vitro* and in atherosclerosis have been demonstrated to have increased proliferation, migration and are characterised by an increased expression of extracellular matrix proteins and cytokines [310]. When extracellular matrix is synthesised by smooth muscle cells, these cells become embedded in the matrix and become separated from each other. This causes the extracellular matrix to suppress phenotype switching, resulting in the smooth muscle cells staying in a contractile state [34]. In contrast, when matrix metalloproteinases break down the extracellular matrix, phenotypic switching of the smooth muscle cells to a synthetic phenotype is encouraged, causing increased proliferation and migration [311].

Given the importance of smooth muscle cell death, proliferation and changes in phenotype in the context of atherogenesis, the effects of chlorinated nucleosides on these factors were explored in this chapter.

4.2. Hypothesis and aims

Given the effects of the incorporation of chlorinated nucleosides to cell function and viability of HCAEC. It was hypothesised that chlorinated nucleosides would also incorporate into the DNA and RNA of HCASMC. Furthermore, it was hypothesised that the incorporation of chlorinated nucleosides would influence cell signalling and viability. Therefore, this chapter aimed to elucidate the effects of chlorinated nucleoside on HCASMC by assessing their incorporation into DNA, RNA and the nucleotide pool. The effect of chlorinated nucleosides on metabolic activity, proliferation and cell viability was also determined. Furthermore, this chapter aimed to determine whether there are alterations in the gene expression of inflammatory, antioxidant and phenotypic markers in HCASMC exposed to chlorinated nucleosides.

4.3. Methods

The incorporation of chlorinated nucleosides into the DNA and RNA of HCASMC was determined using LC-MS/MS (Section 2.5). After treatment of HCASMC with various chlorinated nucleosides, the DNA or RNA was isolated using the Isolate II DNA/RNA/Protein kit (Section 2.5.1) followed by enzymatic hydrolysis and dephosphorylation (Section 2.5.2) in order to prepare nucleoside samples for analysis using LC-MS/MS (Section 2.5.3).

The metabolic activity of HCASMC after exposure to chlorinated nucleosides was determined by staining with PrestoBlue cell viability reagent followed by measurement of fluorescence using a plate reader at excitation and emission wavelengths at 560 and

590 nm, respectively (Section 2.7.1). The proliferation of treated HCASMC was then determined by trypan blue staining in order to count live cells (and exclude dead cells) at varying time points (Section 2.7.2).

Flow cytometry was performed with different stains or antibodies in order to measure different aspects of cellular function. In order to determine proliferation, the expression of KI-67 was measured (Section 2.8.3). Cell death by apoptosis or necrosis was determined using Annexin/PI staining (Section 2.8.2), with calcium accumulation determined using Fluo-4AM (Section 2.8.1) and mitochondrial function assessed with JC-1 staining.

Alterations in ATP concentrations after HCASMC were exposed to chlorinated nucleosides was determined using the ATPlite luminescence assay system (Section 2.7.3). The incorporation of 8ClA into the nucleotide pool to form 8-ClATP was assessed in HCASMC exposed to 8ClA as described in (Section 2.6).

The mRNA expression of HCASMC after exposure to 8ClA and 5CldC was determined using qPCR (Section 2.9). RNA was isolated after treatment using the ReliaPrep RNA Cell Miniprep System (Section 2.9.1) with RNA concentration quantified (Section 2.9.2) and normalised for cDNA synthesis (Section 2.9.3). qPCR was then performed using iQ SYBR Green Supermix with forward and reverse primer sequences outlined in Table 2.6. The activity of MMP2 and MMP9 was determined using gelatin zymography (Section 2.7.9).

4.4. Results

4.4.1. Chlorinated nucleosides incorporate into HCASMC DNA and RNA

Studies were performed in order to determine the extent of incorporation of chlorinated nucleosides into the DNA and RNA of HCASMC after exposure for up to 72 h. Cells were exposed to each chlorinated nucleoside for various incubation times before isolation of DNA and RNA and quantification by LC-MS/MS. HCASMC that were exposed to the chlorinated ribose nucleosides 8ClA, 8ClG and 5ClC (16 µM) had differing levels of chlorinated nucleoside incorporated into the RNA (Figure 4.1A-C). This incorporation was time dependent with 8ClA reaching maximum incorporation after 24 h, whereas 8ClG and 5ClC had maximal incorporation after 6 h (Figure 4.1A-C). Similarly, the deoxyribose chlorinated nucleosides, 8CldA, 8CldG and 5CldC, incorporated into the DNA of HCASMC. Maximal incorporation was achieved after 6 h of exposure to 8CldA and 8CldG, with maximal incorporation after 2 h with 5CldC (Figure 4.1D-F). No evidence for the presence of chlorinated nucleosides was obtained in experiments performed with non-treated control cells in either DNA or RNA. Similarly, ribose chlorinated nucleosides were not found to incorporate into the DNA and deoxyribose chlorinated nucleosides were found not to incorporate into cellular RNA of HCASMC.

Another experiment was performed to determine the ability of the cells to clear chlorinated nucleosides from their DNA or RNA. HCASMC were exposed to chlorinated nucleosides for 24 h prior to removal of the treatment media and re-incubation of the cells in complete media, which lacked chlorinated nucleosides for a further 48 h. In HCASMC treated with the ribose chlorinated nucleosides, 8ClA, 8ClG or 5ClC, there was no statistically significant decrease in chlorinated nucleoside present in RNA under these

treatment conditions when compared to the chlorinated nucleoside concentration observed at each time point, where the chlorinated nucleoside was present for the duration of the experiment. The incorporation of 8ClA, 8ClG or 5ClC into the RNA of HCASMC after exposure for 24 h followed by re-incubation without chlorinated nucleoside for a further 48 h, was slightly decreased when compared to exposure for a total of 24 h. This suggests that there may be some removal or repair of the chlorinated ribose nucleosides from the RNA, but only to a relatively minor extent. When HCASMC were exposed to deoxyribose chlorinated nucleosides under similar conditions, it was found that there was a significant decrease in 8CldA after 48 h incubation in the absence of this nucleotide when compared to that seen on exposure for 6 and 24 h (Figure 4.1D). A significant decrease in 8CldG was also observed after re-incubation when compared to 2 and 6 h exposure (Figure 4.1E). Similarly, when treated with 5CldC under these conditions, the HCASMC had significantly decreased concentrations of the chlorinated nucleoside in DNA when compared to 2 and 48 h exposure (Figure 4.1F). These data suggest that the clearance of chlorinated nucleosides from DNA may occur more readily than that seen with RNA, but there is a large degree of variation in the initial incorporation of the nucleosides, particularly with the RNA experiments, between individual HCASMC donors. This results in a large error bar on the data in this case.

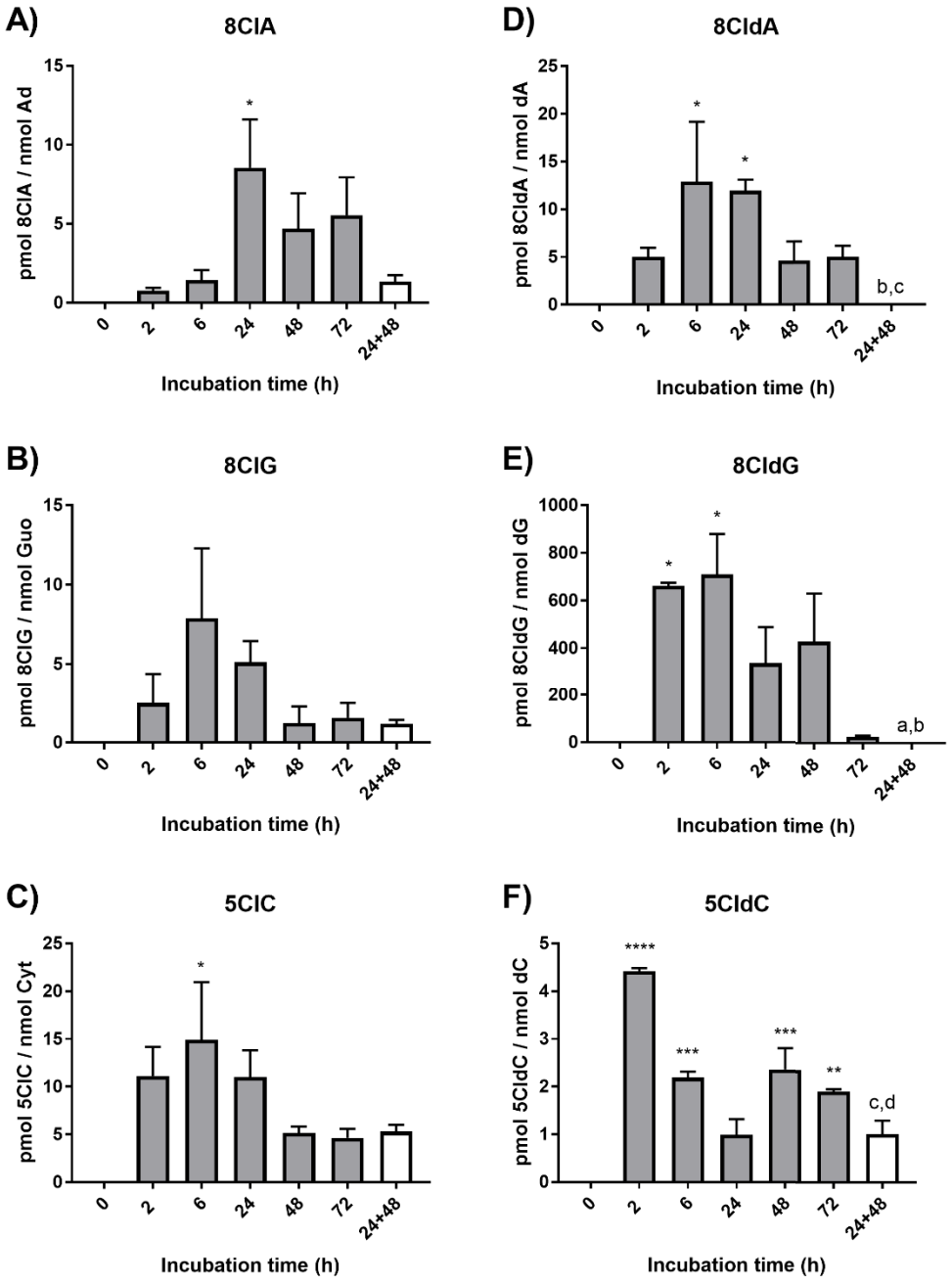

Figure 4.1: *Accumulation and clearance of chlorinated nucleosides into the DNA and RNA of HCASMC.*

*HCASMC (1 × 10^6 cells) were treated with 16 µM 8ClA (A), 8ClG (B), 5ClC (C), 8CldA (D), 8CldG (E) or 5CldC (F) for a period of 2 – 72 h (grey) or incubated with the chlorinated nucleoside for 24 h prior to washing and re-incubation without treatment in complete media for 48 h (white). After treatment, DNA and RNA was extracted, then hydrolysed and dephosphorylated prior to analysis by LC-MS/MS. The concentration of chlorinated nucleoside is shown as a 1:1000 ratio with parent nucleoside where results show the mean ± SEM of experiments performed with at least 3 separate donors. *, **, *** and **** show a significant difference (p < 0.05, 0.01, 0.001 and 0.0001, respectively) in incorporation of chlorinated nucleoside when compared to non-treated control. a, b, c and d show a significant decrease (p < 0.05) in chlorinated nucleoside compared to 2, 6, 24 and 48 h, respectively. Statistics were calculated using a one-way ANOVA with Sidak's multiple comparison test.*

4.4.2. Metabolic activity of HCASMC decreases with exposure to 8ClA, 8ClG, 8CldG and 5CldC

Given that each chlorinated nucleoside incorporated into the DNA or RNA of HCASMC, with some being cleared from the cells, studies were extended to determine whether there were functional changes to these cells. Initial experiments examined the metabolic activity of cells exposed to chlorinated nucleosides (4, 8 and 16 µM) using the PrestoBlue assay, after 24, 48 and 72 h of exposure (Figure 4.2). It was demonstrated that there were significant decreases in metabolic activity when HCASMC were exposed to 8ClA (16 µM), 8CldG (16 µM) and 5CldC (8 µM) for 72 h (Figure 4.2C). When HCASMC were exposed to 8ClA for 72 h, there is a dose dependent decrease in metabolic activity, though there is only a statistically significant decrease evident when the cells are exposed to 16 µM 8ClA (Figure 4.2C). This is similar to the effects of 8CldG on these cells, though decreases are found to occur to a lesser extent (Figure 4.2C). When HCASMC are exposed to 16 µM 5CldC, there was evidence suggesting a slight non-significant increase in metabolic activity (Figure 4.2A,B). However, after 72 h exposure to 5CldC, the metabolic activity of HCASMC was found to be unchanged compared to control when exposed to 4 µM and 16 µM 5CldC. Experiments were also performed with parent nucleosides and it was demonstrated that there were no significant alterations in the metabolic activity when compared to non-treated control.

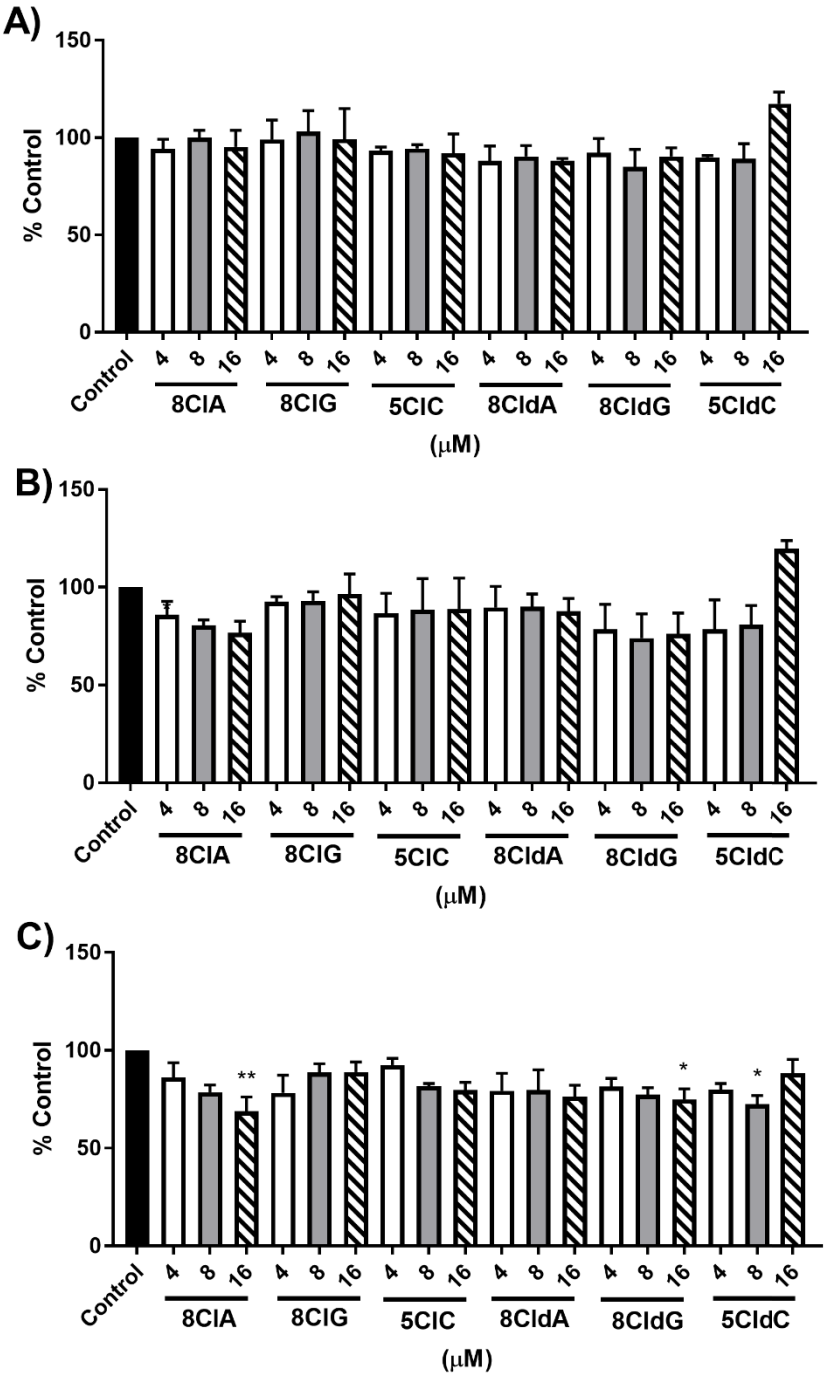

Figure 4.2: *Alterations in metabolic activity on HCASMC exposed to chlorinated nucleosides.*

*HCASMC (10^4 cells) were treated with multiple concentrations (4, 8 and 16 μM) for 24 (A), 48 h (B) or 72 h (C) of each chlorinated nucleoside prior to assessment of metabolic activity using Prestoblue reagent. The conversion of resazurin to resarufin was measured at λ_{ex} = 560 nm and λ_{em} = 590 nm using a plate reader. The results show the mean ± SEM of three separate experiments with independent cell donors completed in triplicate. * and ** show a significant difference ($p < 0.05$ and 0.01, respectively) in metabolic activity when compared to control using a one-way ANOVA with Dunnett's multiple comparison test.*

4.4.3. Exposure to 8ClA and 5CldC decreases proliferation of HCASMC

Changes in the metabolic activity can be reflective of altered viability or proliferation in these cells. Therefore, given the decreases in metabolic activity observed, experiments were then performed in order to determine the ability of HCASMC to proliferate following exposure to chlorinated nucleosides. HCASMC were exposed to the chlorinated nucleosides that were demonstrated to have an effect on metabolic activity (8ClA, 8CldG and 5CldC) with proliferation of these cells determined over time using trypan blue staining with the cells counted using a haemocytometer. Similar experiments were performed where HCASMC were exposed to parent nucleosides in order to determine whether the effects seen were related to chlorination of the nucleoside.

Treatments were performed for this experiment at a concentration of 8 µM in order to remain consistent between each chlorinated nucleoside and allow comparison with previous experiments performed with HCAEC. It was demonstrated that there was no alteration in cell number when HCASMC were exposed to 5ClC or 8CldG over a 96 h period (Figure 4.3A-B). However, when cells were exposed to 8ClA (8 µM) for 24 – 96 h, cell numbers were significantly decreased compared to non-treated and Ad treated controls (Figure 4.3C). Treatment with 5CldC also caused significant differences in cell number when compared to control and dC treated cells after 96 h (Figure 4.3D).

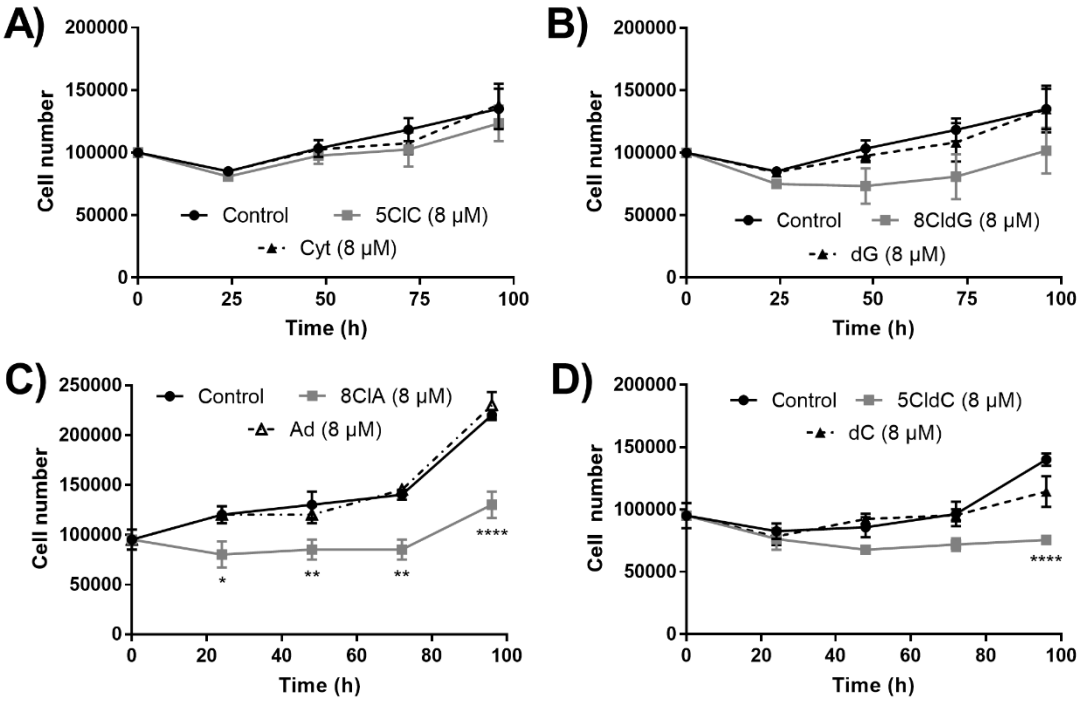

Figure 4.3: Proliferation of HCASMC when exposed to chlorinated nucleosides.
*HCASMC (10^5 cells) were treated with 5ClC (A), 8CldG (B), 8ClA (C) or 5CldC (D) for 24 – 96 h in order to determine cell proliferation. The total cell number was determined by cell counting with trypan blue staining. The results demonstrate mean ± SEM of 3 separate experiments completed with independent cell donors in triplicate. *, ** and **** show a significant decrease ($p < 0.05$, 0.01 and 0.0001, respectively) in cell number compared to untreated control cells using a two-way ANOVA with Tukey's multiple comparison post-hoc test.*

Due to the decrease in cell number observed when HCASMC were treated with 5CldC and 8ClA over a period of 96 h, the expression of KI-67 (a protein marker present in proliferating cells) was determined using flow cytometry (Figure 4.4). After treatment with 8ClA or 5CldC, HCASMC were fixed using ethanol followed by staining with an antibody against KI-67 prior to analysis by flow cytometry. After 24 h of treatment with 8ClA and 5CldC, there were no significant changes in KI-67 expression, though there was a significant increase when cells were treated with Ad and dC (Figure 4.4A), which is representative of increased cell proliferation. The increased expression when cells were exposed to Ad and dC were no longer observed after 48 h of treatment, though

treatment with 8ClA for this period of time significantly decreased the expression of KI-67 compared to control cells (Figure 4.4B). This is consistent with the results observed with trypan blue staining and cell counts using a haemocytometer. After 72 h, there were no significant differences in KI-67 expression between each of the treatments and non-treated control cells (Figure 4.4C). Interestingly, the expression of KI-67 was not shown to decrease when cells were exposed to 5CldC though there was a decrease in total cell number with trypan blue staining and cell counts. This may be due to the incubation time as significant differences were only observed with trypan blue staining and cell counts after incubation for 96 h.

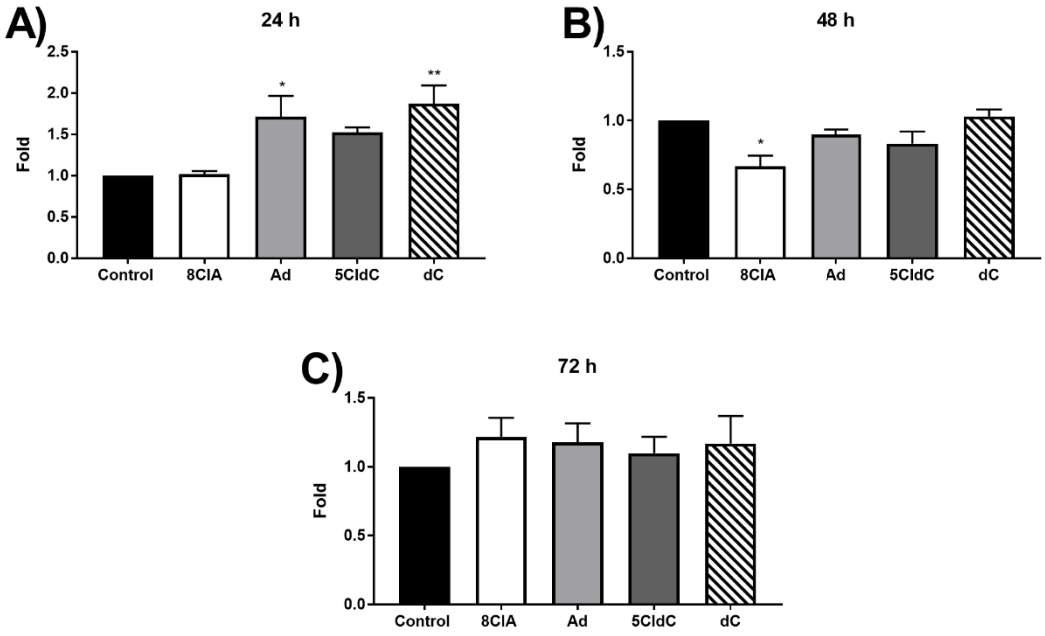

Figure 4.4: Expression of KI-67 in HCASMC exposed to chlorinated and parent nucleoside.

*HCASMC (2 × 10^5 cells) were treated with 8 µM 5ClC, 8CldG, 8ClA or 5CldC for 24 (A), 48 (B) and 72 h (C) prior to determination of KI67 expression by flow cytometry. The results demonstrate mean ± SEM of 3 separate experiments completed with independent cell donors in triplicate. *, ** and **** show a significant decrease (p < 0.05, 0.01 and 0.0001, respectively) in cell number compared to untreated control cells using a way ANOVA with Dunnett's multiple comparison post-hoc test.*

4.4.4. 8ClA and 5CldC do not cause apoptosis or necrosis in HCASMC

Due to the disturbances observed in metabolic activity and proliferation in HCASMC exposed to 8ClA and 5CldC, whether these effects were a result of cell death or cell senescence was examined. The effect of chlorinated nucleosides on apoptosis and necrosis in HCASMC was determined with Annexin V and propidium iodide staining, respectively. Treatment with 8ClA caused a non-significant decrease in the live population of cells when compared to control cells, which was not evident with Ad treated cells (Figure 4.5A). There were also no significant differences in cell death by apoptosis or necrosis when HCASMC were exposed to 5CldC for 72 h (Figure 4.5B).

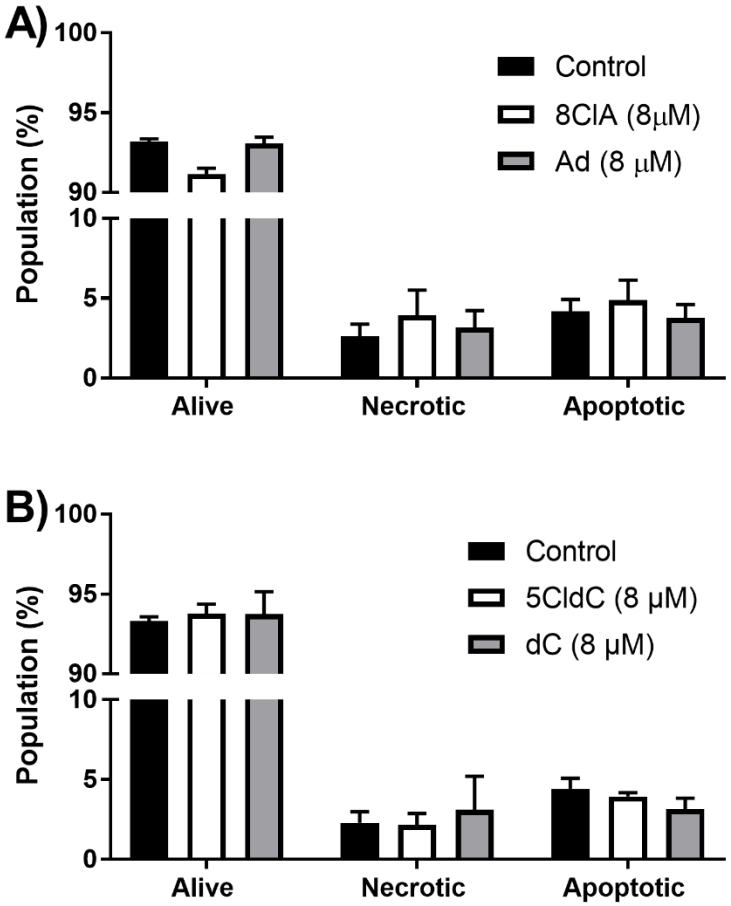

Figure 4.5: *Effects of 8ClA and 5CldC on cell death by apoptosis and necrosis.*
*HCASMC (2 × 10^5 cells) were exposed to 8 μM 8ClA (A), Ad (A), 5CldC (B) or dC (B) for 72 h prior to staining with Annexin PI and propidium iodide then analysed using flow cytometry to determine mechanism of cell death. Data represents mean ± SEM of experiments from 3 separate cell donors performed in triplicate. *, *** and **** (p < 0.05, 0.001 and 0.0001, respectively) represent a significant decrease when compared to non-treated control as determined by two-way ANOVA with Dunnett's multiple comparison post-hoc test.*

4.4.5. 8ClA and 5CldC do not cause calcium accumulation in HCASMC

Due to the decrease in live population in HCASMC exposed to 8ClA, further studies examined whether there were alterations in calcium signalling in these cells. The accumulation of calcium within the cytosol was assessed using Fluo-4AM staining with flow cytometric analysis. It was demonstrated that there was no significant change in

calcium staining when HCASMC were treated with 8ClA, Ad, 5CldC or dC (8 µM) for 24 or 48 h (Figure 4.6).

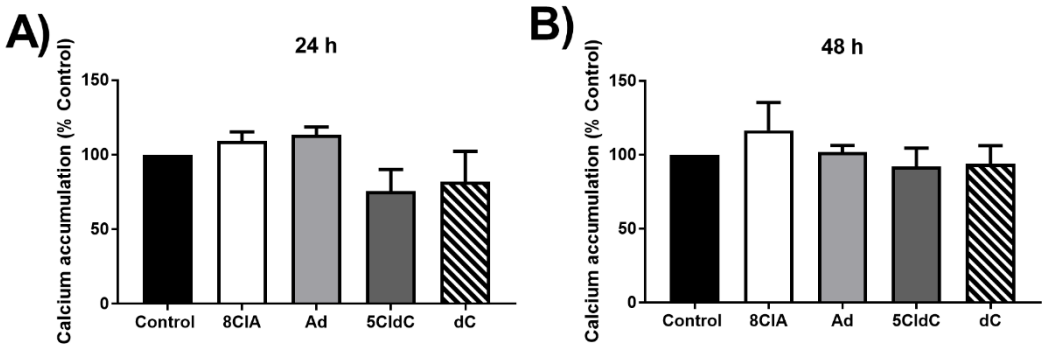

Figure 4.6: *Effects of 8ClA and 5CldC on calcium accumulation in the cytosol of HCASMC.*

*HCASMC (2 × 10^5 cells) were exposed to 8 µM 8ClA, Ad, 5CldC or dC for 24 (A) or 48 h (B) prior to staining with Fluo-4AM and analysis using flow cytometry. Data represents mean ± SEM of experiments from 3 separate cell donors performed in triplicate. *, *** and **** (p < 0.05, 0.001 and 0.0001, respectively) represent a significant decrease when compared to non-treated control as determined by one-way ANOVA with Dunnett's multiple comparison post-hoc test.*

4.4.6. 8ClA decreases mitochondrial function in HCASMC

There were no apparent differences in intracellular calcium or cell death by apoptosis or necrosis in the experiments with 8ClA and 5CldC and HCASMC, though there were effects on metabolic activity and proliferation. Therefore, experiments were performed to determine whether these chlorinated nucleosides altered mitochondrial function. The effects of chlorinated nucleosides on mitochondrial membrane depolarisation was determined by JC-1 staining coupled with flow cytometry, where a decreased red : green ratio was indicative of mitochondrial dysfunction. It was found that treatment with 8ClA induced mitochondrial dysfunction in HCASMC, evident through the significant decrease in red : green ratio when compared to non-treated and Ad controls (Figure 4.7C). These

effects were not evident when HCASMC were treated with 5CldC or dC (Figure 4.7D). In each of these experiments, carbonyl cyanide 3-chlorophenylhydrazone (CCCP), a mitochondrial uncoupler was used as a positive control for increased mitochondrial membrane permeability.

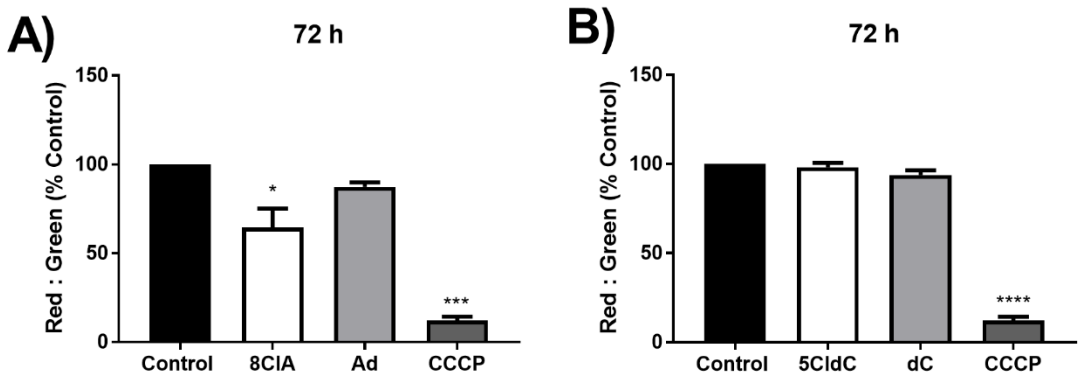

Figure 4.7: *Effects of 8ClA and 5CldC on mitochondrial membrane depolarisation.*
*HCASMC (2 × 10^5 cells) were exposed to 8 µM 8ClA (A), Ad (A), 5CldC (B) or dC (B) for 72 h prior to staining with JC-1 with or without CCCP prior to analysis using flow cytometry to determine mitochondrial membrane depolarisation. Data represents mean ± SEM of experiments from 3 separate cell donors performed in triplicate. *, *** and **** ($p < 0.05$, 0.001 and 0.0001, respectively) represent a significant decrease when compared to non-treated control as determined by one-way ANOVA with Dunnett's multiple comparison post-hoc test.*

4.4.7. 8ClA causes the decrease in cellular ATP through its incorporation to form 8-ClATP

Previous studies have demonstrated that chlorinated nucleosides, in particular 8ClA, can incorporate into the nucleotide pool and deplete stores of ATP [266, 280]. Therefore, due to the alterations observed in mitochondrial function and metabolic activity when cells were treated with 8ClA, the effect of this nucleotide, and also 5CldC, which decreased cellular proliferation, on the concentration of intracellular ATP was examined.

Cells were treated with chlorinated nucleoside prior to assessment of ATP concentration using the ATPlite luminescence assay system. When HCASMC were exposed to 8ClA for 24 and 48 h, the concentrations of ATP present within the cell were significantly decreased when compared to non-treated and Ad treated cells (Figure 4.8A, B). These differences were not observed when HCASMC were treated with 5CldC or dC (Figure 4.8C, D). However, as these concentrations were not normalised to protein concentration, loss in ATP concentrations when HCASMC were exposed to 8ClA may be due to cell death or cell lysis.

Within the literature [260, 266, 280] and in Chapter 3, it has been demonstrated that depletion of ATP when cells are exposed to 8ClA is associated with the formation of the chlorinated analogue of ATP, 8-ClATP. Therefore, the concentrations of 8-ClATP after treatment of HCASMC for 48 h with 8ClA (8 μM) were determined by HPLC. In this case, a BCA protein assay was performed in order to normalise the data to cell protein levels. It was demonstrated that when HCASMC were exposed to 8ClA for 48 h, that there was 8-ClATP formed, which was not the case in non-treated or Ad controls (Figure 4.8E, F). The HPLC experiments showed that there were no changes in the ATP levels between control and 8ClA or Ad treatment, which suggests that the decrease in ATP levels observed with the ATPlite luminescence assay system could reflect a degree of cell death or lysis.

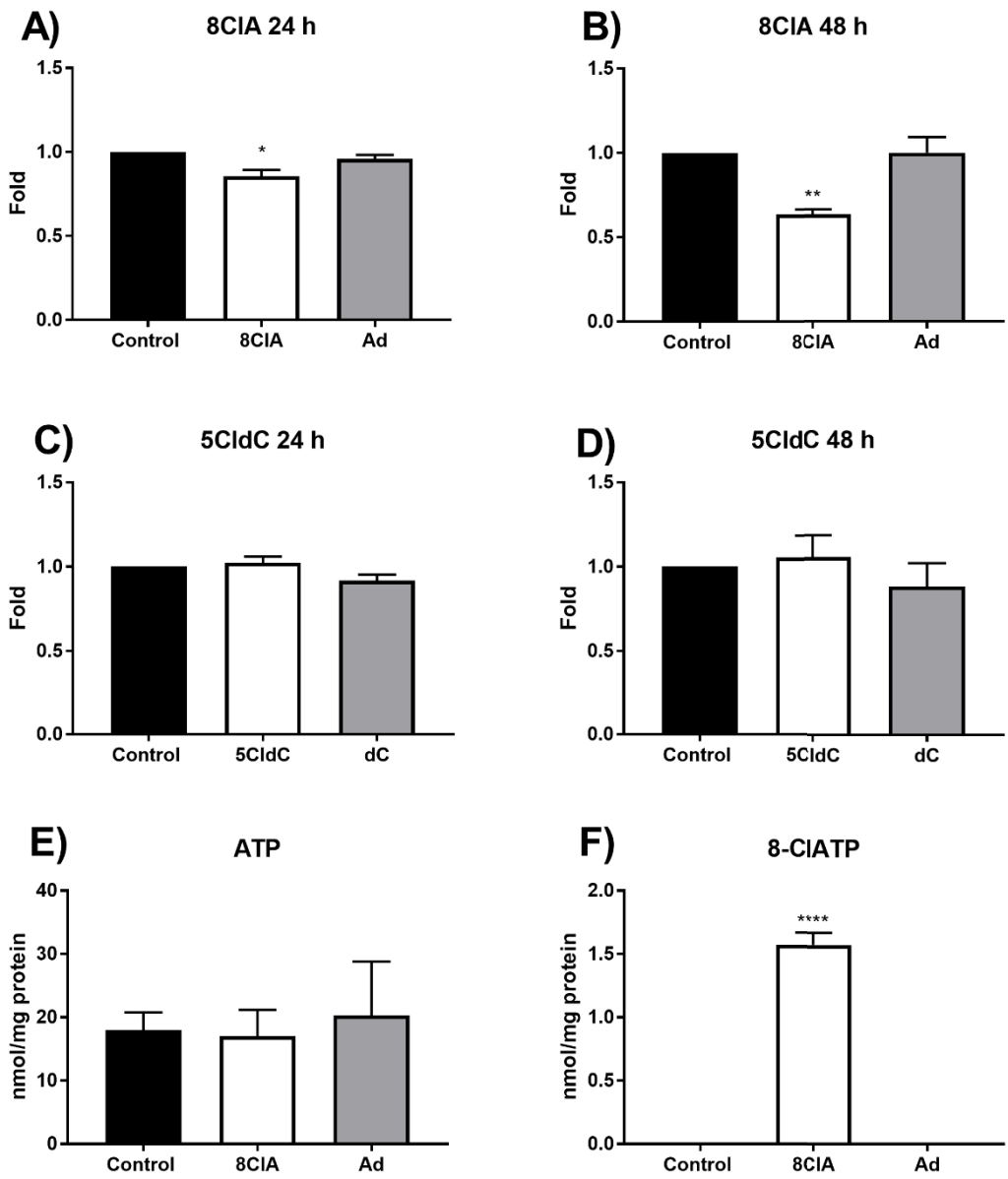

Figure 4.8: *Treatment with 8ClA causes the formation of ATP analogue, 8Cl-ATP.*
*HCASMC (1 × 10^4 cells) were treated with 8 µM 8ClA, Ad, 5CldC or dC for 24 (A,C) and 48 h (B,D) prior to determination of ATP concentration using ATPlite luminescence assay. HCAEC (6 × 10^5 cells) were treated with 8ClA and Ad (8 µM) for 48 h prior to quantification of ATP (E) and 8Cl-ATP (F) within the nucleotide pool using HPLC. Results show the mean ± SEM of experiments from 3 separate donors in triplicate. *, ** and **** show a significant decrease ($p < 0.05$, 0.01 and 0.0001, respectively) compared to untreated control cells using one-way ANOVA with Dunnett's multiple comparison post-hoc test.*

4.4.8. Exposure to 8ClA causes activation of the UPR and antioxidant responses in HCASMC

It was shown that in HCAEC, exposure to 8ClA caused cell death, which was attributed to activation of the unfolded protein response. Given the similarities in the behaviour of HCASMC and HCAEC on exposure to 8ClA, including altered metabolic activity and the accumulation of 8-ClATP, whether exposure to 8ClA caused activation of the unfolded protein response in HCASMC, was examined in this study. When HCASMC were exposed to 8ClA (8 μM) for 24 h, there were no significant changes in gene expression of ATF4 or CHOP (Figure 4.9A, D), which are part of the PERK signalling pathway in the unfolded protein response. However, there was a significant increase in the mRNA expression of GADD34 and sXBP1 (Figure 4.9B, C), which signifies reversal of PERK activation and the activation of the IRE1 signalling pathway, respectively. These results are consistent with the activation of the unfolded protein response, though the effects of 8ClA on HCASMC are not as profound as those observed in HCAEC.

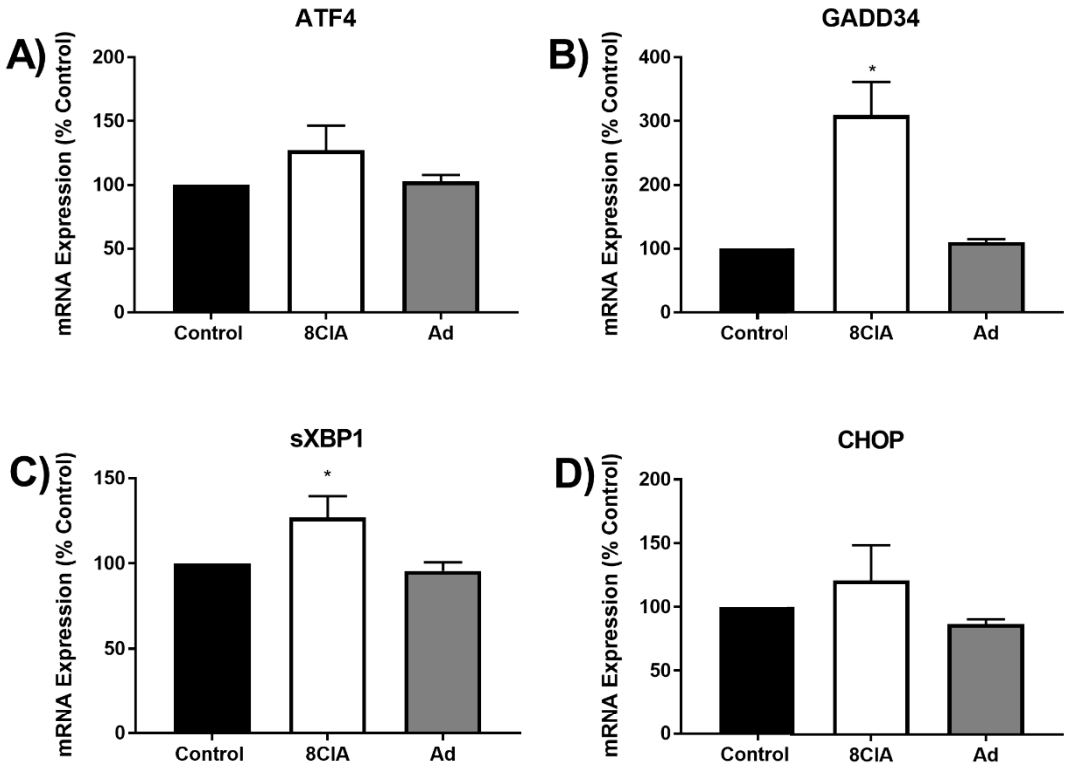

Figure 4.9: *Alterations on mRNA expression of genes related to the unfolded protein response.*

*Gene expression related to the unfolded protein response was determined in HCASMC (1 × 10^5 cells) treated with 8ClA or Ad (8 µM) for 24 h prior to analysis by qPCR. mRNA expression of ATF4 (A), GADD34 (B), sXBP1 (C) and CHOP (D) were normalised to two housekeeping genes, 18S and RPL13. Results represent the mean ± SEM of three independent experiments performed in triplicate. * demonstrates a significant increase ($p < 0.05$) compared to non-treated control using a one-way ANOVA with Dunnett's multiple comparison test.*

Furthermore, in the previous chapter, it was demonstrated that 8ClA induced antioxidant responses in HCAEC after exposure to 8ClA. ER stress (demonstrated through the activation of the UPR) has been correlated with the activation of cellular antioxidant responses including the Nrf2-Keap1 pathway [291]. Therefore, the mRNA expression of antioxidant genes was determined in HCASMC after exposure to 8ClA. There was evidence showing the activation of Nrf2 in HCASMC treated with 8ClA, through the significant increase in mRNA expression of GCLC (Figure 4.10A) and HO-1

(Figure 4.10B). However, in contrast to HCAEC, there were no significant changes in the mRNA expression of NQO1 (Figure 4.10C). Another marker of cellular stress, TXNIP, was also shown to have significantly increased mRNA expression in HCASMC after treatment with 8ClA (Figure 4.10D).

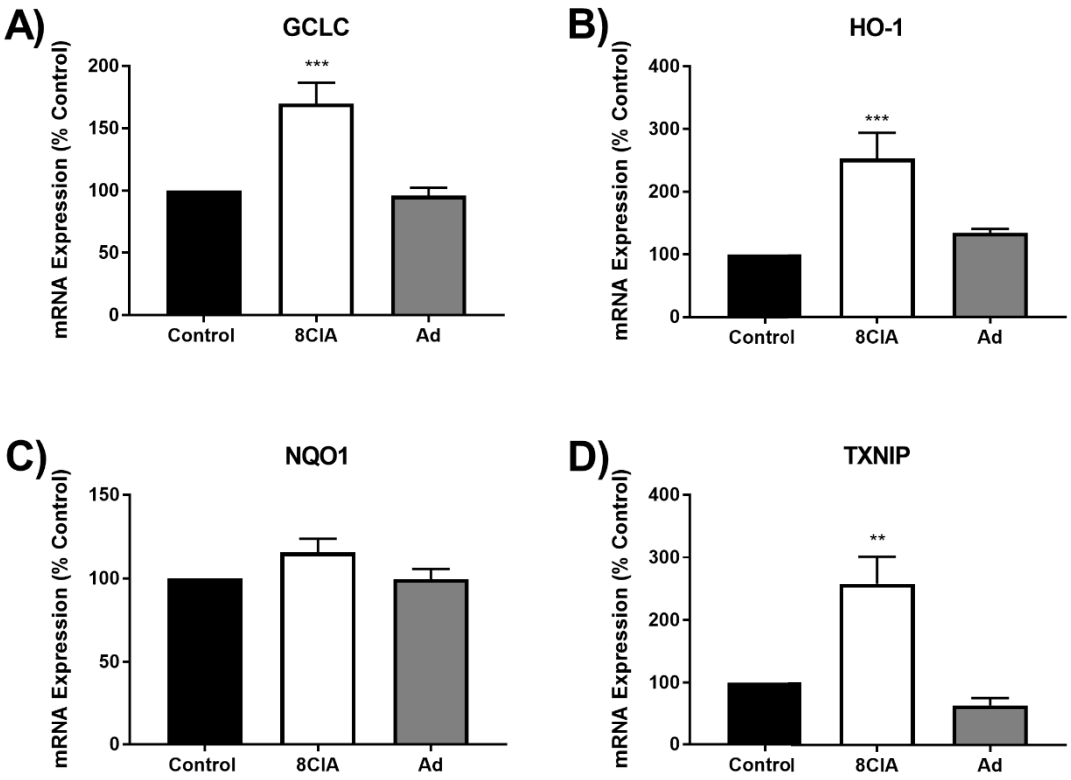

Figure 4.10: *The mRNA expression of genes relating to antioxidant response.*
*Gene expression related to the antioxidant response was determined in HCASMC (1 × 10^5 cells) treated with 8ClA or Ad (8 µM) for 24 h prior to analysis by qPCR. mRNA expression of GCLC (A), HO-1 (B), NQO1 (C) and TXNIP (D) were normalised to two housekeeping genes, 18S and RPL13. Results represent the mean ± SEM of three independent experiments performed in triplicate. ** and *** demonstrate a significant increase ($p < 0.01$ and 0.001, respectively) compared to non-treated control using a one-way ANOVA with Dunnett's multiple comparison test.*

4.4.9. 5ClдC caused increased expression of MMP2 and MMP9 in HCASMC

Due to the alterations in cell proliferation and metabolic activity when HCASMC were exposed to 8ClA and 5ClдC, studies were extended to examine the inflammatory response in HCASMC. Previous studies have demonstrated that treatment of macrophages with chlorinated nucleosides increased expression of pro-inflammatory cytokines and chemokines [259]. In addition, MMPs have been shown to be modulators of inflammation, with MMP2 shown to activate pro-IL-1β [312]. Therefore, the gene expression of MMP2 and MMP9 were determined after treatment of the HCASMC with each chlorinated nucleoside for 72 h. It was found that under these conditions, treatment with 8ClA (8 μM) did not significantly change the mRNA expression of MMP2 or MMP9 after 24 of 48 h treatment (Figure 4.11A-D). Similarly, the mRNA expression of MMP2 remained unchanged compared to non-treated control when HCASMC were exposed to 8 μM 8ClA for 72 h (Figure 4.11E). However, the expression of MMP9 in HCASMC after treatment for 72 h with 8ClA was significantly decreased when compared to non-treated control (Figure 4.11F). These differences were not observed when HCASMC were treated with Ad showing the causal role of the chlorination of the parent compound in the effects on mRNA expression shown.

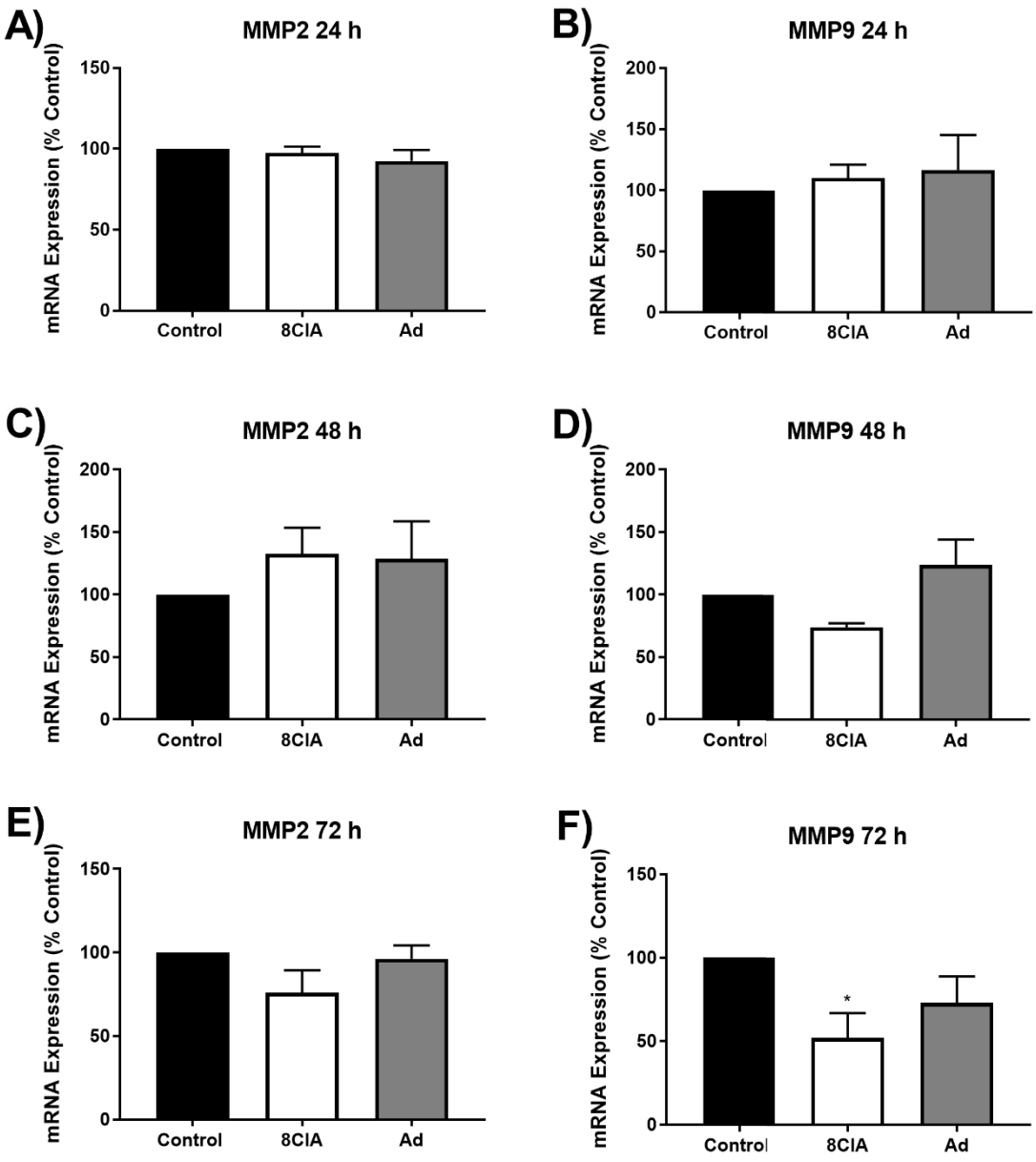

Figure 4.11: *mRNA expression of MMP2 and MMP9 in HCASMC exposed to 8ClA and Ad.*

*HCASMC (10^5 cells) were exposed to 8 µM 8ClA and Ad for 24 (A,B), 48 (C,D) and 72 h (E,F) prior to the determination of mRNA expression of MMP2 (A,C,E) and MMP9 (B,D,F) by PCR. Results were normalised to the expression of 2 housekeeping genes, 18S and RPL13. Data represent the mean ± SEM of experiments performed with 3 independent donors, completed in triplicate. * shows a significant difference ($p < 0.05$) compared to non-treated control using one-way ANOVA with Dunnett's multiple comparison post-hoc test.*

In contrast to the effects on MMP expression observed in HCASMC exposed to 8 µM 8ClA, exposure to 8 µM 5CldC was shown to significantly increase the mRNA expression of MMP9 but not MMP2 after exposure to this chlorinated nucleoside for 24 h (Figure 4.12A, B). Furthermore, after exposure to 5CldC for 48 h, marked increases in both MMP2 and MMP9 mRNA expression are observed when compared to non-treated control (Figure 4.12C, D). By 72 h of incubation with 5CldC, MMP2 mRNA expression levels were no longer significantly different when compared to non-treated control (Figure 4.12E). However, the mRNA expression of MMP9 after HCASMC were treated with 8 µM 5CldC for 72 h remains significantly elevated when compared to non-treated control (Figure 4.12F). These effects were not evident in the parent nucleoside controls consistent with the chlorination of dC driving the effects observed.

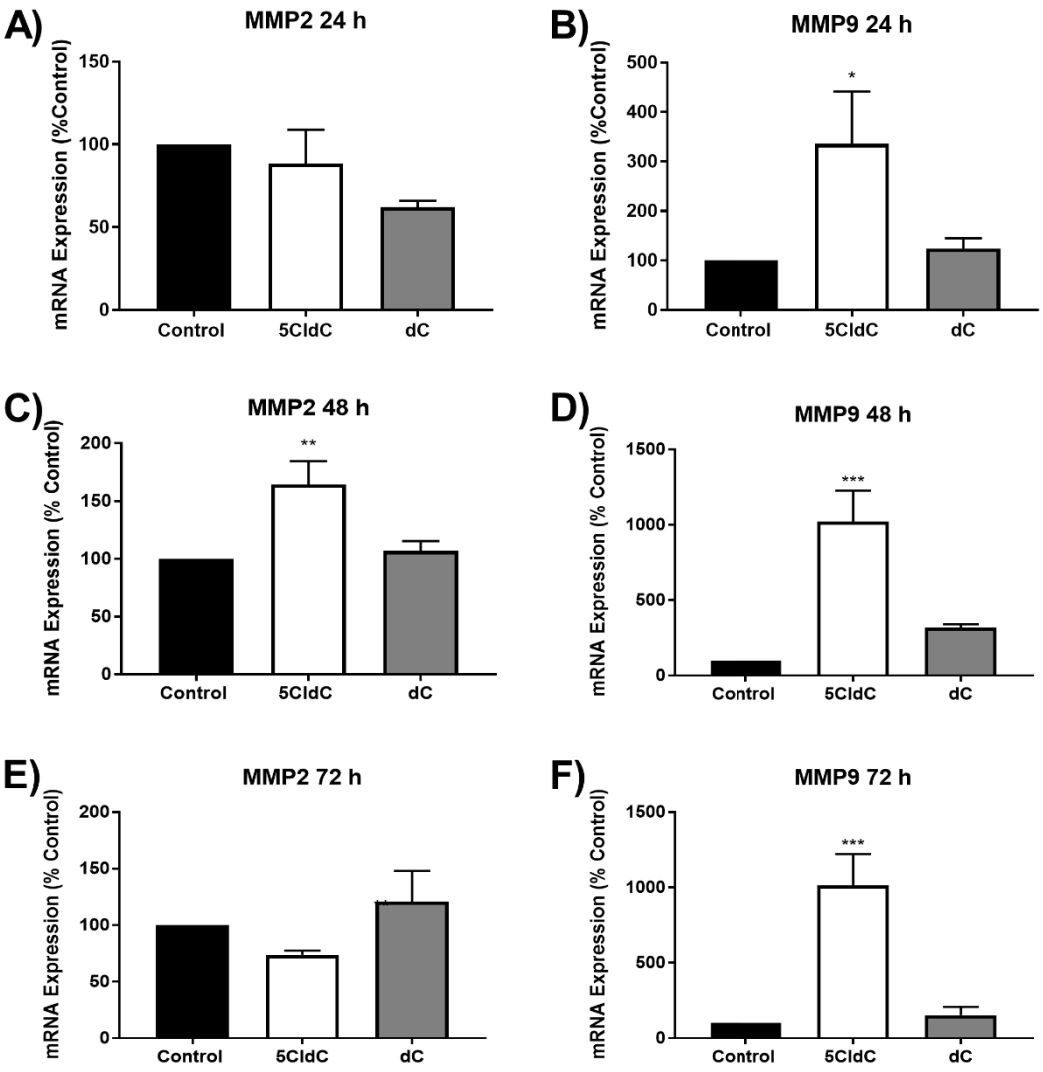

Figure 4.12: *mRNA expression of MMP2 and MMP9 in HCASMC exposed to 5CldC and dC.*

*HCASMC (10^5 cells) were exposed to 8 µM 5CldC and dC for 24 (A,B), 48 (C,D) and 72 h (E,F) prior to the determination of mRNA expression of MMP2 (A,C,E) and MMP9 (B,D,F) by PCR. Results were normalised to the expression of 2 housekeeping genes, 18S and RPL13. Data represent the mean ± SEM of experiments performed with 3 independent donors, completed in triplicate. *, **, *** show a significant difference ($p < 0.05, 0.01, 0.001$, respectively) compared to non-treated control using one-way ANOVA with Dunnett's multiple comparison post-hoc test.*

Given the increased mRNA expression of MMP9 in HCASMC exposed to 5CldC, the proteinase activity of MMP9 was measured. The activity of MMP9 and also MMP2 was determined by gelatin zymography, with quantification of the band density analysed using ImageJ (Figure 4.13A). These experiments showed that there were no significant changes in MMP2 activity (Figure 4.13B), though there was a small, but significant, increase in MMP9 activity (Figure 4.13C). This data shows that although there is an increased mRNA expression of MMP9, there seems to be no appreciable secretion of this matrix metalloproteinase into the cell media.

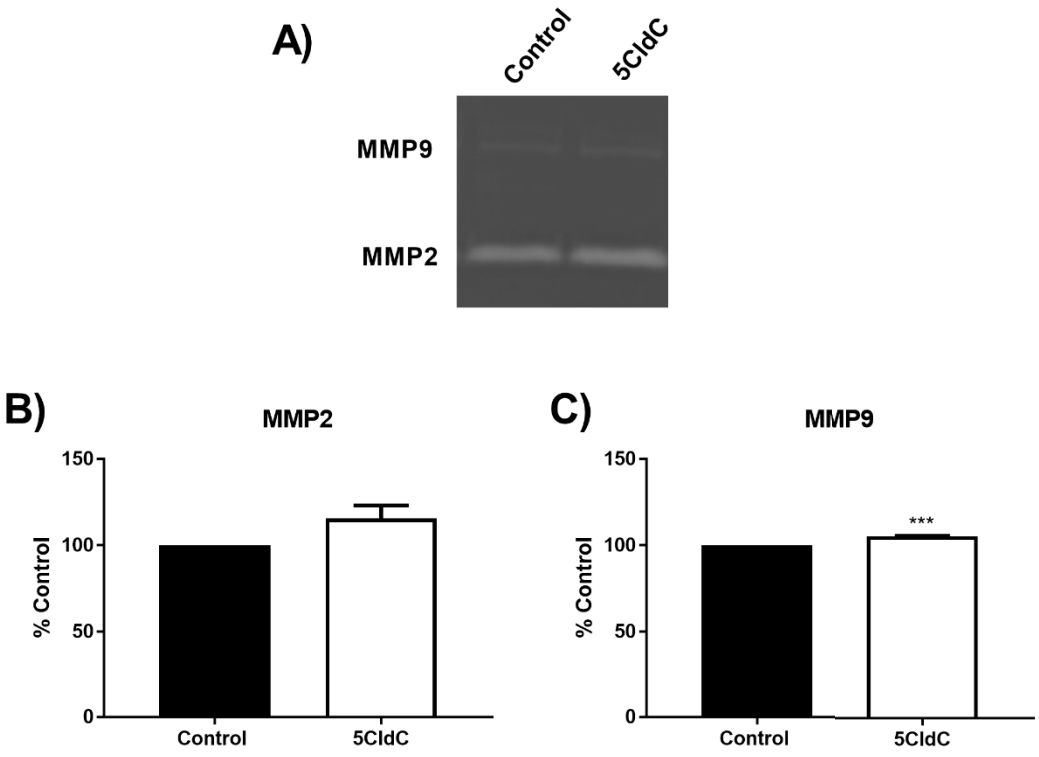

Figure 4.13: *Proteinase activity of MMP2 and MMP9 in HCASMC exposed to 8ClA and 5CldC.*

*The activity of MMP2 and MMP9 were determined in HCASMC treatment media by zymography (A) with density normalised to control (B,C). Data represent the mean ± SEM of experiments performed with 3 independent donors, completed in triplicate. *** shows a significant difference ($p < 0.001$) compared to non-treated control using a t-test.*

4.4.10. HCASMC exposed to 5CldC have increased expression of adhesion molecules

Due to the profound effects that exposure to 5CldC had on the mRNA expression of MMP2 and MMP9 in HCASMC, the mRNA expression of pro-inflammatory cytokines was determined. Recent studies have demonstrated that vascular smooth muscle cells express the adhesion molecules ICAM and VCAM causing the accumulation of leukocytes and activation of monocytes in atherosclerosis [313]. Therefore, the mRNA expression of ICAM and VCAM in HCASMC after exposure to 8 µM 5CldC was determined by qPCR. After HCASMC were exposed to 5CldC for 24 h, there was significant increase in the mRNA expression of ICAM when compared to non-treated control (Figure 4.14A). These changes were not observed in the mRNA expression of VCAM after 24 h exposure to 5CldC (Figure 4.14B). After 48 h of incubation with 5CldC, mRNA expression of VCAM had returned to levels similar to those in non-treated control cells (Figure 4.14C). In contrast, the mRNA expression of VCAM after HCASMC were exposed to 5CldC for 48 h was significantly increased when compared to non-treated control (Figure 4.14D). These changes in the mRNA expression of ICAM and VCAM were not evident when HCASMC were treated with the parent nucleoside dC showing the causal role for the chlorine on 5CldC in the alterations of mRNA expression.

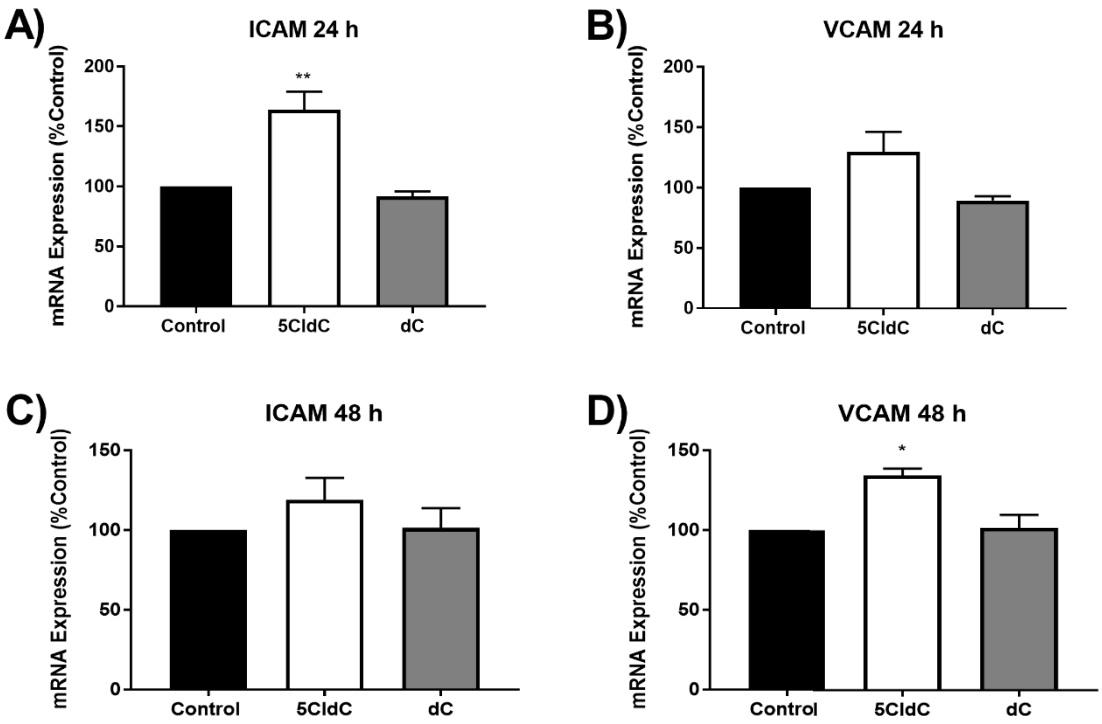

Figure 4.14: *Expression of adhesion molecules after HCASMC were exposed to 5CldC and dC.*

*HCASMC (10^5 cells) were exposed to 8 µM 5CldC and dC for 24 (A,B) and 48 (C,D) prior to the determination of mRNA expression of ICAM (A,C) and VCAM (B,D) by PCR. Results were normalised to the expression of 2 housekeeping genes, 18S and RPL13. Data represent the mean ± SEM of experiments performed with 3 independent donors, completed in triplicate. *, ** show a significant difference ($p < 0.05, 0.01$, respectively) compared to non-treated control using one-way ANOVA with Dunnett's multiple comparison post-hoc test.*

4.4.11. Exposure of HCASMC to 5CldC induces phenotypic changes

As MMPs have been demonstrated to modulate migration and proliferation of smooth muscle cells by degrading the extracellular matrix [314], the effect of 5CldC on phenotypic markers were determined. The mRNA expression of genes associated with the synthetic smooth muscle cell phenotype was determined by qPCR. It was found that the mRNA expression of OPN was significantly decreased on exposure to 5CldC (Figure 4.15A). However, these differences were also observed with dC treatment, which demonstrates a lack of specificity with regards to chlorination of the parent nucleoside. In contrast, when the mRNA expression of other markers of synthetic phenotype were measured, there were no significant differences observed when compared to non-treated control cells. Thus, the mRNA expression of S100A4 (Figure 4.15B), CX43 (Figure 4.15C), Decorin (Figure 4.15D) and Olfml3 (Figure 4.15E) remained unchanged compared to non-treated control cells when HCASMC were exposed to 5CldC.

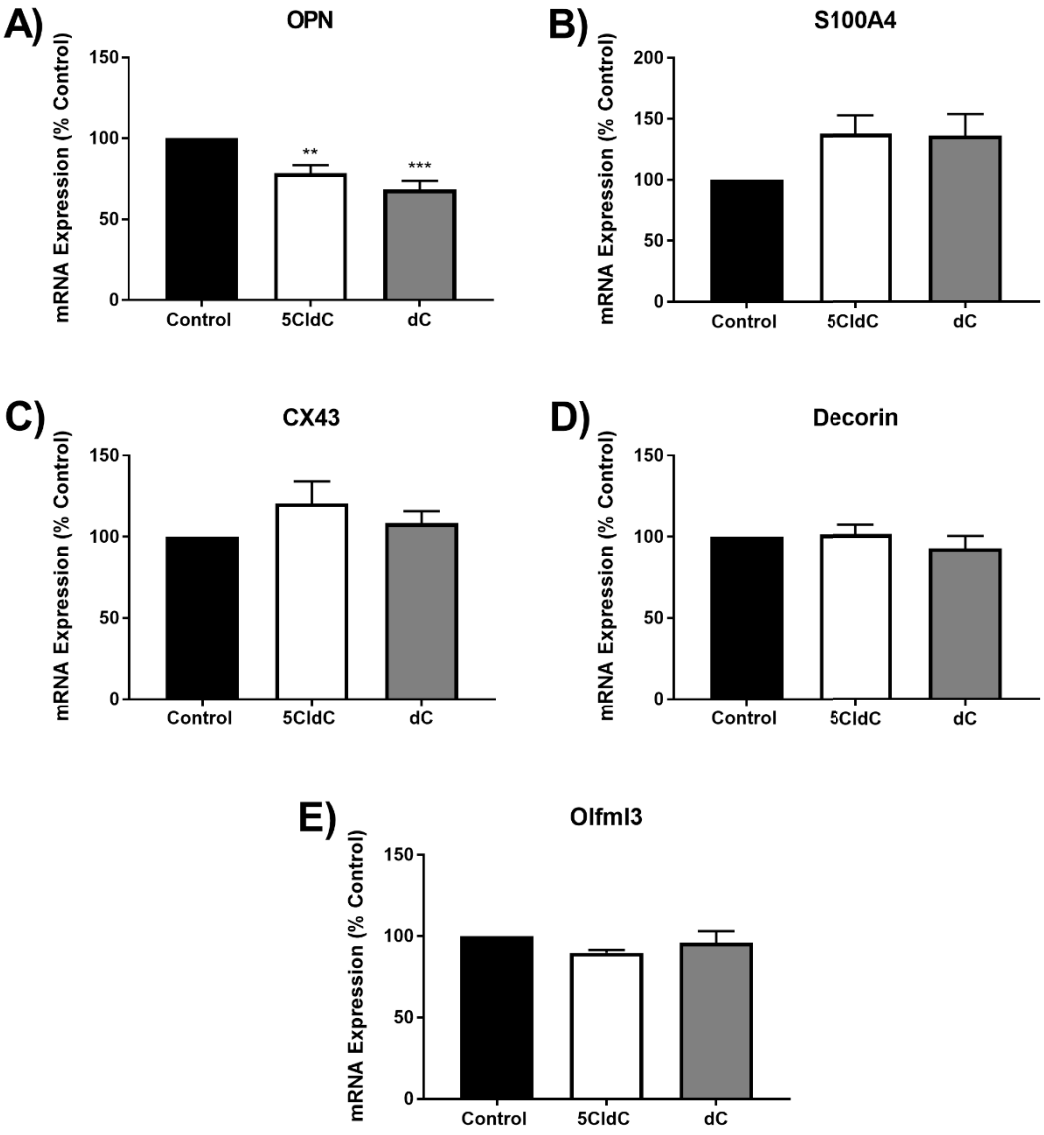

Figure 4.15: *mRNA expression of synthetic smooth muscle cell phenotypic markers.*
*HCASMC (10^5 cells) were exposed to 8 µM 5ClC or dC for 48 h prior to the determination of mRNA expression of OPN (A), S100A4 (B), CX43 (C), Decorin (D) and Olfml3 (E) compared to two housekeeping genes, 18S and RPL13, by qPCR. *, ** and **** show a significant difference ($p < 0.05$, 0.01 and 0.0001, respectively) compared to non-treated control using one-way ANOVA with Dunnett's multiple comparison post-hoc test.*

Further studies were performed in order to determine the effect of 5CldC on the mRNA expression of markers of the contractile phenotype. By qPCR, it was found that there were significant decreases in the mRNA expression of desmin (Figure 4.16A) and calponin (Figure 4.16B) when HCASMC were exposed to 5CldC. Treatment with the parent nucleoside dC did not induce changes in the mRNA expression of desmin when compared to non-treated control. However, mRNA expression of calponin was decreased when treated with dC compared to non-treated control, though to a lesser extent than HCASMC exposed to 5CldC. These data suggest that there may be a decrease in the contractile phenotypic markers measured in smooth muscle cells.

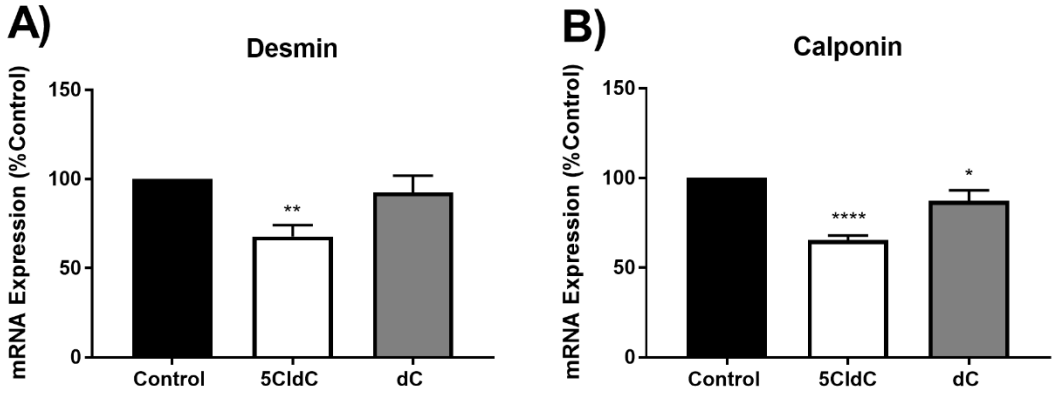

Figure 4.16: *mRNA expression of contractile smooth muscle cell phenotypic markers.*
*HCASMC (10^5 cells) were exposed to 8 µM 5CldC or dC for 48 h prior to the determination of mRNA expression of desmin (A) and calponin (B) by qPCR. Results were normalised to two housekeeping genes, 18S and RPL13. *, ** and **** show a significant difference ($p < 0.05$, 0.01 and 0.0001, respectively) compared to non-treated control using one-way ANOVA with Dunnett's multiple comparison post-hoc test.*

4.5. Discussion

In this Chapter, HCASMC were exposed to chlorinated nucleosides at concentrations that are similar to concentrations of chlorinated nucleosides formed when cells are exposed to HOCl at physiologically relevant concentrations [6], and those reported in patients supplemented with 8ClA or 8Cl-cAMP [283]. Initial studies were performed to determine the incorporation of each chlorinated nucleoside into the DNA and RNA of HCASMC by LC-MS/MS. The current study showed that chlorinated nucleosides incorporate into the DNA and RNA of HCASMC with exposure over a period of 2 - 72 h. Results demonstrate that 8ClA, 8ClG and 5ClC incorporate into the RNA of HCASMC and not into the DNA. Similarly, the deoxyribose chlorinated nucleosides 8CldA, 8CldG and 5CldC incorporate into the DNA of HCASMC and not into the RNA. These findings support those that were observed in HCAEC under the same conditions as described in Chapter 3.

Each chlorinated nucleoside reached maximal incorporation within 6 – 24 h of exposure, with the exception of 5CldC, which reached a maximum after incubation for 2 h. When HCASMC were exposed to 8ClA, maximal incorporation was found to occur after 24 h treatment, after which concentrations in the RNA decrease in a time dependent manner. This data is supported by the observation of the incorporation of 8ClA into the RNA of HCAEC (described in Chapter 3) and also in J774.A1 macrophages where 8ClA was demonstrated to incorporate into the RNA after 4 h [259]. The incorporation of this nucleoside into the RNA of HCAEC is 100-fold larger than the concentrations found in J774.A1 cells, which may reflect the differences observed in primary cell cultures and immortalised cells lines. The incorporation of 8ClA into the RNA of cells has significance

at previous studies have demonstrated the consequences of exposure to this chlorinated nucleoside [260, 266, 282, 315, 316].

Furthermore, 8ClG and 5ClC were demonstrated to incorporate into the RNA as well as 8CldA and 8CldG into the DNA of HCASMC. Maximal incorporation of these nucleosides occurred after exposure for 6 h, after which concentrations of chlorinated nucleoside decreased in the RNA or DNA over time. These results are supported by observations in HCAEC as described in Chapter 3. In addition, studies in J774.A1 macrophages demonstrated the incorporation of 5ClC into RNA, though the incorporation of 8ClG was not measured in these cells [259]. However, in contrast to the current study, the study performed in J774.A1 macrophages, demonstrated that 8CldA and 8CldG were not shown to be incorporated into DNA [259]. Furthermore, research performed using EA.hy926 cell line showed that 8Cl(d)G and 5Cl(d)C accumulated into the nucleotide pool and only 5ClC was found to incorporate into the RNA [224]. However, it has also been shown that the incorporation of chlorinated nucleosides was 40 – 227 times higher in a primary epithelial prostate cell line than compared to the EA.hy926 cell line which may reflect the reactivity of primary cells when compared to immortalised cell lines. In addition, the differences observed between the study conducted by Noyon et al. and the current study may be due to differences in the concentrations of chlorinated nucleosides used [224].

In this study, it was found that 8CldG was incorporated into the DNA of HCASMC much faster than other chlorinated nucleosides and also to the greatest extent. The mechanism by which the incorporation occurs and how quickly this process takes place

is unknown but would be interesting for future studies. The extent of incorporation of different chlorinated nucleosides may be due to the different affinities to their individual kinase. This is because the uptake and incorporation of these chlorinated nucleosides occurs firstly by transfer across the plasma membrane using a facilitated diffusion mechanism, followed by the phosphorylation of nucleosides by specific nucleoside kinases [317]. In addition, it has been demonstrated in non-modified nucleosides that the uptake is dependent on the concentrations of nucleoside extracellularly along with those present in the nucleotide pool [318], though this has not been studied in chlorinated nucleosides. What is known about the incorporation of chlorinated nucleosides, is that this is dependent on the structure on the nucleoside [256] as well as the cell type, as mentioned previously, which may account for the results observed in HCASMC.

Whether the HCASMC were able to clear the chlorinated nucleosides from the DNA or RNA was then determined by incubation with the chlorinated nucleoside for 24 h, prior to the removal of the exogenous source and re-incubation in complete cell culture medium for a further 48 h. It was found that when the cells were exposed to ribose chlorinated nucleosides that there were no statistically significant changes observed between incorporation and clearance studies. However, despite the incorporation of these chlorinated nucleosides into the RNA and the inability of the cells to remove them, only 8ClA and 5ClC were demonstrated to have significantly decreased metabolic activity.

When HCASMC were exposed to re-incubation conditions with deoxyribose chlorinated nucleosides, it was determined that only cells exposed to 8CldA had significantly decreased concentrations of 8CldA within the DNA. The concentration of 5CldC incorporated into the DNA of HCASMC remained unchanged in clearance studies compared to incubation for 24 h alone. The inability of 5CldC to be cleared from the DNA is demonstrated in HCASMC, which may explain the decrease in metabolic activity after exposure to 5CldC. This suggests that 5CldC is not cleared from the DNA of HCASMC by deamination as suggested in previous studies [200, 259]. In contrast, in studies with J774.A1 macrophages, it was demonstrated that concentrations of 5CldC in cellular DNA increased after re-incubation without exogenous source of 5CldC suggesting that 5CldC was incorporated into both the nucleotide pool as well as DNA in these cells [259].

In HCASMC, metabolic activity was used as a method to quickly determine which chlorinated nucleosides may have an influence on cellular function. It was determined was a significant decrease in metabolic activity with treatment with 8ClA, 5ClC, 8CldG and 5CldC. However, in studies performed in J774.A1 macrophages it was demonstrated that exposure to various chlorinated nucleosides at comparable concentrations induced increased expression of pro-inflammatory cytokines and chemokines, which occurred in the absence of significant changes in metabolic activity [259, 260]. This shows that though there were no changes to metabolic activity in HCASMC exposed to 8ClG and 8CldA, these chlorinated nucleosides may alter cellular function despite lack of changes to metabolic activity.

The studies performed in this chapter on HCASMC showed that 8ClA incorporated into the nucleotide pool to form 8-ClATP. As described in Chapter 3, exposure of HCAEC to 8ClA causes apoptotic cell death by activation of the unfolded protein response and the incorporation of 8ClA into the nucleotide pool to form 8-ClATP. Similar observations have been previously described with the toxicity of 8ClA being attributed to the depletion of ATP through the formation of 8-ClATP in macrophages [260], leukemic [280], myeloma [266, 268, 269], breast cancer [270] and mantle cell lymphoma [272] cell lines. In contrast, in HCASMC, 8ClA induces activation of the unfolded protein response, however these cells are able to recover and 8ClA doesn't induce apoptosis. Furthermore, the incorporation of 8ClA into the nucleotide pool of HCASMC to form 8-ClATP does not deplete ATP as shown in different cancer cell lines. This suggests that HCASMC are less sensitive to the exposure of 8ClA than HCAEC and cancer cell lines.

In vascular smooth muscle cells under normal conditions, there is low proliferation and low turnover [58]. However, during early atherogenesis and after vascular injury, there is increased proliferation [34]. This study has shown that treatment with 8ClA and 5CldC significantly decreased the cell number when compared to non-treated control cells when assessed over a period of 0 – 96 h. These differences were not observed with 5ClC and 8CldG treatment, though exposure to these agents also caused a decrease in metabolic activity. When HCASMC were treated with 8CldG, there was a trend towards a decrease in cell number over time. However, this was not found to be significant and this may be due to the concentration used in proliferation studies being lower than that used in the studies of metabolic activity.

The decrease in cell number was supported by a significant decrease in KI-67, a protein present in all active phases of the cell cycle but absent in cells that are non-proliferative [275], in HCASMC exposed to 8ClA. These differences were not evident in Ad treated cells, consistent with a causal role in the chlorination of Ad in these effects observed. However, in contrast, neither 5CldC nor the parent nucleoside dC altered the expression of KI-67, though there were decreases in cell number shown for 5CldC by cell counting methods. These findings are significant as it has been postulated that in advanced lesions, increased proliferation is beneficial in terms of improving plaque stability, which is not the case for cells exposed to 8ClA and 5CldC at least under the conditions examined here [34].

Interestingly, exposure of HCASMC to 8ClA induced mitochondrial dysfunction as demonstrated by JC-1 staining, however these cells did not die via apoptosis. The mitochondrial membrane potential is generated by the ETC and used by ATP synthase in order to fuse free phosphate to ADP to form ATP. This is consistent with observations in HCAEC where production of ATP by glycolysis was significantly impaired and other cells types where there are significant alterations observed with depletion of ATP [271, 272, 280]. Furthermore, during apoptosis, the mitochondrial membrane potential decreases due to the opening of mitochondrial permeable pores and causes the loss of the electrochemical gradient [319], though this is not the case in HCASMC as there were no significant increases in apoptosis despite activation of UPR with exposure to 8ClA.

In this study, it was demonstrated that 8ClA caused ER stress resulting in the activation of the UPR in HCASMC. Results showed that there were no significant changes to the

mRNA expression of ATF4 and CHOP. However, there were significant increases in the expression of GADD34 and sXBP1. GADD34 actions to dephosphorylate eIF2α thereby inhibiting translation of ATF4 activation [320]. Therefore, given that ATF4 mRNA expression was no longer significantly increased compared to control cells, it demonstrated the successful reversal of UPR activation. This contrasts what is seen in HCAEC, where exposure of these cells to 8ClA causes UPR activation and apoptotic cell death (see Chapter 3). Furthermore, Nrf2 was demonstrated to be activated in HCASMC and HCAEC after exposure to 8ClA, which is supported by studies demonstrating the correlation between endoplasmic reticulum stress and the activation of Nrf2-Keap1 pathway [287].

Studies also demonstrated that 5CldC induced mRNA expression of MMPs in HCASMC, which have been shown to be modulators of inflammation, in particular IL-1β [321]. This is supported by studies in J774.A1 macrophages where exposure to 5ClC significantly increased expression of IL-1β. Though the mRNA expression of MMP9 was elevated, the secretion of MMP9 into the cell media reflected by activity measurements was not significantly different compared to non-treated or dC treated control. In these studies, gelatin zymography was used to assess the activity of MMP2 and MMP9, however, this method may not have been sensitive enough to detect minute changes in the activity of these gelatinases. Therefore, future studies could use fluorescence probe methods in order to assess MMP activity [322, 323].

MMP9 has been shown to be elevated in atherosclerosis and lead to decreased plaque stability [324]. This suggests that exposure of smooth muscle cells to 5CldC may lead to

decreased plaque stability in atherosclerosis. Similarly, increased expression of MMP2 and MMP9 were demonstrated to increase the synthetic phenotype causing the migration of smooth muscle cells from the media to the intima [325]. However, in contrast, knockout of MMP9 shows an increase in plaque development, showing that increased MMP9 may prevent plaque development [326]. The increased expression of MMPs was not observed when HCASMC were treated with 8ClA. These findings suggest that 8ClA and 5CldC may have different mechanisms of action.

Previous studies have demonstrated that vascular smooth muscle cells express the adhesion molecules, ICAM and VCAM causing the accumulation of leukocytes and activation of monocytes in atherosclerosis [313]. In HCASMC, the mRNA expression of ICAM and VCAM were upregulated with 5CldC treatment. Previous studies have demonstrated that IL-1β induces ICAM expression [327], which may provide a link between the increased mRNA expression of MMP2 and 9 and the increase in ICAM expression in the current study as MMPs are modulators of IL-1β [321]. Therefore, future studies should determine the mRNA expression of IL-1β in order to confirm the link between the expression of MMP2/MMP9 and ICAM expression.

Though the mechanism by which ICAM and VCAM expression is activated is not fully elucidated, this could occur by activation of NF-KB. Furthermore, VCAM and ICAM can also be activated by the JAK/STAT pathway [328, 329], which may explain the time difference in the increased expression of these adhesion molecules. Despite the exact pathway causing the significant increase in the mRNA expression of adhesion molecules

in HCASMC exposed to 5ClдC not having been elucidated, the overexpression of these can propagate disease progression.

MMP2 and MMP9 are gelatinases that are responsible for the degradation of extracellular matrix in smooth muscle cells [330]. There is also evidence that MMP expression can promote smooth muscle cell migration [331]. In the current study, there was significant increase in MMP2 and MMP9 expression in HCASMC when exposed to 5ClдC for 48 h, therefore the effect of 5ClдC on phenotype was determined. Smooth muscle cells exhibit two broad phenotypes, contractile and synthetic [56, 307, 332-334]. Synthetic phenotype smooth muscle cells have differing morphology compared to contractile cells as well as increased proliferative and migratory properties [308]. In this study, markers of the synthetic phenotype, OPN, S100A4, Olfml3, CX43 and decorin were measured by qPCR. There were no significant alterations in these markers with the exception of OPN, where mRNA expression was significantly decreased after treatment with 5ClдC. However, this significant decrease in OPN expression was also observed in HCASMC treated with the parent nucleoside дC, which demonstrates that the effects observed are not specific to the chlorinated nucleoside. Further studies examined the mRNA expression of two contractile phenotype markers, desmin and calponin. When HCAEC were exposed to 5ClдC, there was a significant decrease observed in these contractile markers. A decrease in these markers demonstrates a shift into a more synthetic phenotype, which is more prevalent in early atherogenesis [334-337].

Taken together, the results of this chapter demonstrate that chlorinated nucleosides, in particular 8ClA and 5CldC may influence the development and progression of atherosclerosis.

4.6. Summary

The data presented in this chapter shows that chlorinated nucleosides have an impact on the homeostasis of HCASMC, in particular, 8ClA and 5CldC. The treatment of HCASMC with 8ClA induced similar effects to those observed in HCAEC, causing a decrease in metabolic activity and ATP concentrations due to the formation of 8-ClATP. Unlike what is observed in HCAEC, treatment with 8ClA does not cause detrimental effects to cell survival though the UPR is activated.

In contrast to studies performed in HCAEC, HCASMC function is altered by exposure to 5CldC. Exposure to 5CldC caused the decrease in metabolic activity and increases in the mRNA expression of MMP9. In 5CldC treated HCASMC, markers of synthetic phenotype remain unchanged, whereas markers of contractile phenotype were significantly decreased when compared to non-treated control. Given these observations, exposure of HCASMC to chlorinated nucleosides may affect the plaque stability and progression in atherosclerosis.

Chapter 5 – DNA damage in neutrophil extracellular trap formation

5.1. Introduction

Neutrophils are part of the innate immune system and subsequently part of the first line of defence to invading pathogen. They are the most abundant leukocyte, accounting for approximately 50% of the leukocytes in healthy people and 80% of the leukocytes in those who are fighting an infection [338]. Neutrophils are produced in the bone marrow in large amounts daily, in the magnitude of 10^{11} cells, from hematopoietic stem cells [339]. From there, they mature and enter the blood stream, where the cells will circulate until recruitment into tissue, through a process called the leukocyte adhesion cascade [340, 341]. The key function of neutrophils in immunity is to phagocytose and degrade foreign organisms such as bacteria, by activating proteases and producing reactive oxygen species, particularly HOCl via the activity of MPO [342].

In 2004, a landmark publication described the release of web-like structures released by neutrophils, which were able to capture bacteria [77]. These structures were termed NETs, released in a novel method of cell death, termed NETosis [343]. When neutrophils undergo NETosis, the traps released from the cell are composed of chromatin, with cytoplasmic and granular proteins, such as histones, neutrophil elastase and MPO decorating the DNA strands [77]. PMA is the most well studied inducer of NETosis, which has led to the elucidation of some of the key molecular mechanisms responsible for this phenomenon. PMA is a direct binder of protein kinase C, causing the release of internal stores of calcium with activation of the Raf-MEK-ERK pathway [344]. Subsequently, the

NADPH complex assembles at the membrane of the phagosome, causing the generation of ROS [343], which is necessary for the formation of NETs [77]. The release of ROS then activated granular proteases, inducing the formation of NETs [345]. Though PMA-induced NETosis is the most well described mechanism, there are multiple other inducers which have been identified including HOCl [102, 346], bacteria [77, 96, 343, 347, 348], fungi [349-356], viruses [356, 357], hydrogen peroxide [343, 358, 359], activated platelets [360-362], cigarette smoke [363] and calcium ionophores [358, 364-366].

NETs have since been detected in multiple pathologies including diabetes [367], systemic lupus erythematosus [368, 369], cystic fibrosis [370], cancer [371, 372] and cardiovascular disease [373, 374]. In cardiovascular disease, NETs have been implicated in thrombosis [375], myocardial infarction and also in atherosclerosis [78, 80, 376, 377]. Extracellular traps have been found to induce endothelial dysfunction by directly activating and damaging endothelial cells [378]. Once a plaque has developed, neutrophils have been found to adhere to atherosclerotic plaques through the release of NETs. Within the atherosclerotic plaque, NET components such as Cathepsin G attract more monocytes into the plaque [379].

Though primary neutrophils can be isolated from whole venous blood through various methods such as density centrifugation, the cells have a short lifespan, and there are variations between cell donors in relation to the sensitivity of the cells to undergo NETosis. Moreover, a high density of cells is required for experiments to characterise specific NET products, particularly oxidation products, which may be present in relatively

low abundance. The PLB-985 cell line is derived from the peripheral blood of an acute non-lymphocytic leukemia patient, and can be differentiated into cells with neutrophil-like properties [380]. Differentiation can be completed using stimuli such as DMSO, ATRA and dibutyryl cyclic adenosine monophosphate, which causes granulocytic maturation [380]. After granulocytic maturation into a neutrophil-like cell, PLB-985 can be stimulated with PMA in order to form extracellular traps [381] analogous to primary human neutrophils.

DNA oxidation and other modifications including chlorination, have been observed in inflammatory fluids and tissues, and are implicated in the development of disease. The oxidation of 2'-deoxyguanosine produces 8oxodG, which has been found to be a biomarker of oxidative stress [382], and is observed in pro-inflammatory conditions [211, 213, 215, 216]. Urinary excretion of 8oxodG is a good predictor of risk for the development of various cancers [215, 383, 384] and mortality in diabetes [248], with increased excretion correlating to poor outcome. 8oxodG has also been detected in the circulation and tissues of patients in many disease states such as Alzheimer's, diabetes [216, 385, 386], cardiovascular diseases [218, 387] and also in aging [388].

Another important physiological and pathological DNA modification is the formation of chlorinated nucleosides. Under inflammatory conditions, MPO catalyses the formation of HOCl, which reacts with DNA and RNA to form a range of chlorinated nucleosides [148]. The presence of chlorinated nucleosides has been described in pathologies including diabetes and atherosclerosis [16, 18]. Previous studies have used differing methods when quantifying chlorinated nucleosides including LC-MS, GC-MS or

immunochemical detection [17, 18, 226]. Overall, the most used method for quantification is LC-MS due to the ability to separate chlorinated and parent nucleosides through chromatographic separation and detection by monitoring the cleavage of the sugar moiety by MS.

In previous chapters of this thesis, chlorinated nucleosides were shown to cause various effects in vascular cells. Furthermore, there is evidence showing elevated levels of chlorinated nucleosides in atherosclerosis [16]. However, the source of these products is yet to be elucidated. Similarly, there are many studies demonstrating the pro-atherogenic properties of NET production, and catalytically active MPO is present on NET DNA [102]. This, together with the fact that NETs are released during chronic inflammatory conditions in the presence of HOCl and other oxidants, suggests that NET DNA could be subject to oxidative modification. Therefore, this chapter examines whether NETs produced by a model neutrophil cell line contain DNA with modified nucleosides.

5.2. Hypothesis and aims

It has been previously determined that HOCl is capable of inducing NETs in human neutrophils. Given than HOCl also reacts with DNA to form chlorinated nucleosides, it was hypothesised that HOCl-induced NETs in a human neutrophil cell line would contain chlorinated nucleosides. Therefore, the studies in this chapter aimed to optimise the differentiation of PLB-985 cells into a neutrophil-like cell, as well as optimise the

conditions required to induce NET formation using PMA and HOCl. The study also aimed to quantify the formation of chlorinated and oxidised nucleosides using LC-MS/MS.

5.3. Methods

PLB-985 cells were cultured and differentiated into neutrophils using RPMI-1640 supplemented with ATRA (1 µM or 2 µM), 1% FBS and 1.3% DMSO for 72 h (Section 2.3.2). The differentiation of PLB-985 was confirmed using May-Grünwald-Giemsa staining as described in Section 2.3.2.1.

A qualitative analysis of the stimulation of differentiated PLB-985 cells to produce NETs was optimised for treatment with PMA or HOCl (Section 2.4.1). The production of these NETs was quantified using Sytox Green staining (Section 2.4.2.1) or PicoGreen staining (2.4.2.2) plate reader methods.

After the optimisation of NET production in PLB-985, experiments were performed to quantify any DNA modifications present on NETs. After stimulation with PMA (50 nM) or HOCl (0.75 mM) for 4 h, the NETs were digested and released from the flask using DNase I. The DNA was then isolated from treatment media by precipitation with sodium acetate and ethanol and extracted using a DNA isolation kit (Section 2.5.1.1). The NET samples were prepared for LC-MS/MS as described in Section 2.5.2. The chromatographic separation and MS detection of parent and modified nucleosides of NETs was performed by LC-MS/MS as described in Section 2.5.3. A modified method was also developed for specific detection of 8CldG with increased sensitivity (Section 2.5.4).

5.4. Results

5.4.1. Differentiation of PLB-985 cells into neutrophils

Initial experiments were performed to optimise the differentiation of PLB-985 into a neutrophil-like cell. PLB-985 were differentiated using ATRA (1 µM or 2 µM) for 72 h in order to promote haematopoiesis and the formation of concaved nuclei [380, 389]. Cells that were incubated in complete media for 72 h in the absence of ATRA had round nuclei when visualised by May-Grünwald-Giemsa staining (Figure 5.1A). After differentiation with 1 µM (Figure 5.1B) and 2 µM ATRA (Figure 5.1C) for 72 h, the cell nuclei were more concave with a lobular morphology when visualised by May-Grünwald-Giemsa staining. This is consistent with PLB-985 having undergone haematopoesis and adopting a more neutrophil-like morphology.

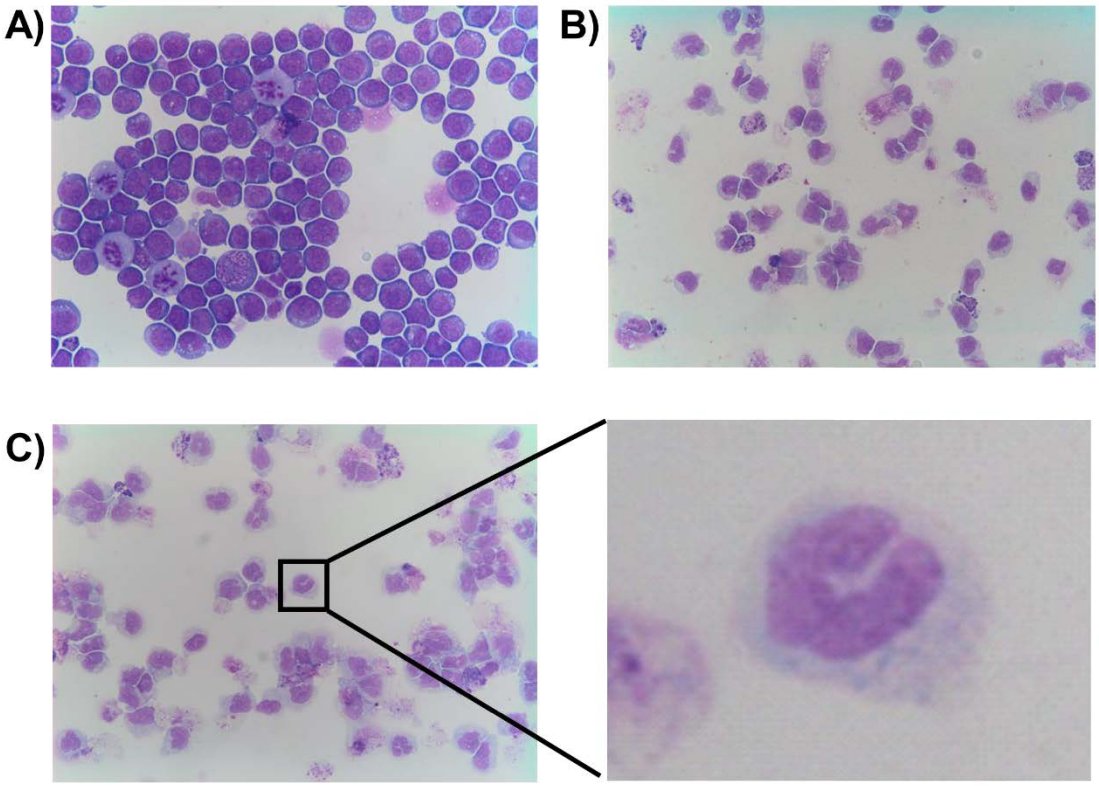

Figure 5.1: *May-Grünwald-Giemsa staining of differentiated PLB-985.*
PLB-985 were allowed to proliferate for 72 h (A) or differentiated in 1 µM (B) or 2 µM ATRA (C) for 72 h followed by staining with May-Grünwald-Giemsa. Images were taken using an Olympus Bx43 microscope with a 60 × magnification.

5.4.2. Optimisation of PMA-induced and HOCl-induced NET production in differentiated PLB-985

After the PLB-985 cells were differentiated, further optimisation experiments were performed for the treatment conditions required to induce NET release. Multiple concentrations of either PMA or HOCl were tested in order to determine if the release of NETs could be induced by these stimuli in accordance with experiments performed in primary human neutrophils [77]. NET release was visualised by Sytox Green, which binds to extracellular DNA [390]. It was found that cells differentiated with 1 µM ATRA for 72 h were not able to produce NETs, although the morphology of the cells was neutrophil-like (Figure 5.2). However, PLB-985 cells differentiated with 2 µM ATRA exposed to 25, 50 and 100 nM PMA (in HBSS supplemented with 0.5% FBS) for 4 h did release NETs (Figure 5.2A-C). It was found that 50 nM PMA produced NETs to the greatest extent as determined by microscopy (Figure 5.2A). Similarly, 2 µM ATRA differentiated cells were stimulated with 0.50, 0.75 and 1 mM HOCl (in RPMI-1640 containing 0.5% FBS) (Figure 5.2D-F) for 4 h, with 0.75 mM HOCl inducing the production of NETs (Figure 5.2E).

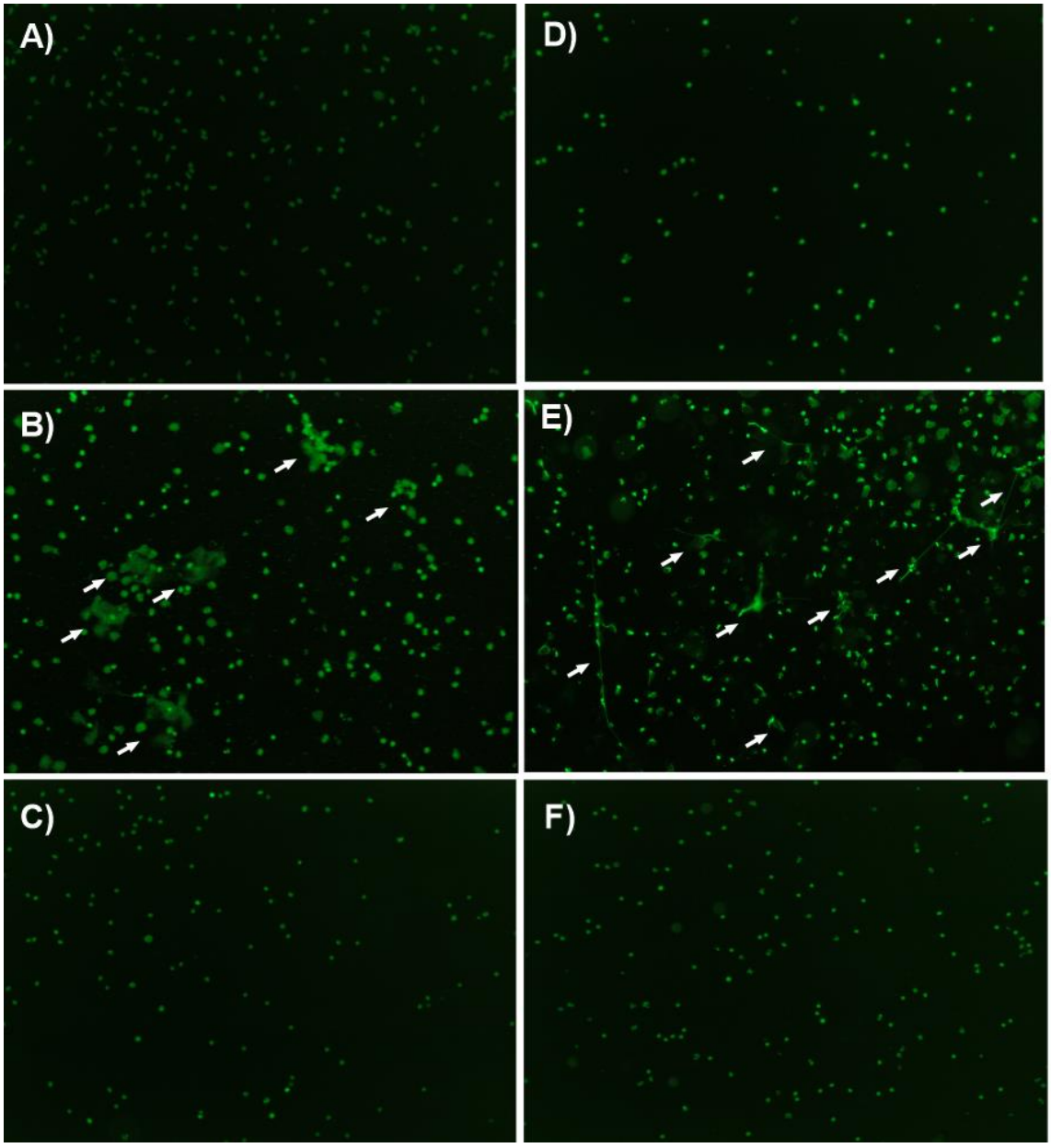

Figure 5.2: *Sytox Green staining of PMA and HOCl-induced extracellular trap release.*
Differentiated PLB-985 cells were stimulated with 25 nM PMA (A), 50 nM PMA (B), 100 nM PMA (C), 0.50 mM HOCl (D), 0.75 mM HOCl (E) or 1 mM HOCl (F). Samples were stained with 2 µM Sytox Green prior to imaging with an Olympus Bx43 FITC microscope with a 20 × objective. White arrows show NETs in (B) and (E).

5.4.3. Quantification of NETs produced by PLB-985 using Sytox Green reagent

In order to quantify the release of NETs by differentiated PLB-985 after treatment with PMA (10, 20, 25, 50 or 100 nM) for 4 h, experiments were performed where Sytox Green was added immediately following PMA treatment. The fluorescence of Sytox Green was measured using a plate reader, once an hour for 4 h at excitation and emission wavelengths of 504 nm and 523 nm, respectively. Exposure of differentiated cells to PMA did not induce an increase in Sytox Green fluorescence over time (Figure 5.3A). Similarly, there were no differences between non-treated differentiated control cells. It was also demonstrated that PLB-985 that have not been differentiated with or without stimulation with PMA have less Sytox Green fluorescence than differentiated cells; this may be indicative of DNA from cells that died during the differentiation process.

A second method of quantification was performed where differentiated PLB-985 cells were stimulated with PMA (10, 20, 25, 50 or 100 nM) for 4 h, after which DNase was then added to detach the NETs from cells. The cells were pelleted by centrifugation, then the supernatant was removed and stained using Sytox Green. It was demonstrated that there were no significant differences in Sytox Green fluorescence between each type of treatment (Figure 5.3B). Moreover, there was no difference between non-treated differentiated control and PMA-treated cells, suggesting that there was no increase in extracellular DNA in PMA treated cells. Similar to the first Sytox Green plate reader method, there was decreased Sytox Green fluorescence measured in non-differentiated control cells and non-differentiated cells exposed to 25 nm PMA.

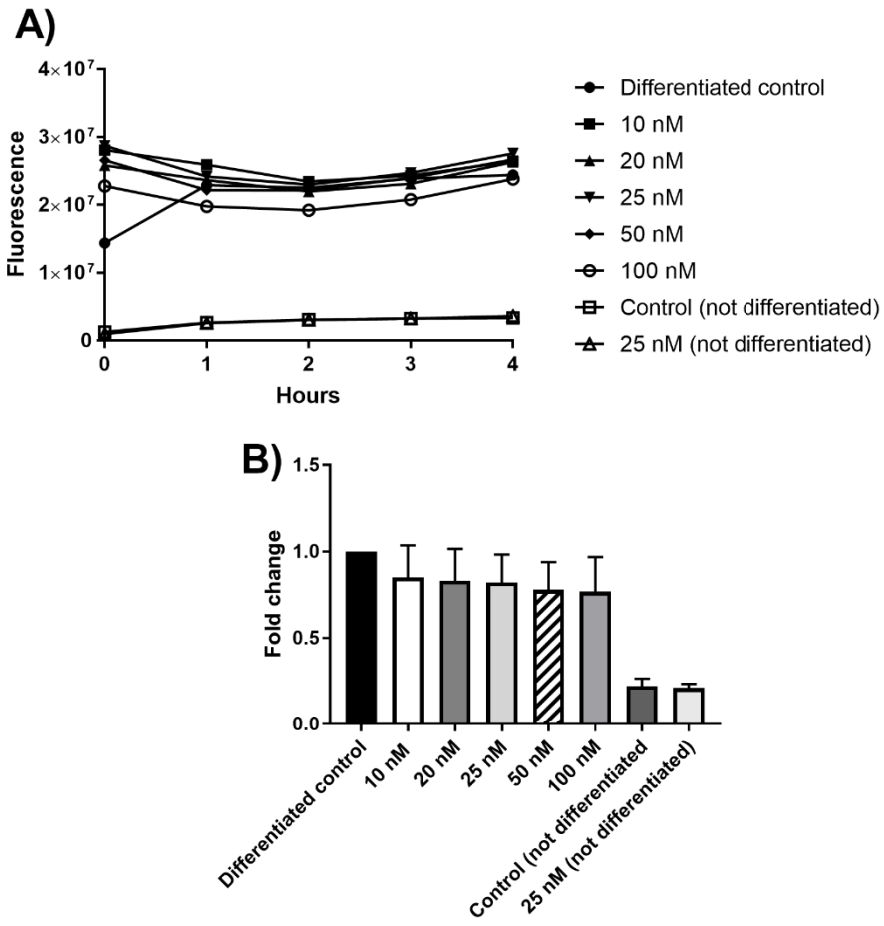

Figure 5.3: *Quantification of NET production by Sytox Green plate reader assay.*
Differentiated PLB-985 were incubated with increasing concentrations of PMA (10, 20, 25, 50 or 100 nM) and 2 µM Sytox Green before analysis using a plate reader, every hour for 4 h (A). (B) PLB-985 were incubated with PMA for 4 h before removal of NETs using DNase and EDTA. NETs were then stained using Sytox Green and fluorescence was measured by plate reader at an excitation and emission of 504 and 523 nm, respectively.

Overall, quantification of NETs stained with Sytox Green using the two plate reader methods described above did not reflect what was shown by microscopy. By microscopy, there was evidence demonstrating the production of NETs when differentiated PLB-985 cells were treated with 50 nM PMA in HBSS with 0.5% FBS or 0.75 mM HOCl in RPMI-1640 with 0.5% FBS. This suggests that the plate reader method is not reliable for quantifying NETS under these conditions.

5.4.4. Quantification of NETs produced by PLB-985 using PicoGreen reagent

Another method of quantifying NETs produced by PLB-985 with PicoGreen reagent was also employed. In this case, differentiated PLB-985 cells were incubated with PMA and HOCl for 4 h prior to detaching NETs from the cells using MNase and EDTA. Cells were then pelleted by centrifugation and the supernatant was stained with PicoGreen reagent. A significant increase in PicoGreen fluorescence was detected in differentiated PLB-985 treated with PMA (10, 25, 50 or 100 nM) (Figure 5.4A). Cells treated with PMA at each concentration tested had approximately 1.4-fold increase in PicoGreen fluorescence compared to the non-treated differentiated control. This showed that there was no dose-dependent effect on the fluorescence of PicoGreen. However, in cells stimulated with HOCl (0.25, 0.5, 0.75 or 1 mM) in RPMI-1640 with 0.5% FBS, it was found that there was no increase in fluorescence after 4 h when compared to non-treated control (Figure 5.4B).

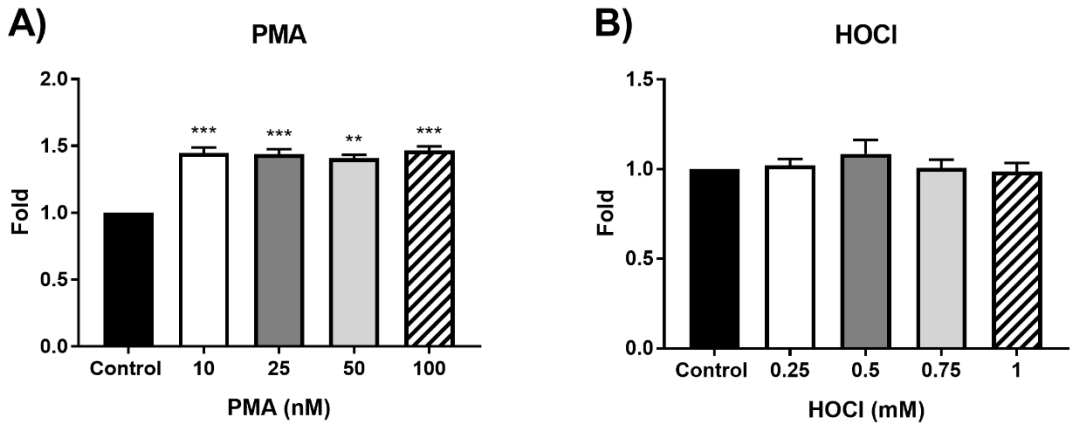

Figure 5.4: *Quantification of NET production in PLB-985 by PicoGreen plate reader assay. Differentiated PLB-985 cells were incubated with PMA (10, 25, 50 or 100 nM) (A) and HOCl (0.25, 0.5, 0.75 or 1 mM) (B) for 4 h. NETs were then digested using MNase and EDTA prior to PicoGreen staining. Fluorescence of PicoGreen was measured using a plate reader at an excitation and emission wavelength of 504 and 523 nm, respectively. Results represent mean ± SEM of three experiments performed in triplicate. **, *** show statistical significance p < 0.01 and 0.001 compared to control using a one-way ANOVA with Dunnett's multiple comparison test.*

Though there were significant increases in PicoGreen fluorescence in differentiated PLB-985 cells treated with PMA, these concentrations were not shown to induce NET formation when examined by microscopy (see Figure 5.2). This shows that staining with PicoGreen reagent may not be specific to staining extracellular DNA resulting only from NET release. Therefore, using a plate reader coupled with Sytox Green staining or PicoGreen staining cannot be used to quantify NET production under these conditions. Therefore, experiments were performed using LC-MS/MS to quantify DNA nucleosides, following isolation, and enzymatic hydrolysis and dephosphorylation of the NET DNA.

5.4.5. Detection and quantification of parent and modified deoxyribose nucleosides in NETs and cellular DNA

From the microscopy data, it is apparent that both PMA and HOCl induced NETs in PLB-985 cells differentiated with ATRA. After PLB-985 were differentiated in RPMI-1640 containing 1% FBS, 2 µM ATRA and 1.3% DMSO for 72 h, treatment with 50 nM PMA (in HBSS with 0.5% FBS) or 0.75 mM HOCl (in RPMI-1640 with 0.5% FBS) induced NET formation (see Figure 5.2). Experiments were performed with both control cells after differentiation and cells following stimulation with 50 nM PMA with quantification of DNA in the supernatant (NETs) and cells (nuclear).

Concentrations of parents nucleosides dA (Figure 5.5A), dG (Figure 5.5B) and dC (Figure 5.5C) were determined by LC-MS/MS. It was found that there was no DNA released into the cell media in differentiated control cells. As such, there were no nucleosides detected in the supernatant of differentiated controls (Figure 5.5). Quantification of dA and dG by LC-MS/MS demonstrated that there was a significant increase in dA and dG

present in the nuclear DNA of control cells when compared both NET and nuclear samples in PMA treated cells (Figure 5.5A, B). Concentrations of dC were shown to be significantly lower in nuclear DNA of cells treated with 50 nM PMA. In contrast to dA and dG, there were no differences between the concentration of dC between the NET samples in PMA stimulated cells when compared to non-treated control nuclear DNA samples (Figure 5.5C).

The analysis was extended to determine whether there were any oxidation products present on the DNA. 8oxodG was found to be present in PMA-induced NET lysate, control cell lysate and PMA treated nuclear lysate to varying extents. The total amount of 8oxodG was quantified to be 158.98, 66.78 and 58.67 pg in PMA-trap (from supernatant), control cell lysate and PMA-cell lysate, respectively, with a significant increase in the concentrations found with the NET DNA (from supernatant) rather than the DNA contained within the cell (lysate samples). Other chlorinated deoxyribose nucleoside modifications such as 8CldA, 8CldG and 5CldC were not found to be present in nuclear or NET DNA in control or 50 nM PMA-induced cells.

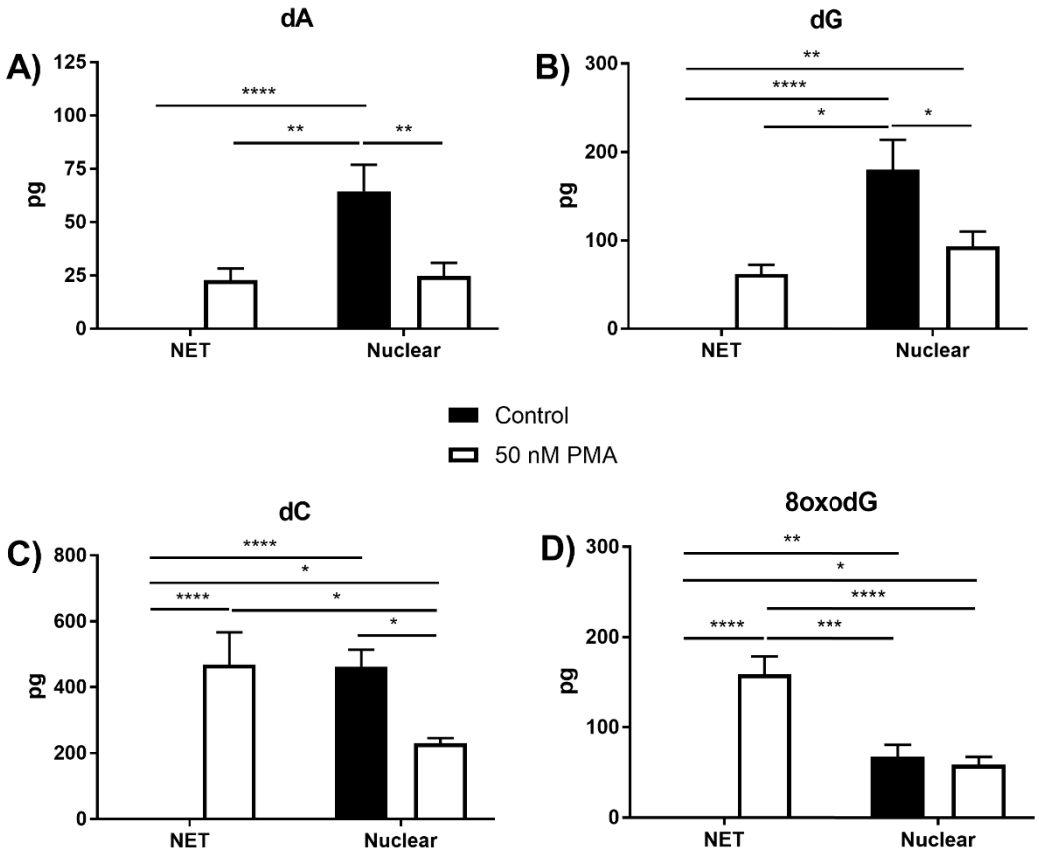

Figure 5.5: *Quantification of deoxyribose nucleosides from PMA-induced NETs and nuclear DNA.*

*DNA was extracted from the supernatant (NETs) or cells (nuclear) of differentiated PLB-985 cells with (white bars) or without treatment (black bars) with 50 nM PMA. Parent nucleosides, dA (A), dG (B), dC (C) and modified nucleoside, 8oxodG (D) concentrations were quantified by LC-MS/MS. Results demonstrate mean ± SEM of 3 separate experiments performed at different passage numbers. *, **, *** and **** show a significant difference (p < 0.05, 0.01, 0.001 and 0.0001, respectively). Statistics were calculated using a one-way ANOVA with Tukey's multiple comparison test.*

Similarly, experiments were also performed with differentiated PLB-985 control cells and those stimulated with 0.75 mM HOCl in RPMI-1640 with 0.5% FBS. Parent and modified nucleoside concentrations present in NET and nuclear DNA were quantified by LC-MS/MS. There was no DNA found to be released into the cell media in differentiated control cells shown by the absence of parent nucleosides in differentiated control supernatant samples (Figure 5.6).

Parent nucleosides (dA, dG and dC) were also quantified in control cell lysates, HOCl-induced NET samples and HOCl treated cell samples by LC-MS/MS. Concentrations of dA and dG were slightly decreased in HOCl cell samples compared to non-treated control cells, which may be due to the presence of these nucleosides in NET samples (Figure 5.6A, B). In these cases, the concentration of dA and dG were significantly decreased in HOCl-induced NET samples compared to non-treated control cell samples. dC was also found to be present in control cell lysates, HOCl-induced NET samples and HOCl treated cell samples, though there were no significant differences between these samples (Figure 5.6C).

There was also evidence shown for the presence of 8oxodG in HOCl-induced NET DNA (supernatant), control cell lysate and HOCl-treated nuclear lysate to varying extents. In HOCl NET DNA from the supernatant, control cell lysate and HOCl-cell lysate, the amount of 8oxodG was 318.06, 111.83 and 140.47 pg (Figure 5.6.D), respectively. There was a significant increase in 8oxodG present in HOCl-induced NET samples when compared to HOCl-treated cell samples and control cell samples. The chlorinated nucleoside, 5CldC, was also present in the cells and traps after stimulation with 0.75 mM HOCl for 4 h. The

total amount of 5CldC present in HOCl-trap samples was 36.76 pg and 83.24 pg in HOCl-cell samples (Figure 5.6.E). In comparison, there was no evidence for the presence of chlorinated nucleosides in differentiated control cell samples. 8CldA and 8CldG could not be detected in any control or 0.75 mM HOCl stimulated samples.

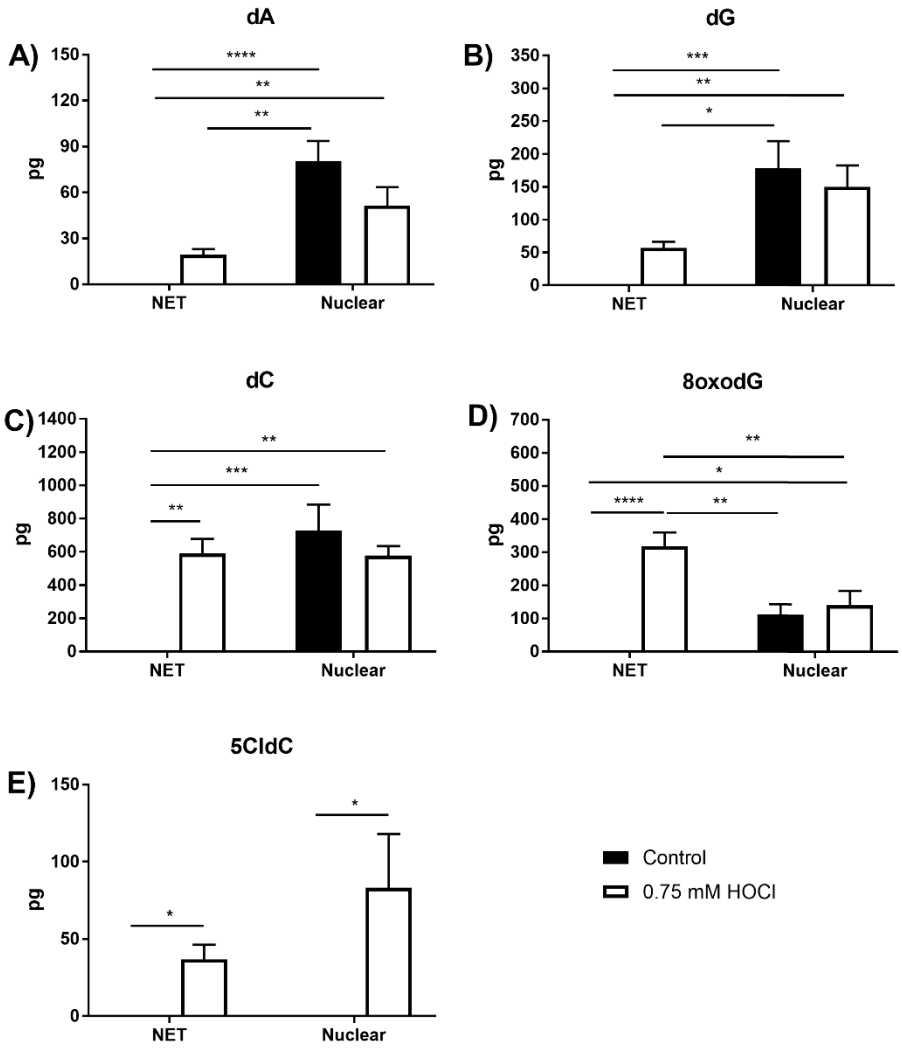

Figure 5.6: *Quantification of deoxyribose nucleosides from HOCl-induced NETs and nuclear DNA.*

*DNA was extracted from the supernatant (NETs) or cells (nuclear) of differentiated PLB-985 cells with (white bars) or without treatment (black bars) with 0.75 mM HOCl. Parent nucleosides, dA (A), dG (B), dC (C) and modified nucleosides, 8oxodG (D) and 5CldC (E) concentrations were quantified by LC-MS/MS. Results demonstrate mean ± SEM of 3 separate experiments performed at different passage numbers. *, **, *** and **** show a significant difference (p < 0.05, 0.01, 0.001 and 0.0001, respectively). Statistics were calculated using a one-way ANOVA with Tukey's multiple comparison test.*

5.5. Discussion

PLB-985 are a diploid cell line derived from the peripheral blood of an acute non-lymphocytic leukemia patient. These cells are able to be differentiated to form granulocytic or monocytic cells, dependent on the inducing agent [380]. In their normal state, PLB-985 cells are myelomonoblasts, which can be characterised by morphological, surface antigen and cytochemical staining analysis [380]. The growth of these cells in the presence of dibutyryl cyclic adenosine monophosphate, ATRA or DMSO promotes granulocytic maturation to neutrophils [380]. This was previously determined by histochemical staining, morphology and also by incorporation of 35S-methionine into neutrophil elastase and cathepsin G [380]. Once differentiated into neutrophils, studies have shown that treatment with PMA induced NET formation in these cells much like in human neutrophils isolated from whole blood [391].

Morphologically, PLB-985 cells have round nuclei and upon successful differentiation to a neutrophil, the nucleus becomes concaved [389]. The differentiation into neutrophils is generally confirmed using May-Grünwald-Giemsa staining, the presence of secretory vesicles and specific neutrophilic granules and cell surface receptor expression [389, 392]. In this study, it was demonstrated using May-Grünwald-Giemsa staining that PLB-985 incubated in RPMI-1640 with ATRA (1 or 2 µM), 1% FBS and 1.3% DMSO for 72 h induced differentiation into neutrophils. However, cells differentiated using 1 µM ATRA were unable to produce NETs upon stimulation with PMA despite appearing to have the morphology of a neutrophil.

Many studies have demonstrated differing methods of differentiation into neutrophils. Previously, PLB-985 have been differentiated into neutrophils using 0.5% dimethylformamide (DMF) with 1% Nutridoma-SP and 1% FBS in RPMI-1640 over a 6 day incubation period [393]. Another study used 0.5% DMF, 2 µM ATRA and 5% FBS in RPMI-1640 medium and reported that after a 6-day differentiation period PLB-985 were consistent with a neutrophil-like cell as analysed by May-Grünwald-Giemsa staining, cell surface CD11b expression and production of hydrogen peroxide [391]. In these studies, it was found that greater than 95% of the cells were found to be viable after the 6-day differentiation period. However, when the differentiation period was extended to 6 days as described in previous studies [391, 393], with a medium change on day 3, the cell viability was found to be <10% when stained with trypan blue. This is consistent with previously published data demonstrating a high cell death rate when differentiating with ATRA for a 6-day period [394].

In differentiated PLB-985 cells, it was demonstrated that PMA at a 50 nM concentration triggered NETosis after 4 h. In human primary neutrophils isolated from peripheral blood, many studies have reported the concentrations of PMA required to induce NET formation. In the initial study describing NETs by Brinkmann et al., it was determined that there were multiple stimuli that were able to induce NETosis, including PMA, interleukin-8 (IL-8) and lipopolysaccharide (LPS) [77]. This study determined that within 30 min of stimulation with 25 nM PMA, that NETs had begun to form. This has been demonstrated by other studies performed in primary neutrophils where NETs are shown to be induced using PMA after 3 h [74, 77, 96]. However, in this study, it was found that a higher concentration of PMA (50 nM) in HBSS supplemented with 0.5% FBS was

sufficient to induce extracellular trap formation and this was not observed at an earlier time point. Thus, the optimal differentiation parameters as well as concentration of PMA for the induction of NETosis were determined in this study.

Moreover, in differentiated PLB-985 cells, 0.75 mM HOCl in RPMI-1640 supplemented with 0.5% FBS was shown to induce NET formation. Though HOCl-induced NETs in PLB-985 cells has not previously been described, studies in primary neutrophils have shown that 0.75 mM HOCl can induce NET formation [346, 395]. In PLB-985 cells, HOCl is demonstrated to induce NET formation after 4 h of exposure, where release was demonstrated to occur between 30 min and 70 min after direct exposure of primary human neutrophils to 0.75 mM HOCl [346]. This may be due to the difference in reactivities between primary neutrophils isolated from whole blood and the differentiated, immortalised cell line PLB-985 used in this study, or changes in the composition of the media used, which could also alter the reactivity. Interestingly, in studies of HOCl-induced NETosis, HOCl is added to cell culture in the presence of media containing FBS [346]. Due to this, it is likely that HOCl reacts with serum, producing N-chloramines or other HOCl-derived oxidation products [396], which may induce NET production rather than HOCl itself.

NETs released after stimulation with 50 nM PMA or 0.75 mM HOCl for 4 h were visualised in this study using Sytox Green to stain extracellular DNA and microscopy using a FITC light filter. This method was used for qualitative assessment to provide evidence for NET formation during the optimisation process. Further studies were performed in an attempt to quantify NET production in PLB-985 stimulated with PMA or

HOCl. Previous studies have reported the use of Sytox Green staining of extracellular DNA coupled with a fluorescence plate reader in order to quantify the amount of extracellular traps produced after addition of stimuli [397, 398]. This study aimed to determine the amount of extracellular trap formed by PLB-985 after stimulation using similar methods. However, it was found that when the supernatant was stained with Sytox Green, that there was no increase in the fluorescence over time when Sytox Green was added along with the stimuli, with fluorescence measured hourly for 4 h. Similarly, when the extracellular DNA was digested using DNase and EDTA after 4 h of treatment to detach NETs from the cell prior to staining with Sytox Green, there was no significant change in the fluorescence between treated samples and non-treated control. The inability to detect changes in fluorescence with this method may be due to low sensitivity of the plate reader, or non-specific background fluorescence in the control cells. Therefore, it was determined that this was not a viable method in quantifying the NET production using the methods specified in this study.

This led to the use of another DNA stain, PicoGreen, which has been used in other studies in order to quantify NETs [399-401]. In this study, differentiated cells were stimulated with PMA or HOCl prior to digestion of the NETs using MNase to detach extruded DNA from the cells. It was shown that with PMA stimulation for 4 h, there was an increase in fluorescence compared to non-treated control. This was however evident at each concentration of PMA tested, which suggested a lack of specificity as microscopy demonstrated that only 50 nM PMA induced NET formation. This implies that fluorescence assay using PicoGreen stain is not a suitable method for the quantification NETs produced using the methods from this thesis. A limitation to the use of PicoGreen

is due to the assay detecting DNA that is released by non-NET pathways which may account for the results observed. The increase in fluorescence was not shown with HOCl treatment of differentiated PLB-985.

Further studies were performed using LC-MS/MS as a means to quantify DNA release and examine whether the extracellular DNA was modified by chlorination or oxidation. This method is valuable as it can separate all compounds of interest (dA, dG, dC, 8CldA, 8CldG, 5CldC and 8oxodG) using one method. However, the length of time required to complete one run is a limitation of this method. This method relies on the detection of MRM fragmentation in ESI+ mode where the m/z ratio decreases by approximately 116, signalling the loss of the deoxyribose sugar moiety. In the PMA-induced extracellular trap samples, the parent compounds and 8oxodG were detected. When the extracellular traps were induced by HOCl, it was found that parent compounds, 8oxodG and 5CldC were detected. Given the implications on the presence of elevated 8oxodG as shown in the literature in the context of cardiovascular disease and the effects of 5CldC on HCASMC (as demonstrated in Chapter 4), this may have implications in the progression of atherosclerosis.

In this study, the chlorinated nucleoside, 5CldC, was found on nuclear DNA and extracellular DNA in cells exposed to HOCl. This may reflect direct chlorination of the cellular DNA by added HOCl, rather than by activation or oxidant production by the PLB-985 cells as no evidence for chlorination was obtained in PMA-stimulated cells. Given that 5CldC is present in the nuclear DNA of PLB-985 cells that have released NETs as well as on the NET DNA, this suggests that the DNA may have been chlorinated in the nucleus

prior to extrusion of DNA by NETosis. The chlorination of dC to form 5CldC but not with other parent nucleosides is consistent with previous studies demonstrating a higher reactivity of HOCl with dC [6, 13, 200].

Though PLB-985 cells exposed to HOCl were demonstrated to have 5CldC present in cellular and extruded DNA, it is uncertain as to whether these products are formed by the reaction with HOCl or N-chloramines that can be formed through the reaction of HOCl and amino acids present in the treatment media. This is supported by previous studies, which have demonstrated that 5CldC can also be formed through the reaction of N-chloramines and DNA [6]. Previous studies have shown that 5CldC can be deaminated by cellular enzymes forming 5CldU [265]. The deamination of 5CldC produces significant effects as 5CldU has been established as a thymidine mutagen analogue, mispairing with guanosine and induces sister chromatid exchange [402-404]. Furthermore, these findings are significant as 5CldC has been demonstrated to incorporate into the DNA of different cell types [259, 265] and also to influence cellular function in HCASMC as described in Chapter 4.

Another modified product produced on PMA-induced NETs and nuclear DNA in PLB-985 was 8oxodG. There was evidence of 8oxodG in nuclear and NET DNA in both PMA-stimulated and HOCl-stimulated cells. In PLB-985 stimulated with PMA, the parent dG from the DNA in the nuclear and NET fractions together are similar to the amount of nuclear DNA from the non-treated control. However, with 8oxodG, the levels of oxidised nucleoside are elevated in the NET fraction showing that this oxidative modification occurs during NET release. These findings are not unexpected, as the exposure of cells

to PMA is known to activate NOX2 generating ROS [405], which is able to modify the dG moiety of DNA. However, it may also be possible that there is artefactual oxidation of dG during sample processing which has been previously described [222, 223, 227].

These findings are significant as 8oxodG is a marker of increased oxidative stress produced by the increase in ROS during inflammation [236]. Furthermore, studies have demonstrated that free 8oxodG has mutagenic properties as it is bypassed by DNA polymerases and due to its tendency to pair with adenine during DNA replication [237, 239]. 8oxodG has been shown to be present in multiple pathologies including cancer, diabetes and atherosclerosis, with some studies showing a correlation between concentrations of 8oxodG and the severity of disease [208, 236, 240, 253]. Given the presence of NETs in these pathologies [74, 78], the findings in this study may provide a source of DNA oxidation.

5.6. Summary

The differentiation of PLB-985 cells into neutrophils was optimised and it was demonstrated that differentiation caused granulopoiesis to occur, demonstrated by the change in nuclear morphology. After differentiation, PLB-985 can be induced using 50 nM PMA and 0.75 mM HOCl in order to produce extracellular traps. The process of extracellular trap production causes modification to the deoxyribose nucleosides in the extruded DNA and also within the cell. PMA-induced NETosis causes the production of 8oxodG, where HOCl-induced NETosis causes both 8oxodG and 5CldC to be present.

This may have important implications in atherosclerosis as NETs have been found in atherosclerotic lesions. Similarly, the formation of 8oxodG and chlorinated nucleosides have also shown to have detrimental outcomes within disease states. Overall, this data may provide new insight into the cellular source or origin of chlorinated and oxidised nucleosides in disease.

Chapter 6 – General Discussion

6.1. Overview

The role of the MPO-derived oxidant, HOCl, in various inflammatory diseases has been well described [107, 406-408]. Studies have demonstrated that HOCl readily reacts with most biomolecules including proteins, lipids and nucleic acids [12, 134, 180, 396]. At sites of inflammation, HOCl and chloramines react with DNA and RNA, which can result in the formation of chlorinated nucleosides. The presence of chlorinated nucleosides has been shown in various inflammatory diseases including infection, diabetes and atherosclerosis [16, 18]. These modified products have been detected in urine and inflammatory fluids from patients with these inflammatory diseases, suggesting that they may have relevance in disease.

Importantly, these products have been demonstrated to incorporate into the cellular RNA and DNA of various cell types [259]. In some cases, the downstream effects of chlorinated nucleosides, particularly 8ClA, which is used therapeutically, have been well described in the context of cancer [262, 266, 271, 272, 296, 315]. However, in general, the effects of these products have not been well studied in the context of atherosclerosis. Studies have shown that chlorinated nucleosides can induce the increased expression of pro-inflammatory cytokines and chemokines in murine macrophage cell models, which may promote lesion formation in atherosclerosis [259, 260]. In EA.hy926 endothelial cells, it was demonstrated that exposure to HOCl induced the chlorination 2-deoxycytidine, forming 5CldC. Furthermore, 5ClC and 5CldC are present in the plasma [224] and leukocytes [13] of healthy donors, respectively.

However, whether chlorinated nucleosides influence viability and cellular signalling in other vascular cells remained to be elucidated. Therefore, it was hypothesised that the exposure of different vascular cell types to chlorinated nucleosides would influence the function of vascular cells, promoting the development and progression of atherosclerosis. In line with the hypothesis, Chapters 3 and 4 in this Thesis aimed to examine the effect of chlorinated nucleosides on these vascular cells.

Though oxidised and chlorinated nucleosides are present in different inflammatory diseases, the source of these products is not certain or well defined. NET formation is linked with the development of atherosclerosis, with the presence of these structures shown to propagate atherogenesis [78, 81, 86]. The mechanisms by which NETs are released have been more well studied [96, 102, 352]. However, whether damage by oxidation or chlorination of the extruded DNA is relevant to disease remains to be elucidated. This is important as it could be a potential pathway by which NETs exert biological effects. Therefore, it was hypothesised that neutrophil extracellular traps may be a source of modified nucleosides in inflammatory environments. The experiments in Chapter 5 of this thesis aimed to characterise the modified and chlorinated nucleosides present in the nuclear and NET DNA of the model neutrophil cell line, PLB-985.

6.2. Sources and detection of modified DNA and RNA

DNA damage products have been studied as biomarkers of disease as they are present in inflammatory diseases such as cancer and atherosclerosis [205-210, 253]. There are a variety of DNA damage products that are formed *in vivo* with some providing insight into

the origin and nature of the oxidant resulting in their formation [204]. Prolonged oxidative stress prevalent in inflammatory states is known to result in the chlorination and oxidation of nucleic acids and results in the formation of modified nucleosides [6, 14, 15, 207, 409]. Given the stability of chlorinated nucleosides produced by HOCl-mediated modification of nucleic acids [6] and the detection of these in inflammatory diseases [13], they may be a suitable biomarker of disease.

In Chapter 5, results demonstrated that HOCl-induced NETosis in PLB-985 resulted in the formation of 5CldC but not 8CldA or 8CldG in both NET and nuclear DNA. These findings support the hypothesis that the exposure of PLB-985 cells would produce chlorinated nucleosides, though not all deoxyribose nucleosides were formed. The results are consistent with previous studies showing that 5CldC is produced to the greatest extent in DNA and cells exposed to HOCl [14]. Whether 5CldC is formed via NET-bound MPO or the HOCl used to stimulate the cells is not certain, but given the lack of chlorination with PMA stimulation, it may reflect the reaction with HOCl. Primary human neutrophils are more sensitive to stimuli as NETs are shown to be produced after 30 min incubation with HOCl [346], rather than the 4 h required with PLB-985 cells, which is a limitation. Future studies with primary neutrophils would therefore be useful, though there is the possibility for more donor variation and limitations due to the high number of cells required for analysis by LC-MS/MS.

As NETs are present in atherosclerotic lesions, where there is also an overproduction of HOCl [410], this source of extracellular DNA could lead to chlorinated nucleoside formation in a disease setting. Though only 5CldC was shown to be generated in PLB-

985 cells, it has been demonstrated that other chlorinated nucleosides can be produced during inflammation [6, 12-14, 16-18, 224, 256]. Other studies have also shown that chlorinated DNA damage products are elevated in animal models of oxidative stress. In a rodent model of inflammation, exposure to LPS induced elevated levels of 8CldG in the liver, 2 to 12 h after exposure [18]. In these animals, it was also demonstrated that there were elevated levels of 8CldG excreted in the urine 24 h after exposure to LPS [18]. In addition, another study performed in a murine model of inflammation, demonstrated that exposure to LPS resulted in the increased immunohistochemical staining of 5CldC [411]. Studies on human atherosclerotic lesions were conducted and it was shown that concentrations of 5ClUra were 10 times those found in healthy aortic tissue [16]. Given these findings, this implicates HOCl induced damage on DNA in inflammation and atherosclerosis. However, future studies should include the detection of other chlorinated nucleosides in atherosclerotic tissue samples.

A key limitation to the use of nucleic acid damage products as biomarkers relates to the abundance of these products compared to those produced in lipids, proteins and other metabolites [204]. Therefore, the detection of these products requires sensitive methods such as those coupled to MS. Furthermore, chlorinated and modified nucleosides have been shown to be further oxidised by ROS, reactive nitrogen species or reactive chlorine species when detected by GC-MS [201, 412, 413]. HOCl and peroxynitrite are produced at sites of inflammation and are both able to oxidised 8oxodG in order to form secondary oxidation products such as oxazolone and oxaluric acid [413]. Furthermore, when 8ClA was exposed to peroxynitrite, levels of 8ClA were shown to decrease in a concentration-dependent manner [201]. These effects were also

observed upon exposure of 5ClUra to peroxynitrite, though to a lesser extent [201]. Given the presence of these reactive species in chronic inflammation, this could make accurate quantification of chlorinated and modified nucleosides in disease states difficult.

In Chapter 5, both PMA-induced and HOCl-induced NETs were shown to have significantly increased concentrations of 8oxodG in NET and nuclear DNA. These findings also support the hypothesis that modified nucleosides would be present in PLB-985 stimulated with PMA or HOCl. Oxidised nucleic acid products, 8oxoG and 8oxodG, are also elevated in different inflammatory diseases [211, 213-216, 238, 239, 414, 415]. As such, NETs in these diseases may provide a potential source of 8oxodG. 8oxodG is elevated in serum and excreted in the urine of patients with diabetes [216, 248]. In addition to this, it has been demonstrated that diabetic patients with complications have significantly increased levels of 8oxodG excreted in their urine when compared to diabetic patients without complications [248]. Though these observations have been made, there has been no link described between 8oxodG levels and mortality rates in diabetic patients [221, 249].

In cancer and atherosclerosis, the formation of 8oxodG is related to an increase in ROS during disease development [208, 236, 253]. Some studies have shown a correlation between the concentrations of 8oxodG detected with the severity of CVD [208, 253]. It has also been shown within the literature that in atherosclerotic lesions, there is an increase in staining for 8oxodG when using immunohistochemistry methods and a significant increase in DNA repair pathways [207]. However, not only is 8oxodG a

biomarker used in disease, it has been shown to mispair in DNA with adenine [239]. Furthermore, free 8oxodG has mutagenic properties [239], and so it would be important to perform studies to understand these mutagenic properties in disease.

Chapters 3, 4 and 5 in this Thesis used LC-MS/MS in order to detect and quantify chlorinated and modified nucleosides. The method used in this Thesis was based on a previously published method, where the LOD was found to be 0.1 pmol for each chlorinated nucleoside (8ClA, 8ClG, 5ClC, 8CldA, 8CldG and 5CldC) by monitoring m/z of the molecular ion and the fragment ion formed from cleavage of the nucleoside at the sugar moiety [14]. In contrast, the LC-MS/MS method used in this Thesis found the LOD for each of the compounds to be in the high fmol range. A study performed in human leukocytes was more sensitive to chlorinated nucleosides where the LOQ was between 2 and 25 fmol for each of the chlorinated nucleosides [13]. However, a limitation of using this more sensitive method was that 8oxodG was not quantifiable [13], which was a modified nucleoside that was measured in Chapter 5.

In Chapter 5, it was demonstrated that both PMA and HOCl-induced NETs contained 8oxodG, which was also present in the nuclear DNA of PLB-985 cells. It would be interesting to study the effects of 8oxodG on different cells types to better understand the influence of this modified nucleoside on cellular homeostasis, given the presence of this nucleoside in disease. In studies quantifying 8oxodG, the method most often employed is LC-MS, due to the potential for heat-induced artefactual formation of 8oxodG by other methods such as GC-MS [222, 223, 227]. Some studies have quantified 8oxodG by enzymatic methods using FPG with visualisation of DNA cleavage by the

Comet assay [223]. However, the detection of these compounds is less sensitive than LC-MS/MS methods and can lack specificity, which is also the case with antibody detection [223].

The studies performed in this Thesis on HCAEC and HCASMC demonstrated the incorporation of 5ClC and 5CldC into the RNA and DNA, respectively, supporting the hypothesis. Studies in HCAEC and HCASMC showed that after the exogenous source of chlorinated nucleoside was removed and cells were reincubated in complete media, cells were unable to fully clear these compounds from their DNA and RNA. Previous studies have demonstrated that 5ClC and 5CldC can be deaminated forming 5ClUra [416]. GC-MS is the method described in order to detect 5ClUra in atherosclerotic lesions, owing to its high limit of detection compared to methods such as LC-MS and the poor ionizability of 5ClUra in the absence of derivitisation [16]. Therefore, future studies should be extended to measure 5ClUra levels in HCAEC and HCASMC exposed to 5ClC or 5CldC using GC-MS in order to determine whether the chlorinated product is being fully removed or deaminated to another chlorinated product.

Given that there are many methods used in order to quantify chlorinated and oxidised nucleosides, future studies should aim to quantify these products in diseased tissues as well as NETs or even macrophage extracellular traps in primary cells isolated from humans. In particular, measurements should focus on quantifying other chlorinated nucleosides such as 8ClA, 8ClG, 5ClC, 8CldA, 8CldG and 5CldC in atherosclerotic lesions. This would provide an important link between concentrations of chlorinated nucleoside

in atherosclerosis and the biological effects observed in vascular cells as demonstrated in this Thesis.

6.3. Biological impacts of chlorinated nucleosides on cell signalling and viability

Both studies *in vivo* and *in vitro* have reported the presence of chlorinated nucleosides during inflammation [6, 12-14, 16-18, 224, 256]. However, what remains less clear is whether these chlorinated adducts are biomarkers of disease or whether they can alter cell signalling, perturbing cell function. The ribose chlorinated nucleoside 8ClA, 8ClG and 5ClC and deoxyribose chlorinated nucleosides 8CldA, 8CldG and 5CldC are products of the reaction of HOCl with RNA and DNA [6, 12].

The experiments performed in Chapter 3 and Chapter 4 determined the effects of the exposure of HCAEC and HCASMC to chlorinated nucleosides, respectively. Using LC-MS/MS, this study determined that 8ClA, 8ClG and 5ClC incorporated into RNA of HCAEC and HCASMC, reaching maximal concentrations after 24 – 48 h of incubation. Similarly, 8CldA, 8CldG and 5CldC were shown to incorporate into the DNA of HCAEC and HCASMC. These findings support the hypothesis for both Chapters 3 and 4 where chlorinated nucleosides were thought to accumulate in the DNA and RNA of HCAEC and HCASMC. In murine macrophages, 8ClA, 8ClG and 5ClC were demonstrated to incorporate into RNA and only 5CldC but not 8CldA and 8CldG were shown to incorporate into DNA [259]. In the studies performed in HCAEC and HCASMC, there was no evidence for the incorporation of ribose chlorinated nucleosides into cellular DNA or the incorporation

of deoxyribose nucleosides incorporating into RNA. As these compounds are postulated to form during inflammation, the incorporation of or exposure to chlorinated nucleosides in vascular cells may alter atherosclerotic lesion progression due downstream biological effects.

Though each of the chlorinated nucleosides examined was shown to incorporate into RNA or DNA of HCAEC, it was demonstrated that only exposure to 8ClA altered the metabolic activity, cell signalling and viability of HCAEC at the incubation times tested. The effects demonstrated are supported by studies performed in Chapter 4 with HCASMC, as well as published studies in cancer cell lines [269-271, 280]. Though 8ClA incorporates into the RNA of vascular cells influencing cellular function, this chlorinated adduct has not previously been measured in an atherosclerotic lesion. As such, the presence of 8ClA would be important to quantify in order to determine whether 8ClA produced during the inflammation process in atherosclerosis could induce these effects in vascular cells. In a previous study, which determined the plasma pharmacology of 8ClA in mice, it was determined that administration of 8ClA resulted in the presence of 1.3 µM 8ClA in plasma [282]. Though this concentration may not cause functional effects in HCAEC or HCASMC, the concentrations used in Chapters 3 and 4 are comparable to what is seen in cells exposed pathologically relevant concentrations of HOCl [6]. The study of 8ClA in vascular cells is also relevant as 8ClA is currently in clinical trials in the treatment of chronic lymphocytic leukemia and acute myeloid leukemia [261, 262]. 8ClA is delivered by intravenous infusion in the treatment of cancer [261, 262] and therefore could influence the viability of vascular cells.

As well as the incorporation of 8ClA into the RNA of HCAEC, 8ClA was also shown to incorporate into the nucleotide pool to form 8-ClATP in both HCAEC and HCASMC. Furthermore, in HCAEC, these disturbances to cellular ATP occurred together with a decreased glycolytic ability of these cells. However, this contrasts to studies in cancer cells where depletion of ATP results in a significant increase in glycolytic ability [417]. Previous studies performed in cancer cell lines have shown that apoptosis upon exposure to 8ClA was caused by the depletion of ATP due to the formation of 8-ClATP [261, 262, 266, 269-272, 280, 282]. Further differences were observed in studies with murine macrophage cells where exposure to 8ClA caused increased measures of oxidative phosphorylation [260]. This may reflect the difference in bioenergetics between different cell types.

In studies performed in Chapters 3 and 4, 8ClA induced increased expression of antioxidant response genes and genes relating to the UPR. The UPR is a key stress response activated in cells under conditions of prolonged ER stress and has been linked to multiple pathologies including CVD [320]. In the ER, the protein folding capacity can be influenced by various factors including ischemia, oxidative stress and irregularities in calcium homeostasis [418]. The UPR is an adaptive pathway, which is induced during ER stress in order to promote protective cell survival mechanisms or to promote apoptosis [419]. Two ER sensors are involved in these adaptive mechanisms, IRE1 and PERK [420]. These two sensor proteins were activated in both HCAEC and HCASMC evident through the significantly increased expression of ATF4, GADD34, sXBP1 and CHOP. Studies have shown the link between IRE1 activation and the activation of NF-κB, which is responsible

for the expression of multiple pro-inflammatory genes [421], so it may be important to see whether 8ClA can promote inflammatory pathways governing atherosclerosis.

The effects on the UPR demonstrated in HCASMC were less profound than those observed in HCAEC. However, these differences may be due to the concentration of 8ClA (8 µM) used in the study with HCASMC. HCAEC were more sensitive to 8ClA showing significant decreases in metabolic activity at an 8 µM dose, where the metabolic activity of HCASMC was significantly decreased at a 16 µM dose. This may explain the differences observed in the viability between these cell types as there is no significant increase in the mRNA expression of CHOP, a main messenger for apoptosis, when HCASMC were exposed to 8ClA. Though previous studies with 8ClA has shown exposure to this chlorinated adduct to induce apoptosis in cancer cell lines, this is the first study demonstrating the UPR signalling to be responsible for 8ClA-induced apoptosis. In contrast to studies performed in this Thesis, in human hepatoma cell lines, it was demonstrated that 8ClA induced apoptosis through increased expression of tumour necrosis factor related apoptosis inducing ligand (TRAIL)-receptor 2 [316, 422]. These differences in cell signalling show that there may be multiple pathways responsible for the induction of apoptotic cell death upon exposure to 8ClA.

The Nrf2 pathway is responsible for signalling of antioxidant responses including those in the thioredoxin system [423]. Nrf2 is redox sensitive transcription factor, which when activated, causes the expression of multiple genes, including HO-1, NQO1 and GCLC [424, 425]. In HCAEC and HCASMC, exposure to 8ClA was shown to significantly increase mRNA expression of these genes, consistent with activation of Nrf2. In murine models

of atherosclerosis, the overexpression of HO-1 has shown atheroprotective effects. Overexpression of HO-1 has been shown in these models to attenuate atherogenesis and to protect against the formation of vulnerable plaques [426, 427]. Similarly, in murine models of atherosclerosis, specific deletion of HO-1 in bone marrow-derived cells resulted in increased macrophage accumulation and total deletion of HO-1 has been shown to accelerate lesion formation [428, 429]. Furthermore, HO-1 has anti-inflammatory effects and can suppress apoptosis in endothelial cells, which shows a link between activation of UPR-induced apoptosis and activation of Nrf2 [430, 431]. In an atherosclerotic environment, HO-1 and NQO1 can suppress smooth muscle cell proliferation and migration [424, 432, 433]. Given the increased expression of HO-1 and NQO1 in HCASMC exposed to 8ClA, future studies should determine whether this may be atheroprotective by suppressing the proliferation and migration of smooth muscle cells.

In Chapter 4, it was demonstrated that exposure to 5CldC induced metabolic changes and decreased proliferation in HCASMC. This was not evident when HCAEC were exposed to 5CldC in Chapter 3, though the incorporation and clearance in both cell types were similar. This suggests that the effects of 5CldC may be unrelated to DNA incorporation. The changes observed between the two cell types could also be due to differences in the reactivity of various cell types. In addition, in Chapter 3, studies used alterations in metabolic activity as a screen for compounds that induced an effect on HCAEC. As such, 5CldC may induce the effects in HCAEC that are evident in HCASMC, though this was not studied, as no change in metabolic activity was apparent. Therefore,

future studies should determine whether there are changes in cell signalling or proliferation of HCAEC exposed to 5CldC.

In HCASMC, the alterations in homeostasis observed upon incubation with 5CldC are significant, as studies have shown that when DNA or cells are exposed to HOCl, dC is the preferential target with 5CldC being formed [6, 13, 224, 434]. This is reflected in studies performed in Chapter 5 where there was evidence of 5CldC formation in NET (36.76 pg) and nuclear DNA (83.24 pg) of neutrophils exposed to HOCl. As NETs have been shown to be prevalent in atherosclerosis, the production of 5CldC in NET and nuclear DNA may provide a source of this chlorinated nucleoside in this disease. In addition, concentrations of 5CldC in the plasma of healthy individuals was determined to range from 0.06 to 0.4 lesions in 10^6 parent nucleosides [13]. These findings suggest that these chlorinated nucleosides are also present in the circulation even without evidence for inflammatory disease.

Previously, MMPs have been shown to be modulators of inflammation, with MMP2 shown to activate pro-IL-1β [312]. In Chapter 4, exposure of HCASMC to 5CldC was shown to increase the mRNA expression of MMP9 but not MMP2. In studies using a murine model of atherosclerosis, MMP9 leads to a decrease in plaque stability [435]. However, in contrast, knockout of MMP9 causes an increase in atherosclerotic plaque development, which suggests that MMP9 may prevent plaque progression [326]. Considering this, increased MMP9 expression in HCASMC exposed to 5CldC may lead to plaque instability or may prevent plaque progression. Therefore, it would be important

to perform studies to determine other signalling pathways involved in MMP9 expression to determine whether this compound is atheroprotective or atherogenic in HCASMC.

The expression of MMP9 has been shown to induce phenotypic changes in smooth muscle cells to the more proliferative and migratory synthetic phenotype [325, 435]. In these studies, there was an increased migration of smooth muscle cells from the tunica media to tunica intima. However, in Chapter 4, there were no significant increases in the mRNA expression of synthetic phenotype markers, though were significant decreases in the expression of contractile markers. The increase in proliferative ability was also not observed through the determination of total cell counts over time when HCASMC were exposed to 5CldC or the expression of KI-67. Future studies should look at the cell cycle using KI-67 as these cells may be senescent and in G_0 phase where they are non-proliferative. Though there was a large increase in the expression of MMP9 when HCASMC were treated with 5CldC, this was only translated to a slight significant increase in MMP9 activity as measured by gelatin zymography, which may explain the phenotypic marker gene expression.

Overall, studies in this Thesis have demonstrated that chlorinated nucleosides formed during inflammation can influence cellular signalling in vascular cells that could be relevant in the context of atherosclerosis. These studies have provided a potential source for modified nucleosides as well as provide insight into the pathways which may be activated by 8ClA and 5CldC, more specifically.

6.4. Future directions

The findings outlined in this Thesis have provided insight into the role and effects of chlorinated nucleosides in cell types relevant to CVD. However, there are still gaps in knowledge of the extent and concentrations to which each of these chlorinated nucleosides are present *in vivo* in inflammatory diseases. Furthermore, given that methods of quantifying chlorinated nucleosides have been demonstrated both in the literature [1, 6, 224] and the results chapters in this Thesis, they could be modified to quantify the presence of chlorinated nucleosides in various tissue samples from these diseases.

In addition to this, in the results from this Thesis, there were genes related to the UPR and antioxidant responses that were demonstrated to be altered in both HCAEC and HCASMC after exposure to chlorinated nucleosides. Further experiments should be performed in order to determine whether the alterations in mRNA expression of these genes has been translated to protein expression. This would provide a clearer picture of the signalling pathways activated by exposure to chlorinated nucleosides. Studies in HCASMC were performed in order to determine the effect of 5CldC on phenotype in Chapter 4. However, it would also be important to explore the effect of 8ClA on these markers given the distinct alterations observed in the activation of UPR and antioxidant responses and the implication of phenotype switching in atherosclerosis.

The experiments quantifying modified nucleosides present in NETs, which were performed in this Thesis could be expanded. The results from this study showed the increase in 8oxodG present in nuclear and NET DNA in PMA and HOCl-induced NETs in

PLB-985 cells. Similarly, 5CldC was quantified in both nuclear and NET DNA in HOCl-induced NETs in PLB-985. Further experiments should be conducted with the addition of H_2O_2 in order to stimulate further production of HOCl by NET-bound MPO in order to determine whether this would produce other chlorinated nucleosides. Studies comparing the DNA and protein modifications from NET production should also be studied and whether modified products are present on NETs stimulated in primary human neutrophils isolated from whole blood. In addition, the comparison of samples from healthy individuals and those from patients with inflammatory disease would be beneficial.

Given the presence of 8oxodG in NETs and also in nuclear DNA in PLB-985 cells, it would be important to explore the effect of this modified nucleoside on various cells types. 8oxodG has been shown to prevalent in various inflammatory diseases, though the direct implications of this modified nucleoside are yet to be determined in vascular cells. Overall, studies to determine the source of oxidised and chlorinated nucleosides in inflammation *in vivo* alongside the data shown in this thesis demonstrating their effects in vascular cells would provide a better understanding of the role of chlorinated nucleosides in disease.

6.5. Final conclusions

The experiments performed in this Thesis aimed to understand the biological consequences resulting from exposure to chlorinated nucleosides, as well as a potential source for these modified nucleosides in disease. Previous studies showed that these

DNA and RNA damage products can be produced during chronic inflammation, with some studies measuring these products in chronic inflammatory diseases, such as atherosclerosis. However, the functional effects of chlorinated nucleosides on different vascular cell types, as well as the source of these compounds in disease was not well understood.

The studies outlined in this Thesis in HCAEC and HCASMC demonstrated that chlorinated nucleosides had a marked impact on cellular function, signalling and viability in both of these cell types. In addition, studies performed on PLB-985 cells showed the presence of oxidised and chlorinated nucleosides in nuclear and NET DNA of neutrophils. The results shown in this Thesis provide insight into the role of chlorinated nucleosides in the context of disease. However, these data also highlight a need for future studies in order to understand the effects observed in vascular cells.

The alterations in cellular homeostasis may not be due directly to the incorporation of chlorinated nucleosides into the DNA or RNA as there was substantial incorporation of these modified products in the absence of changes in viability. In addition, although the concentrations of chlorinated nucleosides used in this Thesis are produced on reaction of cells to physiologically relevant concentrations of HOCl, it is not certain whether this is representative or realistic compared to what is seen *in vivo*. Therefore, further work needs to be performed in order to quantify chlorinated nucleosides *in vivo.*

Previous studies have suggested that chlorinated nucleosides may be good biomarkers for MPO-mediated inflammation. However, information related to the functional consequences of exposure to these products was limited. Overall, the data presented in

this Thesis provides interesting insight into potential new pathways propagating lesion formation, which could be novel therapeutic targets.

References

1. Tang, V., et al., *8-Chloroadenosine induces apoptosis in human coronary artery endothelial cells through the activation of the unfolded protein response.* Redox Biol, 2019. **26**: p. 101274.
2. AIHW, *Australia's Health 2018.* 2018. **Australia's health series no. 14. Cat. no. AUS 178**.
3. Libby, P., *Inflammation in atherosclerosis.* Nature, 2002. **420**(6917): p. 868.
4. Sitia, S., et al., *From endothelial dysfunction to atherosclerosis.* Autoimmun Rev, 2010. **9**(12): p. 830-834.
5. Weiss, S.J., et al., *Phagocyte-generated oxygen metabolites and cellular injury.* Lab Invest, 1982. **47**(1): p. 5-18.
6. Stanley, N.R., et al., *Ability of Hypochlorous Acid and N-Chloramines to Chlorinate DNA and Its Constituents.* Chem Res Toxicol, 2010. **23**(7): p. 1293-1302.
7. Hazen, S.L., et al., *3-Chlorotyrosine, a specific marker of myeloperoxidase-catalyzed oxidation, is markedly elevated in low density lipoprotein isolated from human atherosclerotic intima.* J Clin Invest, 1997. **99**(9): p. 2075-2081.
8. Heinecke, J.W., *Mechanisms of oxidative damage by myeloperoxidase in atherosclerosis and other inflammatory disorders.* J Lab Clin Med, 1999. **133**(4): p. 321-5.
9. Weitzman, S.A., et al., *Inflammation and cancer: role of phagocyte-generated oxidants in carcinogenesis.* Blood, 1990. **76**(4): p. 655-63.
10. Collins, A.R., et al., *DNA damage in diabetes: correlation with a clinical marker.* Free Radic Biol Med, 1998. **25**(3): p. 373-7.
11. Ohnishi, S., et al., *DNA damage induced by hypochlorite and hypobromite with reference to inflammation-associated carcinogenesis.* Cancer Lett, 2002. **178**(1): p. 37-42.
12. Henderson, J.P., et al., *Chlorination of nucleobases, RNA and DNA by myeloperoxidase: a pathway for cytotoxicity and mutagenesis by activated phagocytes.* Redox Rep, 1999. **4**(6): p. 319-20.

13. Badouard, C., et al., *Detection of chlorinated DNA and RNA nucleosides by HPLC coupled to tandem mass spectrometry as potential biomarkers of inflammation.* J Chromatogr B, 2005. **827**(1): p. 26-31.
14. Masuda, M., et al., *Chlorination of Guanosine and Other Nucleosides by Hypochlorous Acid and Myeloperoxidase of Activated Human Neutrophils: Catalysis by Nicotine and Trimethylamine.* J Biol Chem, 2001. **276**(44): p. 40486-40496.
15. Jiang, Q., et al., *5-Chlorouracil, a Marker of DNA Damage from Hypochlorous Acid during Inflammation: a gas chromatography mass spectrometry assay.* J Biol Chem, 2003. **278**(35): p. 32834-32840.
16. Takeshita, J., et al., *Myeloperoxidase Generates 5-Chlorouracil in Human Atherosclerotic Tissue: A Potential Pathway for Somatic Mutagenesis by Macrophages.* J Biol Chem, 2006. **281**(6): p. 3096-3104.
17. Henderson, J.P., et al., *Phagocytes Produce 5-Chlorouracil and 5-Bromouracil, Two Mutagenic Products of Myeloperoxidase, in Human Inflammatory Tissue.* J Biol Chem, 2003. **278**(26): p. 23522-23528.
18. Asahi, T., et al., *Chemical and Immunochemical Detection of 8-Halogenated Deoxyguanosines at Early Stage Inflammation.* J Biol Chem, 2010. **285**(12): p. 9282-9291.
19. Sanz, J., et al., *Imaging of atherosclerotic cardiovascular disease.* Nature, 2008. **451**(7181): p. 953-957.
20. Ross, R., *Atherosclerosis - an inflammatory disease.* N Engl J Med, 1999. **340**(2): p. 115-26.
21. Clarke, M., et al., *The Emerging Role of Vascular Smooth Muscle Cell Apoptosis in Atherosclerosis and Plaque Stability.* Am J Nephrol, 2006. **26**(6): p. 531-535.
22. Förstermann, U., et al., *Nitric oxide synthases: regulation and function.* Eur Heart J, 2012. **33**(7): p. 829-837d.
23. Alheid, U., et al., *Endothelium-derived relaxing factor from cultured human endothelial cells inhibits aggregation of human platelets.* Thromb Res, 1987. **47**(5): p. 561-71.

24. Rudic, R.D., et al., *Direct evidence for the importance of endothelium-derived nitric oxide in vascular remodeling.* J Clin Invest, 1998. **101**(4): p. 731-6.
25. Alkhalil, M., et al., *Quantification of carotid plaque lipid content with magnetic resonance T2 mapping in patients undergoing carotid endarterectomy.* PLoS One, 2017. **12**(7): p. e0181668.
26. Eshtehardi, P., et al., *Association of coronary wall shear stress with atherosclerotic plaque burden, composition, and distribution in patients with coronary artery disease.* J Am Heart Assoc, 2012. **1**(4): p. e002543.
27. Harker, L.A., et al., *The role of endothelial cell injury and platelet response in atherogenesis.* Thromb Haemost, 1978. **39**(2): p. 312-21.
28. Ross, R., et al., *Response to injury and atherogenesis.* Am J Pathol, 1977. **86**(3): p. 675-84.
29. Mundi, S., et al., *Endothelial permeability, LDL deposition, and cardiovascular risk factors—a review.* Cardiovasc Res, 2017. **114**(1): p. 35-52.
30. Delporte, C., et al., *Low-density lipoprotein modified by myeloperoxidase in inflammatory pathways and clinical studies.* Mediators Inflamm, 2013. **2013**: p. 971579.
31. Boudjeltia, K.Z., et al., *Myeloperoxidase-dependent LDL modifications in bloodstream are mainly predicted by angiotensin II, adiponectin, and myeloperoxidase activity: a cross-sectional study in men.* Mediators Inflamm, 2013. **2013**: p. 750742.
32. Schachter, M., *The pathogenesis of atherosclerosis.* Int J Cardiol, 1997. **62 Suppl 2**: p. S3-7.
33. Moore, K.J., et al., *Macrophages in the pathogenesis of atherosclerosis.* Cell, 2011. **145**(3): p. 341-55.
34. Bennett, M.R., et al., *Vascular Smooth Muscle Cells in Atherosclerosis.* Circ Res, 2016. **118**(4): p. 692-702.
35. Doran, A.C., et al., *Role of Smooth Muscle Cells in the Initiation and Early Progression of Atherosclerosis.* Arterioscler Thromb Vasc Biol, 2008. **28**(5): p. 812-819.

36. Clarke, M.C., et al., *Apoptosis of vascular smooth muscle cells induces features of plaque vulnerability in atherosclerosis.* Nat Med, 2006. **12**(9): p. 1075-80.
37. Gonzalez, L., et al., *Macrophage Apoptosis and Necrotic Core Development in Atherosclerosis: A Rapidly Advancing Field with Clinical Relevance to Imaging and Therapy.* Can J Cardiol, 2017. **33**(3): p. 303-312.
38. Seimon, T., et al., *Mechanisms and consequences of macrophage apoptosis in atherosclerosis.* J Lipid Res, 2009. **50 Suppl**(Suppl): p. S382-S387.
39. Glaudemans, A.W.J.M., et al., *Molecular imaging in atherosclerosis.* Eur J Nucl Med Mol I, 2010. **37**(12): p. 2381-2397.
40. Kouraklis, G., *Role of cellular adhesion molecules and growth factors in early atherogenesis.* Med Sci Monit, 2002. **8**(7): p. LE26.
41. Price, D.T., et al., *Cellular adhesion molecules and atherogenesis.* Am J Med, 1999. **107**(1): p. 85-97.
42. Deisher, T.A., et al., *The role of protein kinase C in the induction of VCAM-1 expression on human umbilical vein endothelial cells.* FEBS Lett, 1993. **331**(3): p. 285-90.
43. Pober, J.S., et al., *Evolving functions of endothelial cells in inflammation.* Nat Rev Immunol, 2007. **7**(10): p. 803-815.
44. Ignarro, L.J., et al., *Nitric Oxide as a Signaling Molecule in the Vascular System: An Overview.* J Cardiovasc Pharmacol, 1999. **34**(6): p. 879-886.
45. Lusis, A.J., *Atherosclerosis.* Nature, 2000. **407**(6801): p. 233-41.
46. Shami, A., et al., *Collagen and related extracellular matrix proteins in atherosclerotic plaque development.* Curr Opin Lipidol, 2014. **25**(5): p. 394-9.
47. Ponticos, M., et al., *Extracellular matrix synthesis in vascular disease: hypertension, and atherosclerosis.* J Biomed Res, 2014. **28**(1): p. 25-39.
48. Fuster, V., et al., *Atherosclerotic plaque rupture and thrombosis. Evolving concepts.* Circulation, 1990. **82**(3 Suppl): p. II47-59.
49. Hu, D., et al., *Vascular Smooth Muscle Cells Contribute to Atherosclerosis Immunity.* Front Immunol, 2019. **10**: p. 1101.

50. Corjay, M.H., et al., *Differential effect of platelet-derived growth factor- versus serum-induced growth on smooth muscle alpha-actin and nonmuscle beta-actin mRNA expression in cultured rat aortic smooth muscle cells.* J Biol Chem, 1989. **264**(18): p. 10501-6.
51. Hautmann, M.B., et al., *A transforming growth factor beta (TGFbeta) control element drives TGFbeta-induced stimulation of smooth muscle alpha-actin gene expression in concert with two CArG elements.* J Biol Chem, 1997. **272**(16): p. 10948-56.
52. Li, X., et al., *Suppression of smooth-muscle alpha-actin expression by platelet-derived growth factor in vascular smooth-muscle cells involves Ras and cytosolic phospholipase A2.* Biochem J, 1997. **327 (Pt 3)**: p. 709-16.
53. Hedin, U., et al., *A substrate of the cell-attachment sequence of fibronectin (Arg-Gly-Asp-Ser) is sufficient to promote transition of arterial smooth muscle cells from a contractile to a synthetic phenotype.* Dev Biol, 1989. **133**(2): p. 489-501.
54. Thyberg, J., et al., *Fibronectin and the basement membrane components laminin and collagen type IV influence the phenotypic properties of subcultured rat aortic smooth muscle cells differently.* Cell Tissue Res, 1994. **276**(2): p. 263-71.
55. Pidkovka, N.A., et al., *Oxidized phospholipids induce phenotypic switching of vascular smooth muscle cells in vivo and in vitro.* Circ Res, 2007. **101**(8): p. 792-801.
56. Su, B., et al., *Redox regulation of vascular smooth muscle cell differentiation.* Circ Res, 2001. **89**(1): p. 39-46.
57. Ang, A.H., et al., *Collagen synthesis by cultured rabbit aortic smooth-muscle cells. Alteration with phenotype.* Biochem J, 1990. **265**(2): p. 461-9.
58. Basatemur, G.L., et al., *Vascular smooth muscle cells in atherosclerosis.* Nat Rev Cardiol, 2019. **16**(12): p. 727-744.
59. Randolph, G.J., *Mechanisms that regulate macrophage burden in atherosclerosis.* Circ Res, 2014. **114**(11): p. 1757-71.
60. Seimon, T., et al., *Mechanisms and consequences of macrophage apoptosis in atherosclerosis.* J Lipid Res, 2009. **50 Suppl**: p. S382-7.

61. Martinez, F.O., et al., *Macrophage activation and polarization.* Front Biosci, 2008. **13**: p. 453-61.
62. Chistiakov, D.A., et al., *Macrophage phenotypic plasticity in atherosclerosis: The associated features and the peculiarities of the expression of inflammatory genes.* Int J Cardiol, 2015. **184**: p. 436-45.
63. Bobryshev, Y.V., et al., *Macrophages and Their Role in Atherosclerosis: Pathophysiology and Transcriptome Analysis.* Biomed Res Int, 2016. **2016**: p. 9582430.
64. Al-Sharea, A., et al., *Native LDL promotes differentiation of human monocytes to macrophages with an inflammatory phenotype.* Thromb Haemost, 2016. **115**(4): p. 762-72.
65. Brown, M.S., et al., *Reversible accumulation of cholesteryl esters in macrophages incubated with acetylated lipoproteins.* J Cell Biol, 1979. **82**(3): p. 597-613.
66. Suzuki, H., et al., *A role for macrophage scavenger receptors in atherosclerosis and susceptibility to infection.* Nature, 1997. **386**(6622): p. 292-6.
67. Naito, M., et al., *Coexpression of type I and type II human macrophage scavenger receptors in macrophages of various organs and foam cells in atherosclerotic lesions.* Am J Pathol, 1992. **141**(3): p. 591-9.
68. Kunjathoor, V.V., et al., *Scavenger receptors class A-I/II and CD36 are the principal receptors responsible for the uptake of modified low density lipoprotein leading to lipid loading in macrophages.* J Biol Chem, 2002. **277**(51): p. 49982-8.
69. Lougheed, M., et al., *Mechanism of uptake of copper-oxidized low density lipoprotein in macrophages is dependent on its extent of oxidation.* J Biol Chem, 1996. **271**(20): p. 11798-805.
70. Zhang, H., et al., *Structural requirements for the binding of modified proteins to the scavenger receptor of macrophages.* J Biol Chem, 1993. **268**(8): p. 5535-42.
71. Podrez, E.A., et al., *Macrophage scavenger receptor CD36 is the major receptor for LDL modified by monocyte-generated reactive nitrogen species.* J Clin Invest, 2000. **105**(8): p. 1095-108.

72. Febbraio, M., et al., *Targeted disruption of the class B scavenger receptor CD36 protects against atherosclerotic lesion development in mice.* J Clin Invest, 2000. **105**(8): p. 1049-56.
73. Mortaz, E., et al., *Update on Neutrophil Function in Severe Inflammation.* Front Immunol, 2018. **9**(2171).
74. Papayannopoulos, V., *Neutrophil extracellular traps in immunity and disease.* Nat Rev Immunol, 2018. **18**(2): p. 134-147.
75. Drechsler, M., et al., *Hyperlipidemia-triggered neutrophilia promotes early atherosclerosis.* Circulation, 2010. **122**(18): p. 1837-45.
76. Rotzius, P., et al., *Distinct infiltration of neutrophils in lesion shoulders in ApoE-/- mice.* Am J Pathol, 2010. **177**(1): p. 493-500.
77. Brinkmann, V., et al., *Neutrophil Extracellular Traps Kill Bacteria.* Science, 2004. **303**(5663): p. 1532-1535.
78. Döring, Y., et al., *Neutrophil Extracellular Traps in Atherosclerosis and Atherothrombosis.* Circ Res, 2017. **120**(4): p. 736-743.
79. Döring, Y., et al., *Footprints of Neutrophil Extracellular Traps as Predictors of Cardiovascular Risk.* Arterioscler Thromb Vasc Biol, 2013. **33**(8): p. 1735-1736.
80. Megens, R.T., et al., *Presence of luminal neutrophil extracellular traps in atherosclerosis.* Thromb Haemost, 2012. **107**(3): p. 597-8.
81. Warnatsch, A., et al., *Inflammation. Neutrophil extracellular traps license macrophages for cytokine production in atherosclerosis.* Science (New York, N.Y.), 2015. **349**(6245): p. 316-320.
82. Karlsson, A., et al., *Assembly and activation of the neutrophil NADPH oxidase in granule membranes.* Antioxid Redox Signal, 2002. **4**(1): p. 49-60.
83. Papayannopoulos, V., et al., *Neutrophil elastase and myeloperoxidase regulate the formation of neutrophil extracellular traps.* J Cell Biol, 2010. **191**(3): p. 677-91.
84. Yipp, B.G., et al., *NETosis: how vital is it?* Blood, 2013. **122**(16): p. 2784-2794.

85. Pilsczek, F.H., et al., *A novel mechanism of rapid nuclear neutrophil extracellular trap formation in response to Staphylococcus aureus.* J Immunol, 2010. **185**(12): p. 7413-25.

86. Megens, R.T.A., et al., *Presence of luminal neutrophil extracellular traps in atherosclerosis.* J Thromb Haemost, 2012. **107**(3): p. 597-598.

87. Liu, Y., et al., *Myeloid-Specific Deletion of Peptidylarginine Deiminase 4 Mitigates Atherosclerosis.* Front Immunol, 2018. **9**.

88. Quillard, T., et al., *TLR2 and neutrophils potentiate endothelial stress, apoptosis and detachment: implications for superficial erosion.* Eur Heart J, 2015. **36**(22): p. 1394-1404.

89. Franck, L.G., et al., *Roles of PAD4 and NETosis in Experimental Atherosclerosis and Arterial Injury: Implications for Superficial Erosion.* Circ Res, 2018. **123**(1): p. 33-42.

90. Knight, S.J., et al., *Peptidylarginine Deiminase Inhibition Reduces Vascular Damage and Modulates Innate Immune Responses in Murine Models of Atherosclerosis.* Circ Res, 2014. **114**(6): p. 947-956.

91. Neeli, I., et al., *Histone Deimination As a Response to Inflammatory Stimuli in Neutrophils.* J Immunol, 2008. **180**(3): p. 1895.

92. Wang, Y., et al., *Histone hypercitrullination mediates chromatin decondensation and neutrophil extracellular trap formation.* J Cell Biol, 2009. **184**(2): p. 205-213.

93. Nakashima, K., et al., *PAD4 regulates proliferation of multipotent haematopoietic cells by controlling c-myc expression.* Nat Commun, 2013. **4**: p. 1836.

94. Vossenaar, E.R., et al., *PAD, a growing family of citrullinating enzymes: genes, features and involvement in disease.* Bioessays, 2003. **25**(11): p. 1106-18.

95. Sorensen, O.E., et al., *Neutrophil extracellular traps - the dark side of neutrophils.* J Clin Invest, 2016. **126**(5): p. 1612-20.

96. Li, P., et al., *PAD4 is essential for antibacterial innate immunity mediated by neutrophil extracellular traps.* J Exp Med, 2010. **207**(9): p. 1853-1862.

97. Knight, J.S., et al., *Peptidylarginine deiminase inhibition disrupts NET formation and protects against kidney, skin and vascular disease in lupus-prone MRL/lpr mice.* Ann Rheum Dis, 2015. **74**(12): p. 2199-206.

98. Fuchs, T.A., et al., *Extracellular DNA traps promote thrombosis.* Proc Natl Acad Sci U S A, 2010. **107**(36): p. 15880-5.

99. Gould, T.J., et al., *Neutrophil extracellular traps promote thrombin generation through platelet-dependent and platelet-independent mechanisms.* Arterioscler Thromb Vasc Biol, 2014. **34**(9): p. 1977-84.

100. Oklu, R., et al., *Detection of extracellular genomic DNA scaffold in human thrombus: implications for the use of deoxyribonuclease enzymes in thrombolysis.* J Vasc Interv Radiol, 2012. **23**(5): p. 712-8.

101. Longstaff, C., et al., *Mechanical stability and fibrinolytic resistance of clots containing fibrin, DNA, and histones.* J Biol Chem, 2013. **288**(10): p. 6946-56.

102. Parker, H., et al., *Reactive oxidants and myeloperoxidase and their involvement in neutrophil extracellular traps.* Front Immunol, 2013. **3**(424).

103. Hampton, M.B., et al., *Inside the neutrophil phagosome: oxidants, myeloperoxidase, and bacterial killing.* Blood, 1998. **92**(9): p. 3007-17.

104. Davies, M.J., et al., *Mammalian Heme Peroxidases: From Molecular Mechanisms to Health Implications.* Antioxid Redox Signal, 2008. **10**(7): p. 1199-1234.

105. Kettle, A., et al., *Myeloperoxidase: a key regulator of neutrophil oxidant production.* Redox Rep, 1997. **3**(1): p. 3-15.

106. Winterbourn, C.C., et al., *Biomarkers of myeloperoxidase-derived hypochlorous acid.* Free Radic Biol Med, 2000. **29**(5): p. 403-409.

107. Podrez, E.A., et al., *Myeloperoxidase-generated oxidants and atherosclerosis.* Free Radical Biology and Medicine, 2000. **28**(12): p. 1717-1725.

108. Harrison, J.E., et al., *Studies on the chlorinating activity of myeloperoxidase.* J Biol Chem, 1976. **251**(5): p. 1371-4.

109. Morgan, P.E., et al., *High plasma thiocyanate levels in smokers are a key determinant of thiol oxidation induced by myeloperoxidase.* Free Radic Biol Med, 2011. **51**(9): p. 1815-1822.

110. Anatoliotakis, N., et al., *Myeloperoxidase: expressing inflammation and oxidative stress in cardiovascular disease.* Curr Top Med Chem, 2013. **13**(2): p. 115-38.

111. Brennan, M.L., et al., *Increased atherosclerosis in myeloperoxidase-deficient mice.* J Clin Invest, 2001. **107**(4): p. 419-30.

112. Correa, S., et al., *Myeloperoxidase and the Risk of CKD Progression, Cardiovascular Disease, and Death in the Chronic Renal Insufficiency Cohort (CRIC) Study.* Am J Kidney Dis, 2019.

113. Daugherty, A., et al., *Myeloperoxidase, a catalyst for lipoprotein oxidation, is expressed in human atherosclerotic lesions.* J Clin Invest, 1994. **94**(1): p. 437-444.

114. Fernandes, R., et al., *Increased myeloperoxidase plasma levels in rheumatoid arthritis.* Rheumatol Int, 2012. **32**(6): p. 1605-1609.

115. Hasanpour, Z., et al., *Association between serum myeloperoxidase levels and coronary artery disease in patients without diabetes, hypertension, obesity, and hyperlipidemia.* Adv Biomed Res, 2016. **5**: p. 103.

116. Wang, W., et al., *Increased levels of serum myeloperoxidase in patients with active rheumatoid arthritis.* Life Sci, 2014. **117**(1): p. 19-23.

117. Monteseirin, J., et al., *Elevated secretion of myeloperoxidase by neutrophils from asthmatic patients: the effect of immunotherapy.* J Allergy Clin Immunol, 2001. **107**(4): p. 623-6.

118. Reynolds, W.F., et al., *Myeloperoxidase polymorphism is associated with gender specific risk for Alzheimer's disease.* Exp Neurol, 1999. **155**(1): p. 31-41.

119. Green, P.S., et al., *Neuronal expression of myeloperoxidase is increased in Alzheimer's disease.* J Neurochem, 2004. **90**(3): p. 724-33.

120. VanderVeen, L.A., et al., *Evaluation of the mutagenic potential of the principal DNA adduct of acrolein.* J Biol Chem, 2001. **276**(12): p. 9066-70.

121. Hanahan, D., et al., *Hallmarks of cancer: the next generation.* Cell, 2011. **144**(5): p. 646-74.

122. Zhang, W., et al., *Inflammation and diabetic retinal microvascular complications.* J Cardiovasc Dis Res, 2011. **2**(2): p. 96-103.

123. Gray, E., et al., *Elevated myeloperoxidase activity in white matter in multiple sclerosis.* Neurosci Lett, 2008. **444**(2): p. 195-8.

124. Malle, E., et al., *Myeloperoxidase in kidney disease.* Kidney Int, 2003. **64**(6): p. 1956-1967.

125. Hasanpour, Z., et al., *Association between serum myeloperoxidase levels and coronary artery disease in patients without diabetes, hypertension, obesity, and hyperlipidemia.* Adv Biomed Res, 2016. **5**: p. 103-103.

126. Teng, N., et al., *The roles of myeloperoxidase in coronary artery disease and its potential implication in plaque rupture.* Redox Rep, 2017. **22**(2): p. 51-73.

127. Zhang, R., et al., *Association between myeloperoxidase levels and risk of coronary artery disease.* JAMA, 2001. **286**(17): p. 2136-2142.

128. Sugiyama, S., et al., *Macrophage myeloperoxidase regulation by granulocyte macrophage colony-stimulating factor in human atherosclerosis and implications in acute coronary syndromes.* Am J Pathol, 2001. **158**(3): p. 879-91.

129. Rashid, I., et al., *Myeloperoxidase is a potential molecular imaging and therapeutic target for the identification and stabilization of high-risk atherosclerotic plaque.* Eur Heart J, 2018. **39**(35): p. 3301-3310.

130. Baldus, S., et al., *Myeloperoxidase serum levels predict risk in patients with acute coronary syndromes.* Circulation, 2003. **108**(12): p. 1440-5.

131. Baldus, S., et al., *Endothelial transcytosis of myeloperoxidase confers specificity to vascular ECM proteins as targets of tyrosine nitration.* J Clin Invest, 2001. **108**(12): p. 1759-70.

132. Bergt, C., et al., *The myeloperoxidase product hypochlorous acid oxidizes HDL in the human artery wall and impairs ABCA1-dependent cholesterol transport.* Proc Natl Acad Sci U S A, 2004. **101**(35): p. 13032-7.

133. Pennathur, S., et al., *A hydroxyl radical-like species oxidizes cynomolgus monkey artery wall proteins in early diabetic vascular disease.* J Clin Invest, 2001. **107**(7): p. 853-60.

134. Malle, E., et al., *Modification of low-density lipoprotein by myeloperoxidase-derived oxidants and reagent hypochlorous acid.* Biochim Biophys Acta, 2006. **1761**(4): p. 392-415.

135. Hevonoja, T., et al., *Structure of low density lipoprotein (LDL) particles: basis for understanding molecular changes in modified LDL.* Biochim Biophys Acta, 2000. **1488**(3): p. 189-210.

136. Panasenko, O.M., *The mechanism of the hypochlorite-induced lipid peroxidation.* Biofactors, 1997. **6**(2): p. 181-90.

137. Pattison, D.I., et al., *Hypochlorous acid-mediated oxidation of lipid components and antioxidants present in low-density lipoproteins: absolute rate constants, product analysis, and computational modeling.* Chem Res Toxicol, 2003. **16**(4): p. 439-49.

138. Hazell, L.J., et al., *Secondary radicals derived from chloramines of apolipoprotein B-100 contribute to HOCl-induced lipid peroxidation of low-density lipoproteins.* Biochem J, 1999. **339 (Pt 3)**: p. 489-95.

139. Delporte, C., et al., *Impact of myeloperoxidase-LDL interactions on enzyme activity and subsequent posttranslational oxidative modifications of apoB-100.* Journal of lipid research, 2014. **55**(4): p. 747-757.

140. Koeth, R.A., et al., *Myeloperoxidase in cardiovascular disease.* Adv Clin Chem, 2013. **62**: p. 1-32.

141. Hazen, S.L., et al., *3-Chlorotyrosine, a specific marker of myeloperoxidase-catalyzed oxidation, is markedly elevated in low density lipoprotein isolated from human atherosclerotic intima.* J Clin Invest, 1997. **99**(9): p. 2075-81.

142. Emerging Risk Factors, C., et al., *Major lipids, apolipoproteins, and risk of vascular disease.* JAMA, 2009. **302**(18): p. 1993-2000.

143. Khera, A.V., et al., *Cholesterol efflux capacity, high-density lipoprotein function, and atherosclerosis.* N Engl J Med, 2011. **364**(2): p. 127-35.

144. Shao, B., et al., *Myeloperoxidase: an oxidative pathway for generating dysfunctional high-density lipoprotein.* Chem Res Toxicol, 2010. **23**(3): p. 447-54.

145. Fisher, E.A., et al., *High-density lipoprotein function, dysfunction, and reverse cholesterol transport.* Arterioscler Thromb Vasc Biol, 2012. **32**(12): p. 2813-20.

146. Nicholls, S.J., et al., *Myeloperoxidase, modified lipoproteins, and atherogenesis.* J Lipid Res, 2009. **50**(Supplement): p. S346-S351.

147. Undurti, A., et al., *Modification of high density lipoprotein by myeloperoxidase generates a pro-inflammatory particle.* J Biol Chem, 2009. **284**(45): p. 30825-35.

148. Whiteman, M., et al., *Hypochlorous Acid-Induced Base Modifications in Isolated Calf Thymus DNA.* Chem Res Toxicol, 1997. **10**(11): p. 1240-1246.

149. Hawkins, C.L., et al., *Hypochlorite-induced oxidation of proteins in plasma: formation of chloramines and nitrogen-centred radicals and their role in protein fragmentation.* Biochem J, 1999. **340**(Pt 2): p. 539-548.

150. Carr, A.C., et al., *Chlorination of Cholesterol in Cell Membranes by Hypochlorous Acid.* Arch Biochem Biophys, 1996. **332**(1): p. 63-69.

151. Panasenko, O.M., *The mechanism of the hypochlorite-induced lipid peroxidation.* BioFactors, 1997. **6**(2): p. 181-190.

152. Rayner, B.S., et al., *Comparative reactivity of myeloperoxidase-derived oxidants with mammalian cells.* Free Radic Biol Med, 2014. **71**: p. 240-255.

153. Pattison, D.I., et al., *Absolute rate constants for the reaction of hypochlorous acid with protein side chains and peptide bonds.* Chem Res Toxicol, 2001. **14**(10): p. 1453-64.

154. Hawkins, C.L., et al., *Hypochlorite-induced oxidation of amino acids, peptides and proteins.* Amino Acids, 2003. **25**(3-4): p. 259-74.

155. Pattison, D.I., et al., *Absolute Rate Constants for the Reaction of Hypochlorous Acid with Protein Side Chains and Peptide Bonds.* Chem Res Toxicol, 2001. **14**(10): p. 1453-1464.

156. Drozdz, R., et al., *Oxidation of amino acids and peptides in reaction with myeloperoxidase, chloride and hydrogen peroxide.* Biochim Biophys Acta, 1988. **957**(1): p. 47-52.

157. Pereira, W.E., et al., *Chlorination studies. II. The reaction of aqueous hypochlorous acid with alpha-amino acids and dipeptides.* Biochim Biophys Acta, 1973. **313**(1): p. 170-80.

158. Karimi, M., et al., *Reactivity of disulfide bonds is markedly affected by structure and environment: implications for protein modification and stability.* Sci Rep, 2016. **6**(1): p. 38572.

159. Beal, J.L., et al., *Hypochlorous acid reacts with the N-terminal methionines of proteins to give dehydromethionine, a potential biomarker for neutrophil-induced oxidative stress.* Biochemistry, 2009. **48**(46): p. 11142-8.

160. Peskin, A.V., et al., *Oxidation of methionine to dehydromethionine by reactive halogen species generated by neutrophils.* Biochemistry, 2009. **48**(42): p. 10175-82.

161. Magon, N.J., et al., *Oxidation of calprotectin by hypochlorous acid prevents chelation of essential metal ions and allows bacterial growth: Relevance to infections in cystic fibrosis.* Free Radic Biol Med, 2015. **86**: p. 133-44.

162. Shao, B., et al., *Myeloperoxidase impairs ABCA1-dependent cholesterol efflux through methionine oxidation and site-specific tyrosine chlorination of apolipoprotein A-I.* J Biol Chem, 2006. **281**(14): p. 9001-4.

163. Thomas, E.L., et al., *Cytotoxicity of chloramines.* Methods Enzymol, 1986. **132**: p. 585-93.

164. Pattison, D.I., et al., *Kinetic Analysis of the Role of Histidine Chloramines in Hypochlorous Acid Mediated Protein Oxidation.* Biochemistry, 2005. **44**(19): p. 7378-7387.

165. Fu, S., et al., *Reactions of hypochlorous acid with tyrosine and peptidyl-tyrosyl residues give dichlorinated and aldehydic products in addition to 3-chlorotyrosine.* J Biol Chem, 2000. **275**(15): p. 10851-8.

166. Domigan, N.M., et al., *Chlorination of tyrosyl residues in peptides by myeloperoxidase and human neutrophils.* J Biol Chem, 1995. **270**(28): p. 16542-8.

167. Winterbourn, C.C., *Biological reactivity and biomarkers of the neutrophil oxidant, hypochlorous acid.* Toxicol 2002. **181-182**: p. 223-7.

168. Strobel, N.A., et al., *Oxidative stress biomarkers as predictors of cardiovascular disease.* Int J Cardiol, 2011. **147**(2): p. 191-201.

169. Mocatta, T.J., et al., *Plasma concentrations of myeloperoxidase predict mortality after myocardial infarction.* J Am Coll Cardiol, 2007. **49**(20): p. 1993-2000.

170. Buss, I.H., et al., *3-Chlorotyrosine as a Marker of Protein Damage by Myeloperoxidase in Tracheal Aspirates From Preterm Infants: Association With Adverse Respiratory Outcome.* Pediatr Res, 2003. **53**(3): p. 455-462.

171. Davies, M.D., et al., *The role of myeloperoxidase (MPO) in biomolecule modification, chronic inflammation and disease.* Antioxid Redox Signal, 2020.

172. Biedron, R., et al., *Oxidation by neutrophils-derived HOCl increases immunogenicity of proteins by converting them into ligands of several endocytic receptors involved in antigen uptake by dendritic cells and macrophages.* PLoS One, 2015. **10**(4): p. e0123293.

173. Spickett, C.M., et al., *The reactions of hypochlorous acid, the reactive oxygen species produced by myeloperoxidase, with lipids.* Acta Biochim Pol, 2000. **47**(4): p. 889-99.

174. Yuan, X.M., et al., *Lysosomal destabilization during macrophage damage induced by cholesterol oxidation products.* Free Radic Biol Med, 2000. **28**(2): p. 208-18.

175. Vissers, M.C., et al., *Fatty acid chlorohydrins and bromohydrins are cytotoxic to human endothelial cells.* Redox Rep, 2001. **6**(1): p. 49-55.

176. Micheletta, F., et al., *Vitamin E supplementation in patients with carotid atherosclerosis: reversal of altered oxidative stress status in plasma but not in plaque.* Arterioscler Thromb Vasc Biol, 2004. **24**(1): p. 136-40.

177. Buttari, B., et al., *7-Oxo-cholesterol potentiates pro-inflammatory signaling in human M1 and M2 macrophages.* Biochem Pharmacol, 2013. **86**(1): p. 130-7.

178. Schroter, J., et al., *Chlorinated Phospholipids and Fatty Acids: (Patho)physiological Relevance, Potential Toxicity, and Analysis of Lipid Chlorohydrins.* Oxid Med Cell Longev, 2016. **2016**: p. 8386362.

179. Philippova, M., et al., *Oxidised phospholipids as biomarkers in human disease.* Swiss Med Wkly, 2014. **144**: p. w14037.

180. Ford, D.A., *Lipid oxidation by hypochlorous acid: chlorinated lipids in atherosclerosis and myocardial ischemia.* Clin Lipidol, 2010. **5**(6): p. 835-852.

181. Hazen, S.L., et al., *Isolation of a human myocardial cytosolic phospholipase A2 isoform. Fast atom bombardment mass spectroscopic and reverse-phase high pressure liquid chromatography identification of choline and ethanolamine glycerophospholipid substrates.* J Clin Invest, 1993. **91**(6): p. 2513-22.

182. Gross, R.W., *High plasmalogen and arachidonic acid content of canine myocardial sarcolemma: a fast atom bombardment mass spectroscopic and gas chromatography-mass spectroscopic characterization.* Biochemistry, 1984. **23**(1): p. 158-65.

183. Post, J.A., et al., *Plasmalogen content and distribution in the sarcolemma of cultured neonatal rat myocytes.* FEBS Lett, 1988. **240**(1-2): p. 78-82.

184. Ford, D.A., et al., *Plasmenylethanolamine is the major storage depot for arachidonic acid in rabbit vascular smooth muscle and is rapidly hydrolyzed after angiotensin II stimulation.* Proc Natl Acad Sci U S A, 1989. **86**(10): p. 3479-83.

185. Flemmig, J., et al., *Modification of phosphatidylserine by hypochlorous acid.* Chem Phys Lipids, 2009. **161**(1): p. 44-50.

186. Messner, M.C., et al., *Identification of lysophosphatidylcholine-chlorohydrin in human atherosclerotic lesions.* Lipids, 2008. **43**(3): p. 243-9.

187. Brites, P., et al., *Functions and biosynthesis of plasmalogens in health and disease.* Biochim Biophys Acta, 2004. **1636**(2-3): p. 219-31.

188. Thukkani, A.K., et al., *Reactive chlorinating species produced during neutrophil activation target tissue plasmalogens: production of the chemoattractant, 2-chlorohexadecanal.* J Biol Chem, 2002. **277**(6): p. 3842-9.

189. Messner, M.C., et al., *2-Chlorohexadecanal and 2-chlorohexadecanoic acid induce COX-2 expression in human coronary artery endothelial cells.* Lipids, 2008. **43**(7): p. 581-8.

190. Thukkani, A.K., et al., *Identification of alpha-chloro fatty aldehydes and unsaturated lysophosphatidylcholine molecular species in human atherosclerotic lesions.* Circulation, 2003. **108**(25): p. 3128-33.
191. Coussens, L.M., et al., *Inflammation and cancer.* Nature, 2002. **420**(6917): p. 860.
192. Cochrane, C.G., *Cellular injury by oxidants.* Am J Med, 1991. **91**(3C): p. 23S-30S.
193. Prütz, W.A., *Interactions of hypochlorous acid with pyrimidine nucleotides, and secondary reactions of chlorinated pyrimidines with GSH, NADH, and other substrates.* Arch Biochem Biophys, 1998. **349**(1): p. 183-91.
194. Hawkins, C.L., et al., *Hypochlorite-induced damage to nucleosides: formation of chloramines and nitrogen-centered radicals.* Chem Res Toxicol, 2001. **14**(8): p. 1071-81.
195. Hawkins, C.L., et al., *Hypochlorite-induced damage to DNA, RNA, and polynucleotides: formation of chloramines and nitrogen-centered radicals.* Chem Res Toxicol, 2002. **15**(1): p. 83-92.
196. Hayatsu, H., et al., *Reaction of sodium hypochlorite with nucleic acids and their constituents.* Chem Pharm Bull (Tokyo), 1971. **19**(10): p. 2189-92.
197. Gould, J.P., et al., *The formation of stable organic chloramines during the aqueous chlorination of cytosine and 5-methylcytosine.* Water Res, 1984. **18**(8): p. 991-999.
198. Patton, W., et al., *Chlorination studies. I. The reaction of aqueous hypochlorous acid with cytosine.* Biochem Biophys Res Commun, 1972. **48**(4): p. 880-884.
199. Evans, M.D., et al., *Factors contributing to the outcome of oxidative damage to nucleic acids.* BioEssays, 2004. **26**(5): p. 533-542.
200. Spencer, J.P., et al., *Nitrite-induced deamination and hypochlorite-induced oxidation of DNA in intact human respiratory tract epithelial cells.* Free Radic Biol Med, 2000. **28**(7): p. 1039-50.
201. Whiteman, M., et al., *Loss of oxidized and chlorinated bases in DNA treated with reactive oxygen species: implications for assessment of oxidative damage in vivo.* Biochem Biophys Res Commun, 2002. **296**(4): p. 883-9.

202. Whiteman, M., et al., *Hypochlorous acid-induced DNA base modification: potentiation by nitrite: biomarkers of DNA damage by reactive oxygen species.* Biochem Biophys Res Commun, 1999. **257**(2): p. 572-6.

203. Gould, J.P., et al., *The kinetics and primary products of uracil chlorination.* Water Res, 1984. **18**(2): p. 205-212.

204. Dedon, P.C., et al., *Challenges in developing DNA and RNA biomarkers of inflammation.* Biomark Med, 2007. **1**: p. 293+.

205. Lonkar, P., et al., *Reactive species and DNA damage in chronic inflammation: reconciling chemical mechanisms and biological fates.* Int J Cancer, 2011. **128**(9): p. 1999-2009.

206. Trosko, J.E., et al., *An integrative hypothesis linking cancer, diabetes and atherosclerosis: the role of mutations and epigenetic changes.* Med Hypotheses, 1980. **6**(5): p. 455-68.

207. Martinet, W., et al., *Elevated levels of oxidative DNA damage and DNA repair enzymes in human atherosclerotic plaques.* Circulation, 2002. **106**(8): p. 927-32.

208. Botto, N., et al., *Elevated levels of oxidative DNA damage in patients with coronary artery disease.* Coron Artery Dis, 2002. **13**(5): p. 269-74.

209. Andreassi, M.G., *Coronary atherosclerosis and somatic mutations: an overview of the contributive factors for oxidative DNA damage.* Mutat Res, 2003. **543**(1): p. 67-86.

210. Jaruga, P., et al., *DNA damage products (5'R)- and (5'S)-8,5'-cyclo-2'-deoxyadenosines as potential biomarkers in human urine for atherosclerosis.* Biochemistry, 2012. **51**(9): p. 1822-4.

211. Broedbaek, K., et al., *Urinary 8-oxo-7,8-dihydro-2'-deoxyguanosine as a biomarker in type 2 diabetes.* Free Radic Biol Med, 2011. **51**(8): p. 1473-9.

212. Broedbaek, K., et al., *Urinary albumin and 8-oxo-7,8-dihydroguanosine as markers of mortality and cardiovascular disease during 19 years after diagnosis of type 2 diabetes – A comparative study of two markers to identify high risk patients.* Redox Biol, 2017. **13**: p. 363-369.

213. Gackowski, D., et al., *8-Oxo-7,8-dihydroguanine and 8-oxo-7,8-dihydro-2'-deoxyguanosine levels in human urine do not depend on diet.* Free Radic Res, 2001. **35**(6): p. 825-832.

214. Kjær, L.K., et al., *Cardiovascular and All-Cause Mortality Risk Associated With Urinary Excretion of 8-oxoGuo, a Biomarker for RNA Oxidation, in Patients With Type 2 Diabetes: A Prospective Cohort Study.* Diabetes Care, 2017. **40**(12): p. 1771.

215. Roszkowski, K., et al., *Oxidative damage DNA: 8-oxoGua and 8-oxodG as molecular markers of cancer.* Med Sci Monit, 2011. **17**(6): p. CR329-CR333.

216. Sun, J., et al., *Serum 8-hydroxy-2'-deoxyguanosine (8-oxo-dG) levels are elevated in diabetes patients.* Int J Diabetes Dev Ctries, 2015. **35**(3): p. 368-373.

217. Di Minno, A., et al., *8-Hydroxy-2-Deoxyguanosine Levels and Cardiovascular Disease: A Systematic Review and Meta-Analysis of the Literature.* Antioxid Redox Signal, 2016. **24**(10): p. 548-555.

218. Kroese, L.J., et al., *8-hydroxy-2'-deoxyguanosine and cardiovascular disease: a systematic review.* Curr Atheroscler Rep, 2014. **16**(11): p. 452.

219. Broedbaek, K., et al., *Urinary markers of nucleic acid oxidation and cancer in type 2 diabetes.* Redox Biol, 2015. **4**: p. 34-9.

220. Broedbaek, K., et al., *Urinary markers of nucleic acid oxidation and long-term mortality of newly diagnosed type 2 diabetic patients.* Diabetes Care, 2011. **34**(12): p. 2594-6.

221. Broedbaek, K., et al., *Association between urinary markers of nucleic acid oxidation and mortality in type 2 diabetes: a population-based cohort study.* Diabetes care, 2013. **36**(3): p. 669-676.

222. Bruskov, V.I., et al., *Heat-induced formation of reactive oxygen species and 8-oxoguanine, a biomarker of damage to DNA.* Nucleic Acids Res, 2002. **30**(6): p. 1354-1363.

223. Collins, A.R., et al., *Are we sure we know how to measure 8-oxo-7,8-dihydroguanine in DNA from human cells?* Arch Biochem Biophys, 2004. **423**(1): p. 57-65.

224. Noyon, C., et al., *Validation of a sensitive LC/MSMS method for chloronucleoside analysis in biological matrixes and its applications.* Talanta, 2016. **154**: p. 322-328.

225. Henriksen, T., et al., *Automated method for the direct analysis of 8-oxo-guanosine and 8-oxo-2'-deoxyguanosine in human urine using ultraperformance liquid chromatography and tandem mass spectrometry.* Free Radic Biol Med, 2009. **47**(5): p. 629-35.

226. Henderson, J.P., et al., *Molecular Chlorine Generated by the Myeloperoxidase-Hydrogen Peroxide-Chloride System of Phagocytes Produces 5-Chlorocytosine in Bacterial RNA.* J Biol Chem, 1999. **274**(47): p. 33440-33448.

227. Dizdaroglu, M., *Facts about the artifacts in the measurement of oxidative DNA base damage by gas chromatography-mass spectrometry.* Free Radic Res, 1998. **29**(6): p. 551-63.

228. Senturker, S., et al., *The effect of experimental conditions on the levels of oxidatively modified bases in DNA as measured by gas chromatography-mass spectrometry: how many modified bases are involved? Prepurification or not?* Free Radic Biol Med, 1999. **27**(3-4): p. 370-80.

229. Jaruga, P., et al., *Endogenous oxidative DNA base modifications analysed with repair enzymes and GC/MS technique.* Nucleic Acids Res, 2000. **28**(6): p. E16.

230. Chapman, A.L., et al., *Chlorination of bacterial and neutrophil proteins during phagocytosis and killing of Staphylococcus aureus.* J Biol Chem, 2002. **277**(12): p. 9757-62.

231. Azqueta, A., et al., *The essential comet assay: a comprehensive guide to measuring DNA damage and repair.* Arch Toxicol, 2013. **87**(6): p. 949-68.

232. Boiteux, S., et al., *Substrate specificity of the Escherichia coli Fpg protein (formamidopyrimidine-DNA glycosylase): excision of purine lesions in DNA produced by ionizing radiation or photosensitization.* Biochemistry, 1992. **31**(1): p. 106-10.

233. Croteau, D.L., et al., *Repair of oxidative damage to nuclear and mitochondrial DNA in mammalian cells.* J Biol Chem, 1997. **272**(41): p. 25409-12.

234. Cooke, M.S., et al., *Evaluation of enzyme-linked immunosorbent assay and liquid chromatography–tandem mass spectrometry methodology for the analysis of 8-oxo-7,8-dihydro-2'-deoxyguanosine in saliva and urine.* Free Radic Biol Med, 2006. **41**(12): p. 1829-1836.

235. Dizdaroglu, M., et al., *Free radical-induced damage to DNA: mechanisms and measurement.* Free Radic Biol Med, 2002. **32**(11): p. 1102-15.

236. Kawanishi, S., et al., *Crosstalk between DNA Damage and Inflammation in the Multiple Steps of Carcinogenesis.* Int J Mol Sci, 2017. **18**(8): p. 1808.

237. Paz-Elizur, T., et al., *DNA repair of oxidative DNA damage in human carcinogenesis: potential application for cancer risk assessment and prevention.* Cancer letters, 2008. **266**(1): p. 60-72.

238. Faucher, F., et al., *8-oxoguanine DNA glycosylases: one lesion, three subfamilies.* Int J Mol Sci, 2012. **13**(6): p. 6711-6729.

239. Taggart, D.J., et al., *Mutagenic potential of 8-oxo-7,8-dihydro-2'-deoxyguanosine bypass catalyzed by human Y-family DNA polymerases.* Chem Res Toxicol, 2014. **27**(5): p. 931-940.

240. Dandona, P., et al., *Oxidative damage to DNA in diabetes mellitus.* Lancet, 1996. **347**(8999): p. 444-5.

241. Rehman, A., et al., *Increased oxidative damage to all DNA bases in patients with type II diabetes mellitus.* FEBS Lett, 1999. **448**(1): p. 120-2.

242. Lorenzi, M., et al., *Increased single strand breaks in DNA of lymphocytes from diabetic subjects.* J Clin Invest, 1987. **79**(2): p. 653-6.

243. Dincer, Y., et al., *Assessment of DNA base oxidation and glutathione level in patients with type 2 diabetes.* Mutat Res, 2002. **505**(1-2): p. 75-81.

244. Blasiak, J., et al., *DNA damage and repair in type 2 diabetes mellitus.* Mutat Res, 2004. **554**(1-2): p. 297-304.

245. Leinonen, J., et al., *New biomarker evidence of oxidative DNA damage in patients with non-insulin-dependent diabetes mellitus.* FEBS Lett, 1997. **417**(1): p. 150-2.

246. Hinokio, Y., et al., *Oxidative DNA damage in diabetes mellitus: its association with diabetic complications.* Diabetologia, 1999. **42**(8): p. 995-8.

247. Dong, Q.Y., et al., *Urinary 8-hydroxydeoxyguanosine levels in diabetic retinopathy patients.* Eur J Ophthalmol, 2008. **18**(1): p. 94-8.

248. Broedbaek, K., et al., *Urinary 8-oxo-7,8-dihydro-2'-deoxyguanosine as a biomarker in type 2 diabetes.* Free Radic Biol Med, 2011. **51**(8): p. 1473-1479.

249. Broedbaek, K., et al., *Urinary markers of nucleic acid oxidation and long-term mortality of newly diagnosed type 2 diabetic patients.* Diabetes care, 2011. **34**(12): p. 2594-2596.

250. Kjaer, L.K., et al., *Indicator of RNA oxidation in urine for the prediction of mortality in patients with type 2 diabetes and microalbuminuria: A post-hoc analysis of the Steno-2 trial.* Free Radic Biol Med, 2018. **129**: p. 247-255.

251. Cervelli, T., et al., *DNA damage and repair in atherosclerosis: current insights and future perspectives.* Int J Mol Sci, 2012. **13**(12): p. 16929-16944.

252. Simon, A.S., et al., *Altered DNA repair, oxidative stress and antioxidant status in coronary artery disease.* J Biosci, 2013. **38**(2): p. 385-9.

253. Botto, N., et al., *Evidence for DNA damage in patients with coronary artery disease.* Mutat Res, 2001. **493**(1-2): p. 23-30.

254. Evans, H.J., *Parental mutagenesis and familial cancer.* Nature, 1982. **296**(5857): p. 488-489.

255. Fedeles, B.I., et al., *Intrinsic mutagenic properties of 5-chlorocytosine: A mechanistic connection between chronic inflammation and cancer.* Proc Natl Acad Sci U S A, 2015. **112**(33): p. E4571-80.

256. Noyon, C., et al., *The presence of modified nucleosides in extracellular fluids leads to the specific incorporation of 5-chlorocytidine into RNA and modulates the transcription and translation.* Mol Cell Biochem, 2017. **429**(1-2): p. 59-71.

257. Kim, C.H., et al., *Polymerase incorporation and miscoding properties of 5-chlorouracil.* Chem Res Toxicol, 2010. **23**(4): p. 740-8.

258. Patra, A., et al., *Structure, stability and function of 5-chlorouracil modified A:U and G:U base pairs.* Nucleic Acids Res, 2013. **41**(4): p. 2689-97.

259. Macer-Wright, J.L., et al., *A Role for Chlorinated Nucleosides in the Perturbation of Macrophage Function and Promotion of Inflammation.* Chem Res Toxicol, 2019. **32**(6): p. 1223-1234.

260. Macer-Wright, J.L., et al., *8-Chloroadenosine Alters the Metabolic Profile and Downregulates Antioxidant and DNA Damage Repair Pathways in Macrophages.* Chem Res Toxicol, 2019.

261. Medicine, U.S.N.L.o. *8-Chloro-Adenosine in Chronic Lymphocytic Leukemia*. 2016 October 13, 2016.

262. Medicine, U.S.N.L.o. *8-Chloroadenosine in Treating Patients With Relapsed or Refractory Acute Myeloid Leukemia*. 2020 January 3, 2020.

263. Perez, L.M., et al., *Sensitization to X ray by 5-chloro-2'-deoxycytidine co-administered with tetrahydrouridine in several mammalian cell lines and studies of 2'-chloro derivatives.* Int J Radiat Biol, 1986. **12**(8): p. 1523-1527.

264. Greer, S., et al., *Five-chlorodeoxycytidine, a tumor-selective enzyme-driven radiosensitizer, effectively controls five advanced human tumors in nude mice.* Int J Radiat Biol, 2001. **51**(3): p. 791-806.

265. Santos, O., et al., *Radiation, pool size and incorporation studies in mice with 5-chloro-2'-deoxycytidine.* Int J Radiat Oncol Biol Phys, 1990. **19**(2): p. 357-65.

266. Gandhi, V., et al., *8-chloro-cAMP and 8-chloro-adenosine act by the same mechanism in multiple myeloma cells.* Cancer Res, 2001. **61**(14): p. 5474-9.

267. Chen, L.S., et al., *Inhibition of ATP synthase by chlorinated adenosine analogue.* Biochem Pharmacol, 2009. **78**(6): p. 583-591.

268. Halgren, R.G., et al., *8Cl-cAMP cytotoxicity in both steroid sensitive and insensitive multiple myeloma cell lines is mediated by 8Cl-adenosine.* Blood, 1998. **92**(8): p. 2893-8.

269. Stellrecht, C.M., et al., *RNA-directed actions of 8-chloro-adenosine in multiple myeloma cells.* Cancer Res, 2003. **63**(22): p. 7968-74.

270. Stellrecht, C.M., et al., *A unique RNA-directed nucleoside analog is cytotoxic to breast cancer cells and depletes cyclin E levels.* Breast Cancer Res Treat, 2010. **121**(2): p. 355-64.

271. Stellrecht, C.M., et al., *ATP directed agent, 8-chloro-adenosine, induces AMP activated protein kinase activity, leading to autophagic cell death in breast cancer cells.* J Hematol Oncol, 2014. **7**: p. 23-23.

272. Dennison, J.B., et al., *Preclinical activity of 8-chloroadenosine with mantle cell lymphoma: roles of energy depletion and inhibition of DNA and RNA synthesis.* Br J Haematol, 2009. **147**(3): p. 297-307.

273. Love, D.T., *The role of HOSCN in the oxidation of proteins and cellular damage in atherosclerosis*. 2015, University of Sydney.

274. Frankowski, H., et al., *Use of gel zymography to examine matrix metalloproteinase (gelatinase) expression in brain tissue or in primary glial cultures.* Methods Mol Biol, 2012. **814**: p. 221-233.

275. Sun, X., et al., *Ki-67: more than a proliferation marker.* Chromosoma, 2018. **127**(2): p. 175-186.

276. Perelman, A., et al., *JC-1: alternative excitation wavelengths facilitate mitochondrial membrane potential cytometry.* Cell Death Dis, 2012. **3**(11): p. e430-e430.

277. Rayner, B.S., et al., *Comparative reactivity of myeloperoxidase-derived oxidants with mammalian cells.* Free Radic Biol Med, 2014. **71**(0): p. 240-255.

278. Vita, J.A., et al., *Serum myeloperoxidase levels independently predict endothelial dysfunction in humans.* Circulation, 2004. **110**(9): p. 1134-9.

279. Whiteman, M., et al., *8-Chloroadenine: a novel product formed from hypochlorous acid-induced damage to calf thymus DNA.* Biomarkers, 1999. **4**(4): p. 303-310.

280. Balakrishnan, K., et al., *Cell death of bioenergetically compromised and transcriptionally challenged CLL lymphocytes by chlorinated ATP.* Blood, 2005. **105**(11): p. 4455-62.

281. Han, J.H., et al., *Involvement of AMP-activated protein kinase and p38 mitogen-activated protein kinase in 8-Cl-cAMP-induced growth inhibition.* J Cell Physiol, 2009. **218**(1): p. 104-12.

282. Gandhi, V., et al., *Plasma and cellular pharmacology of 8-chloro-adenosine in mice and rats.* Cancer Chemother Pharmacol, 2002. **50**(2): p. 85-94.
283. Tortora, G., et al., *Phase I clinical study with 8-chloro-cAMP and evaluation of immunological effects in cancer patients.* Clin Cancer Res, 1995. **1**(4): p. 377-84.
284. Cao, S.S., et al., *Unfolded protein response.* Curr Biol, 2012. **22**(16): p. R622-R626.
285. Tabas, I., *The role of endoplasmic reticulum stress in the progression of atherosclerosis.* Circ Res, 2010. **107**(7): p. 839-50.
286. Zhou, A.X., et al., *The UPR in atherosclerosis.* Semin Immunopathol, 2013. **35**(3): p. 321-32.
287. Espinosa-Diez, C., et al., *Antioxidant responses and cellular adjustments to oxidative stress.* Redox Biol, 2015. **6**: p. 183-197.
288. Tang, V., et al., *Chlorinated nucleosides - Novel mediators or biomarkers of disease?* 2015.
289. Guo, X., et al., *Glycolysis in the control of blood glucose homeostasis.* Acta Pharm Sin, 2012. **2**(4): p. 358-367.
290. Lee, S., et al., *The Interface Between ER and Mitochondria: Molecular Compositions and Functions.* Mol Cells, 2018. **41**(12): p. 1000-1007.
291. Cullinan, S.B., et al., *Nrf2 Is a Direct PERK Substrate and Effector of PERK-Dependent Cell Survival.* Mol Cell Biol, 2003. **23**(20): p. 7198-7209.
292. Li, X., et al., *Up-regulation of thioredoxin interacting protein (Txnip) by p38 MAPK and FOXO1 contributes to the impaired thioredoxin activity and increased ROS in glucose-treated endothelial cells.* Biochem Biophys Res Commun, 2009. **381**(4): p. 660-5.
293. Spindel, O.N., et al., *Thioredoxin-interacting protein mediates nuclear-to-plasma membrane communication: role in vascular endothelial growth factor 2 signaling.* Arterioscler Thromb Vasc Biol, 2012. **32**(5): p. 1264-70.
294. Faitova, J., et al., *Endoplasmic reticulum stress and apoptosis.* Cell Mol Biol, 2006. **11**(4): p. 488-505.
295. Sano, R., et al., *ER stress-induced cell death mechanisms.* Biochim Biophys Acta, 2013. **1833**(12): p. 3460-3470.

296. Langeveld, C.H., et al., *The antiproliferative effect of 8-chloro-adenosine, an active metabolite of 8-chloro-cyclic adenosine monophosphate, and disturbances in nucleic acid synthesis and cell cycle kinetics.* Biochem Pharmacol, 1997. **53**(2): p. 141-8.

297. DiMarco, J.P., et al., *Adenosine: electrophysiologic effects and therapeutic use for terminating paroxysmal supraventricular tachycardia.* Circulation, 1983. **68**(6): p. 1254-63.

298. Mimura, J., et al., *Role of Nrf2 in the pathogenesis of atherosclerosis.* Free Radical Biology and Medicine, 2015. **88**: p. 221-232.

299. Lee, S., et al., *Thioredoxin-interacting protein regulates protein disulfide isomerases and endoplasmic reticulum stress.* EMBO Mol Med, 2014. **6**(6): p. 732-43.

300. Zhao, Q., et al., *Thioredoxin-interacting protein links endoplasmic reticulum stress to inflammatory brain injury and apoptosis after subarachnoid haemorrhage.* J Neuroinflammation, 2017. **14**(1): p. 104.

301. Szpigel, A., et al., *Lipid environment induces ER stress, TXNIP expression and inflammation in immune cells of individuals with type 2 diabetes.* Diabetologia, 2018. **61**(2): p. 399-412.

302. Kim, S.M., et al., *Endothelial dysfunction induces atherosclerosis: increased aggrecan expression promotes apoptosis in vascular smooth muscle cells.* BMB Rep, 2019. **52**(2): p. 145-150.

303. Masoudkabir, F., et al., *The interplay of endothelial dysfunction, cardiovascular disease, and cancer: What we should know beyond inflammation and oxidative stress.* Eur J Prev Cardiol, 2019: p. 2047487319895415.

304. Libby, P., et al., *Immune effector mechanisms implicated in atherosclerosis: from mice to humans.* Immunity, 2013. **38**(6): p. 1092-104.

305. Rodier, F., et al., *Four faces of cellular senescence.* J Cell Biol, 2011. **192**(4): p. 547-56.

306. Tchkonia, T., et al., *Cellular senescence and the senescent secretory phenotype: therapeutic opportunities.* J Clin Invest, 2013. **123**(3): p. 966-72.

307. Thyberg, J., et al., *Adult human arterial smooth muscle cells in primary culture. Modulation from contractile to synthetic phenotype.* Cell Tissue Res, 1985. **239**(1): p. 69-74.

308. Rensen, S.S.M., et al., *Regulation and characteristics of vascular smooth muscle cell phenotypic diversity.* Neth Heart J, 2007. **15**(3): p. 100-108.

309. Regan, C.P., et al., *Molecular mechanisms of decreased smooth muscle differentiation marker expression after vascular injury.* J Clin Invest, 2000. **106**(9): p. 1139-47.

310. Alexander, M.R., et al., *Epigenetic control of smooth muscle cell differentiation and phenotypic switching in vascular development and disease.* Annu Rev Physiol, 2012. **74**: p. 13-40.

311. Vacek, T.P., et al., *Matrix metalloproteinases in atherosclerosis: role of nitric oxide, hydrogen sulfide, homocysteine, and polymorphisms.* Vasc Health Risk Manag, 2015. **11**: p. 173-183.

312. Schonbeck, U., et al., *Generation of biologically active IL-1 beta by matrix metalloproteinases: a novel caspase-1-independent pathway of IL-1 beta processing.* J Immunol, 1998. **161**(7): p. 3340-6.

313. Braun, M., et al., *Cellular adhesion molecules on vascular smooth muscle cells.* Cardiovasc Res, 1999. **41**(2): p. 395-401.

314. Newby, A.C., *Matrix metalloproteinases regulate migration, proliferation, and death of vascular smooth muscle cells by degrading matrix and non-matrix substrates.* Cardiovasc Res, 2006. **69**(3): p. 614-624.

315. Kearney, A.Y., et al., *8-Chloroadenosine Sensitivity in Renal Cell Carcinoma Is Associated with AMPK Activation and mTOR Pathway Inhibition.* PLoS One, 2015. **10**(8).

316. Wang, M., et al., *8-Chloro-adenosine sensitizes a human hepatoma cell line to TRAIL-induced apoptosis by caspase-dependent and -independent pathways.* Oncol Rep, 2004. **12**(1): p. 193-9.

317. Rozengurt, E., et al., *Uptake of nucleosides in density-inhibited cultures of 3T3 cells.* Nature, 1977. **267**(5610): p. 442-4.

318. Marz, R., et al., *Purine and pyrimidine transport and phosphoribosylation and their interaction in overall uptake by cultured mammalian cells. A re-evaluation.* J Biol Chem, 1979. **254**(7): p. 2329-38.

319. Webster, K.A., *Mitochondrial membrane permeabilization and cell death during myocardial infarction: roles of calcium and reactive oxygen species.* Future Cardiol, 2012. **8**(6): p. 863-884.

320. Hetz, C., *The unfolded protein response: controlling cell fate decisions under ER stress and beyond.* Nat Rev Mol Cell Biol, 2012. **13**(2): p. 89-102.

321. Manicone, A.M., et al., *Matrix metalloproteinases as modulators of inflammation.* Semin Cell Dev Biol, 2008. **19**(1): p. 34-41.

322. Yang, J., et al., *Detection of MMP activity in living cells by a genetically encoded surface-displayed FRET sensor.* Biochimica et Biophysica Acta (BBA) - Molecular Cell Research, 2007. **1773**(3): p. 400-407.

323. Hawkins, K.E., et al., *Fluorometric immunocapture assay for the specific measurement of matrix metalloproteinase-9 activity in biological samples: application to brain and plasma from rats with ischemic stroke.* Molecular Brain, 2013. **6**(1): p. 14.

324. Heo, S.H., et al., *Plaque Rupture is a Determinant of Vascular Events in Carotid Artery Atherosclerotic Disease: Involvement of Matrix Metalloproteinases 2 and 9.* J Clin Neurol, 2011. **7**(2): p. 69-76.

325. Thomas, A.C., et al., *Effect of matrix metalloproteinase-9 knockout on vein graft remodelling in mice.* J Vasc Res, 2010. **47**(4): p. 299-308.

326. Johnson, J.L., et al., *Divergent effects of matrix metalloproteinases 3, 7, 9, and 12 on atherosclerotic plaque stability in mouse brachiocephalic arteries.* Proc Natl Acad Sci U S A, 2005. **102**(43): p. 15575-80.

327. Yang, C.M., et al., *Interleukin-1beta induces ICAM-1 expression enhancing leukocyte adhesion in human rheumatoid arthritis synovial fibroblasts: involvement of ERK, JNK, AP-1, and NF-kappaB.* J Cell Physiol, 2010. **224**(2): p. 516-26.

328. Han, X., et al., *Enhancement of ICAM-1 via the JAK2/STAT3 signaling pathway in a rat model of severe acute pancreatitis-associated lung injury.* Exp Ther Med, 2016. **11**(3): p. 788-796.

329. Duzagac, F., et al., *JAK/STAT pathway interacts with intercellular cell adhesion molecule (ICAM) and vascular cell adhesion molecule (VCAM) while prostate cancer stem cells form tumor spheroids.* J buon, 2015. **20**(5): p. 1250-7.

330. Brown, B.A., et al., *Evidence for the Involvement of Matrix-Degrading Metalloproteinases (MMPs) in Atherosclerosis.* Prog Mol Biol Transl Sci, 2017. **147**: p. 197-237.

331. Belo, V.A., et al., *Matrix Metalloproteinase 2 as a Potential Mediator of Vascular Smooth Muscle Cell Migration and Chronic Vascular Remodeling in Hypertension.* J Vasc Res, 2015. **52**(4): p. 221-31.

332. Thyberg, J., et al., *Modulation of arterial smooth muscle cells from contractile to synthetic phenotype requires induction of ornithine decarboxylase activity and polyamine synthesis.* Exp Cell Res, 1987. **170**(1): p. 153-9.

333. Ghrib, F., et al., *The expression of tissue factor and tissue factor pathway inhibitor in aortic smooth muscle cells is up-regulated in synthetic compared to contractile phenotype.* Thromb Haemost, 2002. **87**(6): p. 1051-6.

334. Gomez, D., et al., *Smooth muscle cell phenotypic switching in atherosclerosis.* Cardiovasc Res, 2012. **95**(2): p. 156-64.

335. Owens, G.K., et al., *Molecular regulation of vascular smooth muscle cell differentiation in development and disease.* Physiol Rev, 2004. **84**(3): p. 767-801.

336. Hao, H., et al., *Arterial smooth muscle cell heterogeneity: implications for atherosclerosis and restenosis development.* Arterioscler Thromb Vasc Biol, 2003. **23**(9): p. 1510-20.

337. Rensen, S.S., et al., *Regulation and characteristics of vascular smooth muscle cell phenotypic diversity.* Neth Heart J, 2007. **15**(3): p. 100-8.

338. Dancey, J.T., et al., *Neutrophil kinetics in man.* J Clin Invest, 1976. **58**(3): p. 705-15.

339. Gorgens, A., et al., *Revision of the human hematopoietic tree: granulocyte subtypes derive from distinct hematopoietic lineages.* Cell Rep, 2013. **3**(5): p. 1539-52.

340. Ley, K., et al., *Getting to the site of inflammation: the leukocyte adhesion cascade updated.* Nat Rev Immunol, 2007. **7**(9): p. 678-89.

341. Chavakis, E., et al., *Novel aspects in the regulation of the leukocyte adhesion cascade.* Thromb Haemost, 2009. **102**(2): p. 191-7.

342. Mayadas, T.N., et al., *The multifaceted functions of neutrophils.* Annu Rev Pathol, 2014. **9**: p. 181-218.

343. Fuchs, T.A., et al., *Novel cell death program leads to neutrophil extracellular traps.* J Cell Biol, 2007. **176**(2): p. 231-241.

344. Urban, C.F., et al., *Neutrophil extracellular traps contain calprotectin, a cytosolic protein complex involved in host defense against Candida albicans.* PLoS pathogens, 2009. **5**(10): p. e1000639-e1000639.

345. Nguyen, G.T., et al., *Neutrophils to the ROScue: Mechanisms of NADPH Oxidase Activation and Bacterial Resistance.* Front Cell Infect Microbiol, 2017. **7**: p. 373-373.

346. Palmer, L.J., et al., *Hypochlorous acid regulates neutrophil extracellular trap release in humans.* Clin Exp Immunol, 2012. **167**(2): p. 261-8.

347. Kolaczkowska, E., et al., *Molecular mechanisms of NET formation and degradation revealed by intravital imaging in the liver vasculature.* Nature Comm 2015. **6**: p. 6673-6673.

348. Van Avondt, K., et al., *Signal Inhibitory Receptor on Leukocytes-1 Limits the Formation of Neutrophil Extracellular Traps, but Preserves Intracellular Bacterial Killing.* J Immunol, 2016. **196**(9): p. 3686.

349. Urban, C.F., et al., *Neutrophil extracellular traps capture and kill Candida albicans yeast and hyphal forms.* Cell Microbiol, 2006. **8**(4): p. 668-676.

350. Branzk, N., et al., *Neutrophils sense microbe size and selectively release neutrophil extracellular traps in response to large pathogens.* Nature Immunol 2014. **15**(11): p. 1017-1025.

351. Metzler, K.D., et al., *A myeloperoxidase-containing complex regulates neutrophil elastase release and actin dynamics during NETosis.* Cell Rep, 2014. **8**(3): p. 883-896.

352. Papayannopoulos, V., et al., *Neutrophil elastase and myeloperoxidase regulate the formation of neutrophil extracellular traps.* J Cell Biol, 2010. **191**(3): p. 677-691.

353. Metzler, K.D., et al., *Myeloperoxidase is required for neutrophil extracellular trap formation: implications for innate immunity.* Blood, 2011. **117**(3): p. 953-959.

354. Röhm, M., et al., *NADPH oxidase promotes neutrophil extracellular trap formation in pulmonary aspergillosis.* Infect Immun, 2014. **82**(5): p. 1766-1777.

355. Loures, F.V., et al., *Recognition of Aspergillus fumigatus hyphae by human plasmacytoid dendritic cells is mediated by dectin-2 and results in formation of extracellular traps.* PLoS pathogens, 2015. **11**(2): p. e1004643-e1004643.

356. Funchal, G.A., et al., *Respiratory syncytial virus fusion protein promotes TLR-4-dependent neutrophil extracellular trap formation by human neutrophils.* PloS one, 2015. **10**(4): p. e0124082-e0124082.

357. Saitoh, T., et al., *Neutrophil Extracellular Traps Mediate a Host Defense Response to Human Immunodeficiency Virus-1.* Cell Host & Microbe, 2012. **12**(1): p. 109-116.

358. Neeli, I., et al., *Regulation of Extracellular Chromatin Release from Neutrophils.* J Innate Immunol, 2009. **1**(3): p. 194-201.

359. Lim, M.B.H., et al., *Rac2 is required for the formation of neutrophil extracellular traps.* J Leukoc Biol, 2011. **90**(4): p. 771-776.

360. Etulain, J., et al., *P-selectin promotes neutrophil extracellular trap formation in mice.* Blood, 2015. **126**(2): p. 242-246.

361. von Brühl, M.-L., et al., *Monocytes, neutrophils, and platelets cooperate to initiate and propagate venous thrombosis in mice in vivo.* J Exp Med, 2012. **209**(4): p. 819.

362. Clark, S.R., et al., *Platelet TLR4 activates neutrophil extracellular traps to ensnare bacteria in septic blood.* Nature Medicine, 2007. **13**: p. 463.

363. Qiu, S.-L., et al., *Neutrophil extracellular traps induced by cigarette smoke activate plasmacytoid dendritic cells.* Thorax, 2017. **72**(12): p. 1084.

364. Martinod, K., et al., *Neutrophil elastase-deficient mice form neutrophil extracellular traps in an experimental model of deep vein thrombosis.* J Thromb Haemost, 2016. **14**(3): p. 551-558.

365. Douda, D.N., et al., *SK3 channel and mitochondrial ROS mediate NADPH oxidase-independent NETosis induced by calcium influx.* PNAS, 2015. **112**(9): p. 2817-2822.

366. Neeli, I., et al., *Opposition between PKC isoforms regulates histone deimination and neutrophil extracellular chromatin release.* Front Immunol, 2013. **4**: p. 38-38.

367. Wong, S.L., et al., *Diabetes primes neutrophils to undergo NETosis, which impairs wound healing.* Nature Medicine, 2015. **21**: p. 815.

368. Garcia-Romo, G.S., et al., *Netting neutrophils are major inducers of type I IFN production in pediatric systemic lupus erythematosus.* Sci Transl Med, 2011. **3**(73): p. 73ra20.

369. Villanueva, E., et al., *Netting neutrophils induce endothelial damage, infiltrate tissues, and expose immunostimulatory molecules in systemic lupus erythematosus.* J Immunol, 2011. **187**(1): p. 538-52.

370. Martínez-Alemán, S.R., et al., *Understanding the Entanglement: Neutrophil Extracellular Traps (NETs) in Cystic Fibrosis.* Front Cell Infect Microbiol, 2017. **7**: p. 104-104.

371. Berger-Achituv, S., et al., *A proposed role for neutrophil extracellular traps in cancer immunoediting.* Front Immunol, 2013. **4**: p. 48.

372. Garley, M., et al., *NETs in cancer.* Tumour Biol, 2016. **37**(11): p. 14355-14361.

373. Kessenbrock, K., et al., *Netting neutrophils in autoimmune small-vessel vasculitis.* Nat Med, 2009. **15**(6): p. 623-5.

374. Chistiakov, D.A., et al., *Neutrophil's weapons in atherosclerosis.* Exp Mol Pathol, 2015. **99**(3): p. 663-71.

375. Martinod, K., et al., *Thrombosis: tangled up in NETs.* Blood, 2014. **123**(18): p. 2768.

376. Warnatsch, A., et al., *Inflammation. Neutrophil extracellular traps license macrophages for cytokine production in atherosclerosis.* Science, 2015. **349**(6245): p. 316-20.

377. Quillard, T., et al., *TLR2 and neutrophils potentiate endothelial stress, apoptosis and detachment: implications for superficial erosion.* Eur Heart J, 2015. **36**(22): p. 1394-404.

378. Gupta, A.K., et al., *Activated endothelial cells induce neutrophil extracellular traps and are susceptible to NETosis-mediated cell death.* FEBS Lett, 2010. **584**(14): p. 3193-7.

379. Kougias, P., et al., *Defensins and cathelicidins: neutrophil peptides with roles in inflammation, hyperlipidemia and atherosclerosis.* J Cell Mol Med, 2005. **9**(1): p. 3-10.

380. Tucker, K.A., et al., *Characterization of a new human diploid myeloid leukemia cell line (PLB- 985) with granulocytic and monocytic differentiating capacity.* Blood, 1987. **70**(2): p. 372.

381. Marin-Esteban, V., et al., *Afa/Dr Diffusely Adhering Escherichia coli Strain C1845 Induces Neutrophil Extracellular Traps That Kill Bacteria and Damage Human Enterocyte-Like Cells.* Infect Immun, 2012. **80**(5): p. 1891.

382. Valavanidis, A., et al., *8-hydroxy-2' -deoxyguanosine (8-OHdG): A critical biomarker of oxidative stress and carcinogenesis.* J Environ Sci Health C Environ Carcinog Ecotoxicol Rev, 2009. **27**(2): p. 120-39.

383. Sova, H., et al., *8-Hydroxydeoxyguanosine: a new potential independent prognostic factor in breast cancer.* Br J Cancer, 2010. **102**: p. 1018.

384. Sheridan, J., et al., *Nuclear oxidative damage correlates with poor survival in colorectal cancer.* Br J Cancer, 2009. **100**(2): p. 381-388.

385. Hofer, T., et al., *Nucleic acid oxidative damage in Alzheimer's disease-explained by the hepcidin-ferroportin neuronal iron overload hypothesis?* J Trace Elem Med Biol, 2016. **38**: p. 1-9.

386. Lovell, M.A., et al., *Increased DNA oxidation and decreased levels of repair products in Alzheimer's disease ventricular CSF.* J Neurochem, 1999. **72**(2): p. 771-6.

387. Xiang, F., et al., *Association of serum 8-hydroxy-2'-deoxyguanosine levels with the presence and severity of coronary artery disease.* Coron Artery Dis, 2011. **22**(4): p. 223-7.

388. Herrero, A., et al., *Effect of aging on mitochondrial and nuclear DNA oxidative damage in the heart and brain throughout the life-span of the rat.* J Am Aging Assoc, 2001. **24**(2): p. 45-50.

389. Pedruzzi, E., et al., *Differentiation of PLB-985 myeloid cells into mature neutrophils, shown by degranulation of terminally differentiated compartments in response to N-formyl peptide and priming of superoxide anion production by granulocyte–macrophage colony-stimulating factor.* Br J Haematol, 2002. **117**(3): p. 719-726.

390. Masuda, S., et al., *Measurement of NET formation in vitro and in vivo by flow cytometry.* Cytometry A, 2017. **91**(8): p. 822-829.

391. Sémiramoth, N., et al., *Afa/Dr-Expressing, Diffusely Adhering Escherichia coli Strain C1845 Triggers F1845 Fimbria-Dependent Phosphatidylserine Externalization on Neutrophil-Like Differentiated PLB-985 Cells through an Apoptosis-Independent Mechanism.* Infect Immun, 2010. **78**(7): p. 2974.

392. Sémiramoth, N., et al., *Escherichia coli type 1 pili trigger late IL-8 production by neutrophil-like differentiated PLB-985 cells through a Src family kinase- and MAPK-dependent mechanism.* J Leukoc Biol, 2009. **85**(2): p. 310-321.

393. Volk, A.P.D., et al., *Priming of neutrophils and differentiated PLB-985 cells by pathophysiological concentrations of TNF-α is partially oxygen dependent.* J Innate Immunol, 2011. **3**(3): p. 298-314.

394. Rincón Gila, E., et al., *A map of gene expression in neutrophil-like cell lines.* BMC Genomics, 2018. **19**.

395. Akong-Moore, K., et al., *Influences of Chloride and Hypochlorite on Neutrophil Extracellular Trap Formation.* PloS one, 2012. **7**: p. e42984.

396. Hawkins, Clare L., *Hypochlorous acid-mediated modification of proteins and its consequences.* Essays Biochem, 2019.

397. Carmona-Rivera, C., et al., *Induction and Quantification of NETosis*. 2016. p. 14.41.1-14.41.14.

398. Bekeschus, S., et al., *Neutrophil extracellular trap formation is elicited in response to cold physical plasma.* J Leukoc Biol, 2016. **100**(4): p. 791-799.

399. Muñoz Caro, T., et al., *Neutrophil Extracellular Traps as Innate Immune Reaction against the Emerging Apicomplexan Parasite Besnoitia besnoiti.* PLOS ONE, 2014. **9**(3): p. e91415.

400. Hu, Q., et al., *Increased neutrophil extracellular traps activate NLRP3 and inflammatory macrophages in adult-onset Still's disease.* Arthritis Res Ther, 2019. **21**(1): p. 9.

401. Kraaij, T., et al., *A novel method for high-throughput detection and quantification of neutrophil extracellular traps reveals ROS-independent NET release with immune complexes.* Autoimmun Rev, 2016. **15**(6): p. 577-584.

402. Pal, B.C., et al., *Environmental pollutant 5-chlorouracil is incorporated in mouse liver and testes DNA.* Mutat Res, 1981. **91**(4): p. 395-401.

403. Morris, S.M., *The genetic toxicology of 5-fluoropyrimidines and 5-chlorouracil.* Mutat Res, 1993. **297**(1): p. 39-51.

404. Yu, H., et al., *Ionization of bromouracil and fluorouracil stimulates base mispairing frequencies with guanine.* J Biol Chem, 1993. **268**(21): p. 15935-43.

405. Cox, J.A., et al., *Activation of the human neutrophil nicotinamide adenine dinucleotide phosphate (NADPH)-oxidase by protein kinase C.* The Journal of clinical investigation, 1985. **76**(5): p. 1932-1938.

406. Nicholls, S.J., et al., *Myeloperoxidase and cardiovascular disease.* Arterioscler Thromb Vasc Biol, 2005. **25**(6): p. 1102-11.

407. Jeitner, T.M., et al., *Linking Inflammation and Parkinson Disease: Hypochlorous Acid Generates Parkinsonian Poisons.* Toxicol Sci, 2016. **151**(2): p. 388-402.

408. Sam, C.-H., et al., *The role of hypochlorous acid as one of the reactive oxygen species in periodontal disease.* J Dent Sci, 2009. **4**(2): p. 45-54.

409. Malik, Q., et al., *Oxidative and non-oxidative DNA damage and cardiovascular disease.* Free Radic Res, 2012. **46**(4): p. 554-64.

410. Nicholls Stephen, J., et al., *Myeloperoxidase and Cardiovascular Disease.* Arterioscler Thromb Vasc Biol, 2005. **25**(6): p. 1102-1111.

411. Kawai, Y., et al., *Endogenous Formation of Novel Halogenated 2'-Deoxycytidine: Hypohalous Acids-Mediated DNA Modification at the Site of Inflammation.* J Biol Chem, 2004. **279**(49): p. 51241-51249.

412. Uppu, R.M., et al., *Competitive reactions of peroxynitrite with 2'-deoxyguanosine and 7,8-dihydro-8-oxo-2'-deoxyguanosine (8-oxodG): relevance to the formation of 8-oxodG in DNA exposed to peroxynitrite.* Free Radic Biol Med, 1996. **21**(3): p. 407-11.

413. Burney, S., et al., *DNA damage in deoxynucleosides and oligonucleotides treated with peroxynitrite.* Chem Res Toxicol, 1999. **12**(6): p. 513-20.

414. Weimann, A., et al., *Quantification of 8-oxo-guanine and guanine as the nucleobase, nucleoside and deoxynucleoside forms in human urine by high-performance liquid chromatography–electrospray tandem mass spectrometry.* Nucleic Acids Res, 2002. **30**(2): p. e7-e7.

415. Yoshida, R., et al., *Urinary 8-Oxo-7,8-dihydro-2'-deoxyguanosine Values Measured by an ELISA Correlated Well with Measurements by High-Performance Liquid Chromatography with Electrochemical Detection.* Cancer Epidemiol Biomarkers Prev, 2002. **11**(10): p. 1076-1081.

416. Duncan, B.K., et al., *Mutagenic deamination of cytosine residues in DNA.* Nature, 1980. **287**(5782): p. 560-1.

417. Wu, M., et al., *Multiparameter metabolic analysis reveals a close link between attenuated mitochondrial bioenergetic function and enhanced glycolysis dependency in human tumor cells.* Am J Physiol, 2007. **292**(1): p. C125-C136.

418. Minamino, T., et al., *Endoplasmic reticulum stress as a therapeutic target in cardiovascular disease.* Circ Res, 2010. **107**(9): p. 1071-82.

419. Tabas, I., et al., *Integrating the mechanisms of apoptosis induced by endoplasmic reticulum stress.* Nat Cell Biol, 2011. **13**(3): p. 184-90.

420. Ivanova, E.A., et al., *The Role of Endoplasmic Reticulum Stress and Unfolded Protein Response in Atherosclerosis.* Int J Mol Sci, 2016. **17**(2): p. 193.

421. Kaneko, M., et al., *Activation signal of nuclear factor-kappa B in response to endoplasmic reticulum stress is transduced via IRE1 and tumor necrosis factor receptor-associated factor 2.* Biol Pharm Bull, 2003. **26**(7): p. 931-5.

422. Sun, M., et al., *Sp1 is involved in 8-chloro-adenosine-upregulated death receptor 5 expression in human hepatoma cells.* Oncol Rep, 2008. **19**(1): p. 177-85.

423. Jakobs, P., et al., *Nuclear Factor (Erythroid-Derived 2)-Like 2 and Thioredoxin-1 in Atherosclerosis and Ischemia/Reperfusion Injury in the Heart.* Antioxid Redox Signal, 2017. **26**(12): p. 630-644.

424. Mimura, J., et al., *Role of Nrf2 in the pathogenesis of atherosclerosis.* Free Radic Biol Med, 2015. **88**: p. 221-232.

425. Pi, J., et al., *Activation of Nrf2-mediated oxidative stress response in macrophages by hypochlorous acid.* Toxicol Appl Pharmacol, 2008. **226**(3): p. 236-43.

426. Juan, S.H., et al., *Adenovirus-mediated heme oxygenase-1 gene transfer inhibits the development of atherosclerosis in apolipoprotein E-deficient mice.* Circulation, 2001. **104**(13): p. 1519-25.

427. Cheng, C., et al., *Heme oxygenase 1 determines atherosclerotic lesion progression into a vulnerable plaque.* Circulation, 2009. **119**(23): p. 3017-27.

428. Yet, S.F., et al., *Absence of heme oxygenase-1 exacerbates atherosclerotic lesion formation and vascular remodeling.* FASEB J, 2003. **17**(12): p. 1759-61.

429. Orozco, L.D., et al., *Heme oxygenase-1 expression in macrophages plays a beneficial role in atherosclerosis.* Circ Res, 2007. **100**(12): p. 1703-11.

430. Brouard, S., et al., *Carbon monoxide generated by heme oxygenase 1 suppresses endothelial cell apoptosis.* J Exp Med, 2000. **192**(7): p. 1015-26.

431. Willis, D., et al., *Heme oxygenase: a novel target for the modulation of the inflammatory response.* Nat Med, 1996. **2**(1): p. 87-90.

432. Kim, S.Y., et al., *Activation of NAD(P)H:quinone oxidoreductase 1 prevents arterial restenosis by suppressing vascular smooth muscle cell proliferation.* Circ Res, 2009. **104**(7): p. 842-50.

433. Duckers, H.J., et al., *Heme oxygenase-1 protects against vascular constriction and proliferation.* Nat Med, 2001. **7**(6): p. 693-8.

434. Valinluck, V., et al., *5-halogenated pyrimidine lesions within a CpG sequence context mimic 5-methylcytosine by enhancing the binding of the methyl-CpG-binding domain of methyl-CpG-binding protein 2 (MeCP2).* Nucleic Acids Res, 2005. **33**(9): p. 3057-64.

435. Heo, S.H., et al., *Plaque rupture is a determinant of vascular events in carotid artery atherosclerotic disease: involvement of matrix metalloproteinases 2 and 9.* J Clin Neurol, 2011. **7**(2): p. 69-76.

Appendix 1 – Table of Materials

Table 1: *Table of materials.*

Reagent	Supplier	Location
0.22 µm centrifugal filter	Merck	Kenilworth, NJ, USA
10 kDa centrifugal filter	Merck	Kenilworth, NJ, USA
2- 2-deoxy-2-[(7-nitro-2,1,3-benzoxadiazol-4-yl)-amino]-D-glucose (2-NBDG)	Cayman Chemical	Ann Arbor, MO, USA
2'-deoxycytidine	Sigma Aldrich	St Louis, MO, USA
3 M sodium acetate (pH 5.2)	Sigma Aldrich	St Louis, MO, USA
4-12% Bis-tris gel	Life Technologies	Carlsbad, CA, USA
5ClC	Biolog	Bremen, Germany
5CldC	Biolog	Bremen, Germany
8ClA	Biolog	Bremen, Germany
8-ClATP	Biolog	Bremen, Germany
8CldA	Biolog	Bremen, Germany
8CldG	Biolog	Bremen, Germany
8ClG	Biolog	Bremen, Germany
8oxodG	Biolog	Bremen, Germany
8oxoG	Biolog	Bremen, Germany
Acetic acid	Astral Diagnostics	West Deptford, NJ, USA
Acetonitrile	Honeywell	Charlotte, NC, USA
Acquity C18 UPLC column	Waters	Milford, MA, USA

Acrylamide	Amresco	Solon, OH, USA
Adenosine (Ad)	Sigma Aldrich	St Louis, MO, USA
Alkaline phosphatase	Sigma Aldrich	St Louis, MO, USA
All-trans retinoic acid (ATRA)	Sigma Aldrich	St Louis, MO, USA
Ammonium formate	Sigma Aldrich	St Louis, MO, USA
Ammonium persulphate (APS)	Astral Diagnostics	West Deptford, NJ, USA
Ammonium phosphate monobasic	Sigma Aldrich	St Louis, MO, USA
Annexin V	BD Pharmingen	San Jose, CA, USA
Anti-ATF4 antibody	Santa Cruz Biotechnology	Dallas, TX, USA
Anti-mouse IgG	Cell Signalling Technology	Danvers, MA, USA
Anti-rabbit IgG	Cell Signalling Technology	Danvers, MA, USA
Anti-TXNIP antibody	Invitrogen	Carlsbad, CA, USA
Anti-β-actin antibody	Santa Cruz Biotechnology	Dallas, TX, USA
Apigenin	Cayman Chemical	Ann Arbor, MO, USA
ATP	Sigma Aldrich	St Louis, MO, USA
ATPlite Luminescence Assay System	Perkin Elmer	Waltham, MA, USA
BCA Protein Reagent A	ThermoFisher Scientific	Rockford, IL, USA
Bovine serum albumin (BSA)	Sigma Aldrich	St Louis, MO, USA
Calcium chloride	Sigma Aldrich	St Louis, MO, USA
Carbonyl cyanide m-chlorophenyl hydrazone (CCCP)	Life Technologies	Carlsbad, CA, USA
Cell Lytic Reagent	Sigma Aldrich	St Louis, MO, USA
Cell MitoStress Test Kit	Agilent	Santa Clara, CA, USA

Chloroform	Sigma Aldrich	St Louis, MO, USA
Coomassie brilliant blue	ThermoFisher Scientific	Rockford, IL, USA
Copper sulphate pentahydrate	Sigma Aldrich	St Louis, MO, USA
CTP	Sigma Aldrich	St Louis, MO, USA
Cytidine	Sigma Aldrich	St Louis, MO, USA
DC Protein Assay	Bio-Rad	Hercules, CA, USA
Deoxycytidine	Sigma Aldrich	St Louis, MO, USA
Deoxyguanosine	Sigma Aldrich	St Louis, MO, USA
Deoxyribonuclease (DNase)	Roche	Basel, Switzerland
Dimethyl sulfoxide (DMSO)	Sigma Aldrich	St Louis, MO, USA
Discovery C18 column	Sigma Aldrich	St Louis, MO, USA
DNA isolation kit	Qiagen	Hilden, Germany
EDTA	Sigma Aldrich	St Louis, MO, USA
Ethanol	Sigma Aldrich	St Louis, MO, USA
Fetal bovine serum (FBS)	Gibco	Grand Island, NY, USA
Fluo-4AM	Invitrogen	Carlsbad, CA, USA
Formaldehyde	Sigma Aldrich	St Louis, MO, USA
Gelatin	Sigma Aldrich	St Louis, MO, USA
Giemsa	Sigma Aldrich	St Louis, MO, USA
Glucose	Sigma Aldrich	St Louis, MO, USA
Glucose uptake cell-based assay kit	Cayman Chemical	Ann Arbor, MO, USA
Glyceraldehyde 3-phosphate	Sigma Aldrich	St Louis, MO, USA
Glycine	Sigma Aldrich	St Louis, MO, USA

Glycolysis cell-based assay kit	Cayman Chemical	Ann Arbor, MO, USA
GTP	Sigma Aldrich	St Louis, MO, USA
HBSS	Gibco	Grand Island, NY, USA
HEPES	Sigma Aldrich	St Louis, MO, USA
Human coronary artery endothelial cells (HCAEC)	Cell Applications	San Diego, CA, USA
Human coronary artery smooth muscle cells (HCASMC)	Cell Applications	San Diego, CA, USA
Hypochlorous acid (HOCl)	VWR	Radnor, PA, USA
iBlot 2 PVDF stack membrane	ThermoFisher Scientific	Rockford, IL, USA
iQ SYBR Green Supermix	Bio-Rad	Hercules, CA, USA
iScript cDNA Synthesis Kit	Bio-Rad	Hercules, CA, USA
Isolate II DNA/RNA/Protein Kit	Bioline	London, UK
Isopropanol	Sigma Aldrich	St Louis, MO, USA
JC-1	Life Technologies	Carlsbad, CA, USA
KI-67 monoclonal antibody	Life Technologies	Carlsbad, CA, USA
L-glutamine	Life Technologies	Carlsbad, CA, USA
May – Grünwald stain	Sigma Aldrich	St Louis, MO, USA
MES running buffer	ThermoFisher Scientific	Rockford, IL, USA
MesoEndo Cell Culture Medium	Cell Applications	San Diego, CA, USA
Methanol	Sigma Aldrich	St Louis, MO, USA
Micrococcal nuclease (Mnase)	Roche	Basel, Switzerland
NAD^+, free acid	Roche	Basel, Switzerland
NE-PER nuclear and cytosolic extraction kit	ThermoFisher Scientific	Rockford, IL, USA

Nuclease P_1	Sigma Aldrich	St Louis, MO, USA
Nuclease-free H_2O	Bio-Rad	Hercules, CA, USA
NuPAGE LDS sample buffer (4X)	ThermoFisher Scientific	Rockford, IL, USA
NuPAGE reduction agent (10X)	ThermoFisher Scientific	Rockford, IL, USA
PBS	Gibco	Grand Island, NY, USA
Penicillin-streptomycin	Gibco	Grand Island, NY, USA
Perchloric acid	UNIVAR	Downers Grove, IL< USA
PERTEX	Leica Microsystems	Wetzlar, Germany
Phorbol myristate acetate (PMA)	Sigma Aldrich	St Louis, MO, USA
Phosphate buffer (pH 6.5)	Sigma Aldrich	St Louis, MO, USA
PicoGreen	ThermoFisher Scientific	Rockford, IL, USA
PLB-985	DSMZ	Braunschweig, Germany
Poly-*l*-lysine	Sigma Aldrich	St Louis, MO, USA
Ponceau S	Sigma Aldrich	St Louis, MO, USA
Potassium hydroxide	Sigma Aldrich	St Louis, MO, USA
Precision Plus Protein Kaleidoscope	Bio-Rad	Hercules, CA, USA
PrestoBlue Cell Viability reagent	ThermoFisher Scientific	Rockford, IL, USA
ProLong Gold antifade mountant	Invitrogen	Carlsbad, CA, USA
Propidium iodide	BD Pharmingen	San Jose, CA ,USA
Protease inhibitor cocktail	Sigma Aldrich	St Louis, MO, USA
Quant-iT PicoGreen dsDNA Reagent	ThermoFisher Scientific	Rockford, IL, USA
ReliaPrep RNA Cell Miniprep System	Promega	Madison, WI, USA

Restore PLUS Western blot stripping buffer	ThermoFisher Scientific	Rockford, IL, USA
RIPA buffer	Sigma Aldrich	St Louis, MO, USA
RPMI-1640	Sigma Aldrich	St Louis, MO, USA
Seahorse XF DMEM	Agilent	Santa Clara, CA, USA
Sep-Pak C18 3 cc Vacuum Cartridge	Waters	Milford, MA, USA
Smooth Muscle Cell Growth Medium	Lonza	Basel, Switzerland
Sodium azide	Sigma Aldrich	St Louis, MO, USA
Sodium chloride	Sigma Aldrich	St Louis, MO, USA
Sodium dodecyl sulfate (SDS)	Sigma Aldrich	St Louis, MO, USA
Sodium phosphate	Sigma Aldrich	St Louis, MO, USA
Sodium pyrophosphate	Sigma Aldrich	St Louis, MO, USA
Sodium pyruvate	Sigma Aldrich	St Louis, MO, USA
Sytox Green	ThermoFisher Scientific	Rockford, IL, USA
Tetramethylethylenediamine (TEMED)	Sigma Aldrich	St Louis, MO, USA
Trifluoroacetic acid (TFA)	Sigma Aldrich	St Louis, MO, USA
Tris-base	Astral Scientific	Sydney, NSW, Australia
Tris-HCl	Astral Scientific	Sydney, NSW, Australia
Triton X-100	Sigma Aldrich	St Louis, MO, USA
Trypan blue	Gibco	Grand Island, NY, USA
Trypsin-EDTA	ThermoFisher Scientific	Rockford, IL, USA
Tween-20	Sigma Aldrich	St Louis, MO, USA
UTP	Sigma Aldrich	St Louis, MO, USA
Western Lighting plus ECL	Perkin Elmer	Waltham, MA, USA

Zinc sulfate	Sigma Aldrich	St Louis, MO, USA
ZORBAX SAX HPLC column	Agilent	Santa Clara, CA, USA

Appendix 2 – Example chromatograms from LC-MS/MS

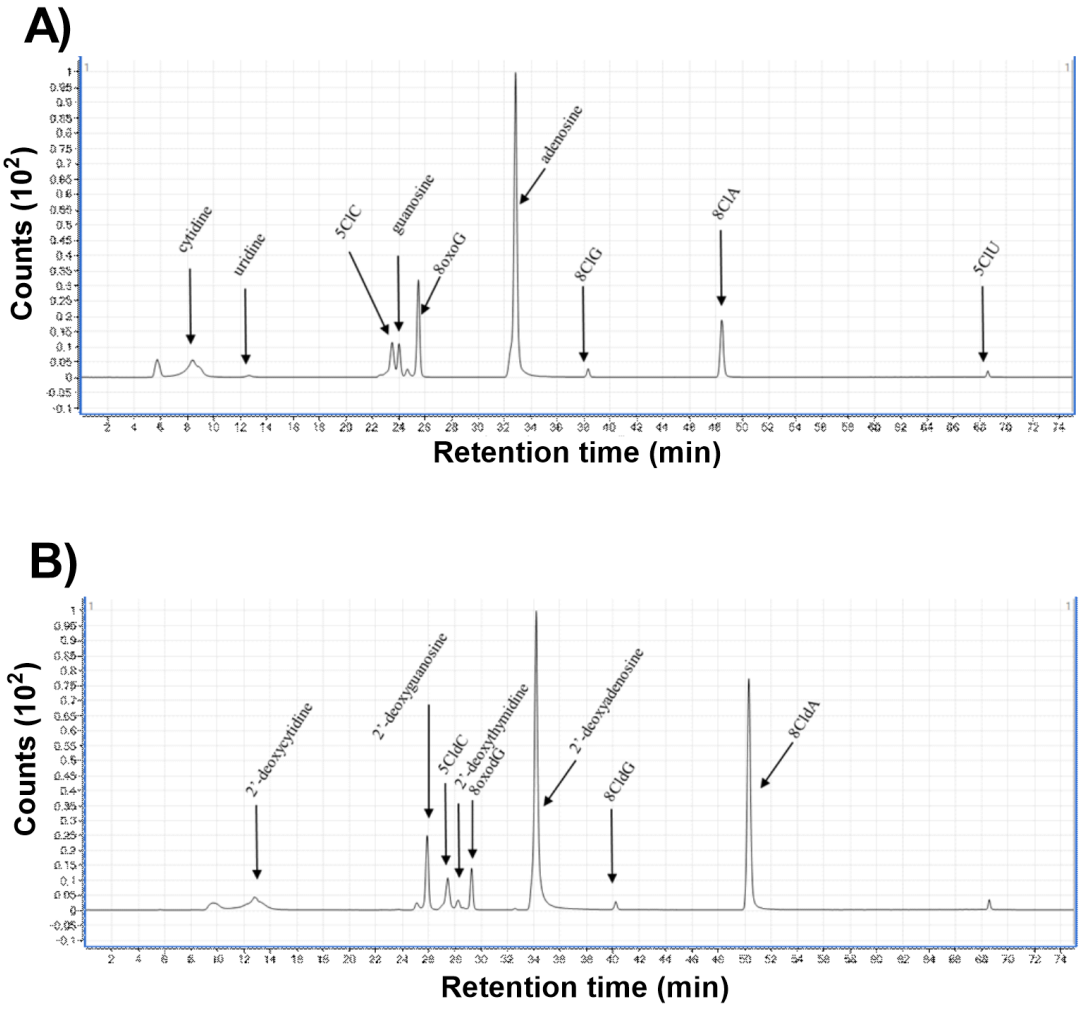

Figure 1: *Total ion chromatogram of unmodified and modified nucleosides detected using MS/MS.*

Chromatographic separation of a mixed ribose standard containing cytidine, uridine, 5ClC, guanosine, 8oxoG, adenosine, 8ClG, 8ClA and 5ClU was achieved using LC-MS/MS (A). (B) shows chromatographic separation of deoxyribose nucleoside standard by MRM using LC-MS/MS. Detection achieved by MRM of m/z specified in Table 2.4.

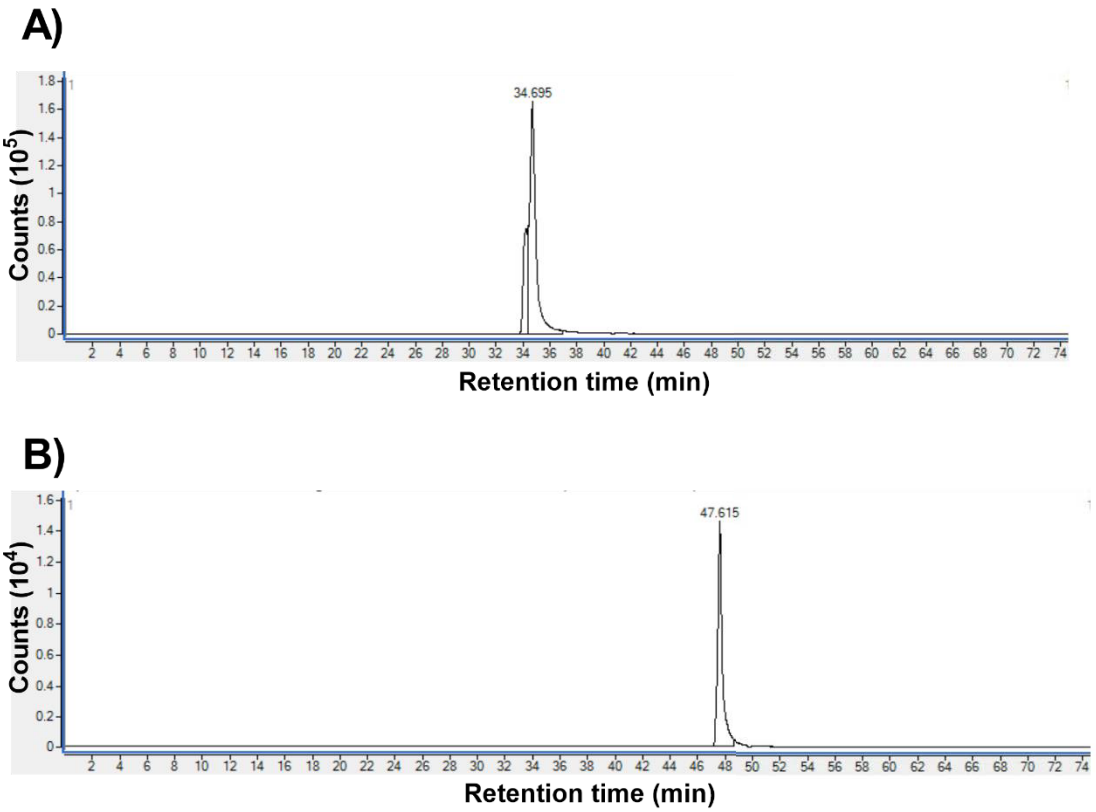

Figure 2: *SRM traces of HCAEC exposed to 8ClA detected using MS/MS.*
HCAEC (1 × 10^6 cells) were treated with 16 µM 8ClA. After treatment, RNA was extracted, then hydrolysed and dephosphorylated prior to analysis by LC-MS/MS. A mass fragmentation of 268.1 → 136.1 was monitored using SRM for positive identification of adenosine (A) and 302.2 → 169.9. for 8ClA (B).

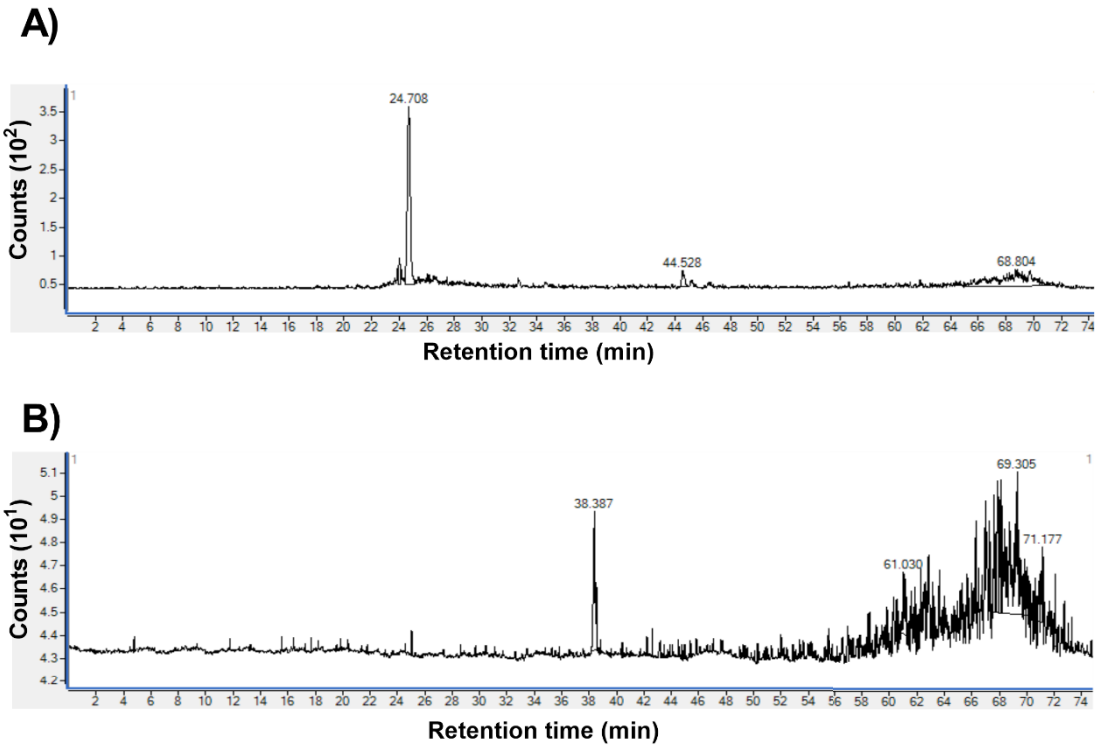

Figure 3: *SRM traces of HCAEC exposed to 8ClG detected using MS/MS.*
HCAEC (1 × 10^6 cells) were treated with 16 µM 8ClG. After treatment, RNA was extracted, then hydrolysed and dephosphorylated prior to analysis by LC-MS/MS. A mass fragmentation of 284.1 → 151.9 was monitored using SRM for positive identification of guanosine (A) and 318.1 → 186.0 for 8ClG (B).

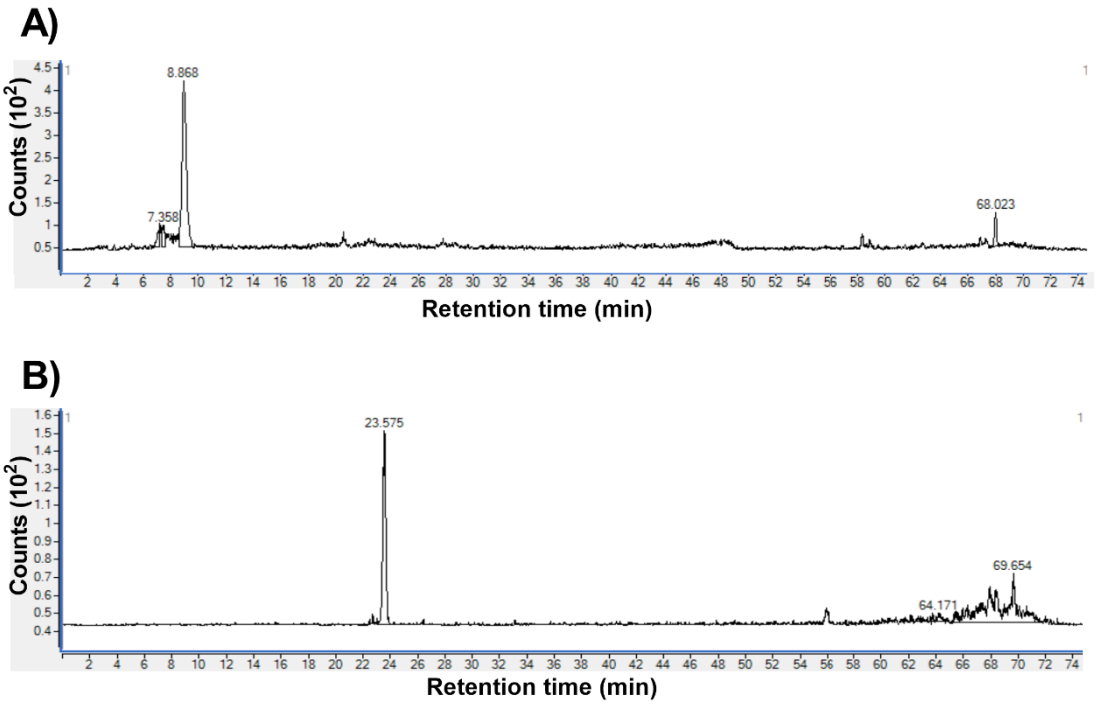

Figure 4: *SRM traces of HCAEC exposed to 5ClC detected using MS/MS.*
HCAEC (1 × 10^6 cells) were treated with 16 µM 5ClC. After treatment, RNA was extracted, then hydrolysed and dephosphorylated prior to analysis by LC-MS/MS. A mass fragmentation of 244.1 → 112.0 was monitored using SRM for positive identification of cytidine (A) and 278.1 → 145.9 for 5ClC (B).

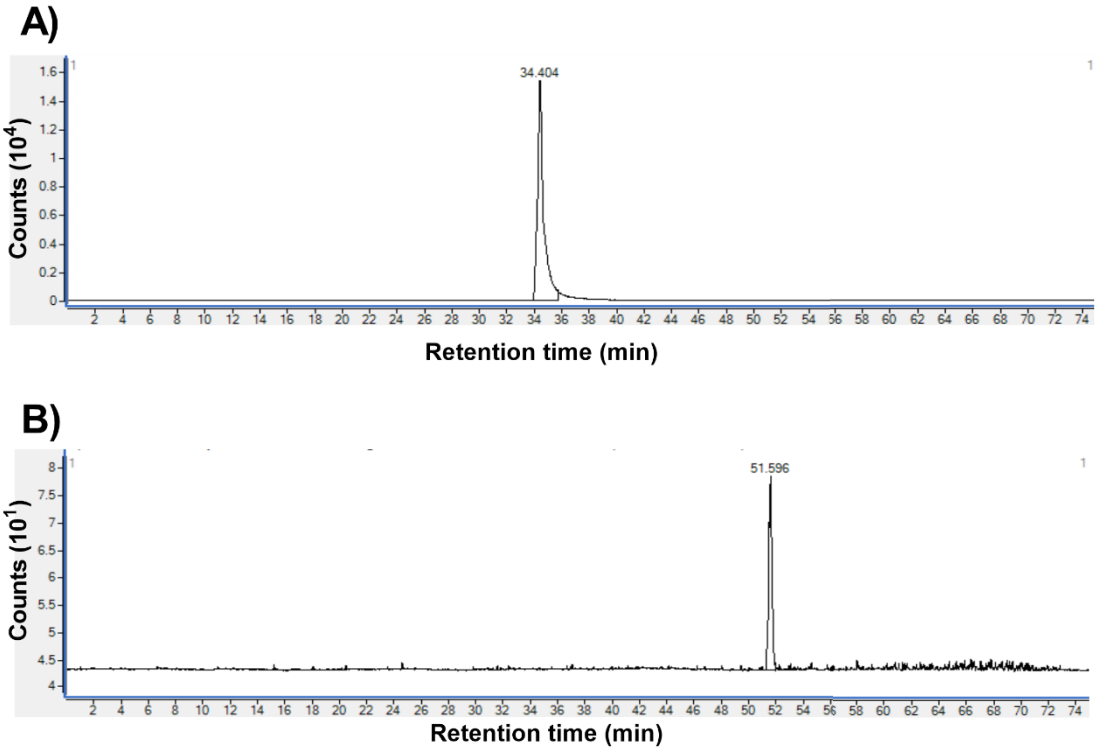

Figure 5: *SRM traces of HCAEC exposed to 8ClдA detected using MS/MS.*
HCAEC (1×10^6 cells) were treated with 16 µM 8ClдA. After treatment, DNA was extracted, then hydrolysed and dephosphorylated prior to analysis by LC-MS/MS. A mass fragmentation of 252.2 → 135.9 was monitored using SRM for positive identification of dA (A) and 286.1 → 169.9 for 8ClдA (B).

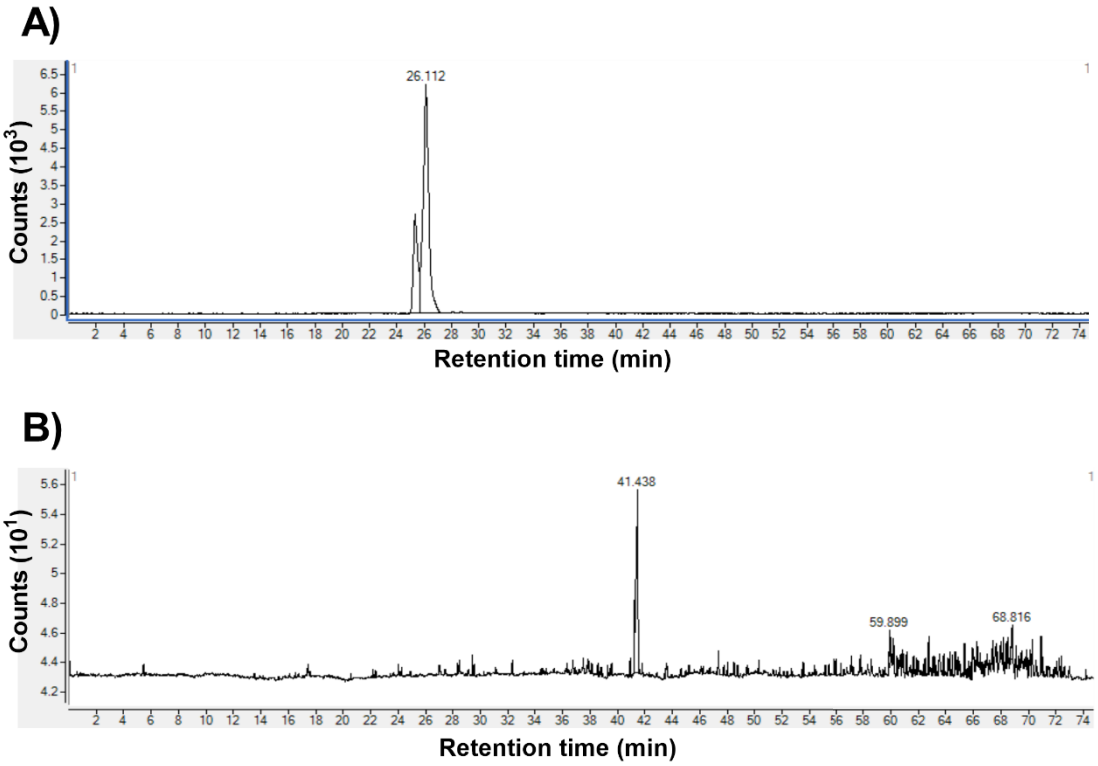

Figure 6: *SRM traces of HCAEC exposed to 8ClдG detected using MS/MS.*
HCAEC (1×10^6 cells) were treated with 16 µM 8ClдG. After treatment, DNA was extracted, then hydrolysed and dephosphorylated prior to analysis by LC-MS/MS. A mass fragmentation of 268.1 → 151.9 was monitored using SRM for positive identification of dG (A) and 302.1 → 186.0 for 8ClдG (B).

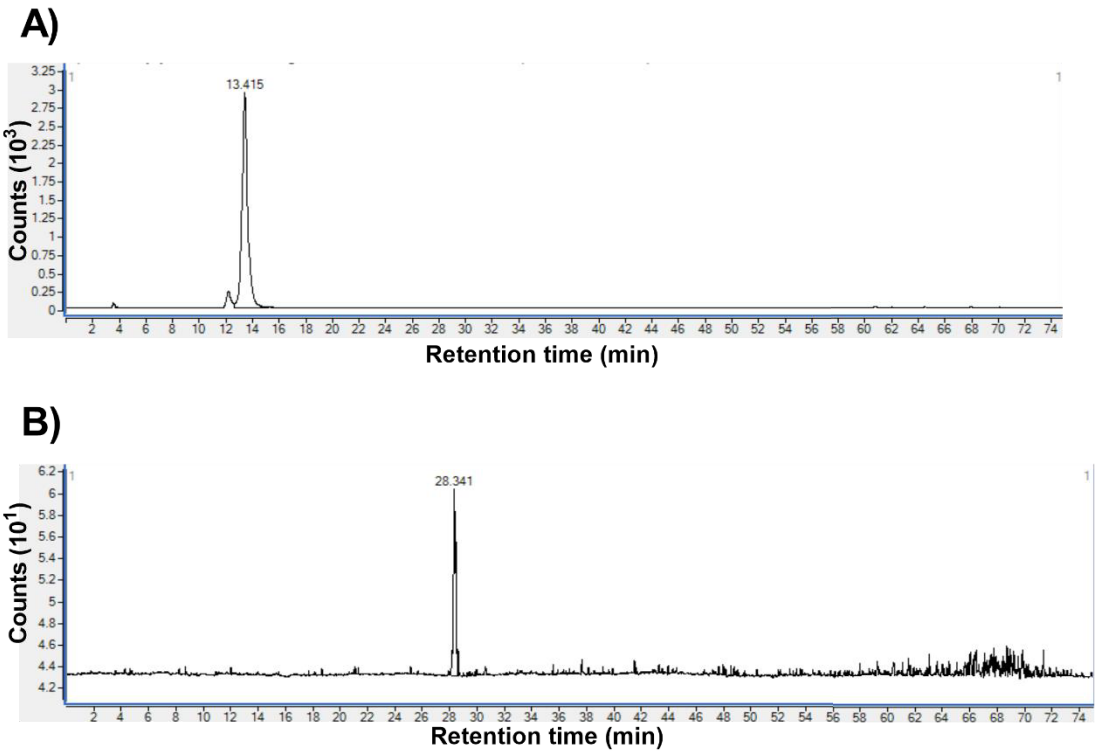

Figure 7: *SRM traces of HCAEC exposed to 5ClдC detected using MS/MS.*
HCAEC (1 × 10^6 cells) were treated with 16 µM 5ClдC. After treatment, DNA was extracted, then hydrolysed and dephosphorylated prior to analysis by LC-MS/MS. A mass fragmentation of 228.1 → 111.9 was monitored using SRM for positive identification of dC (A) and 262.1 → 145.9 for 5ClдC (B).

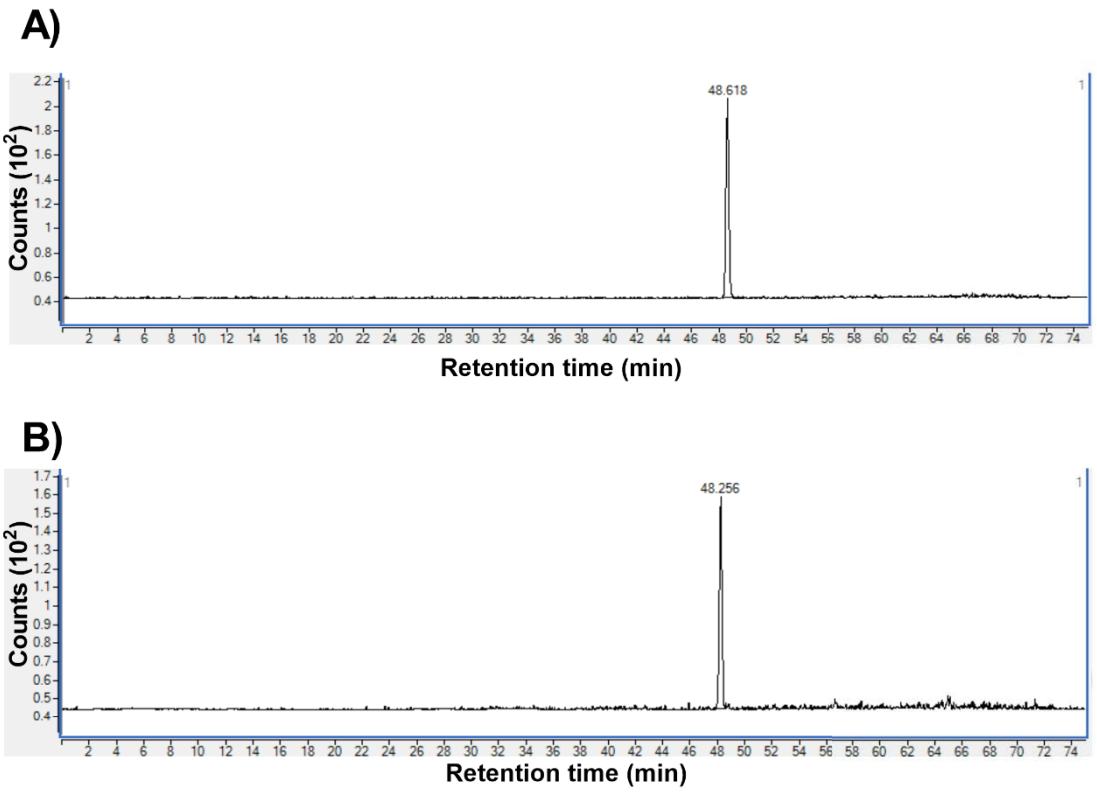

Figure 8: *SRM traces of negative control for 8ClA.*
(A) represents the SRM trace for an injection of 10 nM standard. A 10 nM standard of 8ClA was hydrolysed and dephosphorylated using the same method as cell samples prior to analysis by LC-MS/MS (B). A mass fragmentation of 302.2 → 169.9 was monitored for positive identification of 8ClA by MS/MS.

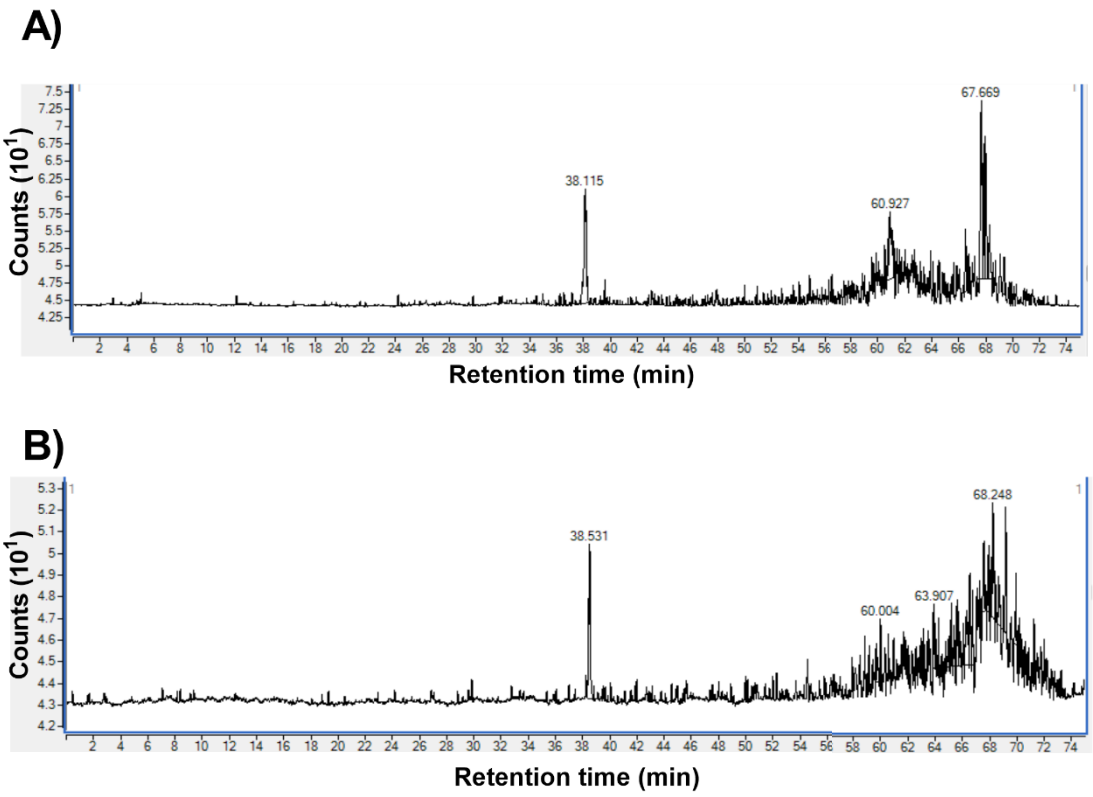

Figure 9: *SRM traces of negative control for 8ClG.*
(A) represents the SRM trace for an injection of 10 nM standard. A 10 nM standard of 8ClG was hydrolysed and dephosphorylated using the same method as cell samples prior to analysis by LC-MS/MS (B). A mass fragmentation of 318.1 → 186.0 was monitored for positive identification of 8ClG by MS/MS.

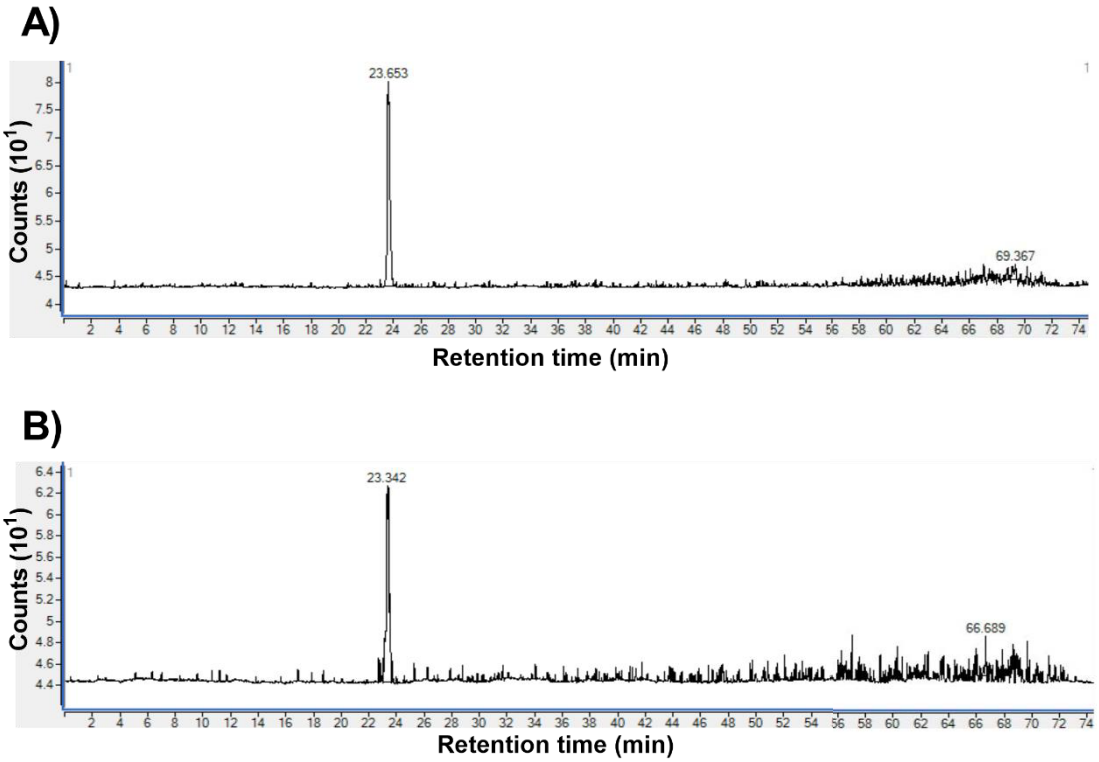

Figure 10: *SRM traces of negative control for 5ClC.*
(A) represents the SRM trace for an injection of 10 nM standard. A 10 nM standard of 5ClC was hydrolysed and dephosphorylated using the same method as cell samples prior to analysis by LC-MS/MS (B). A mass fragmentation of 278.1 → 145.9 was monitored for positive identification of 5ClC by MS/MS.

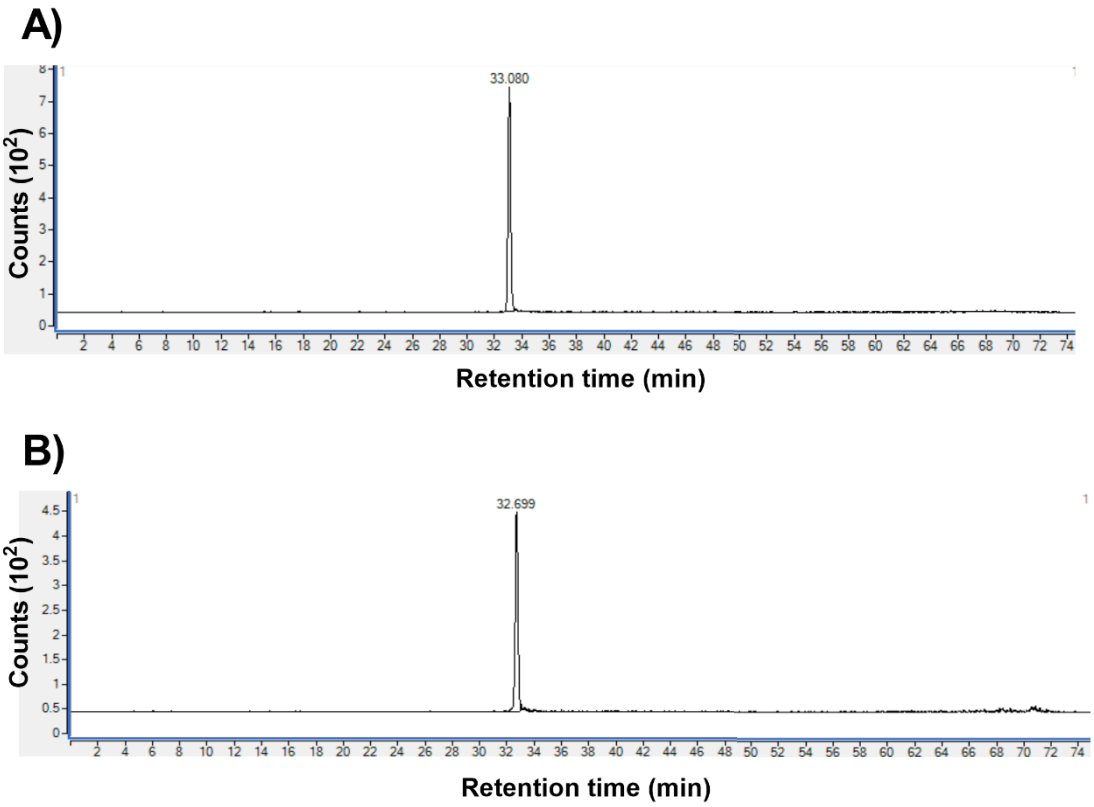

Figure 11: *SRM traces of negative control for adenosine.*
(A) represents the SRM trace for an injection of 10 nM standard. A 10 nM standard of adenosine was hydrolysed and dephosphorylated using the same method as cell samples prior to analysis by LC-MS/MS (B). A mass fragmentation of 268.1 → 136.1 was monitored for positive identification of adenosine by MS/MS.

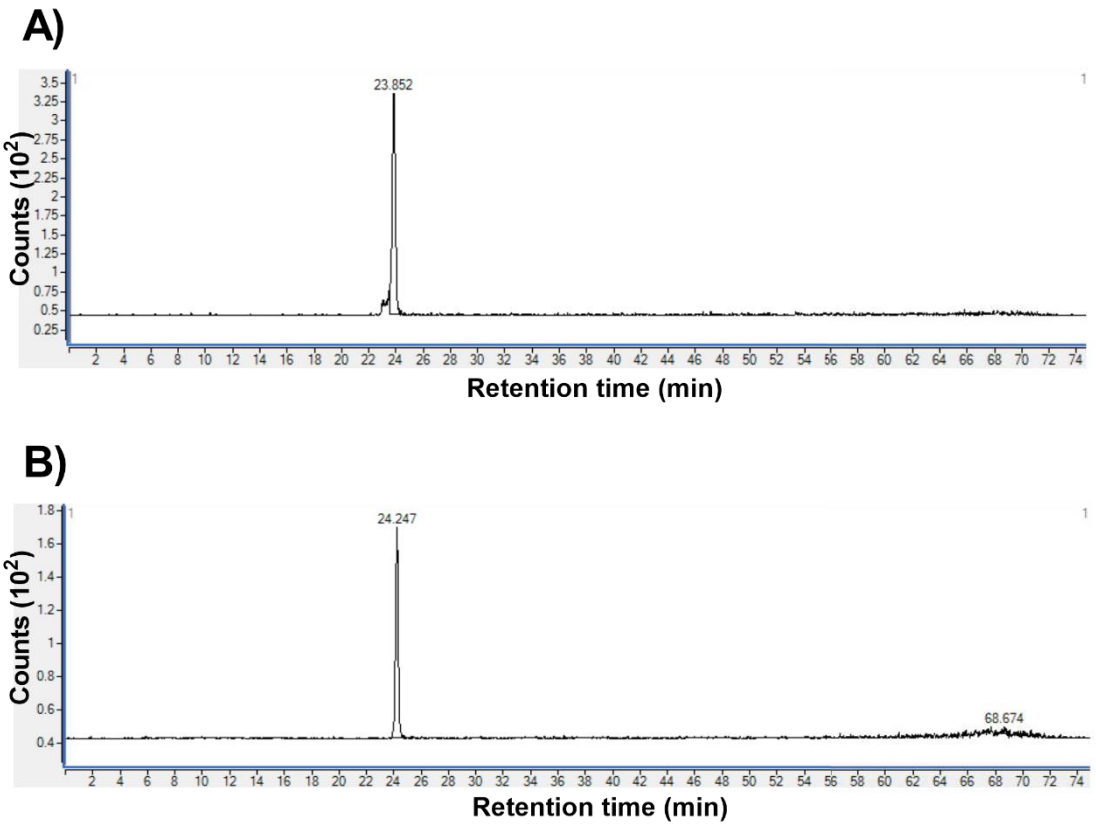

Figure 12: *SRM traces of negative control for guanosine.*
(A) represents the SRM trace for an injection of 10 nM standard. A 10 nM standard of guanosine was hydrolysed and dephosphorylated using the same method as cell samples prior to analysis by LC-MS/MS (B). A mass fragmentation of 284.1 → 151.9 was monitored for positive identification of guanosine by MS/MS.

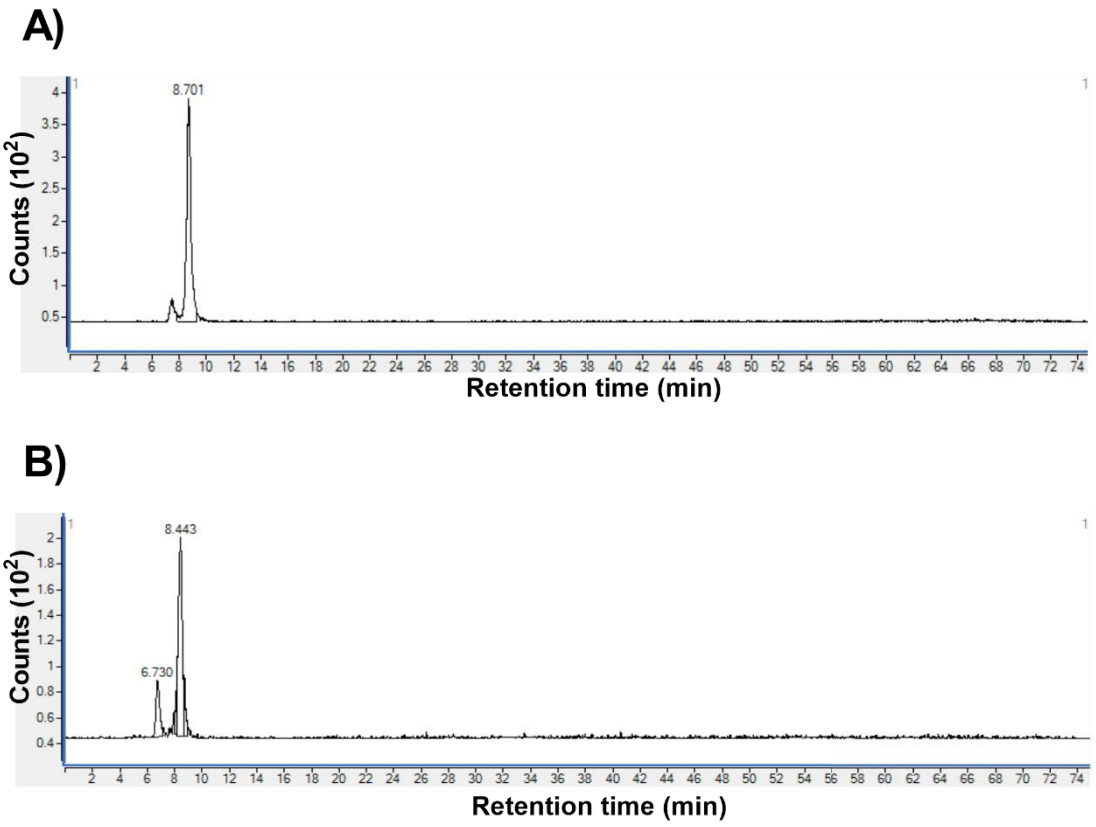

Figure 13: *SRM traces of negative control for cytidine.*
(A) represents the SRM trace for an injection of 10 nM standard. A 10 nM standard of guanosine was hydrolysed and dephosphorylated using the same method as cell samples prior to analysis by LC-MS/MS (B). A mass fragmentation of 244.1 → 112.0 was monitored for positive identification of cytidine by MS/MS.

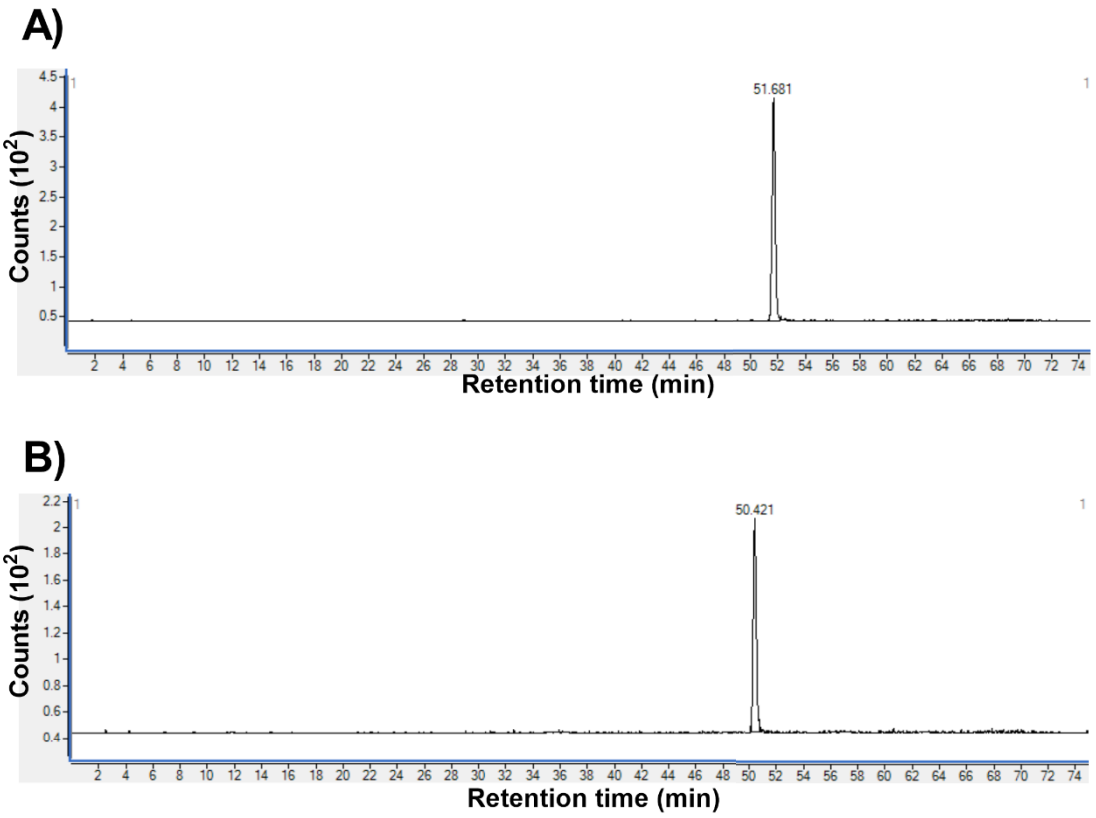

Figure 14: *SRM traces of negative control for 8CldA.*
(A) represents the SRM trace for an injection of 10 nM standard. A 10 nM standard of 8CldA was hydrolysed and dephosphorylated using the same method as cell samples prior to analysis by LC-MS/MS (B). A mass fragmentation of 286.1 → 169.9 was monitored for positive identification of 8CldA by MS/MS.

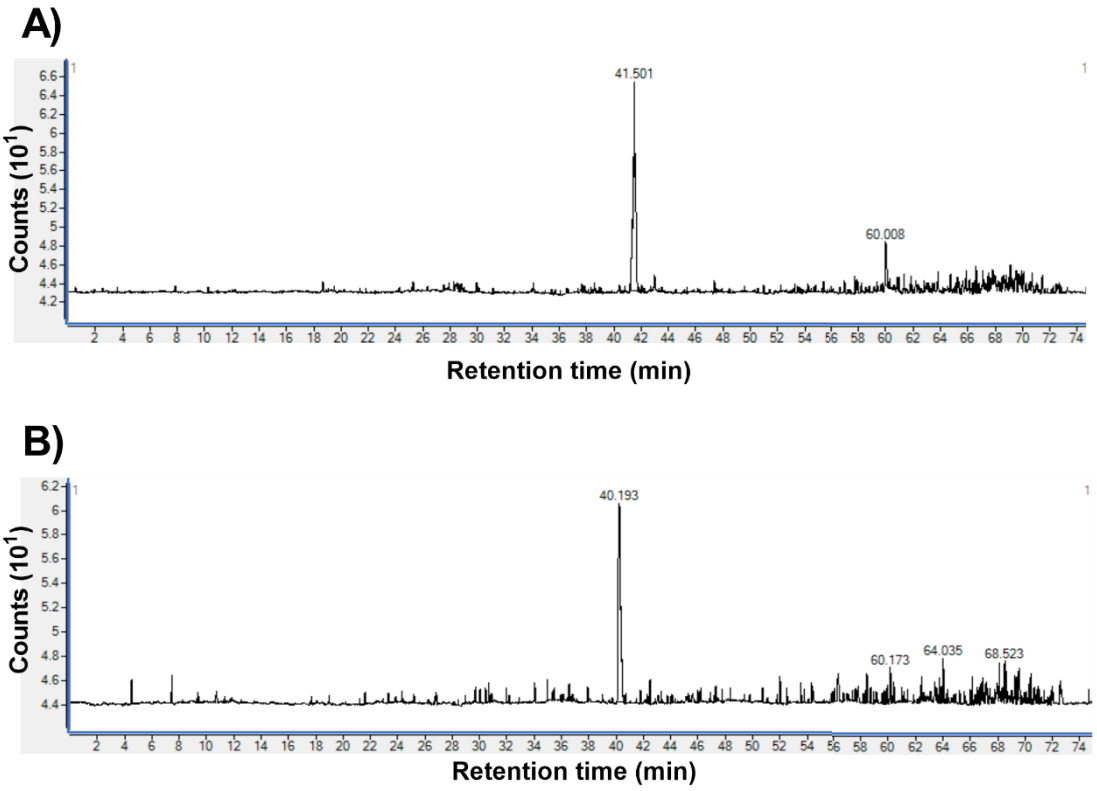

Figure 15: *SRM traces of negative control for 8CldG.*
(A) represents the SRM trace for an injection of 10 nM standard. A 10 nM standard of 8CldG was hydrolysed and dephosphorylated using the same method as cell samples prior to analysis by LC-MS/MS (B). A mass fragmentation of 302.1 → 186.0 was monitored for positive identification of 8CldG by MS/MS.

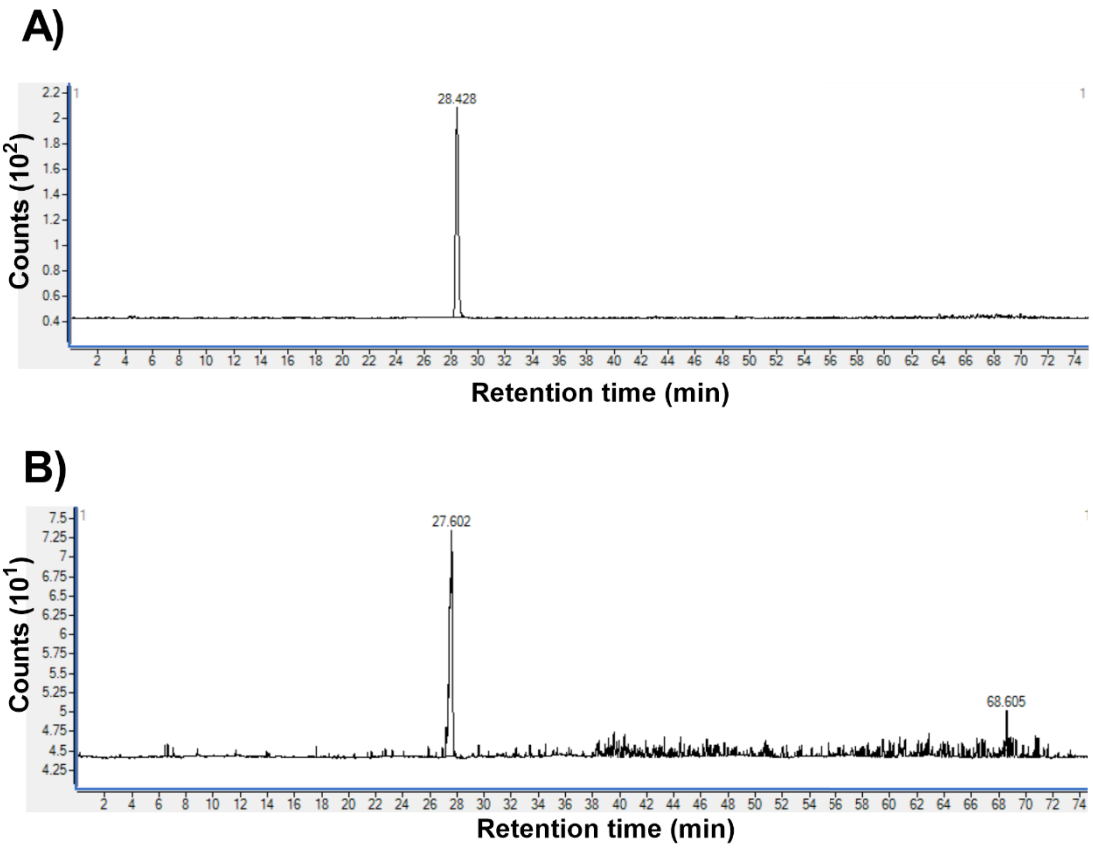

Figure 16: *SRM traces of negative control for 5CldC.*
(A) represents the SRM trace for an injection of 10 nM standard. A 10 nM standard of 5CldC was hydrolysed and dephosphorylated using the same method as cell samples prior to analysis by LC-MS/MS (B). A mass fragmentation of 262.1 → 145.9 was monitored for positive identification of 5CldC by MS/MS.

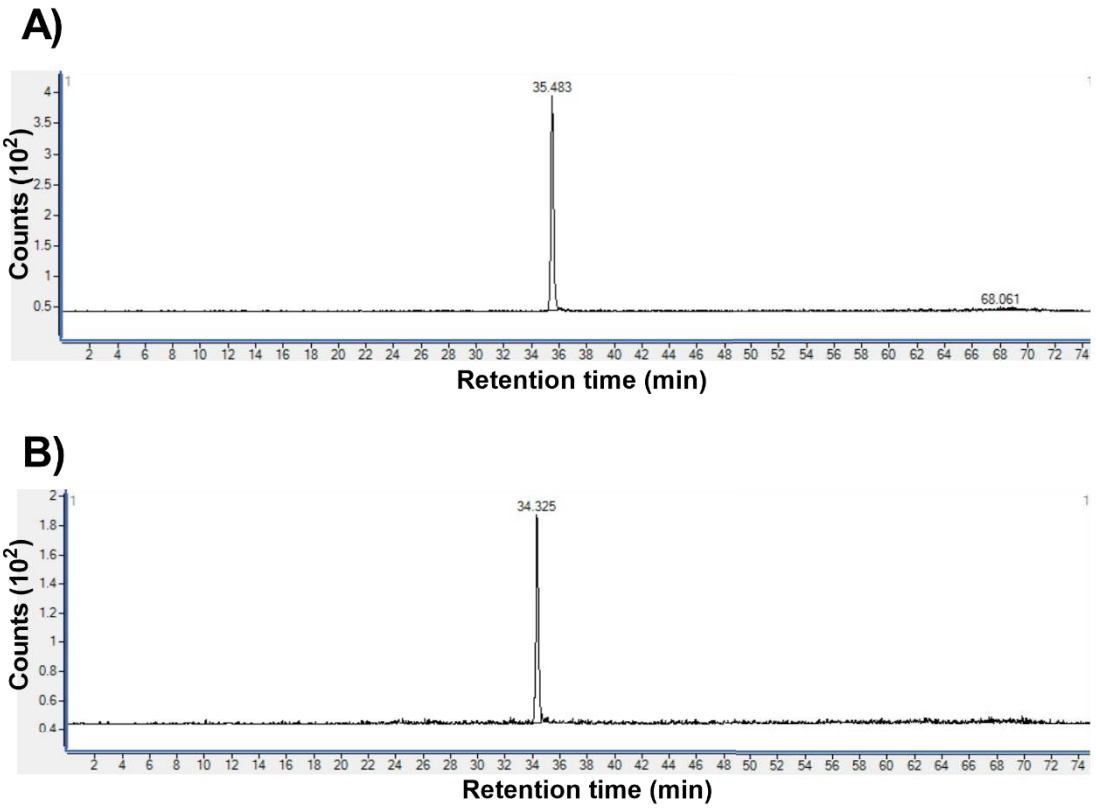

Figure 17: *SRM traces of negative control for dA.*
(A) represents the SRM trace for an injection of 10 nM standard. A 10 nM standard of dA was hydrolysed and dephosphorylated using the same method as cell samples prior to analysis by LC-MS/MS (B). A mass fragmentation of 252.2 → 135.9 was monitored for positive identification of dA by MS/MS.

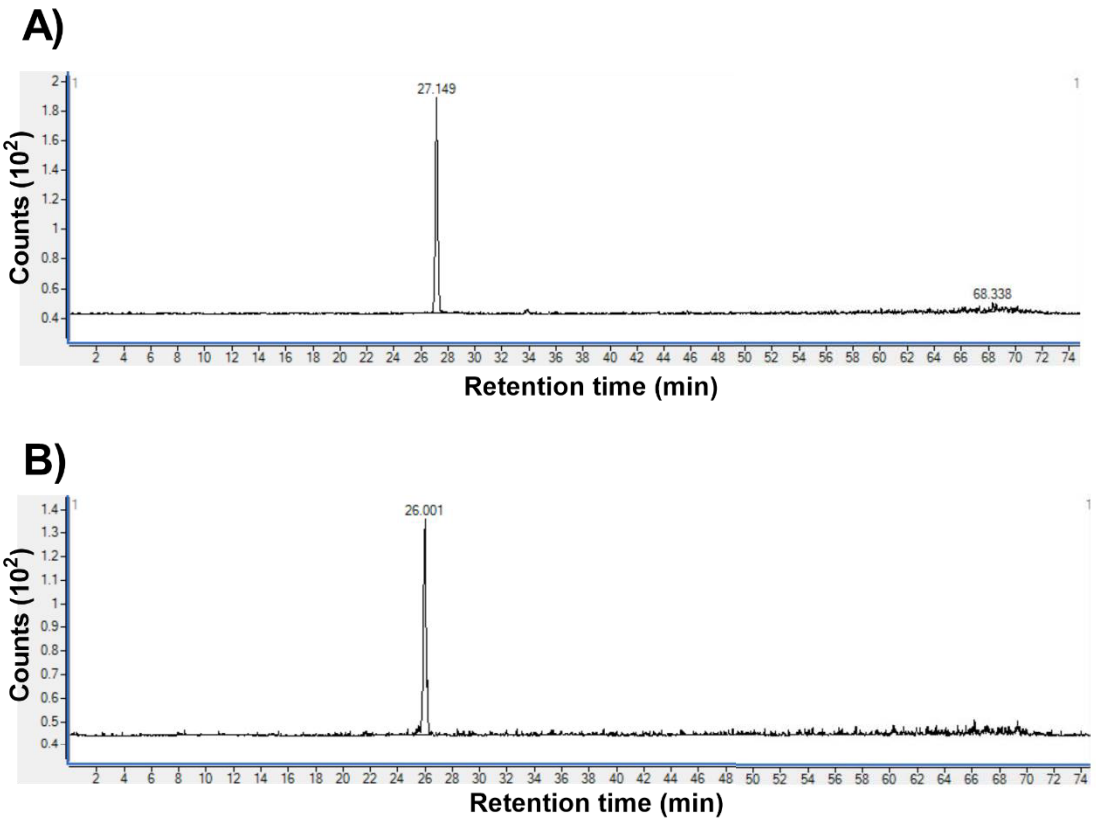

Figure 18: *SRM traces of negative control for dG.*
(A) represents the SRM trace for an injection of 10 nM standard. A 10 nM standard of dG was hydrolysed and dephosphorylated using the same method as cell samples prior to analysis by LC-MS/MS (B). A mass fragmentation of 268.1 → 151.9 was monitored for positive identification of dG by MS/MS.

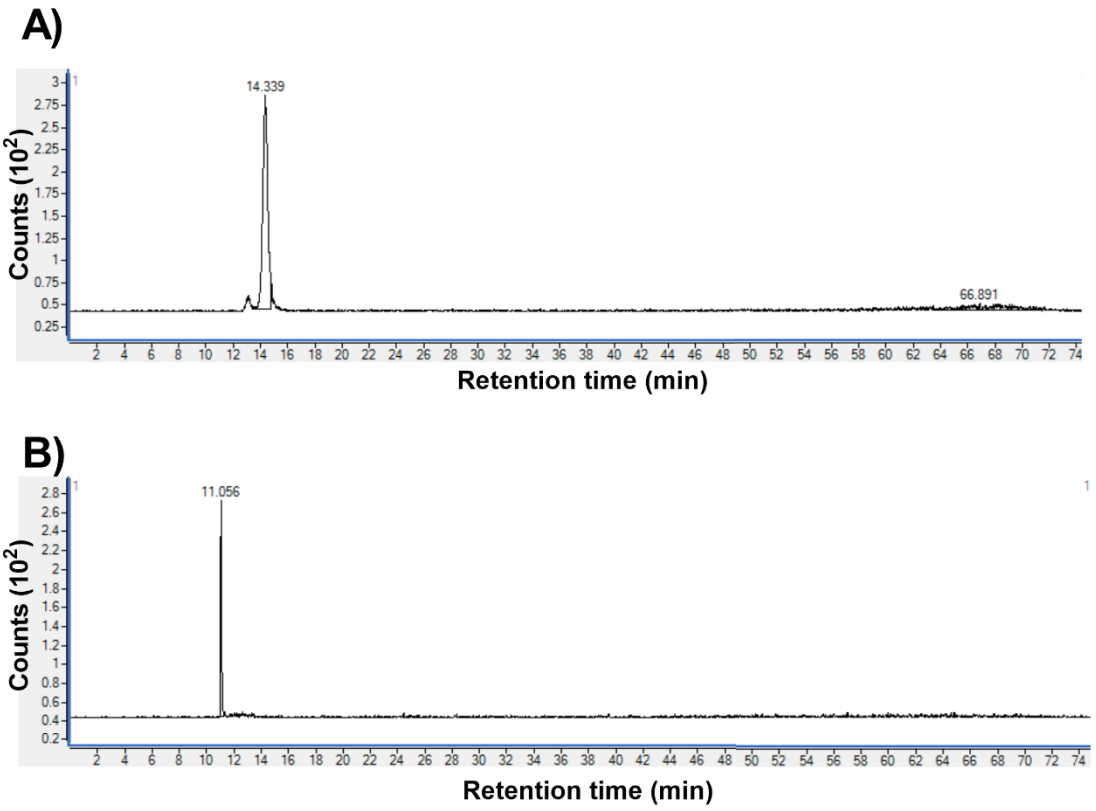

Figure 19: *SRM traces of negative control for dC.*
(A) represents the SRM trace for an injection of 10 nM standard. A 10 nM standard of dC was hydrolysed and dephosphorylated using the same method as cell samples prior to analysis by LC-MS/MS (B). A mass fragmentation of 228.1 → 111.9 was monitored for positive identification of CG by MS/MS.

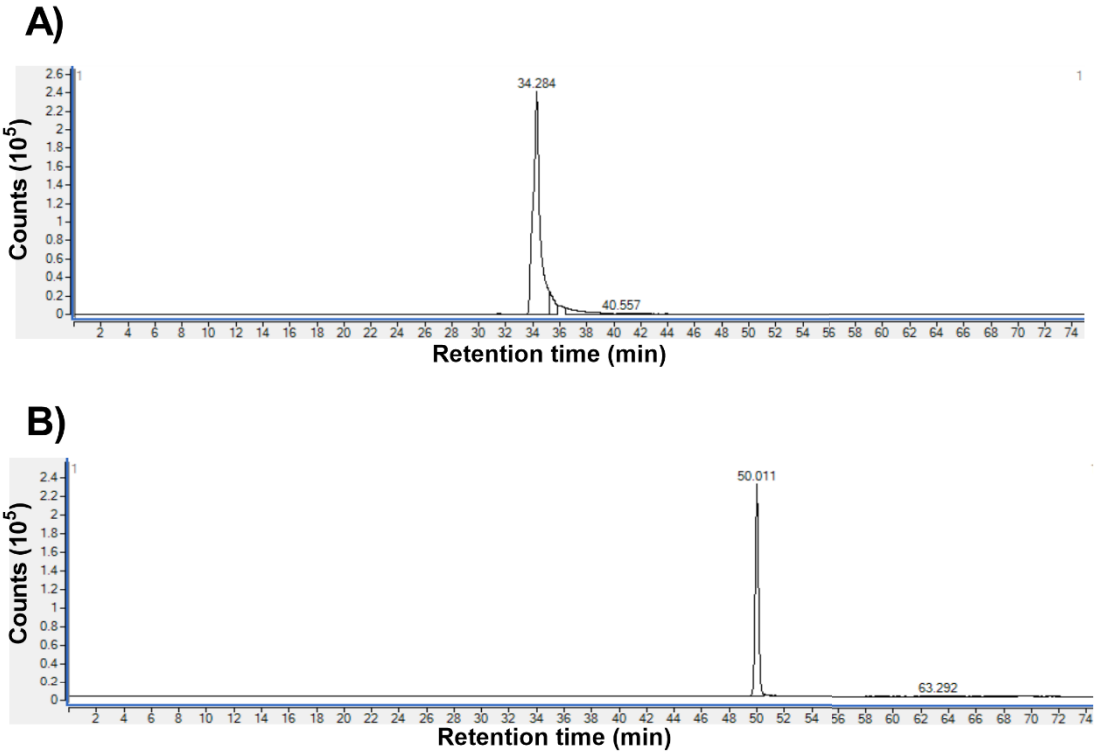

Figure 20: *SRM traces of positive control for 8ClA.*
HCAEC (1 × 10^6 cells) were treated with 16 µM 8ClA. After treatment, RNA was extracted and sample was spiked with 50 fmol of 8ClA. The sample was then hydrolysed and dephosphorylated prior to analysis by LC-MS/MS. A mass fragmentation of 268.1 → 136.1 was monitored using SRM for positive identification of adenosine (A) and 302.2 → 169.9 for 8ClA (B).

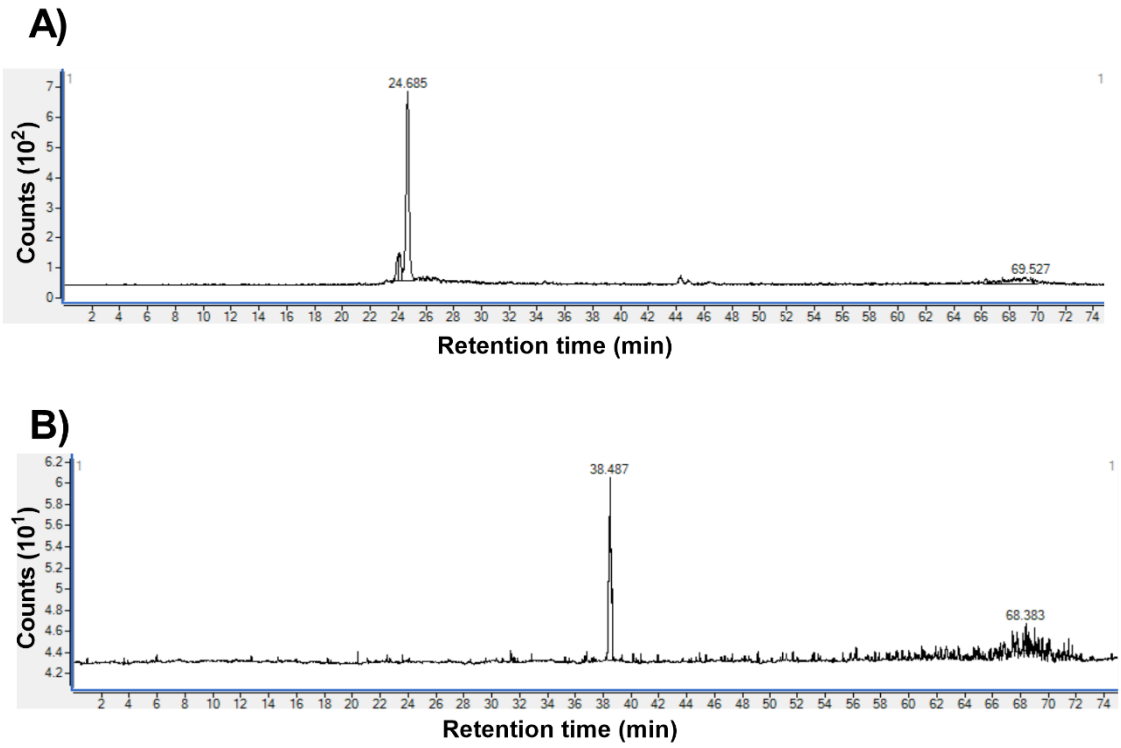

Figure 21: *SRM traces of positive control for 8ClG.*
HCAEC (1 × 10^6 cells) were treated with 16 µM 8ClG. After treatment, RNA was extracted and sample was spiked with 50 fmol of 8ClG. The sample was then hydrolysed and dephosphorylated prior to analysis by LC-MS/MS. A mass fragmentation of 284.1 → 151.9 was monitored using SRM for positive identification of guanosine (A) and 318.1 → 186.0 for 8ClG (B).

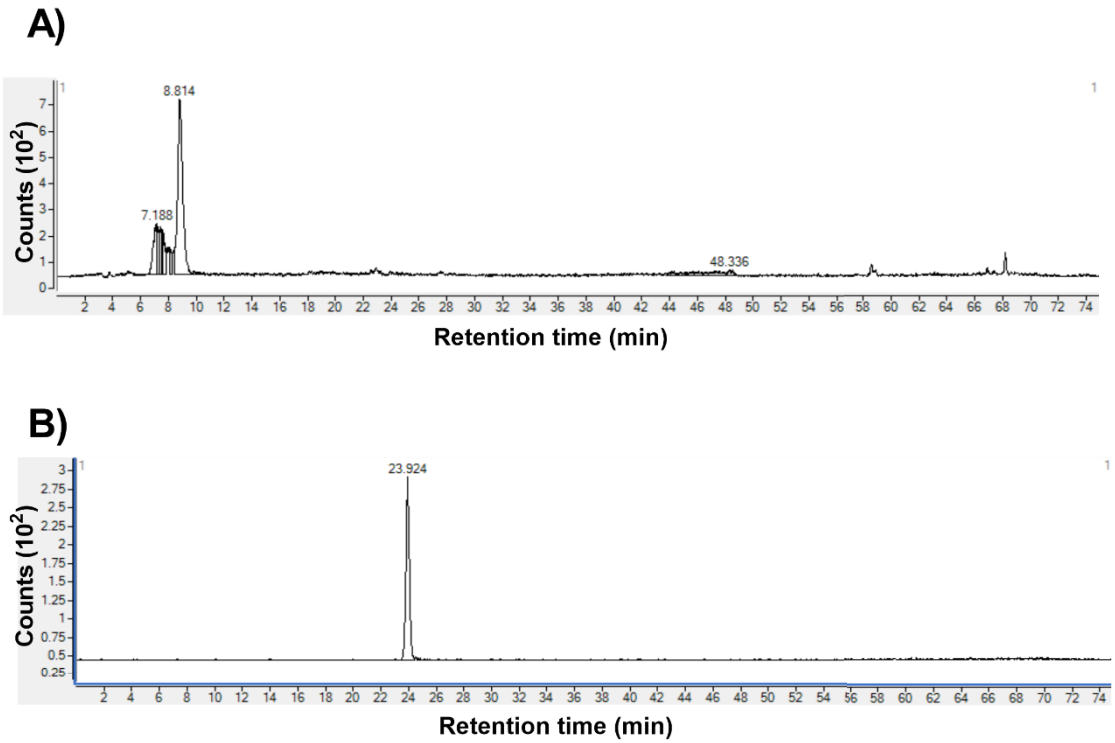

Figure 22: *SRM traces of positive control for 5ClC.*

HCAEC (1 × 10^6 cells) were treated with 16 µM 5ClC. After treatment, RNA was extracted and sample was spiked with 50 fmol of 5ClC. The sample was then hydrolysed and dephosphorylated prior to analysis by LC-MS/MS. A mass fragmentation of 244.1 → 112.0 was monitored using SRM for positive identification of cytidine (A) and 278.1 → 145.9 for 5ClC (B).

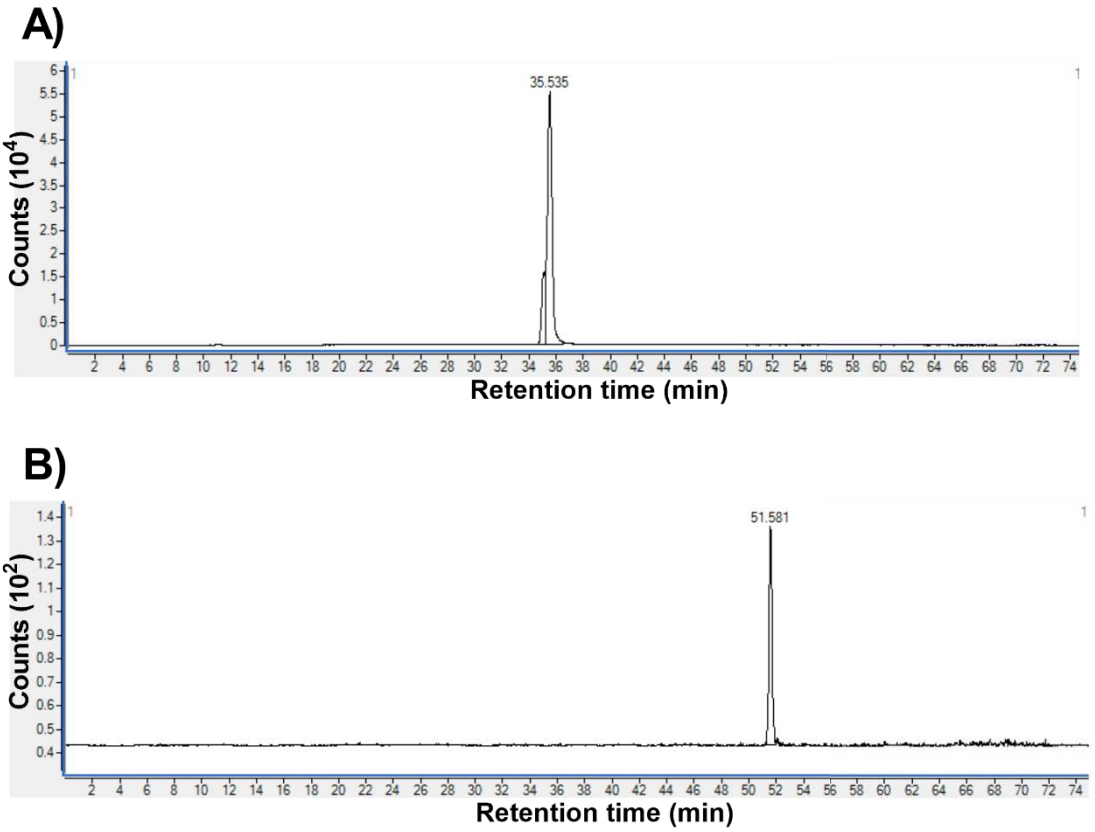

Figure 23: *SRM traces of positive control for 8ClдA.*

HCAEC (1 × 10^6 cells) were treated with 16 µM 8ClдA. After treatment, DNA was extracted and sample was spiked with 50 fmol of 8ClдA. The sample was then hydrolysed and dephosphorylated prior to analysis by LC-MS/MS. A mass fragmentation of 252.2 → 135.9 was monitored using SRM for positive identification of дA (A) and 286.1 → 169.9 for 8ClдA (B).

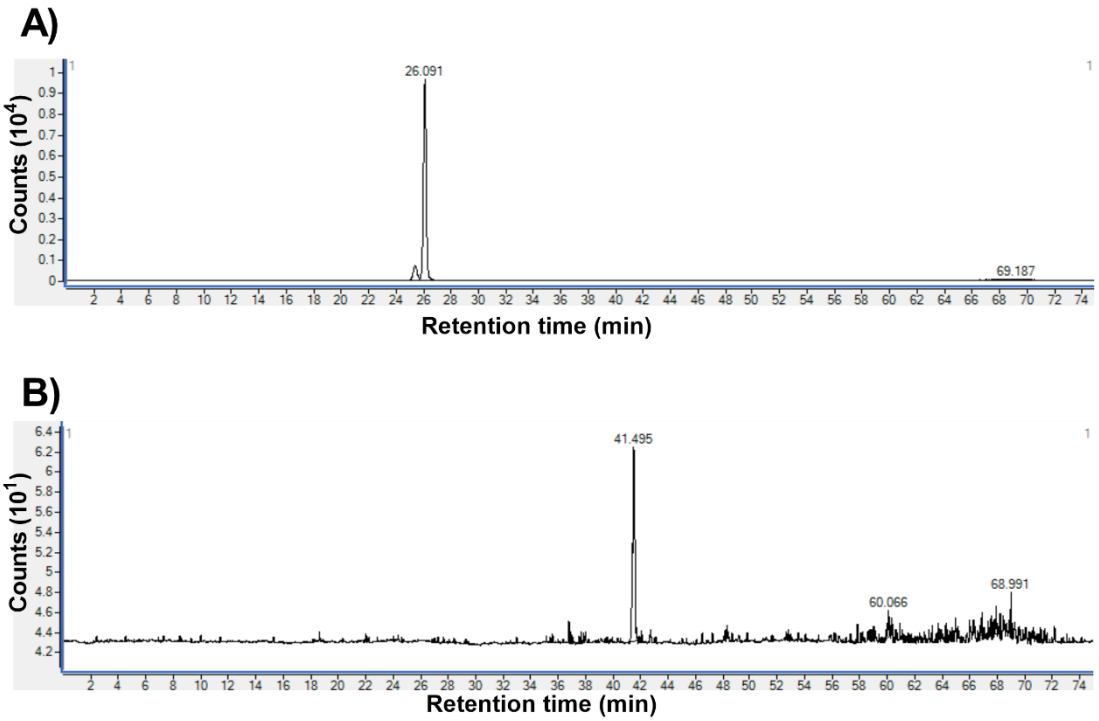

Figure 24: *SRM traces of positive control for 8ClдG.*

HCAEC (1×10^6 cells) were treated with 16 µM 8ClдG. After treatment, DNA was extracted and sample was spiked with 50 fmol of 8ClдG. The sample was then hydrolysed and dephosphorylated prior to analysis by LC-MS/MS. A mass fragmentation of 268.1 → 151.9 was monitored using SRM for positive identification of dG (A) and 302.1 → 186.0 for 8ClдG (B).

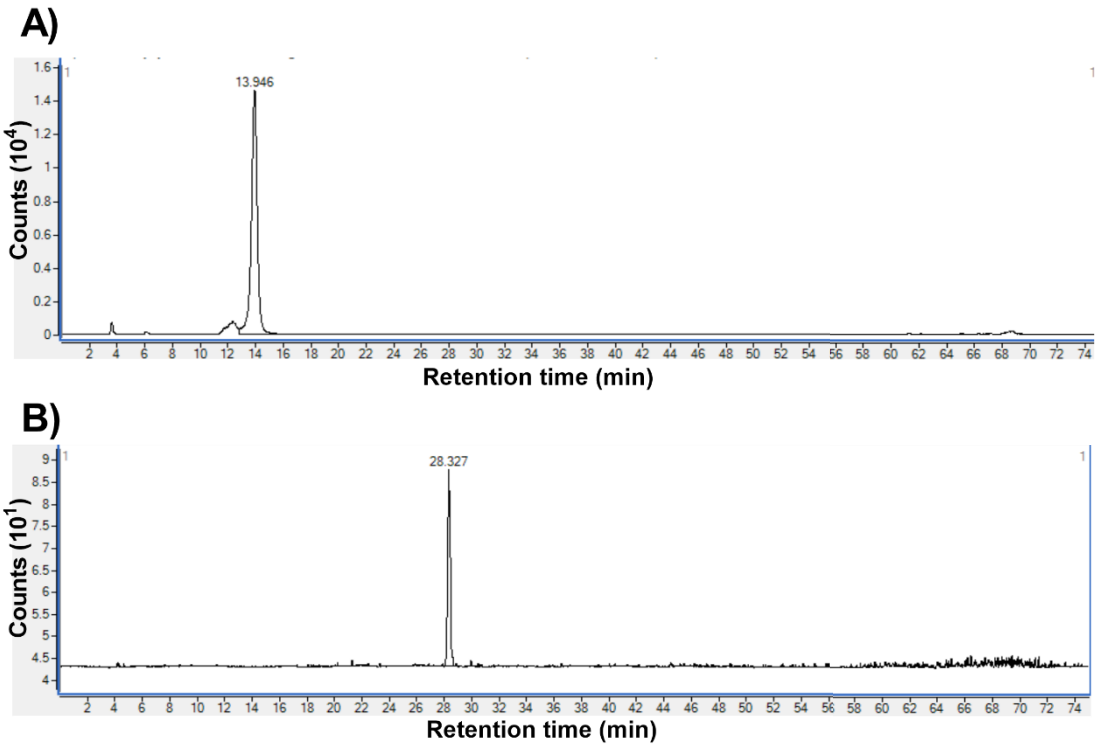

Figure 25: *SRM traces of positive control for 5ClдC.*
HCAEC (1 × 10^6 cells) were treated with 16 µM 5ClдC. After treatment, DNA was extracted and sample was spiked with 50 fmol of 8ClA. The sample was then hydrolysed and dephosphorylated prior to analysis by LC-MS/MS. A mass fragmentation of 228.1 → 111.9 was monitored using SRM for positive identification of dC (A) and 262.1 → 145.9 for 5ClдC (B).